INFORMATION TO USERS

This manuscript has been reproduced from the microfilm master. UMI films the text directly from the original or copy submitted. Thus, some thesis and dissertation copies are in typewriter face, while others may be from any type of computer printer.

The quality of this reproduction is dependent upon the quality of the copy submitted. Broken or indistinct print, colored or poor quality illustrations and photographs, print bleedthrough, substandard margins, and improper alignment can adversely affect reproduction.

In the unlikely event that the author did not send UMI a complete manuscript and there are missing pages, these will be noted. Also, if unauthorized copyright material had to be removed, a note will indicate the deletion.

Oversize materials (e.g., maps, drawings, charts) are reproduced by sectioning the original, beginning at the upper left-hand corner and continuing from left to right in equal sections with small overlaps. Each original is also photographed in one exposure and is included in reduced form at the back of the book.

Photographs included in the original manuscript have been reproduced xerographically in this copy. Higher quality 6" x 9" black and white photographic prints are available for any photographs or illustrations appearing in this copy for an additional charge. Contact UMI directly to order.

UMI

A Bell & Howell Information Company
300 North Zeeb Road, Ann Arbor MI 48106-1346 USA
313/761-4700 800/521-0600

Université d'Ottawa · University of Ottawa

A Study of Fluid Behavior by a General Analytical Solution of the Ornstein-Zernike Equation

Yiping Tang

A thesis submitted to the School of Graduate Studies and Research
for partial fulfillment of the degree of
Doctor of Philosophy
in the Department of Chemical Engineering
University of Ottawa

Abstract

In this work, a fundamental integral equation in statistical thermodynamics, the Ornstein-Zernike (OZ) equation, is solved analytically for the first time for arbitrary intermolecular potentials with a hard core. The proposed solution which combines the perturbation method and the Hilbert transform is applied for both pure fluids and mixtures. Subsequently, the radial distribution function (RDF), which is a crucial function to determine the structure and thermodynamics of fluids, is obtained for a number of typical fluids including the two well-known square-well (SW) and Lennard-Jones (LJ) fluids. RDFs for the SW and LJ fluids are successfully compared with computer simulation data, and the thermodynamic properties derived from these RDFs are found to be better than or comparable to other liquid theories. Furthermore, a two-Yukawa function is suggested in this work to map the LJ potential. The mapping successfully brings the calculations of the structure and thermodynamics of the LJ fluid in a straightforward and analytical manner. The thermodynamics of LJ mixtures are developed analogously. The developed expressions are utilized to describe various types of behavior of LJ mixtures, including vapor-liquid and liquid-liquid equilibria. The description surpasses considerably other liquid theories. The applicability of the present equation of state (EOS) for simple real fluids is also investigated and the superiority of the present EOS over other empirical equations is evidenced by yielding better thermodynamic consistency.

Accompanying the above development, a new strategy for the inverse Laplace transform is proposed to obtain RDF in a completely explicit and analytical manner. A new version of RDF for both pure hard spheres and hard-sphere mixtures is developed based on the first-order OZ solution obtained. A new approximation is suggested to improve the prediction of RDF of the LJ fluid. A RDF for a nonspherical molecule, hard-sphere chain, is also analytically obtained.

Abstrait

Dans ce travail, on a résoud analytiquement, pour la première fois, l' équation de Ornstein - Zernike (OZ), qui est une équation intégrale et fondamentale en thermodynamique statistique, pour des potentiels intermoléculaires et arbitraires avec un noyau dur. On a appliqué la solution proposée, combinant la méthode de perturbation et la transformation de Hilbert, pour des fluides pures et des mélanges. Par la suite, on a obtenu la fonction de distribution radiale (FDR), qui est une fonction cruciale pour déterminer la structure et les propriétés thermodynamiques des fluides, pour un nombre de fluides typiques y compris les fluides bien connus: le puits - carfe (PC) et Lennard - Jones (LJ). Pour les fluides PC et LJ, on a comparé, avec succès, les FDR aux données des simulations par ordinateur. De plus, on a trouvé que les propriétés thermodynamiques dérivées de ces FDR sont mieux ou comparables à celles dérivées d'autres théories des liquides. En outre, on a suggéré la fonction de Deux - Yukawa afin d'ajuster le potentiel de LJ. Cet ajustement a apporté, avec succès, les calculs de la structure et des propriétés thermodynamiques du fluide LJ d'une façon simple et analytique. On a analoguement developpé les propriétés thermodynamiques des mélanges de LJ. On a utilisé les expressions developpées pour décrire les comportements variés des mélanges de LJ y compris les équilibres vapeur - liquide et liquide - liquide. Cette déscription a considérablement surpassé les autres théories des liquides. On a aussi examiné l'applicabilité de la présente équation d'état (EDE) pour des fluides simples et réels. Cette équation a manifesté une supériorité par rapport aux autres équations empiriques, du fait qu'elle a mieux produit des propriétés thermodynamiques uniformes.

Accompagné du développement discuté ci - dessus, on a proposé une nouvelle stratégie pour résoudre l'inverse de la transformation de Laplace, afin d'obtenir une FDR complètement plus explicite et analytique. On a développé une nouvelle version de FDR, basée sur la solution du premier ordre de O-Z obtenue, pour des sphères dures à l'état pur ainsi que pour leurs mélanges. On a suggéré une nouvelle approximation pour améliorer la prédiction de FDR pour le fluide LJ. De plus, on a analytiquement obtenu une FDR pour une molécule non sphérique et une chaîne de sphères dures.

Acknowledgements

Many thanks go to Professor Benjamin C.-Y. Lu for his patient supervision of this work. I thank him especially for his accommodation and encouragement of the theoretical part of this work, which provides me a stable and pleasant environment for research and is crucial in the success of this thesis.

I am grateful to Dr. G. C. Benson for his kindness in providing his computer facilities.

I would like to thank Professors Y. Li, J. Lu and Z. Li of Tsinghua University for making me aware of needs of analytical solutions of the OZ equation, and for their encouragement in this work.

I would also like to thank Mr. J. Wu of the University of California at Berkeley for encouraging and suggestive discussion in the solution of the OZ equation.

Financial supports from the Ontario Graduate Scholarship and the University of Ottawa are also greatly appreciated.

Finally, I would like to thank my wife, Xiaohui, for her support during my Ph.D. studies and for her typing certain portions of this thesis.

Table of Contents

List of Figures

List of Tables

Nomenclature

A = Helmholtz free energy
B_2 = second virial coefficient
a = reduced Helmholtz free energy
a_c = parameter of Kihara potential
C = matrix of direct correlation function
$c(r)$ = direct correlation function
d = BH diameter
$G(s)$ = Laplace transform of $rg(r)$
$g(r)$ = radial distribution function
H = Hilbert transform, matrix of total correlation function
$h(r)$ = total correlation function
i = unit of imaginary part of a complex number
l_{ij} = parameter of the Lorentz combining rule
I = the unit matrix
k = Boltzmann constant, wave vector in Fourier transform
k_0, k_1 = potential parameters of the TY potential
K = potential parameters of Yukawa mixtures
K_0, K_1 = potential parameters of TY mixtures
m = chain length
N = number of molecules, number of components in a mixture
P = pressure
$Q_0(s)$ = factor correlation function of hard spheres
R = diameter of hard spheres
r = absolute value of a distance
s = wave vector in Laplace transform
T = temperature
U = internal energy
u = reduced internal energy
$u(r)$ = molecular interpotential
V = volume
x = composition
$y(r)$ = cavity function
Z = compressibility factor
z = parameter of Yukawa potential
z_1, z_2 = parameters of the TY potential

Greek letters

β = $1/\{\kappa T\}$

γ = surface tension
γ_{ij} = parameter of the Berthelot combining rule
ϵ = potential energy parameter
ε = perturbation parameter
η = $1/6\rho R^3$
λ = well width of SW potential
μ = viscosity
ρ = density of fluid
σ = potential size parameter

Subscripts and other indices
0 = hard spheres
1 = first-order term in a perturbation expansion
i = ith-order term in a perturbation expansion
$\hat{}$ = one-dimensional Fourier transform
$\sim$ = three-dimensional Fourier transform
* = reduced property

Abbreviations
AAD = average absolute deviation
BH = Barker and Henderson
CS = Carnahan Starling
DCF = direct correlation function
EOS = equation of state
EXP = exponential
GMSA = generalized mean spherical approximation
GWL = Guo, Wang and Lu
HNC = hypernetted chain
LB = Lorentz-Berthelot
LLE = liquid-liquid equilibria
LJ = Lennard-Jones
LS = Lee and Sandler
MBWR = modified Benedict-Webb-Rubin
MC = Monte Carlo
MD = molecular dynamic
MSA = mean spherical approximation
NRTL = non-random two liquid
OOP = object-oriented programming
OZ = Ornstein-Zernike
PR = Peng-Robinson

PTH = perturbation theory given by Fotouh and Shukla (1997)
PT = perturbation theory given by Lotif and Fisher (1989)
PVT = pressure, volume and temperature
PY = Percus-Yevick
RDF = radial distribution function
SEXP = simplified exponential
SL = Shen and Lu
SW = square-well
TCF = total correlation function
TY = two-Yukawa
UCST = upper critical solution temperature
UNIFAC = universal functional activity coefficient
UNIQUAC = universal quasi-chemical
VDW = van der Waals
VDW1 = van der Waals one-fluid
VLE = vapor-liquid equilibria
VW = Verlet and Weis
WCA = Weeks, Chandler and Anderson

1. Introduction

Understanding the behavior of fluids is one basic requirement in the design and operation of chemical engineering and petroleum industries. Many processes such as distillation, extraction, adsorption and leaching require a lot of knowledge of properties of pure substances and their mixtures. These requirements constantly inspire the development of thermodynamics, whose task is to correlate and predict the behavior of fluids. Today, the applications of thermodynamics have been found in the treatment of environmental pollution, purification of sea water and even in the field of biochemistry, such as in protein association and separation (Arich, 1992). It has become an indispensable tool to solve quantitatively problems encountered in both science and engineering.

In recent decades, the development of thermodynamics has been very encouraging. Modern thermodynamics has incorporated many new results from other fields, especially statistical physics and computer technology. Traditionally, thermodynamics describes only empirically the behavior of certain fluids. The description works out usually after much information about the fluid is already known. Therefore, either the kind of systems or the range of conditions (temperature, pressure) is highly limited by this phenomenological method or phenomenological thermodynamics. One typical example of phenomenological thermodynamics is the van der Waals (VDW) equation of state (EOS). Although the VDW EOS and its later variations (e. g., Redlich and Kwong, 1949; Peng and Robinson, 1976) are rather popular in practical applications, they always suffer some fundamental inadequacies. For instance, saturated liquid densities and second virial coefficients are given very poorly. Empirical or semi-empirical solution models such as NRTL, UNIQUAC and UNIFAC models are widely utilized in industry to calculate vapor-liquid equilibria (VLE) and liquid-liquid equilibria (LLE). One disturbing thing is that all these models have to adopt two inconsistent sets of parameters for VLE and LLE. The inconsistency reveals an inherent difficulty of phenomenological thermodynamics and is unlikely to be eliminated by some empirical modifications. The failures of phenomenological thermodynamics are the

consequence of neglecting or oversimplifying molecular interactions and fluid structure in its consideration. It is well known that microscopic characteristics of a fluid or molecular interactions fully underlie its macroscopic behavior. Any more efficient methods to describe complex macroscopic behavior should be firmly based on microscopic molecular interactions. Developing fluid bulk properties from the level of molecular interaction is the task of statistical thermodynamics. Progress in modern thermodynamics relies heavily on the development of statistical thermodynamics.

The exact relation between macroscopic properties and molecular interactions has been established for many years. Two well-developed methods, the canonical and the grand canonical ensembles (Lee, 1988), provide two mathematical routines to represent the relation. In principle, any thermodynamic properties can be predicted by the two ensemble methods provided that the intermolecular potential is known. In such a prediction, one crucial intermediate quantity derived from the two ensembles is the radial distribution function (RDF), which is originally defined by (Lee, 1988)

$$g(r) = g(|r_1 - r_2|) = \frac{V^2 \int \cdots \int \exp\left(-\frac{\beta}{2}\sum_i^N \sum_j^N u(r_{ij})\right) dr_3 dr_4 \cdots dr_N}{\int \cdots \int \exp\left(-\frac{\beta}{2}\sum_i^N \sum_j^N u(r_{ij})\right) dr_1 dr_2 \cdots dr_N} \qquad (1)$$

where V and N are the volume and number of molecules, respectively. $\beta = 1/kT$, where T stands for absolute temperature and k is Boltzmann constant. u(r) is the intermolecular potential. The physical meaning of RDF can be interpreted as the probability density of finding one molecule 1 at r_1 and another molecule 2 at r_2, which is dependent only on the relative distance $r = |r_1 - r_2|$ for spherical molecules. For an ideal gas, g(r) is unity throughout the r-space. The deviation from unity of g(r) for a real fluid represents quantitatively the nonideality of the fluid. Generally, g(r) is an oscillating and damped function, approaching unity as r goes to infinity. A typical profile of RDF for the Lennard-Jones (LJ) fluid is illustrated in Figure 1, where $T^*(=kT/\epsilon)$ and $\rho^*(=\rho\sigma^3)$ are the reduced temperature and density, respectively, and ϵ and σ are energy and size parameters of the LJ potential, respectively. The

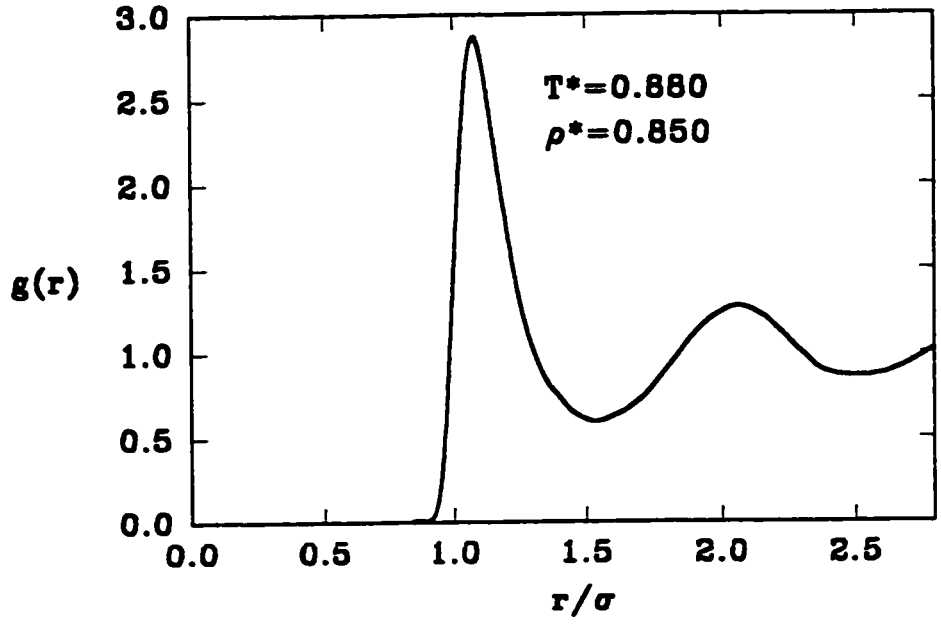

Figure 1. A RDF profile for the LJ fluid

significant point for RDF is that, once this function is known, any thermodynamic properties can be straightforwardly calculated. For instance, the internal energy, pressure and compressibility can be presented respectively by

$$\frac{U}{NkT}=\frac{3}{2}+\frac{\rho}{2kT}\int_0^{\infty} g(r)\,u(r)\,4\pi r^2 dr \qquad (2)$$

$$\frac{PV}{NkT}=1-\frac{\rho}{6kT}\int_0^{\infty} g(r)\,\frac{du(r)}{dr}\,4\pi r^3 dr \qquad (3)$$

$$\frac{1}{NkT}\left(\frac{\partial P}{\partial \rho}\right)_T=\frac{1}{1+\rho\int_0^{\infty}(g(r)-1)\,4\pi r^2 dr} \qquad (4)$$

Other properties such as enthalpy and entropy can be derived by the well-known

Maxwell relations through one of the above relations. It is of value to mention that some other quantities in non-equilibrium and inhomogeneous thermodynamics are inherently connected with RDF. For example, surface tension γ, one characteristic of inhomogeneous fluids, can be determined by (Toda et al., 1992)

$$\gamma=\frac{\rho^2}{32}\int_0^\infty \frac{du(r)}{dr} g(r) 4\pi r^4 dr \tag{5}$$

The viscosity μ, which is widely required in transport phenomena, is associated with the equilibrium g(r) by (Reed and Gubbins, 1973)

$$\frac{\mu}{\mu_0}=\frac{1}{g(1)}+1.676\rho+3.339\rho^2 g(1) \tag{6}$$

for hard spheres, in which μ_0 is the dilute gas viscosity. Therefore, RDF plays a central role in liquid theory and is much demanded in the development of thermodynamics. Unfortunately, an exact calculation of RDF is practically prohibitive because of the astronomical number of integrals in Equation (1). The integration difficulty is the primary obstacle for developing a useful liquid theory from the canonical and the grand canonical ensembles.

It is in recent decades that considerable progress in liquid theory has been made with the aid of computer simulation and integral equation theory. Computer simulation, which is hereafter referred to as either Monte Carlo (MC) or molecular dynamic (MD) simulation, can partially overcome the difficulty in evaluating the canonical partition function and, to a certain extent, predict fluid behavior if the intermolecular potential is known. Another important application of computer simulation is to provide reliable numerical results to test the validity of liquid theories. However, computer simulation requires a tremendous amount of calculations, which are very time-consuming and unaffordable for engineering purposes even with today's high-speed computers. Besides, it is inadequate to provide systematic information about fluid behavior. The integral equation theory, which was developed rapidly in recent years, is a very promising method to solve the problems mentioned above. For

a pure fluid, the theory proposed by Ornstein and Zernike (OZ) (1914) is mathematically presented by

$$h(r) = c(r) + \rho \int d\boldsymbol{r}' c(\boldsymbol{r}') h(\boldsymbol{r}-\boldsymbol{r}') \tag{7}$$

where h(r) is the total correlation function (TCF), defined by h(r) = g(r)-1. c(r) is the direct correlation function (DCF). ρ is the density of the fluid. The integral in Equation (7) is taken over the three-dimensional space. The OZ equation may be written more concisely by taking the Fourier transform of Equation (7):

$$\tilde{h}(k) = \tilde{c}(k) + \rho \tilde{h}(k)\, \tilde{c}(k) \tag{8}$$

where

$$\tilde{h}(k) = \frac{4\pi}{k} \int_0^\infty r h(r) \sin kr dr \tag{9}$$

$$\tilde{c}(k) = \frac{4\pi}{k} \int_0^\infty r c(r) \sin kr dr \tag{10}$$

The OZ equation, once supplemented by another relation (closure) between h(r) and c(r), can be solved and give us the most desired RDF. Two typical closures for the solution are the Percus-Yevick (PY) (1958) approximation

$$c(r) = g(r)(1 - e^{\beta u(r)}) \tag{11}$$

and the mean spherical approximation (MSA) (Lebowitz and Percus, 1966)

$$\begin{aligned} c(r) &= -\beta u(r), \quad r > R \\ h(r) &= -1, \quad r < R \end{aligned} \tag{12}$$

where the molecules are assumed to have an impenetrable hard core. Although a certain mathematical simplicity is introduced here, the two approximations have been proven to perform dramatically well in a number of liquid theories. The PY approximation and MSA are adopted throughout this work in the solution of the OZ equation.

Solving the OZ equation is a very technical and interesting problem in liquid theories. Although the highly nonlinear integral equation could be solved numerically, the numerical solution is of little interest for practical usage due to its extensive computational work. Moreover, a numerical solution often causes some instability problems, e. g., around the critical region. In 1960s, it was surprisingly found that the OZ equation can be solved analytically due to the elegant work done by Wertheim (1963) and Thiele (1963) for hard spheres. Their achievement inspired much interest in the solvability of the OZ equation for other potentials, because analytical results will give us a direct insight into fluid structure, and more significantly provide a favorable foundation for perturbation theory to explore more complex systems.

Subsequently, Lebowitz (1964) obtained the OZ solution for the two-component mixture of hard spheres. Baxter (1968a) found the OZ solution for sticky hard spheres which for the first time accounts for an attractive force in the solution. In 1970s, solutions of the OZ equation were found for molecules interacting through the primitive Coulomb force (Waisman and Lebowitz, 1970), a typical molecular interaction in electrolyte solutions, and for molecules interacting through the Yukawa form (Waisman, 1973). Blum et al. later extended Waisman's solutions to the Yukawa function with multiple tails (Hφye and Blum, 1978), the Yukawa mixtures (Blum and Hφye, 1977) and to non-primitive electrolyte solution (Blum, 1975; Blum and Hφye, 1977). Recently, the OZ solutions which incorporate solvent effect have enabled us to quantitatively understand the nature of the dielectric constant in physical chemistry (Wertheim, 1971; Blum, 1978; Blum and Wei, 1987). Henderson et al. (1976b) have applied the OZ solution for analyzing the phenomena of solid-fluid interface which lead to a theoretical description of adsorption. The above analytical solutions have found some practical applications. For example, vapor-liquid and liquid-liquid phase separations have been investigated by a number of authors through the analytical algorithm developed above (Caccamo and Giunta, 1991; Hoheisel and Zhang, 1991; Arrieta et al., 1991). The Baxter OZ solutions for sticky hard spheres (Baxter, 1968a) and mixtures (Barboy, 1975) greatly facilitate the studies of chain molecules (Chiew, 1990). In recent years, the density functional theory has become a very efficient tool

to study inhomogeneous fluids, which are conceptually different from homogeneous fluids studied in this work and cover a variety of new phenomena such as surface wetting and adsorption. In implementing the density functional theory, the analytical solution of the OZ equation for homogenous fluids is an indispensable input function and the accuracy of such an input function heavily affects the performance of the theory. More recently, the OZ equation has been utilized to interpret the supercritical solubility enhancement (Chialo and Cummings, 1994; Munoz et al., 1995), protein precipitation(Chiew et al, 1995) and phase separation of a PEG-salt-water solution (Kenkare and Hall, 1996). Today, there is a tendency to describe various fluid behavior more and more frequently through the solution of the OZ equation.

However, the solution of the OZ equation was far from accomplished. Except for a very few potentials mentioned above, analytical results for most potentials used in liquid theory were still not available. For example, the OZ solution for the LJ potential, which is an essential force to describe molecular interaction, remained an analytically prohibitive problem. In addition, the mathematical expressions of previous OZ solutions were rather complex and the complexity would tremendously increase with the increasing number of components in a mixture. Up to now, there was no practical equation of state based on the OZ solution available in the literature. Thus, a certain simplification of the OZ solution should be made to enlarge the applications of the OZ equation for both theoretical studies and practical applications.

The purpose of this work is to find an efficient mathematical scheme applicable to an arbitrary potential for the OZ solution, and to reduce the mathematical work in manipulating the solution. Eventually, a new equation of state with strong theoretical background and relatively simple mathematical form is developed to explore the behavior of real fluids. The new EOS for both the pure LJ fluid and LJ mixtures is tested rigorously by comparing it with computer simulation data and is then applied to calculations of thermodynamics of real fluids. Considerable improvement over other empirical EOS is found in this work. This work is an attempt to bridge the gap between statistical thermodynamics and phenomenological thermodynamics.

2. A New Strategy to Solve the OZ Equation

2.1. Pure fluids

The OZ equation has been solved in different ways (Wertheim, 1963; Thiele, 1963; Baxter, 1968b). However, all of these methods are only applicable to a specific potential and can be hardly extended to general cases. The most widely utilized factorization method suggested by Baxter (1968b) is totally dependent on an empirical construction of the factor correlation function, and its application is inevitably limited. Some efforts (Smith, 1979; Perram, 1983) to find a more efficient solution have been made, but appeared unsuccessful in terms of practical usage. In this work, a new mathematical scheme for solving the OZ equation (Tang and Lu, 1993) is proposed. The scheme can yield a general solution to the OZ equation and is free from the prerequisite of the form of the intermolecular potential u(r) as long as the potential is of a hard core. The most important accomplishment resulting from the new scheme is that for the first time analytical RDF expressions are obtained for two classic potentials, square-well (SW) and LJ potentials, whose RDFs were analytically inaccessible for a long time. As far as the mathematical form of the solution is concerned, the proposed scheme automatically generates explicit RDF expressions in terms of the Laplace transform, and therefore considerably reduces the algebraic work. Moreover, the performance of the first-order solution (Tang and Lu; 1994a, 1994b, 1994c) is extensively investigated and found to be better than or comparable to any other liquid theories developed previously.

Details about the new method have been presented previously(Tang and Lu, 1993) and are summarized below. At first, for the intermolecular potential with a hard core, a perturbation expansion about the hard core is made to decompose the OZ equation as well as the PY or MSA closure into a series of new equations. The decompositions are based on the fact that h(r) and c(r) can be expanded by

$$h(r) = h_0(r) + \varepsilon h_1(r) + \varepsilon^2 h_2(r) + \ldots$$
$$c(r) = c_0(r) + \varepsilon c_1(r) + \varepsilon^2 c_2(r) + \ldots \tag{13}$$

or

$$\tilde{h}(k) = \tilde{h}_0(k) + \varepsilon \tilde{h}_1(k) + \varepsilon^2 \tilde{h}_2(k) + \ldots$$
$$\tilde{c}(k) = \tilde{c}_0(k) + \varepsilon \tilde{c}_1(k) + \varepsilon^2 \tilde{c}_2(k) + \ldots \tag{14}$$

where the subscript 0 represents a quantity of hard spheres, 1, 2,..., i indicate the first-order, second-order, and ith-order perturbation, respectively, brought by an attractive force. ε is here a perturbation parameter, which reduces the fluid to hard spheres if $\varepsilon = 0$ and recovers the fluid concerned if $\varepsilon = 1$. Substituting Equations (13) and (14) into the OZ relation (8) yields

$$\tilde{c}_1(k) = \frac{\tilde{h}_1(k)}{(1+\rho\tilde{h}_0(k))^2} \tag{15}$$

$$\tilde{c}_2(k) = \frac{\tilde{h}_2(k)}{(1+\rho\tilde{h}_0(k))^2} - \frac{\rho\tilde{h}_1(k)\,\tilde{c}_1(k)}{1+\rho\tilde{h}_0(k)} \tag{16}$$

$$\tilde{c}_i(k) = \frac{\tilde{h}_i(k)}{(1+\rho\tilde{h}_0(k))^2} - \frac{\rho\sum_{j=1}^{i-1}\tilde{h}_j(k)\,\tilde{c}_{i-j}(k)}{1+\rho\tilde{h}_0(k)} \tag{17}$$

The PY closure (11) can be split into

$$c_1(r) = (h_0(r)+1)\,(e^{-\beta u(r)}-1), \qquad r \geq R \tag{18}$$

$$c_i(r) = (h_{i-1}(r) - c_{i-1}(r))\,(e^{-\beta u(r)}-1), \qquad r \geq R \text{ and } i \geq 2 \tag{19}$$

$$h_i(r) = 0, \quad r < R \text{ for } i \geq 1 \tag{20}$$

and the split for the MSA closure (12) is:

$$c_1(r) = -\beta u(r), \qquad r > R \tag{21}$$

$$c_i(r) = 0, \qquad r > R \quad and \quad i \geq 2 \tag{22}$$

$$h_i(r) = 0, \qquad r < R \quad and \quad i \geq 1 \tag{23}$$

Equations (15), (16) and (17) are referred to as the first, second and ith-order OZ equation, respectively. Each set of relations such as Equations (15), (18) and (20) can be solved independently in principle. The perturbation method to solve the OZ equation has been implemented numerically (Gubbins et al., 1971; Madden and Fitts, 1971) but never analytically, because these sets of relations look more complex than the original OZ equation. The key point in the following development is the adoption of the Hilbert transform to solve each set of these relations. The Hilbert transform denoted by the operator H is defined as (Hochstadt, 1973)

$$H\hat{\phi} = \frac{1}{\pi}\int_{-\infty}^{\infty} \frac{\hat{\phi}(y)}{k-y}\,dy \tag{24}$$

where ϕ with a hat (^) is the one-dimensional Fourier transform of any function ϕ

$$\hat{\phi}(k) = \int_{-\infty}^{\infty} \phi(x)\, e^{-ikx}\,dx \tag{25}$$

A number of important properties of the Hilbert transform are shown in Appendix A. One distinct feature of the Hilbert transform is that there is a singular point y = k in the path of the integral (24). It is due to this singular point that the Hilbert transform can catch the general solution of the integral equation. In practice, the singular point can be avoided by analyzing the integration contour in a complex plane according to the nature of the given potential.

The following development for the OZ solution is very technical. If only the final results are concerned, one may skip this part and directly refer to Equation (37). There are a number of prerequisites for fully comprehending the following algebraic

work: (a) familiarity with the Fourier transform; (b) fully understanding the Hilbert transform in Appendix A; (c) familiarity with complex analysis; (d) fully grasping the Baxter (1968b) solution of the OZ equation for hard spheres.

Returning to Equation (8) and following the factorization method introduced by Baxter (1968b), we shall have

$$(1+\rho\tilde{h}_0(k))^{-1}=1-\rho\tilde{c}_0(k)=Q_0(k)Q_0(-k) \tag{26}$$

where

$$Q_0(k)=1-2\pi\rho\int_0^R q_0(r)e^{-ikr}dr \tag{27}$$

with

$$\begin{gathered} q_0(r)=\frac{1}{2}a_0r^2+b_0r-\frac{1}{2}a_0R^2-b_0R \\ a_0=\frac{1+2\eta}{(1-\eta)^2},\quad b_0=-\frac{3}{2}\frac{R\eta}{(1-\eta)^2},\quad \eta=\frac{\pi}{6}\rho R^3 \end{gathered} \tag{28}$$

$Q_0(k)$ in Equations (26) and (27) is the factorization function of hard spheres and can be explicitly given by

$$\begin{gathered} Q_0(k)=\frac{S(k)+12\eta L(k)e^{-ikR}}{(1-\eta)^2(ikR)^3} \\ S(k)=(1-\eta)^2(ikR)^3+6\eta(1-\eta)(ikR)^2+18\eta^2ikR-12\eta(1+\eta) \\ L(k)=(1+\frac{\eta}{2})ikR+1+2\eta \end{gathered} \tag{29}$$

Obviously, the functions $Q_0(k)$ and $Q_0(-k)$ are valued only in the r-space [0,R] and [-R,0], respectively. Defining the one-dimensional Fourier transforms

$$\hat{h}(k)=\int_0^\infty rh(r)e^{-ikr}dr,\quad \hat{c}(k)=\int_0^\infty rc(r)e^{-ikr}dr \tag{30}$$

and substituting Equations (26) and (30) into (8) yields

$$Q_0^2(k)\,(\hat{h}_1(k)-\hat{h}_1(-k)) = \frac{\hat{c}_1(k)-\hat{c}_1(-k)}{Q_0^2(-k)} \tag{31}$$

With further definition of

$$U_1(k) = \int_R^{\infty} r c_1(r)\, e^{-ikr} dr, \quad S_1(k) = \int_0^R r c_1(r)\, e^{-ikr} dr \tag{32}$$

we have

$$Q_0^2(k)\,(\hat{h}_1(k)-\hat{h}_1(-k)) = \left(\frac{U_1(k)}{Q_0^2(-k)}\right)_{R^-} + \left(\frac{U_1(k)}{Q_0^2(-k)}\right)_{R^+} + \frac{S_1(k)-U_1(-k)-S_1(-k)}{Q_0^2(-k)} \tag{33}$$

In (33), $U_1(k)/Q_0^2(-k)$ is now split into two functions in the r-space $[R,\infty]$ denoted by R^- and the space $[-\infty,R]$ denoted by R^+, respectively. (The details about the split are left in Appendix A). Rearranging (33) yields

$$Q_0^2(k)\,\hat{h}_1(k) - \left(\frac{U_1(k)}{Q_0^2(-k)}\right)_{R^-} = Q_0^2(k)\,\hat{h}_1(-k) + \left(\frac{U_1(k)}{Q_0^2(-k)}\right)_{R^+} + \frac{S_1(k)-U_1(-k)-S_1(-k)}{Q_0^2(-k)} \tag{34}$$

The left-hand side of Equation (34) is in the r-space [R, ∞], while that of the right-hand side is valued in the space [-∞, R]. Hence, both sides should vanish, giving

$$Q_0^2(k)\,\hat{h}_1(k) = \left(\frac{U_1(k)}{Q_0^2(-k)}\right)_{R^-} \tag{35}$$

The split in (33) can be technically performed by the Hilbert transform which is detailed in Appendix A, giving

$$\left(\frac{U_1(k)}{Q_0^2(-k)}\right)_{R^-} = \frac{U_1(k)}{2Q_0^2(-k)} - \frac{e^{-ikR}}{2\pi i}\int_{-\infty}^{\infty} \frac{U_1(y)\,e^{iyR}}{(y-k)\,Q_0^2(-y)}\,dy$$

$$\left(\frac{U_1(k)}{Q_0^2(-k)}\right)_{R^+} = \frac{U_1(k)}{2Q_0^2(-k)} + \frac{e^{-ikR}}{2\pi i}\int_{-\infty}^{\infty} \frac{U_1(y)\,e^{iyR}}{(y-k)\,Q_0^2(-y)}\,dy \qquad (36)$$

Hence, the general solution of the first-order OZ equation is obtained:

$$\hat{h}_1(k) = \frac{1}{Q_0^2(k)}\left[\frac{U_1(k)}{2Q_0^2(-k)} - \frac{e^{-ikR}}{2\pi i}\int_{-\infty}^{\infty} \frac{U_1(y)\,e^{iyR}}{(y-k)\,Q_0^2(-y)}\,dy\right] \qquad (37)$$

One important feature here is that the split is made without concerning the split function in the r-space, thus leading to the general solution (37). An inverse Fourier transform of Equation (37) will give us the first-order indirect correlation function $h_1(r)$, which is equivalent to the first-order RDF $g_1(r)$ due to the definition of h(r) mentioned earlier.

After a similar mathematical analysis, it is found that the ith-order OZ solution is given by

$$\hat{h}_i(k) = \frac{1}{Q_0^2(k)}\left\{\frac{U_i(k)}{2Q_0^2(-k)} - \frac{ik}{4\pi}\frac{Q_0(k)}{Q_0(-k)}\sum_{j=1}^{i-1}\rho\hat{h}_j(k)\,\hat{c}_{i-j}(k) - \right.$$

$$\left.\frac{e^{-ikR}}{2\pi i}\int_{-\infty}^{\infty}\frac{e^{iyR}}{y-k}\left[\frac{U_i(y)}{Q_0^2(-y)} - \frac{iy}{2\pi}\frac{Q_0(y)}{Q_0(-y)}\sum_{j=1}^{i-1}\rho\hat{h}_j(y)\,\hat{c}_{i-j}(y)\right]dy\right\}, \quad i\geq 2 \qquad (38)$$

where

$$U_i(k) = \int_R^{\infty} r c_i(r)\,e^{-ikr}\,dr \qquad (39)$$

Equations (37) and (38) are the foundation of this thesis and any further development will be their derivatives. Obviously, this general solution has no restriction on the function of the intermolecular potential and shows immediately a superiority to previous solutions restricted to a special potential function.

The general solution (37) can be simplified according to the nature of the potential. In case that the potential is a smooth function over the interval [R,∞], and $U_1(k)$ is a monovalued function in the complex plane, $h_1(k)$ can be reduced to (Tang and Lu, 1993)

$$\hat{h}_1(k) = -\frac{e^{-ikR}}{Q_0^2(k)} \underset{\{U_1(y)\}}{Res}\left(\frac{U_1(y)\, e^{iyR}}{(y-k)\, Q_0^2(-y)}\right) \tag{40}$$

The symbol Res in Equation (40) represents the summation of residuals in all singularities of the function $U_1(y)$. If $c_1(r)$ is a smooth function in the interval [R,λR] ($\lambda > 1$) but vanishes outside of the interval such as that of the SW potential, $h_1(k)$ can be reduced to (Tang and Lu, 1997a)

$$\hat{h}_1(k) = -\frac{e^{-ikR}}{Q_0^2(k)} Res\left(\frac{W_{\lambda R}(y)\, e^{iyR}}{(y-k)\, A^2(-y)}\right) \tag{41}$$

where

$$W_{\lambda R}(y) = \int_{\lambda R}^{\infty} r c_1(r)\, e^{-iyr} dr, \quad A(y) = \frac{S(y)}{(1-\eta)^2 (iyR)^3} \tag{42}$$

in which $c_1(r)$ is the extension of $c_1(r)$ from the range [R, λR] to [λR, ∞]. In Equation (41), Res denotes the summation of residues of all singularities of functions inside the parentheses. To retain the Fourier transform $U_1(y)$ of $rc_1(r)$, which is expressed more straightforwardly than $W_{\lambda R}(y)$, one may use an alternative to (41)

$$\hat{h}_1(k) = \frac{e^{-ikR}}{Q_0^2(k)} Res\left(\frac{U_1(y)\, e^{iyR}}{(y-k)\, A^2(-y)}\right) \tag{43}$$

for a short-ranged potential. Equivalence between (41) and (43) can be proven by an algebraic analysis (Tang and Lu, 1997a).

Equations (40) and (41) or (43) are two very useful formulas and would straightforwardly provide RDFs for most potentials used in statistical thermodynamics. Concrete applications for a number of typical potentials are illustrated in Section 3.

2.2 Mixtures

There is a demand to extend the new solution method to mixtures. The bulk properties of mixtures proliferate in a wide range of phenomena, such as vapor-liquid equilibria, liquid-liquid equilibria, aggregation and phase separation. These phenomena represent a number of important applications in the chemical industry and engineering. Numerous experimental data concerning the properties of mixtures have been reported in the literature. However, a quantitative description at the level of microscopic size or intermolecular potential is very scarce. A few years ago, Abramo et al. (1986) first employed the OZ solution formulated by Blum and Hφye (1978) for mixtures of Yukawa interaction to investigate the nonideal characteristics of mixtures including phase separations. Their work has stimulated much interest (Arrieta et al., 1987; 1991; Hoheisel and Zhang, 1991; Caccamo and Giunta, 1993) in the nature of vapor-liquid and liquid-liquid phase transitions. Among these works, one commonly required assumption is that the molecules have to interact with each other through the Yukawa form, even though the interaction does not exist in real fluids. Nevertheless, we could hardly find a better way since available analytical MSA solutions for mixtures are limited to the Yukawa potential just as in the case of pure fluids. If the OZ solution for physically realistic potentials (e. g. Lennard-Jones potential or other arbitrary potentials) is available, we would gain much more knowledge about mixture behavior. Exploring the behavior of mixtures at the level of molecular interaction is another aim of the present work.

With the obtaining of the OZ solution for pure fluids, the extension to mixtures can be proceeded in a similar manner but in terms of matrices. The OZ equation for a N-component mixture is given by

$$h_{ij}(r) = c_{ij}(r) + \sum_k \rho_k \int dr' c_{ik}(r') h_{kj}(r-r') \qquad (44)$$

where $h_{ij}(r) = g_{ij}(r)-1$, $g_{ij}(r)$ is the RDF between species i and j, and ρ_k is the number density of species k. Taking the three-dimensional Fourier transform of Equation (44) and reforming it in a matrix form yields

$$\tilde{H}(k) = \tilde{C}(k) + \tilde{H}(k)\,\tilde{C}(k) \tag{45}$$

or

$$(I+\tilde{H}(k))\,(I-\tilde{C}(k)) = I \tag{46}$$

where *I* is the unit matrix, and the components of H(k) and C(k) are given by

$$\{\tilde{H}(k)\}_{ij} = \frac{4\pi\sqrt{\rho_i\rho_j}}{k}\int_0^\infty r h_{ij}(r)\,\sin krdr \tag{47}$$

$$\{\tilde{C}(k)\}_{ij} = \frac{4\pi\sqrt{\rho_i\rho_j}}{k}\int_0^\infty r c_{ij}(r)\,\sin krdr \tag{48}$$

Substituting a perturbation expansion of H(k) and C(k)

$$\begin{aligned}\tilde{H}(k) &= \tilde{H}_0(k) + \varepsilon\tilde{H}_1(k) + \cdots\cdots \\ \tilde{C}(k) &= \tilde{C}_0(k) + \varepsilon\tilde{C}_1(k) + \cdots\cdots\end{aligned} \tag{49}$$

into Equation (45) and noting that

$$(I+\tilde{H}_0(k))\,(I-\tilde{C}_0(k)) = I$$

one can obtain

$$\tilde{H}_1(k)\,(I-\tilde{C}_0(k)) = (I+\tilde{H}_0(k))\,\tilde{C}_1(k) \tag{51}$$

$$\tilde{H}_\gamma(k)\,(I-\tilde{C}_0(k)) = (I+\tilde{H}_0(k))\,\tilde{C}_\gamma(k) + \sum_{m=1}^{\gamma-1}\tilde{H}_m(k)\,\tilde{C}_{\gamma-m}(k), \quad \gamma\geq 2 \tag{52}$$

where subscript 0 represents a hard sphere quantity. $H_1(k)$, $H_\gamma(k)$, $C_1(k)$ and $C_\gamma(k)$ in Equations (51) and (52) can be regarded as the first-order and γth-order amendment of those of hard spheres. As in the pure fluid case, Equations (51) and (52) are referred to as the first-order and γth-order OZ equations, respectively.

To supply conditions for solving the OZ equation, an additive hard core for mixtures is presumed for purpose of simplicity, although such an assumption may not

have to be imposed. The additive hard core condition indicates that

$$h_{ij}(r) = -1, \quad r < R_{ij} \tag{53}$$

and $R_{ij} = (R_i + R_j)/2$. Closures for solving the OZ equation of mixtures are treated in an analogous manner to those of pure fluids. Following the procedure presented in Section 2.1, the PY approximation

$$h_{ij}(r)\, f_{ij}(r) = (1 + f_{ij}(r))\, c_{ij}(r) - f_{ij}(r), \quad r > R_{ij} \tag{54}$$

with

$$f_{ij}(r) = e^{-\beta u_{ij}(r)} - 1 \tag{55}$$

can be decomposed into a set of new closure approximations:

$$c_{1,ij}(r) = (h_{0,ij} + 1)\, f_{ij}(r), \quad r > R_{ij} \tag{56}$$

$$c_{\gamma,ij}(r) = (h_{\gamma-1,ij}(r) - c_{\gamma-1,ij}(r))\, f_{ij}(r), \quad r > R_{ij} \text{ and } \gamma \geq 2 \tag{57}$$

The MSA closure

$$c_{ij}(r) = -\beta u_{ij}(r), \quad r > R_{ij} \tag{58}$$

can be decomposed to

$$c_{1,ij}(r) = -\beta u_{ij}(r), \quad r > R_{ij} \tag{59}$$

$$c_{\gamma,ij}(r) = 0, \quad r > R \text{ and } \gamma \geq 2 \tag{60}$$

Together with the exact relations

$$h_{0,ij}(r) = -1, \quad r < R \tag{61}$$

$$h_{\gamma,ij} = 0, \quad r < R \text{ and } \gamma \geq 1 \tag{62}$$

the first and γ-th order OZ equation, a decomposition of Equation (44), can be solved

independently. The details about the solution have been presented (Tang and Lu, 1995) and are left in Appendix B. This achievement required further work on the Hilbert transform for matrix and space analysis. The final solution of the first-order OZ equation is

$$Q_0^T(k)\,\hat{H}_1(k)\,Q_0(k)=\frac{1}{2}\,[Q_0(-k)]^{-1}U_1(k)\,[Q_0^T(-k)]^{-1}$$
$$-\frac{E(k)}{2\pi i}\int_{-\infty}^{\infty}\frac{dy}{y-k}\Big[E(-y)\,[Q_0(-y)]^{-1}U_1(y)\,[Q_0^T(-y)]^{-1}E(-y)\Big]E(k) \tag{63}$$

Defining the summation of the right-hand side terms of Equation (63) as $B_1(k)$ yields

$$\hat{H}_1(k)=[Q_0^T(k)]^{-1}B_1(k)\,[Q_0(k)]^{-1} \tag{64}$$

In Equations (63) and (64), superscript -1 represents the inverse of a matrix and superscript T represents the transpose of a matrix. E(k) is a diagonal matrix with elements $\{E(k)\}_{mm}=\exp(-ikR_m/2)(m=1,2,\ldots N)$. Other quantities are defined by

$$\{\hat{H}(k)\}_{ij}=2\pi\sqrt{\rho_i\rho_j}\int_0^{\infty}rh_{ij}(r)\,e^{-ikr}dr \tag{65}$$

$$\{U_1(k)\}_{ij}=2\pi\sqrt{\rho_i\rho_j}\int_{R_{ij}}^{\infty}rC_{1,ij}(r)\,e^{-ikr}dr \tag{66}$$

$$\{Q_0(k)\}_{ij}=\delta_{ij}-\sqrt{\rho_i\rho_j}e^{-ik\lambda_{ij}}\,[\varphi_1(R_i)\,Q'_{ij}+\varphi_2(R_i)\,Q''_j] \tag{67}$$

with

$$Q'_{ij}=\frac{2\pi}{\Delta}\left(R_{ij}+\frac{\pi}{4\Delta}R_iR_j\xi_2\right),\quad Q''_j=\frac{2\pi}{\Delta}\left(1+\frac{\pi}{2\Delta}R_j\xi_2\right) \tag{68}$$

$$\xi_n=\sum_m\rho_mR_m^n,\qquad \Delta=1-\frac{\pi\xi_3}{6} \tag{69}$$

$$\varphi_1(R_i)=\frac{1-ikR_i-e^{-ikR_i}}{(ik)^2},\qquad \varphi_2(R_i)=\frac{1-ikR_i+\frac{(ikR_i)^2}{2}-e^{-ikR_i}}{(ik)^3} \tag{70}$$

After some nontrivial algebraic work (Tang and Lu, 1995), it was further found that

$$\{[Q_0(k)]^{-1}\}_{ij}=\delta_{ij}+A_{ij}(k)\,e^{-ik\lambda_{ij}} \tag{71}$$

with

$$A_{ij}(k)=2\pi\sqrt{\rho_i\rho_j}\;\frac{W_{ij}(k)}{\Delta\det(k)} \tag{72}$$

$$\begin{aligned}W_{ij}(k)=&\varphi_2(R_i)\left(1+\frac{\pi\xi_3}{2\Delta}\right)+\varphi_1(R_i)\left(R_{ij}+\frac{\pi\xi_2R_iR_j}{4\Delta}\right)+\\&\frac{\pi}{2\Delta}\varphi_1(R_i)\sum_m\rho_m\varphi_1(R_m)\,(R_m-R_i)\,(R_m-R_j)+\frac{\pi}{2\Delta}R_i^2\sum_m\rho_m\varphi_2(R_m)\,(R_j-R_m)\end{aligned} \tag{73}$$

$$\begin{aligned}\det(k)=1&-\frac{2\pi}{\Delta}\sum_m\rho_m\varphi_2(R_m)\left(1+\frac{\pi\xi_3}{2\Delta}\right)-\frac{2\pi}{\Delta}\sum_m\rho_m\varphi_1(R_m)\left(R_m+\frac{\pi\xi_2R_m^2}{4\Delta}\right)\\&-\frac{\pi^2}{2\Delta^2}\sum_m\sum_n\rho_m\rho_n\varphi_1(R_m)\,\varphi_1(R_n)\,(R_m-R_n)^2\end{aligned} \tag{74}$$

Although these expressions look lengthy, they are easily programmed in a computer. One interesting point is that these expressions are applicable to mixtures with any number of species as well as to pure fluids in Section 2.1, and seem to bear an universal nature in statistical thermodynamics. Subsequent development on RDF and thermodynamics is made essentially in terms of these expressions.

Once $B_1(k)$ is known, Equation (64) can be utilized to calculate directly the first-order RDF. Equation (63) shows that $B_1(k)$ is subject to $U_1(k)$ which is the only specific quantity for a given mixture. $U_1(k)$ itself can be determined by either the PY, the MSA or some other closure approximations if the direct correlation functions in these approximations are fixed outside of the hard core. As notable as in the pure fluid case, Equation (64) is of an explicit and analytical form and is applicable to an

arbitrary intermolecular potential. It can be easily handled for further theoretical treatment of thermodynamic properties and practical calculations. In contrast, the full MSA solutions, reported in the literature for a very few specific potentials (Barboy, 1975; Blum and Hφye, 1978;) are mathematically very complex and computationally cumbersome in further determining their physically acceptable roots.

The γ-th order OZ solution is given by

$$\begin{aligned} Q_0^T(k)\,\hat{H}_\gamma(k)\,Q_0(k) = &\frac{1}{2}\,[Q_0(-k)]^{-1}U_\gamma(k)\,[Q_0^T(-k)]^{-1} - \\ &\frac{ik}{4\pi}\sum_{m=1}^{\gamma-1} Q_0^T(k)\,\tilde{H}_m(y)\,\tilde{C}_{\gamma-m}(y)\,[Q_0^T(-k)]^{-1} - \\ &\frac{E(k)}{2\pi i}\int_{-\infty}^{\infty}\frac{dy}{y-k}\Bigg\{E(-y)\Bigg[[Q_0(-y)]^{-1}U_\gamma(y)\,[Q_0^T(-y)]^{-1} - \\ &\frac{iy}{2\pi}\sum_{m=1}^{\gamma-1} Q_0^T(y)\,\tilde{H}_m(y)\,\tilde{C}_{\gamma-m}(y)\,[Q_0^T(-y)]^{-1}\Bigg]E(-y)\Bigg\}E(k) \end{aligned} \tag{75}$$

If the sum of the right-hand side of Equation (75) is referred to as $B_\gamma(k)$, one then has

$$\hat{H}_\gamma(k) = [Q_0^T(k)]^{-1}B_\gamma(k)\,[Q_0(k)]^{-1} \tag{76}$$

Thus, Equations (64) and (76) are the general solution of the OZ equation of mixtures for an arbitrary potential with an additive hard core. The general solution paves the way to implement statistical thermodynamics to practical applications. A few examples of application will be demonstrated later on. It should be mentioned here that the attainment of the explicit expression for $B_\gamma(k)$ ($\gamma > 1$) is not so straightforward as $B_1(k)$. As well as $U_\gamma(k)$, $B_\gamma(k)$ is also related to quantities $H_m(k)$ and $C_{\gamma-m}(k)$ ($0 < m < \gamma$), which have to be determined in advance by solving γ-1 lower-order OZ equations. Further effort in space split, which involves some more mathematical analysis, needs to be carried out. Fortunately, in most situations, the first-order OZ solution appears to be sufficient to determine the mixture structure and thermodynamic properties from our experience. The performance of the first-order solution will be investigated in detail in Section 3.4 and 3.6.

Analogous to pure fluids, $B_1(k)$ in (64) can be further simplified according to the

nature of the potential function. For a smooth and monovalued $U_1(k)$, $B_1(k)$ is reduced to

$$B_1(k) = -E(k) \underset{\{U_1(y)\}}{Res} \left(\frac{E(-y)\ [Q_0(-y)]^{-1} U_1(y)\ [Q_0^T(-y)]^{-1} E(-y)}{y-k} \right) E(k) \qquad (77)$$

The residual operation in Equation (77) should be made with respect to each element of the matrix $U_1(y)$. For a short-ranged potential, a similar expression to Equation (41) or (43) may be derived. However, the resulting expressions will be extremely tedious due to the diameter difference between two species. In view of mathematical complexity and relatively fewer practical applications, further work on short-ranged potentials for mixtures is not addressed in this thesis.

3. Radial Distribution Functions

3.1. Laplace transforms of RDF for pure fluids

In this section, the general OZ solution will be utilized to yield RDFs for some typical potentials in thermodynamics with focus on the first-order OZ solution under the MSA assumption, since the solution is of simple analytical form and dominates the structure and properties of fluids. Before proceeding to concrete examples, it is necessary to make some mathematic elucidation. In subsequent discussion, the diameter of hard spheres is set to be unity except that of the LJ potential which may vary with temperature. As well, the Laplace transform will be utilized to replace the one-dimensional Fourier transform in Section 2. The major purpose of the replacement is for mathematical brevity, which will simplify later algebraic work. Transition from the Fourier transform to the Laplace transform can be made easily by setting ik = s in the Fourier transform. For instance, the Laplace transform of rg(r) is defined as

$$G(s) = \int_0^\infty r g(r)\, e^{-sr} dr \tag{78}$$

and the factor correlation function $Q_0(s)$ in (29), (79) is now defined by

$$\begin{aligned} Q_0(s) &= \frac{S(s) + 12\eta L(s)\, e^{-s}}{(1-\eta)^2 s^3} \\ S(s) &= (1-\eta)^2 s^3 + 6\eta(1-\eta) s^2 + 18\eta^2 s - 12\eta(1+\eta) \\ L(s) &= (1+\frac{\eta}{2}) s + 1 + 2\eta \end{aligned} \tag{79}$$

The Laplace transforms of other quantities can be figured out intuitively. In terms of the Laplace transform, Equations (40), (41) and (43) can be rewritten respectively as

$$G_1(s) = -\frac{e^{-s}}{Q_0^2(s)} \underset{\{U_1(t)\}}{Res}\left(\frac{U_1(t)\, e^t}{(t-s) Q_0^2(-t)} \right) \tag{80}$$

$$G_1(s) = -\frac{e^{-s}}{Q_0^2(s)} Res\left(\frac{W_\lambda(t)\, e^t}{(t-s)\, A^2(-t)} \right) \tag{81}$$

$$G_1(s) = \frac{e^{-s}}{Q_0^2(s)} Res\left(\frac{U_1(t)\, e^t}{(t-s)\, A^2(-t)} \right) \tag{82}$$

Obviously, all the residual evaluations in (80)-(82) should be carried out over the t-complex plane. Applications of (80)-(82) need to be elucidated for typical types of potentials encountered in statistical thermodynamics.

i) For a short-ranged potential with $\lambda < 2$, the residuals in (82) can be obtained more explicitly by taking advantage of $U_1(t)$ being an analytical function over the t-complex plane and all singularities of the bracketed functions in (82) being $t=s$ and the zeros t_i of S(t). Consequently, after some algebra it is found that (Tang and Lu, 1997a)

$$G_1(s) = \frac{(1-\eta)^4 e^{-s}}{Q_0^2(s)} \left\{ \frac{U_1(s)\, s^6}{S^2(-s)} e^s - \right.$$

$$\left. \sum_{i=0}^{2} \left[\frac{U_1'(-t_i)\, S_1 + U_1(-t_i)\, (S_1 - 6S_1/t_i + S_2)}{S_1^3(s+t_i)} + \frac{U_1(-t_i)}{S_1^2(s+t_i)^2} \right] t_i^6 e^{-t_i} \right\} \tag{83}$$

It should be mentioned that Equation (83) is applicable to any short-ranged potentials without placing any restrictions on its mathematical form. An extension of the above result for $\lambda > 2$ can be carried out in a similar manner, but the final expression will become rather tedious because of the involved residual evaluation. For a long-ranged potential, (83) may still be quite reliable after introducing a cutoff at a certain distance, typically at $r=2$. Our experience (Tang and Lu, 1997a) shows that the cutoff effect is not appreciable unless the given potential is strongly long-ranged. For a strongly long-ranged potential such as the Coulomb potential, (83) and even the first-order OZ solution itself is inappropriate for fluid structure because of the slow convergence of the expansion (13).

ii). For the potential $K r^n e^{-zr}$, in which K and z are two constants and the integer n

≥ -1, the sole singularity at t=z for $U_1(t)$ in (80) is a pole of order n. A residue evaluation of Equation (80) yields

$$G_1(s) = -\frac{Ke^{-s}}{Q_0^2(s)} \frac{d^{n+1}}{dt^{n+1}} \left(\frac{1}{(t-s)\,Q_0^2(-t)} \right) \Bigg|_{t=-z} \tag{84}$$

$G_1(s)$ can be given more explicitly if n is known. When n=-1, (84) will recover the first-order RDF of the Yukawa potential (Tang and Lu, 1993).

iii). For the potential Ke^{-r}/r^n ($n \geq 2$), (80) will be inadequate for $G_1(s)$ due to a branch point for $U_1(t)$ at t=0. A distinct way to obtain the RDF for the potential, which needs extra work on a contour integration on the t-complex plane, has been presented earlier (Tang and Lu, 1994a). The contour integration yields

$$G_1(s) = \frac{Ke^{-s}}{Q_0^2(s)} \int_0^{\infty} \frac{t^{n-2}e^{-t}}{(n-2)!\,(t+s)\,Q_0^2(t)}\,dt \tag{85}$$

leading to RDFs of the LJ and Kihara fluids.

The discussions above cover most potentials encountered in statistical thermodynamics. One can now obtain easily the first-order RDF for these potentials through (83)-(85). For six typical potentials in statistical thermodynamics, both u(r) and its corresponding $G_1(s)$ are presented below. For convenience of usage, the presentation begins with the case of hard spheres which has been solved before (Wertheim, 1963; Thiele, 1963; Baxter, 1968b).

a). Hard spheres

$$u(r) = \begin{cases} \infty, & r<1 \\ 0, & r>1 \end{cases} \tag{86}$$

Following the PY approximation (Wertheim, 1963; Thiele, 1963; Baxter, 1968b)

$$G_0(s) = \frac{L(s)\,e^{-s}}{(1-\eta)^2 Q_0(s)\,s^2} \tag{87}$$

Based on the generalized mean spherical approximation (GMSA)(Waisman, 1973), a

more accurate RDF has been developed (Tang and Lu, 1995):

$$G_0(s) = \frac{L(s)\,e^{-s}}{(1-\eta)^2 Q_0(s)\,s^2} + \frac{\eta^2}{2(1-\eta)^3}\frac{e^{-s}}{Q_0^2(s)\,(s+z_0)} \tag{88}$$

with

$$z_0 = \frac{2(1+2\eta)}{(4-\eta)(1-\eta)^2}\left(3+\sqrt{21-15\eta+3\eta^2}\right) \tag{89}$$

The development of the new RDF (88) will be illustrated in Section 3.2.

b). Sticky hard spheres

$$u(r) = \begin{cases} \infty, & r<1 \\ -\epsilon\delta(r-1), & r\geq 1 \end{cases} \tag{90}$$

$$G_1(s) = \beta\epsilon\frac{(1+\eta/2)}{(1-\eta)^2}\frac{e^{-s}}{Q_0^2(s)} \tag{91}$$

c). Yukawa potential

$$u(r) = \begin{cases} \infty, & r<1 \\ -\epsilon\dfrac{e^{-z(r-1)}}{r}, & r>1 \end{cases} \tag{92}$$

$$G_1(s) = \frac{\beta\epsilon e^{-s}}{(s+z)\,Q_0^2(s)\,Q_0^2(z)} \tag{93}$$

d). Square-well potential

$$u(r) = \begin{cases} \infty & r<1 \\ -\epsilon & 1<r<\lambda \\ 0 & \lambda<r \end{cases} \tag{94}$$

$$G_1(s) = \beta\epsilon \frac{(1-\eta)^4 e^{-s}}{Q_0^2(s)} \sum_{i=0}^{2} \left[\left(\frac{a_1(i)}{s+t_i} + \frac{a_2(i)}{(s+t_i)^2} \right) e^{(\lambda-1)t_i} - \left(\frac{a_3(i)}{s+t_i} + \frac{a_2(i)}{(s+t_i)^2} \right) e^{-(\lambda-1)s} \right] \tag{95}$$

with

$$a_1(i) = \frac{(\lambda^2-\lambda)\, t_i^5 + (1+4\lambda)\, t_i^4 - 4t_i^3}{S_1^2} + \frac{(t_i^4 - \lambda t_i^5) S_2}{S_1^3}, \quad a_2(i) = \frac{t_i^4 - \lambda t_i^5}{S_1^2}, \tag{96}$$

$$a_3(i) = \frac{5\lambda t_i^4 - 4t_i^3}{S_1^2} + \frac{(t_i^4 - \lambda t_i^5) S_2}{S_1^3}$$

where

$$S_1 = S'(t), \quad S_2 = S''(t) \tag{97}$$

and $t_i (i=0,1,2)$, the roots of equation $S(t)=0$, is given by

$$t_j = [-2\eta + (2\eta f)^{1/3} (y_+ c^j + y_- c^{-j})] / (1-\eta) \tag{98}$$

with

$$f = 3+3\eta-\eta^2, \quad y_\pm = [1 \pm (1+2\eta^4/f^2)^{1/2}]^{1/3}, \quad c = e^{2\pi i/3} \tag{99}$$

e). Lennard-Jones potential

$$u(r) = \begin{cases} \infty, & r<R \\ 4\epsilon \left(\frac{\sigma^{12}}{r^{12}} - \frac{\sigma^6}{r^6} \right), & r>R \end{cases} \tag{100}$$

$$G_1(s) = \frac{4\beta\epsilon e^{-s}}{Q_0^2(s)} \int_0^\infty \frac{\frac{(\sigma/R)^6}{4!} t^4 - \frac{(\sigma/R)^{12}}{10!} t^{10}}{(t+s) Q_0^2(t)} e^{-t} dt \tag{101}$$

where $G_1(s)$ is the Laplace transform of $xg_1(x)$ with the scaled distance $x = r/R$.

Obviously, (100) is a modified LJ potential. To closely account for the structure and properties of the LJ fluid, R is usually set to be a temperature-dependent quantity and may be chosen as (Barker and Henderson, 1967b)

$$R=\int_0^{\sigma}(1-e^{-\beta u(r)})\,dr, \qquad u(r)=4\epsilon(\sigma^{12}/r^{12}-\sigma^{6}/r^{6}) \tag{102}$$

f). Kihara potential

$$u(r)=\begin{cases}\infty, & r<R\\ 4\epsilon\left(\dfrac{(\sigma-a_c)^{12}}{(r-a_c)^{12}}-\dfrac{(\sigma-a_c)^{6}}{(r-a_c)^{6}}\right), & r>R\end{cases} \tag{103}$$

$$G_1(s)=\frac{4\beta\epsilon e^{-s}}{Q_0^2(s)}\int_0^{\infty}\frac{\dfrac{((\sigma-a_c)/R)^6}{4!}t^4-\dfrac{((\sigma-a_c)/R)^{12}}{10!}t^{10}}{(t+s)\,Q_0^2(t)}e^{-t(R-a_c)/R}dt \tag{104}$$

where the quantities x and R are similarly defined or determined as those of the LJ potential.

A few comments should be made here for the above results. Except for the PY solution (87), all the other $G_i(s)$ ($i=0,1$) are developed from (83)-(85). The RDFs for two artificial potentials, sticky hard spheres and Yukawa fluid, were found (Tang and Lu, 1993) identical to those derived from the full solution developed earlier by others (Baxter, 1968a; Hφye and Blum, 1977). In order to see how simple and how good the performance of the newly developed RDF is, comparisons with the formalism of one full solution of the Yukawa fluid reported by Hφye and Blum (1977) and its numerical value for g(1), are presented below and in Table 1. The full MSA solution is

$$G(s)=\frac{s\tau(s)\,e^{-s}}{(1-12\eta q(s))} \tag{105}$$

$$\tau(s) = a\left(\frac{1}{s^3} + \frac{1}{s^2}\right) + \frac{b}{s^2} - \frac{cze^{-z}}{s(s+z)} \tag{106}$$

$$\sigma(s) = \frac{a}{s^3} + \frac{b}{s^2} - \frac{\left(\frac{a}{2} + b + ce^{-z}\right)}{s} + \frac{c+d}{s+z} \tag{107}$$

$$q(s) = \sigma(s) - \tau(s)\, e^{-s} \tag{108}$$

where a,b,c,d are implied by the following relations

$$b = 12\eta\left(-\frac{a}{8} - \frac{b}{6} + c\left(\frac{1}{z^2} - \left(\frac{1+z}{z^2} + \frac{1}{2}\right)e^{-z}\right) + \frac{d}{z^2}\right) \tag{109}$$

$$1 - a = 12\eta\left(-\frac{a}{3} - \frac{b}{2} + c\left(\frac{1}{z} - \frac{1+z}{z}e^{-z}\right) + \frac{d}{z}\right) \tag{110}$$

$$z(c+d) = 12\eta d G(z) \tag{111}$$

$$Ke^{z} = zd(1 - 12\eta q(z)) \tag{112}$$

Obviously, the full solution (105) is much more complex than Equation (93). The numerical RDF determination from the full solution needs to solve a set of simultaneous nonlinear Equations (109)-(112) and singling out the physical acceptable root. Table 1 demonstrates that the first-order solution and the full solution yield very close RDF values at contact. Hence, Equation (93) is much desirable for practical purposes.

Three other potentials, SW, LJ and Kihara potentials, have been investigated for a long time. Because of their intractable mathematical form, it was thought almost impossible to present their RDFs in an analytical manner. The achievement of Equations (95), (101) and (104) demonstrates the power of the novel scheme presented in this work. Table 1 has shown that the first-order RDF is efficient to

replace the full MSA RDF of the Yukawa potential. It is believed that the same conclusion may be drawn for other potentials. Details about them are left in Section 3.4.

Table 1. Values of g(1) for the Yukawa fluid (z=1.8)

ρ	$1/\beta\epsilon$	the full solution	this work
0.4	2.0	1.963	1.944
	1.5	2.040	2.003
	1.0	2.222	2.121
0.6	2.0	2.561	2.555
	1.5	2.598	2.586
	1.0	2.681	2.649
0.8	2.0	3.629	3.628
	1.5	3.646	3.643
	1.0	3.681	3.674

3.2. A new RDF for hard spheres

One interesting application of (93) is that it can provide an improved RDF for hard spheres. The RDF is very basic in the development of liquid theories, especially for perturbation theories (e. g. Barker and Henderson, 1967; Weeks et al., 1971) to study more complex fluids. Notwithstanding that much work has been done for this fluid, its study has not yet been completed. The widely utilized RDF is still the PY solution of the OZ equation developed many years ago (Wertheim, 1963; Thiele, 1963). It is well known that the PY solution is not completely satisfactory as both its pressure and RDF show non-negligible errors at high densities. The pressure discrepancies could be well corrected by the Carnahan-Starling (CS) (1969) equation through a semiempirical combination of the virial pressure and the compressibility pressure developed from the PY solution. The RDF discrepancies, however, are not corrected satisfactorily. In the literature, there are two widely cited methods for this correction. One is the Verlet and Weis (VW)(1972) algorithm, which reproduces a better RDF of hard spheres by a fully semiempirical construction. The empirical nature of the VW algorithm makes it inappropriate for further theoretical work. The other correction method is the so-called generalized mean spherical approximation (GMSA) (Waisman,

1973). The GMSA is more logical in eliminating the PY RDF discrepancies because it assumes that the DCF c(r) of hard spheres is of the Yukawa form outside the hard core, instead of zero in the PY approximation (11), namely

$$c(r) = K\frac{e^{-z(r-1)}}{r}, \qquad r>1 \tag{113}$$

where K and z are two parameters to be located by the CS equation and thermodynamic consistency. It is found in the literature that the performance of the GMSA is comparable to that of the VW algorithm. However, if based on the full MSA solution, the determination of the GMSA RDF is rather cumbersome and K and z have to be evaluated through solving (105)-(112). The complexity would be intolerable with the increasing number of components in hard-sphere mixtures. The simplicity of the first-order RDF (93) suggests that incorporating (93) in the GMSA instead of the full solution (105) may yield a simple improved RDF of hard spheres. Such a RDF for both pure hard spheres and mixtures has been presented (Tang and Lu, 1995). The resulting RDF has been shown in (88) for pure hard spheres and will be given in Section 3.6 for mixtures. The performance of (82) is indicated in Figure 2.

3.3. Explicit RDF expressions for pure fluids

In order to obtain RDF values to extract information about the structure of a fluid, the problem of the Laplace inversions of $G_i(s)(i=0,1)$ in (86)-(104) needs to be resolved. In principle, the inversion could be performed by a numerical method. An examination of several typical numerical methods summarized by Davies and Martin (1979) shows that all of them are highly unreliable except that representing the inversion by a Fourier series. However, the Fourier series method brings intolerable computation work in practical manipulations as well as the instability problem occurring at large r distances. Therefore, an analytical inversion is more desirable. Among analytical efforts reported in the literature, Wertheim (1963) first gave the explicit RDF for $1<r<2$ in his original PY solution; Throop and Bearman (1965) performed the inversion for $1<r<4$, which was later extended to the region $1<r<6$ (Manel et al., 1970; Smith et al., 1970). Perram (1975) has proposed a scheme to

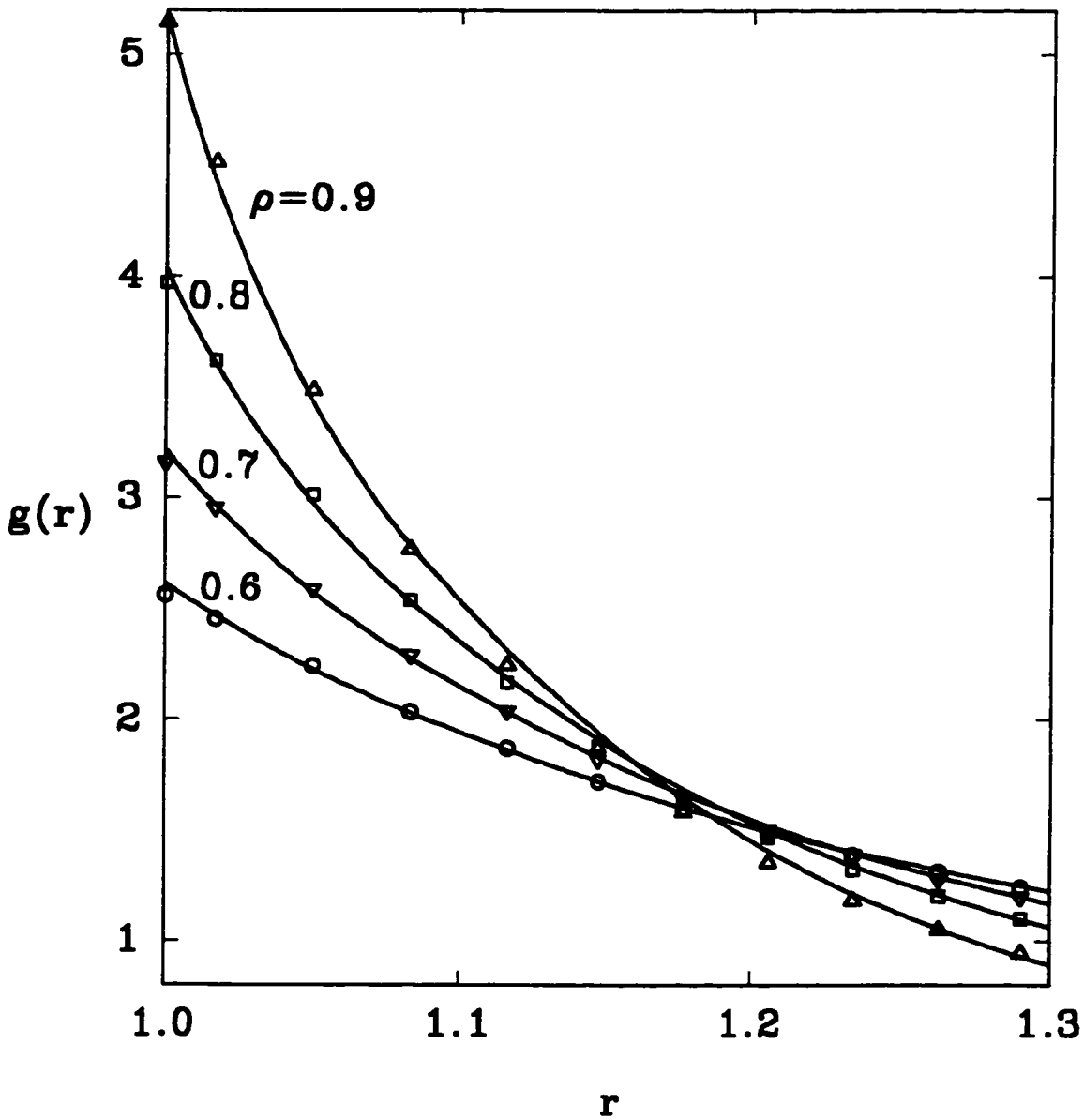

Figure 2. RDF for hard spheres. The symbols (circle, triangle, square) are the MC data (Barker and Henderson, 1971). The solid lines are results from the GMSA in this work.

convert the inversion into a linear, stepwise, differential equation to obtain RDF values. Recently, Chang and Sandler (1994) reported a real-function representation of RDF for 3 shells with $1<r<4$. All these efforts are confined to a limited number of shells and to the system of hard spheres. Extension of the above work to a larger number of shells is practically prohibitive. Very recently, a new method was proposed to obtain the inversion for any specified shell (Tang and Lu, 1997). The final expressions of the inversion are completely explicit and universal for all the classical fluids mentioned above. The starting point in our inversion is the creation of the following functions

$$A(n_1, n_2, k_1, \alpha) =$$

$$\sum_{i=\max(k_1-n_1,0)}^{n_2} \frac{n_2!\,(i+n_1)!}{i!\,(n_2-i)!\,(i+n_1-k_1)!}(1+\eta/2)^i(1+2\eta)^{n_2-i}t_\alpha^{n_1+i-k_1} \tag{114}$$

$$B(n_1, n_2, n_3, i, \alpha) =$$

$$\frac{1}{(1-\eta)^{2n_3}}\sum_{k_1=0}^{n_3-i}\sum_{k_2=0}^{n_3-i-k_1}\frac{(-1)^{n_3-i-k_1}(n_3-1+k_2)!\,(2n_3-1-i-k_1-k_2)!}{k_1!\,k_2!\,(n_3-1-k_1-k_2)!\,((n_3-1)!)^2}\times \tag{115}$$

$$\frac{A(n_1, n_2, k_1, t_\alpha)}{(t_\alpha-t_\beta)^{n_3+k_2}(t_\alpha-t_\gamma)^{2n_3-i-k_1-k_2}}$$

$$C(n_1, n_2, n_3, r) =$$

$$\begin{cases} \displaystyle\sum_{\alpha=0}^{2}\sum_{i=1}^{n_3}\frac{B(n_1, n_2, n_3, i, \alpha)}{(i-1)!}r^{i-1}e^{t_\alpha r}H(r), & n_1+n_2<3n_3 \\ \displaystyle\frac{(1+\eta/2)^{n_2}}{(1-\eta)^{2n_3}}\delta(r)+\sum_{\alpha=0}^{2}\sum_{i=1}^{n_3}\frac{B(n_1, n_2, n_3, i, \alpha)}{(i-1)!}r^{i-1}e^{t_\alpha r}H(r), & n_1+n_2=3n_3 \end{cases} \tag{116}$$

$$D(n_1,n_2,n_3,z,r)=$$

$$\begin{cases} \displaystyle\sum_{\alpha=0}^{2}\sum_{i=1}^{n_3}\frac{(-1)^i B(n_1,n_2,n_3,i,\alpha)}{(t_\alpha+z)^i}\times \\ \qquad\left(e^{-zr}-e^{t_\alpha r}\sum_{j=0}^{i-1}\frac{(-1)^j(t_\alpha+z)^j r^j}{j!}\right)H(r), \quad n_1+n_2<3n_3 \\ \dfrac{(1+\eta/2)^{n_2}}{(1-\eta)^{2n_3}}e^{-zr}H(r)+\displaystyle\sum_{\alpha=0}^{2}\sum_{i=1}^{n_3}\frac{(-1)^i B(n_1,n_2,n_3,i,\alpha)}{(t_\alpha+z)^i}\times \\ \qquad\left(e^{-zr}-e^{t_\alpha r}\sum_{j=0}^{i-1}\frac{(-1)^j(t_\alpha+z)^j r^j}{j!}\right)H(r), \quad n_1+n_2=3n_3 \end{cases} \tag{117}$$

$$E(n_1,n_2,n_3,z,r)=$$

$$\begin{cases} \displaystyle\sum_{\alpha=0}^{2}\sum_{i=1}^{n_3}\frac{(-1)^i B(n_1,n_2,n_3,i,\alpha)}{(t_\alpha+z)^i}\times \\ \left(re^{-zr}+\dfrac{i(e^{-zr}-e^{t_\alpha r})}{t_\alpha+z}-e^{t_\alpha r}\displaystyle\sum_{j=0}^{i-1}(i-j)\frac{(-1)^j(t_\alpha+z)^{j-1}r^j}{j!}\right)H(r), \quad n_1+n_2<3n_3 \\ \dfrac{(1+\eta/2)^{n_2}}{(1-\eta)^{2n_3}}re^{-zr}H(r)+\displaystyle\sum_{\alpha=0}^{2}\sum_{i=1}^{n_3}\frac{(-1)^i B(n_1,n_2,n_3,i,\alpha)}{(t_\alpha+z)^i}\times \\ \left(re^{-zr}+\dfrac{i(e^{-zr}-e^{t_\alpha r})}{t_\alpha+z}-e^{t_\alpha r}\displaystyle\sum_{j=0}^{i-1}(i-j)\frac{(-1)^j(t_\alpha+z)^{j-1}r^j}{j!}\right)H(r), \quad n_1+n_2=3n_3 \end{cases} \tag{118}$$

where $\delta(r)$ is the Dirac delta function and H(r) is the Heaviside function, which is 0 for $r<0$ and 1 for $r\geq 0$. $t_\alpha(\alpha=0,1,2)$ are three zeros of S(t), given explicitly in (98)-(99). An algebraic analysis (Tang and Lu, 1997) of the inversions of (86)-(104) indicates all of them can be expressed in terms of (114)-(118), giving the following results:

a). Hard spheres

For the PY approximation

$$rg_0(r)=\sum_{n=0}^{\infty}(-12\eta)^n C(1,n+1,n+1,r-n-1) \tag{119}$$

and for the GMSA

$$rg_0(r) = \sum_{n=0}^{\infty} (-12\eta)^n C(1, n+1, n+1, r-n-1)$$
$$+ \frac{\eta^2(1-\eta)}{2} \sum_{n=0}^{\infty} (1+n)\,(-12\eta)^n D(6, n, n+2, z_0, r-n-1) \tag{120}$$

b). Sticky hard sphere

$$xg_1(x) = \beta\epsilon(1+\eta/2)\,(1-\eta)^2 \sum_{n=0}^{\infty} (1+n)\,(-12\eta)^n C(6, n, n+2, r-n-1) \tag{121}$$

c). Yukawa potential

$$rg_1(r) = \beta\epsilon \frac{(1-\eta)^4}{Q_0^2(z)} \sum_{n=0}^{\infty} (1+n)\,(-12\eta)^n D(6, n, n+2, z, r-n-1) \tag{122}$$

d). Square-well potential

$$rg_1(r) = \beta\epsilon(1-\eta)^8 \sum_{n=0}^{\infty} \sum_{i=0}^{2} (1+n)\,(-12\eta)^n \{[a_1(i) D(6, n, n+2, t_i, r-n-1) +$$
$$a_2(i) E(6, n, n+2, t_i, r-n-1)]\, e^{(\lambda-1)t_i} - [a_3(i) D(6, n, n+2, t_i, r-n-\lambda)$$
$$+ a_2(i) E(6, n, n+2, t_i, r-n-\lambda)]\} \tag{123}$$

e). Lennard-Jones potential

$$xg_1(x) = 4\beta\epsilon(1-\eta)^4 \int_0^{\infty} dt \frac{\frac{(\sigma/R)^6}{4!} t^4 - \frac{(\sigma/R)^{12}}{10!} t^{10}}{Q_0^2(t)} e^{-t}$$
$$\times \sum_{n=0}^{\infty} (1+n)\,(-12\eta)^n D(6, n, n+2, t, x-n-1) \tag{124}$$

f). Kihara potential

$$xg_1(x) = 4\beta\epsilon(1-\eta)^4 \int_0^\infty dt \frac{\frac{((\sigma-a_c)/R)^6}{4!}t^4 - \frac{((\sigma-a_c)/R)^{12}}{10!}t^{10}}{Q_0^2(t)} e^{-t(R-a_c)/R} \quad (125)$$

$$\times \sum_{n=0}^{\infty} (1+n)(-12\eta)^n D(6, n, n+2, t, x-n-1)$$

Thus, explicit RDF expressions are achieved for these typical potentials. It is notable that the expressions (119)-(125) are presented in a systematic way, thus there are easy for programming. Another distinguishing feature of the method is its suitability for any number of shells, which can hardly be expected from any other methods proposed in the literature. In addition to these classical fluids, the above inversion scheme is also found applicable to hard sphere chains, which is shown in Section 3.9. It should be mentioned that computational time in the above calculations increases with increasing number of shells, and at larger distances ($r > 15$), high digital precision is required to obtain correct results. Practically, these situations might be avoided by assuming $g_1(r) = 0$ after a sufficiently large r value.

3.4. Performance of RDF of pure fluids

With Equations (119)-(125) in hand, we can easily evaluate the performance of the first-order RDF by comparing it with computer simulation data available in the literature. To serve as examples, RDFs for the SW and LJ fluids are utilized for comparison. The RDF of the Kihara fluid is not exhibited here as its nature is nearly the same as the LJ fluid. A comparison is shown for the SW fluid in Figure 3. The agreement with the MC data (Henderson et al., 1976) is surprisingly good and is even better than the hypernetted chain (HNC), PY and superposition approximation numerically solved previously (Smith et al., 1977). It appears that the performance of the first-order RDF is nearly equivalent to the full MSA solution determined by Smith et al. (1977).

A comparison between the results from Equation (124) and the MC data of Verlet (1968) for the LJ fluid is shown in Figure 4 at three states. Overall performance of (124) is rather satisfactory. Only at higher densities and r at near σ, some

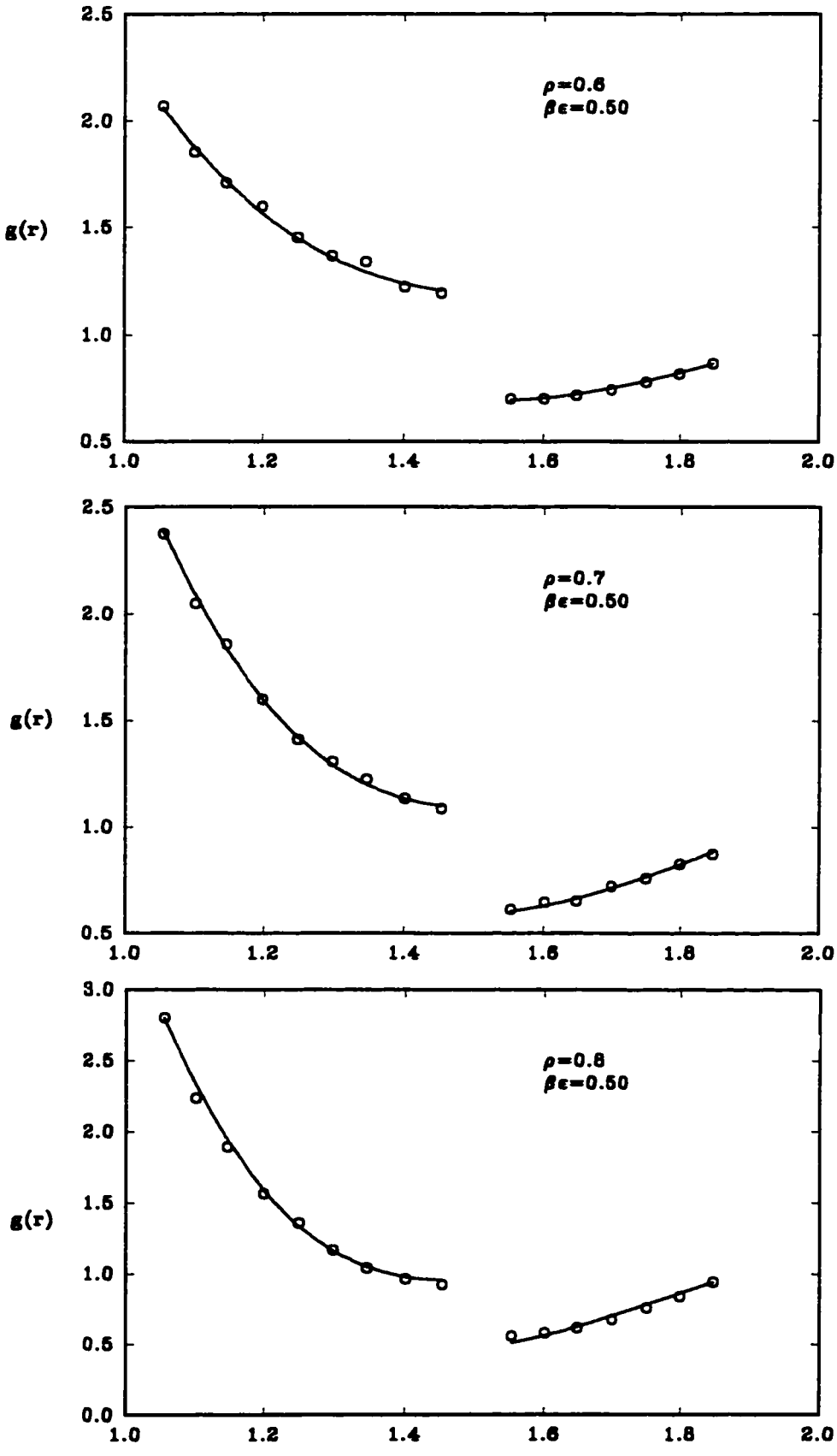

Figure 3. RDF of the SW fluid. The circles are the MC data (Henderson et al., 1976). The solid lines are results from the present theory.

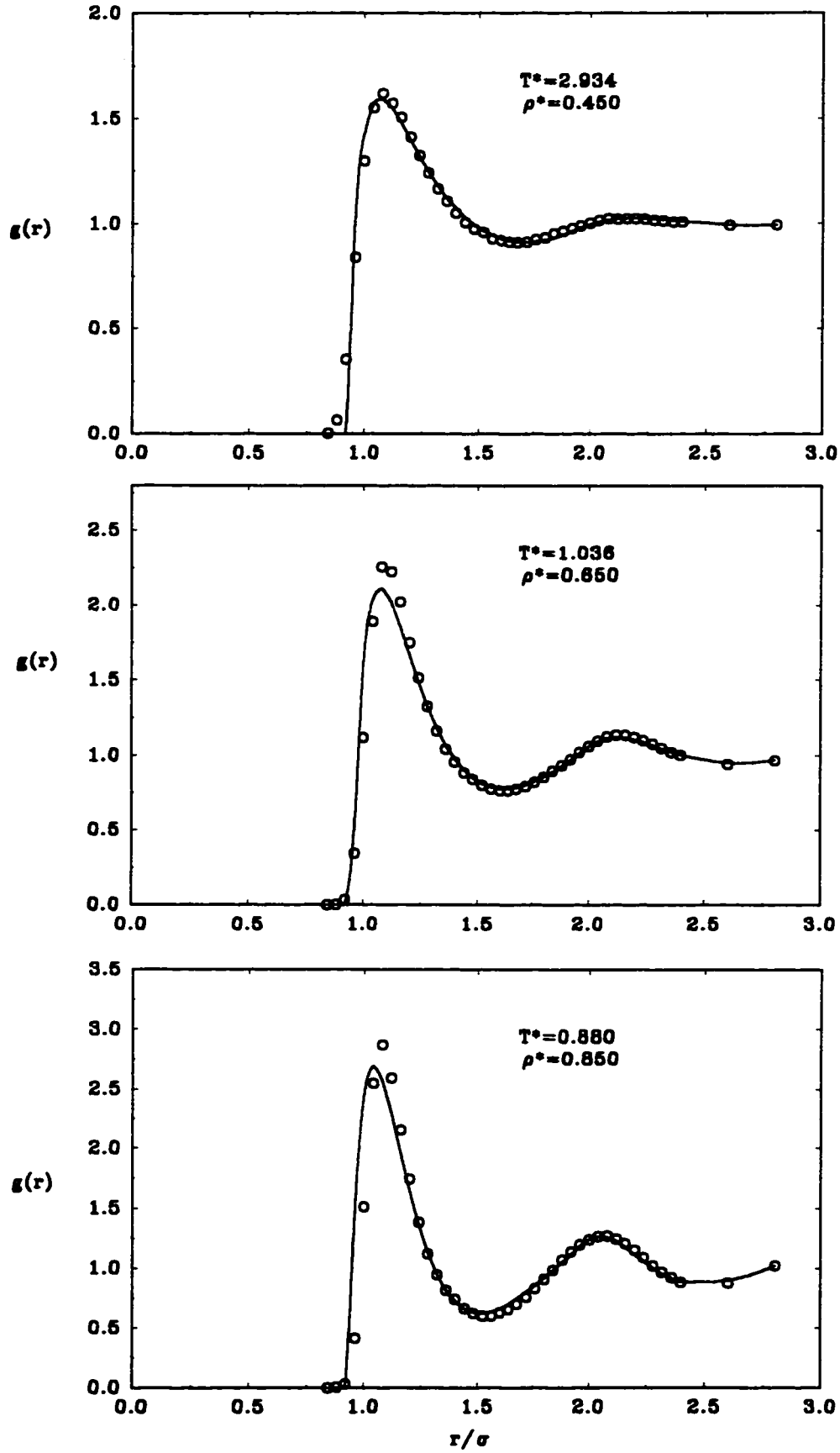

Figure 4. RDF of the LJ fluid. The circles are the MD data (Verlet, 1968). The solid lines are results from the present theory.

discrepancies occur. The discrepancies are not caused by the first-order approximation adopted here but by the MSA assumption (12). The details about the physical inadequacy of the MSA assumption is out of the scope of the discussion here. In Section 3.8, we will present a new approximation, the simplified exponential (SEXP) approximation, to improve the MSA performance. The SEXP approximation which modifies only slightly the MSA, remedies the deficiencies observed above with great success. Even with some defects, Equation (124) is still much better than the PY solution reported by Gubbins et al.(1971). It should be borne in mind that the LJ fluid is a very important fluid in statistical thermodynamics, and Equation (124) is currently the only analytical expression available for this fluid. Such a structure expression provides a new framework to establish more rigorous liquid theories. Neither the BH theory nor the WCA theory is grounded so firmly on the structure of the LJ fluid. A recent investigation (Tang and Lu, 1997c) indicates that the LJ structure is given very badly in the BH theory, and is good at high densities for the WCA theory but deteriorates severely at low densities.

In summary, the performance of the first-order RDF for two typical potentials has been investigated and found rather satisfactory. The investigating range covers densities and temperatures of both gas and liquid states. Hence, a new liquid theory based on the first-order RDF can be developed confidently. The development will be presented in Section 4.

3.5. A two-Yukawa function to map the LJ potential

Any utilization of Equations (101) and (124) will inevitably encounter an integration. The integration has to be carried out by a numerical method and consumes considerable computing time. It is more troublesome that the LJ RDF (101) results in a double integral in developing the LJ thermodynamics (Tang and Lu, 1994b; 1994c). For purposes of both saving time and practical application, there is a need to resolve the integration issue. It is noticed that the RDF of the Yukawa potential is of a simple form. If the LJ potential can be accurately mapped by means of a suitable Yukawa function, the corresponding mapping RDF will get rid of the troublesome integration. The accuracy of the mapping RDF depends solely on the mapping

accuracy of the Yukawa function, not on temperature or density. In other words, the resulting RDF will perform as satisfactorily as (101) or (124). In this work, a two-Yukawa (TY) function

$$u^{TY}(r)=\begin{cases}\infty, & r<R\\ -k_0\epsilon\dfrac{e^{-z_1(r-\sigma)}}{r}+k_0\epsilon\dfrac{e^{-z_2(r-\sigma)}}{r}, & r>R\end{cases} \tag{126}$$

is adopted to map the LJ potential by properly selecting parameters k_0, z_1 and z_2. Such a mapping has been suggested in the literature several times (Jedrzejek and Mansoori, 1980; Foiles and Ashcroft, 1981; Rudisill and Cummings, 1989). But all of them show non-negligible deviations at $r>\sigma$ when using their k_0, z_1 and z_2 values. Here k_0, z_1, z_2 are located by the following constraints:

1)

$$[ru^{TY}(r)]\,|_{r=\sigma}=[ru^{LJ}(r)]\,|_{r=\sigma} \tag{127}$$

which is already implied in the function of $u^{TY}(r)$.

2)

$$[ru^{TY}(r)]'|_{r=\sigma}=[ru^{LJ}(r)]'|_{r=\sigma} \tag{128}$$

3) minimizing

$$I=\int_{\sigma}^{\infty}[ru^{TY}(r)-ru^{LJ}(r)]^2dr \tag{129}$$

which alternatively indicates

$$\frac{\partial I}{\partial z_1}=0, \qquad \frac{\partial I}{\partial z_2}=0 \tag{130}$$

Equations (127)-(128) ensure that the TY function maps the LJ potential accurately around $r=\sigma$ while minimizing (130) is one way to make the mapping closest for $r>\sigma$. Solving (127)-(130) yields $k_0=2.1714\sigma$, $z_1=2.9637/\sigma$, $z_2=14.0167/\sigma$. The diameter of the hard core R was selected here by (102) or more simply by an empirical

function (De Souza and Ben-Amotz, 1993)

$$R=2^{1/6}\left[1+\left(1+\frac{T^*+C_2T^{*2}+C_3T^{*4}}{C_1}\right)^{1/2}\right]^{-1/6}\sigma \tag{131}$$

with $c_1=1.1287$, $c_2=-0.05536$ and $c_3=0.0007278$. $T^*(=kT/\epsilon)$ is the reduced temperature. With these new values, the TY function and the LJ potential are depicted in Figure 5, where differences between the two potentials are practically invisible. The excellent reproduction may be inherited in the calculation of the RDF and the thermodynamic properties of the LJ fluid. Using the first-order MSA solution (84), the first-order RDF $g_1(r)$ for the TY function is given by

$$\int_R^\infty rg_1(r)\,e^{-sr}dr=\frac{\beta\epsilon k_1 e^{-sR}}{(s+z_1)\,Q_0^2(sR)\,Q_0^2(z_1R)}-\frac{\beta\epsilon k_2 e^{-sR}}{(s+z_2)\,Q_0^2(sR)\,Q_0^2(z_2R)} \tag{132}$$

where

$$k_1=k_0e^{z_1(\sigma-R)},\quad k_2=k_0e^{z_2(\sigma-R)} \tag{133}$$

Using the mathematical scheme demonstrated in Section 3.3, the inverse Laplace transform of (132) is found to be

$$\begin{aligned} rg_1(r)=&\beta\epsilon k_1\frac{(1-\eta)^4}{Q_0^2(z_1R)}\sum_{n=0}^{\infty}(1+n)\,(-12\eta)^nD(6,n,n+2,z_1R,r-n-1)\\ &-\beta\epsilon k_2\frac{(1-\eta)^4}{Q_0^2(z_2R)}\sum_{n=0}^{\infty}(1+n)\,(-12\eta)^nD(6,n,n+2,z_2R,r-n-1)\end{aligned} \tag{134}$$

A comparison between the TY RDF and the LJ RDF in Table 2 at $T^*=2.934$ and $\rho^*=\rho\sigma^3=0.45$ indicates that the overall average difference between the two RDFs is within 0.1% and therefore they are graphically indistinguishable. Since our mapping is independent of temperature and density, we can conclude that Equation (134) describes satisfactorily the structure of the LJ fluid and the description is practically identical to (101). The calculation of RDF through (132) or (134) is much less time-consuming than (101) because no integral is involved. In subsequent discussion, the

TY function will be utilized to replace the LJ potential for both pure fluids and mixtures without notification unless the LJ potential is needed in some specific cases.

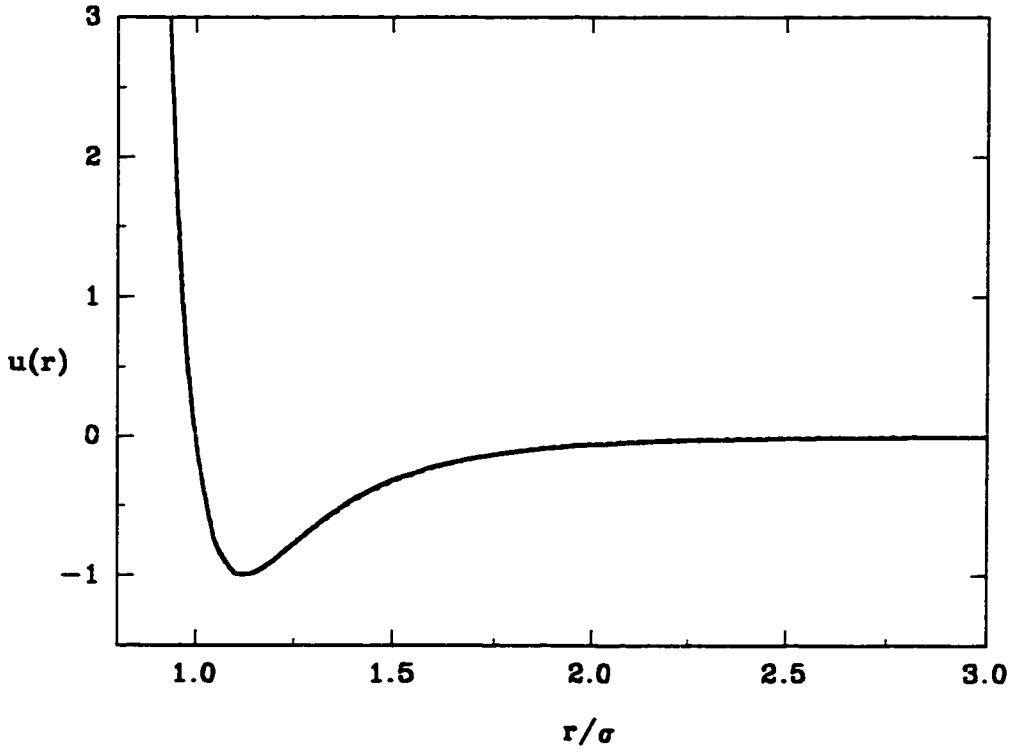

Figure 5. The profile of the LJ potential (solid line) and TY function (dashed line) suggested in this work

Table 2. A comparison between the first-order MSA RDF of the LJ potential and that of the TY potential

r	LJ	TY
1.0000	1.429	1.428
1.0800	1.595	1.593
1.1600	1.481	1.479
1.2400	1.322	1.320
1.3200	1.180	1.181
1.4000	1.072	1.073
1.4800	0.994	0.996
1.5600	0.945	0.946
1.6400	0.919	0.920
1.7200	0.913	0.913
1.8000	0.923	0.923
1.8800	0.948	0.948
1.9600	0.983	0.982
AAD%		0.082

3.6. Laplace transforms of RDF for mixtures

The RDF of mixtures can be developed in an analogous manner to pure fluids. The foundation of such a development is Equation (64) or its derivative (77). Here, the Laplace transforms of RDF, defined by

$$\{G_0(s)\}_{ij}=2\pi\sqrt{\rho_i\rho_j}\int_0^\infty r g_{0,ij}(r)\,e^{-sr}dr$$
$$\{G_1(s)\}_{ij}=2\pi\sqrt{\rho_i\rho_j}\int_0^\infty r g_{1,ij}(r)\,e^{-sr}dr \qquad (135)$$

are presented for the one-Yukawa, multiple-Yukawa, Lennard-Jones and TY potentials. As in the pure fluid case, the following presentation begins with hard-sphere mixtures.

a). Hard spheres

$$u_{ij}(r)=\begin{cases}\infty, & r<R_{ij}\\ 0, & r>R_{ij}\end{cases} \qquad (136)$$

The PY RDF for this mixture is obtained by Blum and Hφye (1977), giving

$$\{G_0^{PY}(s)\}_{ij}=$$
$$\frac{2\pi\sqrt{\rho_i\rho_j}e^{-sR_{ij}}}{\Delta\det(s)}\left[\frac{1}{s^2}\left(1+\frac{\pi\xi_3}{2\Delta}\right)+\frac{1}{s}\left(R_{ij}+\frac{\pi\xi_2R_iR_j}{4\Delta}\right)\right. \tag{137}$$
$$\left.+\frac{\pi}{2\Delta s}\sum_m\rho_m\varphi_1(R_m)\,(R_m-R_i)\,(R_m-R_j)\right]$$

The GMSA RDF, which has been described in detail in Section 3.2 and developed earlier (Tang and Lu, 1995), is

$$\{G_0^{GMSA}(s)\}_{ij}=\{G_0^{PY}(s)\}_{ij}$$
$$+\left(J_{ij}+\sum_n J_{in}A_{nj}(s)+\sum_m J_{mj}A_{mi}(s)+\sum_m\sum_n J_{mn}A_{mi}(s)\,A_{nj}(s)\right)\frac{e^{-sR_{ij}}}{s+z} \tag{138}$$

where

$$J_{ij}=\frac{\pi^3\xi_2^2\sqrt{\rho_i\rho_j}}{288\Delta^3}\left(-R_i^3+5R_i^2R_j+5R_iR_j^2-R_j^3\right) \tag{139}$$

and z in (138) is determined by

$$\frac{1}{z}\left(8\xi_2^2+\frac{\pi}{\Delta}\,(5\xi_2^2\xi_3-\xi_1\xi_2\xi_4)\right)+\frac{1}{z^2}\left(10\xi_1\xi_2-2\xi_0\xi_3+\right.$$
$$\left.\frac{8\pi}{\Delta}\xi_2^3+\frac{\pi^2}{2\Delta^2}\,(5\xi_2^3\xi_3-\xi_1\xi_2^2\xi_4)\right)=\frac{2}{3}\,(3\Delta+\Delta^2)\,\xi_2\xi_3 \tag{140}$$

b). One-Yukawa potential

$$U_{ij}(r)=\begin{cases}\infty, & r<R_{ij}\\ -R_{ij}\epsilon_{ij}\dfrac{e^{-z_{ij}(r-R_{ij})}}{r}, & r>R_{ij}\end{cases} \tag{141}$$

$$\{G_1(s)\}_{ij}=\Big(b_{ij}(s)+\sum_n b_{in}(s)A_{nj}(s)+\sum_m b_{mj}(s)A_{mi}(s)+\sum_m\sum_n A_{mi}(s)A_{nj}(s)b_{mn}(s)\Big)e^{-sR_{ij}} \tag{142}$$

with

$$b_{ij}(s)=\frac{K_{ij}}{s+z_{ij}}+\sum_n\frac{K_{in}A_{jn}(z_{in})}{s+z_{in}}+\sum_m\frac{K_{mj}A_{im}(z_{mj})}{s+z_{mj}}+\sum_m\sum_n\frac{K_{mn}A_{im}(z_{mn})A_{jn}(z_{mn})}{s+z_{mn}} \tag{143}$$

and

$$K_{ij}=2\pi\sqrt{\rho_i\rho_j}R_{ij}\beta\epsilon_{ij} \tag{144}$$

c). Multiple-Yukawa potential

$$U_{ij}(r)=\begin{cases}\infty, & r<R_{ij}\\ -R_{ij}\sum_\gamma\epsilon_{\gamma,ij}\dfrac{e^{-z_{\gamma,ij}(r-R_{ij})}}{r}, & r>R_{ij}\end{cases} \tag{145}$$

$$\{G_1(s)\}_{ij}=\Big(\sum_\gamma b_{\gamma,ij}(s)+\sum_n\sum_\gamma b_{\gamma,in}(s)A_{nj}(s)+\sum_m\sum_\gamma b_{\gamma,mj}(s)A_{mi}(s)+\sum_m\sum_n\sum_\gamma b_{\gamma,mn}(s)A_{mi}(s)A_{nj}(s)\Big)e^{-sR_{ij}} \tag{146}$$

where

$$b_{\gamma,ij}(s)=\frac{K_{\gamma,ij}}{s+z_{\gamma,ij}}+\sum_n\frac{K_{\gamma,in}A_{jn}(z_{\gamma,in})}{s+z_{\gamma,in}}+\sum_m\frac{K_{\gamma,mj}A_{im}(z_{\gamma,mj})}{s+z_{\gamma,mj}}+\sum_m\sum_n\frac{K_{\gamma,mn}A_{im}(z_{\gamma,mn})A_{jn}(z_{\gamma,mn})}{s+z_{\gamma,mn}} \tag{147}$$

and

$$K_{\gamma,ij}=2\pi\sqrt{\rho_i\rho_j}R_{ij}\beta\epsilon_{\gamma,ij} \tag{148}$$

d) Lennard-Jones potential

$$u(r)=\begin{cases}\infty, & r<R_{ij}\\ 4\varepsilon_{ij}\left(\dfrac{\sigma_{ij}^{12}}{r^{12}}-\dfrac{\sigma_{ij}^{6}}{r^{6}}\right), & r>R_{ij}\end{cases} \tag{149}$$

$$\{G_1(s)\}_{ij}=\Big(b_{ij}(s)+\sum_n b_{in}(s)A_{nj}(s)+\sum_m b_{mj}(s)A_{mi}(s)+\sum_m\sum_n A_{mi}(s)A_{nj}(s)b_{mn}(s)\Big)e^{-sR_{ij}} \tag{150}$$

where

$$b_{ij}(s)=\int_0^{\infty}\Big(K_{ij}(t)\,e^{-t\sigma_{ij}}+\sum_n K_{in}(t)A_{jn}(z_{in})\,e^{-t\sigma_{\epsilon}}+\sum_m K_{mj}(t)A_{im}(z_{mj})\,e^{-t\sigma_{mj}}+\sum_m\sum_n K_{mn}(t)A_{im}(z_{mn})A_{jn}(z_{mn})\,e^{-t\sigma_{mn}}\Big)\frac{dt}{t+s} \tag{151}$$

and

$$K_{ij}(t)=8\pi\sqrt{\rho_i\rho_j}\beta\epsilon_{ij}\left(\frac{\sigma_{ij}^{6}t^{4}}{4!}-\frac{\sigma^{12}t^{10}}{10!}\right) \tag{152}$$

e) TY potential

$$u_{ij}^{TY}(r)=\begin{cases}\infty, & r<R_{ij}\\ -k_{0,ij}\epsilon_{ij}\dfrac{e^{-z_{1,ij}(r-\sigma_{ij})}}{r}+k_{0,ij}\epsilon_{ij}\dfrac{e^{-z_{2,ij}(r-\sigma_{ij})}}{r}, & r>R_{ij}\end{cases} \tag{153}$$

where $k_{0,ij}=2.1714\sigma_{ij}$, $z_{1,ij}=2.9637/\sigma_{ij}$, $z_{2,ij}=14.0167/\sigma_{ij}$, as obtained in Section 3.5. Equation (153) can be rewritten as

$$u_{ij}^{TY}(r)=\begin{cases}\infty, & r<R_{ij}\\ -k_{1,ij}\epsilon_{ij}\dfrac{e^{-z_{1,ij}(r-R_{ij})}}{r}+k_{2,ij}\epsilon_{ij}\dfrac{e^{-z_{2,ij}(r-R_{ij})}}{r}, & r>R_{ij}\end{cases} \tag{154}$$

with

$$k_{1,ij}=k_{0,ij}e^{z_{1,ij}(\sigma_{ij}-R_{ij})}\ ,\quad k_{2,ij}=k_{0,ij}e^{z_{2,ij}(\sigma_{ij}-R_{ij})} \tag{155}$$

A comparison between (154) and (145) shows that

$$\begin{aligned}\{G_1(s)\}_{ij}=&\Big(b_{1,ij}(s)-b_{2,ij}(s)+\\ &\sum_n [b_{1,in}(s)-b_{2,in}(s)]A_{nj}(s)+\sum_m [b_{1,mj}(s)-b_{2,mj}(s)]A_{mi}(s)+\\ &\sum_m\sum_n [b_{1,mn}(s)-b_{2,mn}(s)]A_{mi}(s)A_{nj}(s)\Big)e^{-sR_{ij}}\end{aligned} \tag{156}$$

where

$$\begin{aligned}b_{\gamma,ij}(ik)=&\frac{K_{\gamma,ij}}{ik+z_{\gamma,ij}}+\sum_n \frac{K_{\gamma,in}A_{jn}(z_{\gamma,in})}{ik+z_{\gamma,in}}+\sum_m \frac{K_{\gamma,mj}A_{im}(z_{\gamma,mj})}{ik+z_{\gamma,mj}}\\ &+\sum_m\sum_n \frac{K_{\gamma,mn}A_{im}(z_{\gamma,mn})A_{jn}(z_{\gamma,mn})}{ik+z_{\gamma,mn}}\end{aligned} \tag{157}$$

and

$$K_{1,ij}=2\pi\sqrt{\rho_i\rho_j}\beta\epsilon_{ij}k_{1,ij}\ ,\quad K_{2,ij}=2\pi\sqrt{\rho_i\rho_j}\beta\epsilon_{ij}k_{2,ij} \tag{158}$$

In further utilization of (156), there are two problems needed to be addressed in advance. One is about unlike parameters σ_{ij} and ϵ_{ij} ($i\neq j$), which are usually represented by like parameters as follows:

$$\epsilon_{ij}=\gamma_{ij}\sqrt{\epsilon_{ii}\epsilon_{jj}}\ ,\quad \sigma_{ij}=l_{ij}\frac{\sigma_{ii}+\sigma_{jj}}{2} \tag{159}$$

If $\gamma_{ij}=l_{ij}=1$, the unlike parameters obey the so-called Lorentz-Berthelot (LB) combining rule. The LB mixtures are commonly studied in both theory and computer simulation, and therefore this case is treated as the default case if γ_{ij} and l_{ij} are not specified. The other is about the determination of R_{ij}, which is somewhat complex for LJ mixtures. For pure LJ fluids, this diameter is obtained by the BH method (1967b) as shown in (102). The BH diameter can be alternatively derived by a scheme suggested by Hansen and McDonald (1986), which seems to be more general than the original BH

derivation. The scheme is extended here to develop R_{ij} for mixtures. R_{ij} is determined in such a manner that a pseudo-fluid interacting through the repulsive part of the LJ potential should have a Helmholtz free energy close to that of the hard-sphere mixture with diameter R_{ij}. Making a perturbation expansion of the Helmholtz free energy of the pseudo-fluid about the hard-sphere mixture to first order, yields (Hansen and McDonald, 1986)

$$a_{rep}=a_0+\sum_i\sum_j\int_0^{\sigma_{ij}}\left(-\frac{1}{2}\rho x_i x_j y_{0,ij}(r)\right)\left(e^{-\beta u_{rep,ij}(r)}-e^{-\beta u_{0,ij}(r)}\right)dr \quad (160)$$

where *rep* represents the pseudo-fluid and 0 is the hard-spheres mixture. $y_{0,ij}(r)$ is the cavity function of the hard-sphere mixture. The integrand in (160) peaks at $r=\sigma_{ij}$ and therefore in the integration, $y_{0,ij}(r)$ can be approximated by its value at contact, or $g_{0,ij}(R_{ij})$. Thus, Equation (160) reduces to

$$a_{rep}=a_0-2\pi\rho\sum_i\sum_j x_i x_j g_{0,ij}(R_{ij})R_{ij}^2(R_{ij}-d_{ij}) \quad (161)$$

where

$$d_{ij}=\int_0^{\sigma_{ij}}(1-e^{-\beta u_{ij}(r)})\,dr \quad (162)$$

which can be explicitly calculated in a similar manner to (131)

$$d_{ij}=2^{1/6}\left[1+\left(1+\frac{T^*+c_2T^{*2}+c_3T^{*4}}{c_1}\right)^{1/2}\right]^{-1/6}\sigma_{ij} \quad (163)$$

with $c_1=1.1287$, $c_2=-0.05536$ and $c_3=0.0007278$ and $T^*=kT/\epsilon_{ij}$. Now R_{ij} can be determined by Equation (161). One choice made in the literature is $R_{ii}=d_{ii}(i=1,\ldots,N)$ and $R_{ij}=(R_{ii}+R_{jj})/2$. This selection looks simple and natural but unphysical limit results will be brought in, that is, the chemical potential μ_i at infinite dilution ($x_i\to 0$) is dependent on σ_{ii} and ϵ_{ii} (Lotfi and Fischer, 1989). The dependence can be traced back to that $R_{ij}(i\neq j)$ is dependent on σ_{ii} and ϵ_{ii} even $x_i=0.0$. To avoid the dependence, R_{ij}

is chosen by forcing

$$\sum_j x_j (R_{ij}-d_{ij}) = 0 \qquad (164)$$

which gives

$$R_{ii} = 2\sum_j x_j d_{ij} - \sum_i \sum_j x_i x_j d_{ij} \qquad (165)$$

and $R_{ij} = (R_{ii} + R_{jj})/2$. One can easily see that the new R_{ij} is independent of σ_{ii} and ϵ_{ii} at infinite dilution. For the pure LJ fluid, (165) reduces to (102), which has been used in the calculations of previous sections for the LJ fluid. Thus, (165) can be viewed as an extension of the BH diameter for LJ mixtures and is adopted throughout this work.

3.7. Performance of RDF for LJ mixtures

In this section, we make comparisons between the RDF given by Equation (156) and that of computer simulation data. For reason of the availability of simulation data in the literature, only LJ mixtures are concerned here, but the conclusions may be extended to Yukawa mixtures since Equation (156) is developed from a TY function. Unlike pure LJ fluids in Section 3.2, developing an explicit RDF expression from (156) is practically prohibitive if not impossible theoretically. Here, we make the inverse Laplace transform of (156) by a numerical method suggested by Davies and Martin (1979). Obviously, such a inversion is very time-consuming but there is no other choice. Fortunately, by adopting the TY function to map the LJ potential, Equation (156) has reduced the inversion work tremendously.

Figures 6-11 demonstrate the performance of Equation (156) based on the MSA and that of SEXP approximation in Section 3.8 for three two-component mixtures of $x_1 = 0.25$, 0.50 and 0.75 at two temperatures $T^*(kT/\epsilon_{11}) = 1.0$ and 2.0, respectively. In these figures, the reduced density $\rho^* = \rho\sigma_{11}^3$. The comparisons are very encouraging and show a number of similarities to the case of the pure LJ fluid. It is evident that the MSA underestimates RDF values at $r \sim \sigma_{ij}$. The underestimation can be found for all the three RDFs $g_{11}(r)$, $g_{12}(r)$ and $g_{22}(r)$. The MSA RDF is generally good

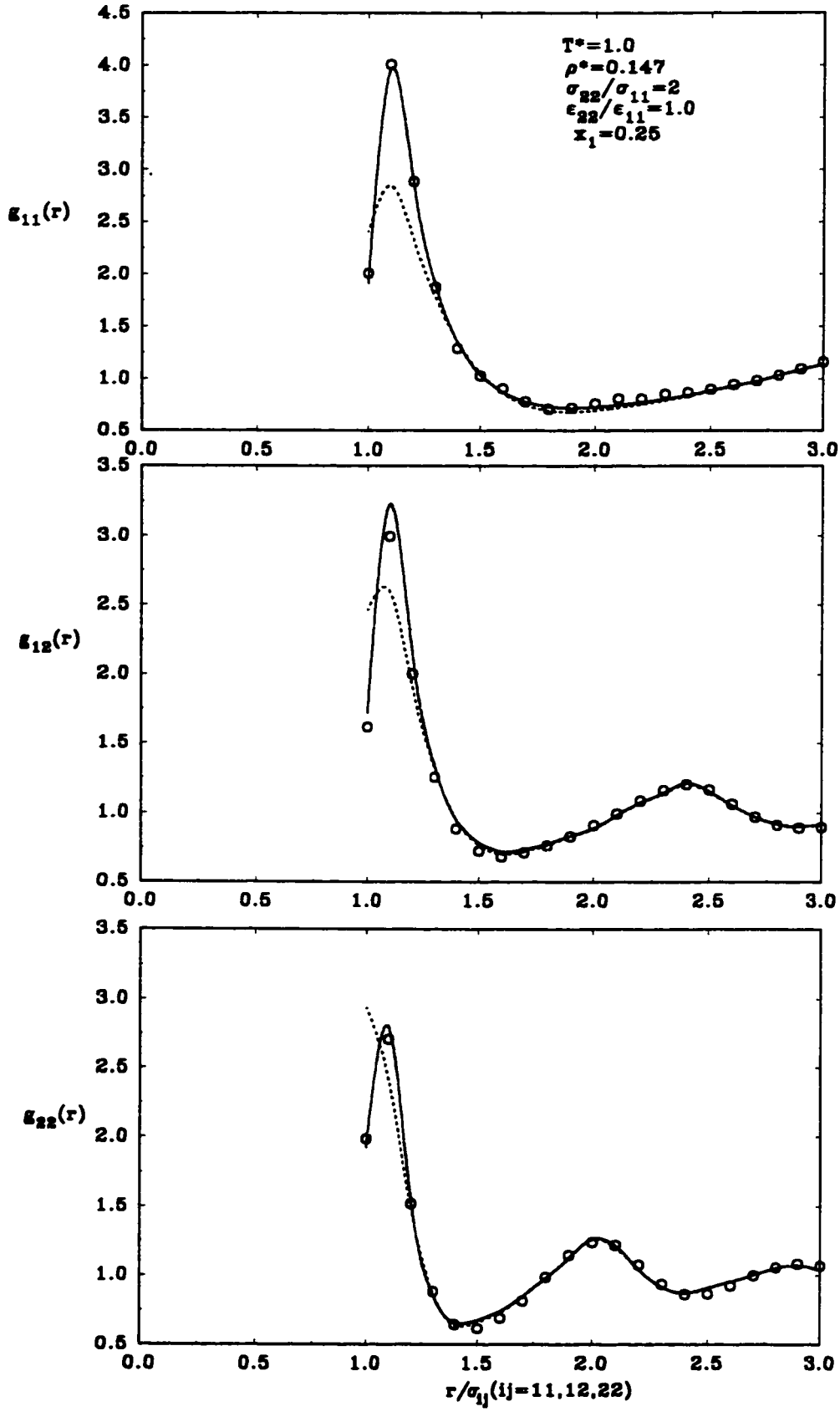

Figure 6. RDF of a LJ mixture. The circles are the MD data (Huber and Ely, 1989). The dashed and solid lines are results from the first-order MSA and SEXP approximation, respectively.

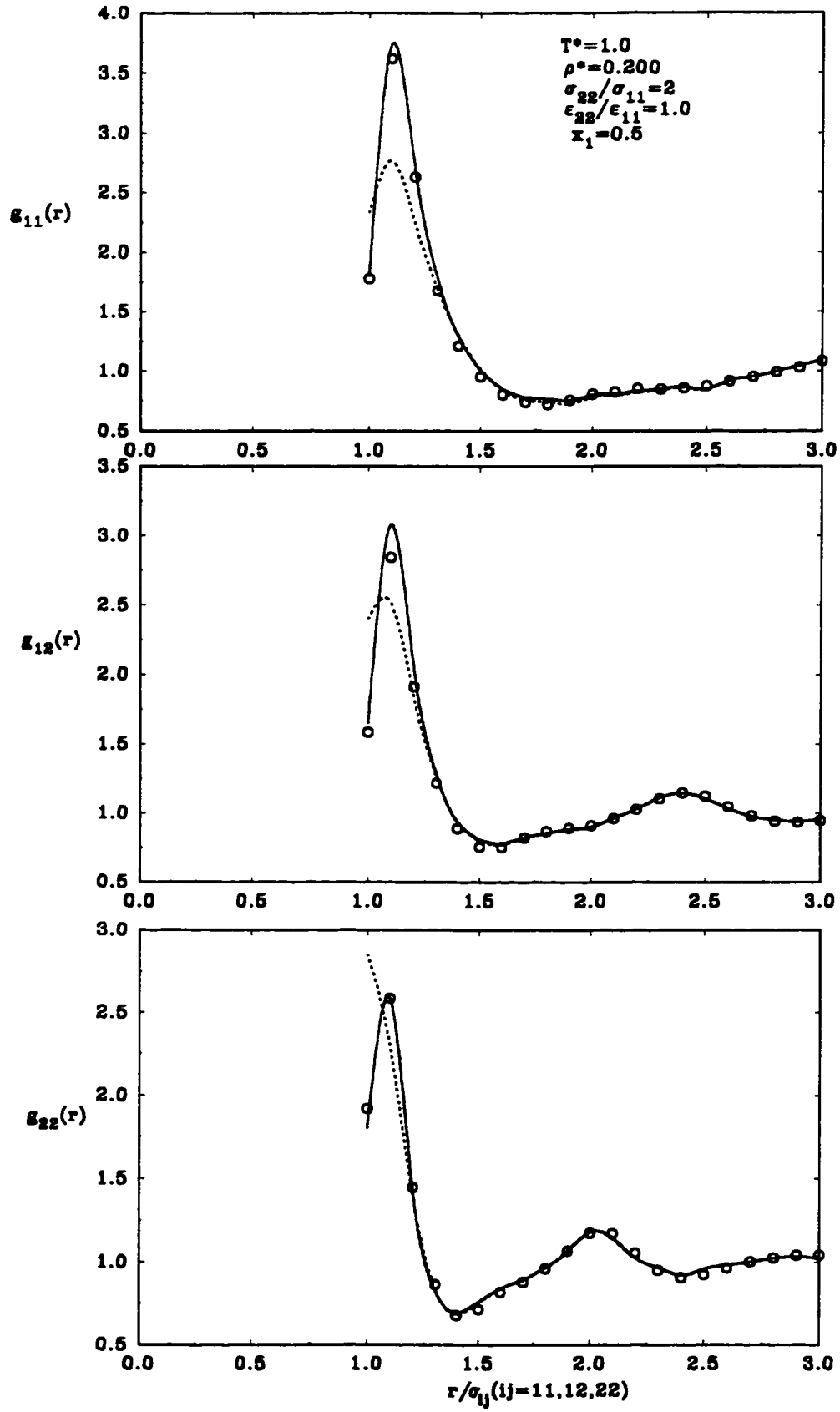

Figure 7. RDF of a LJ mixture. The circles are the MD data (Huber and Ely, 1989). The dashed and solid lines are results from the first-order MSA and SEXP approximation, respectively.

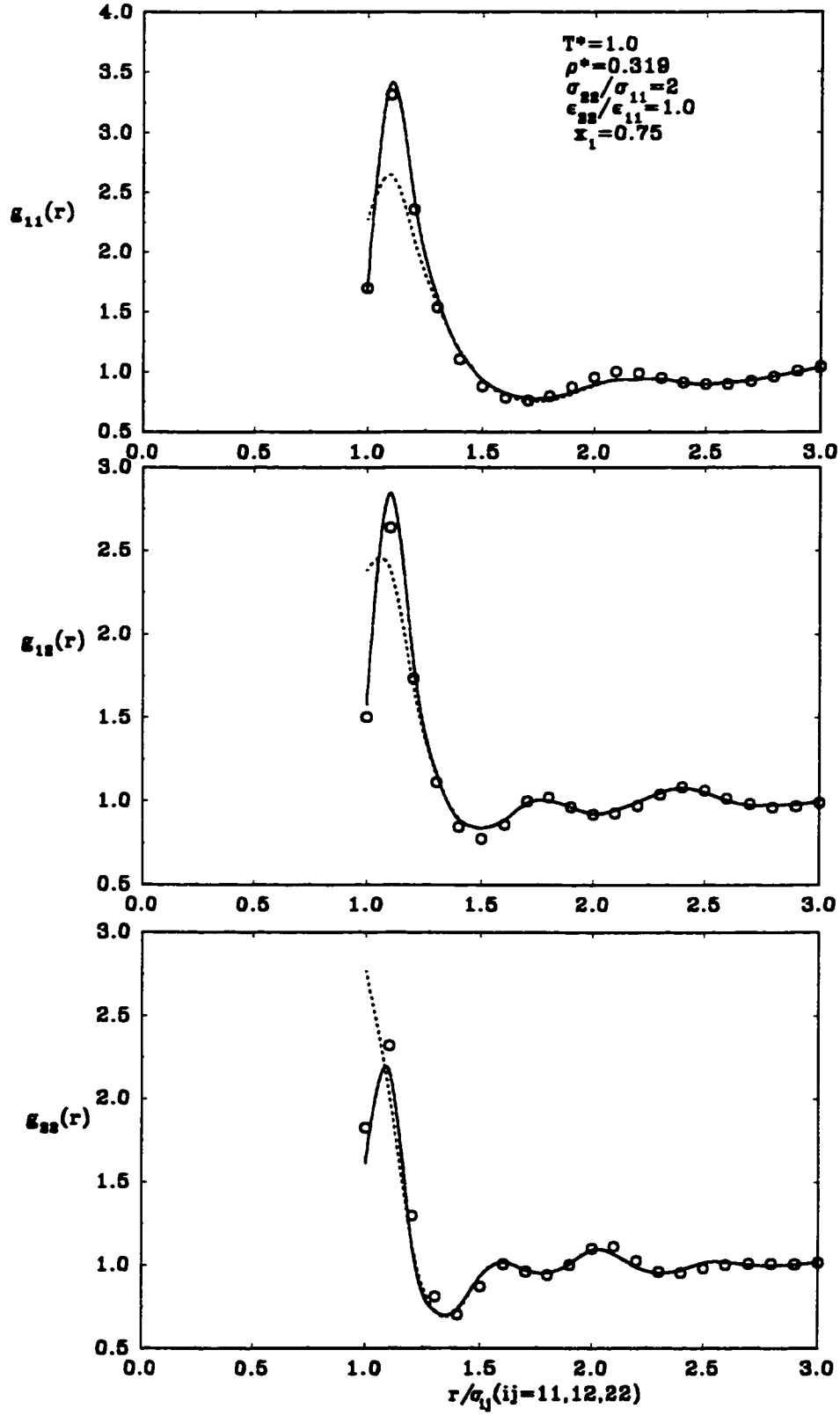

Figure 8. RDF of a LJ mixture. The circles are the MD data (Huber and Ely, 1989). The dashed and solid lines are results from the first-order MSA and SEXP approximation, respectively.

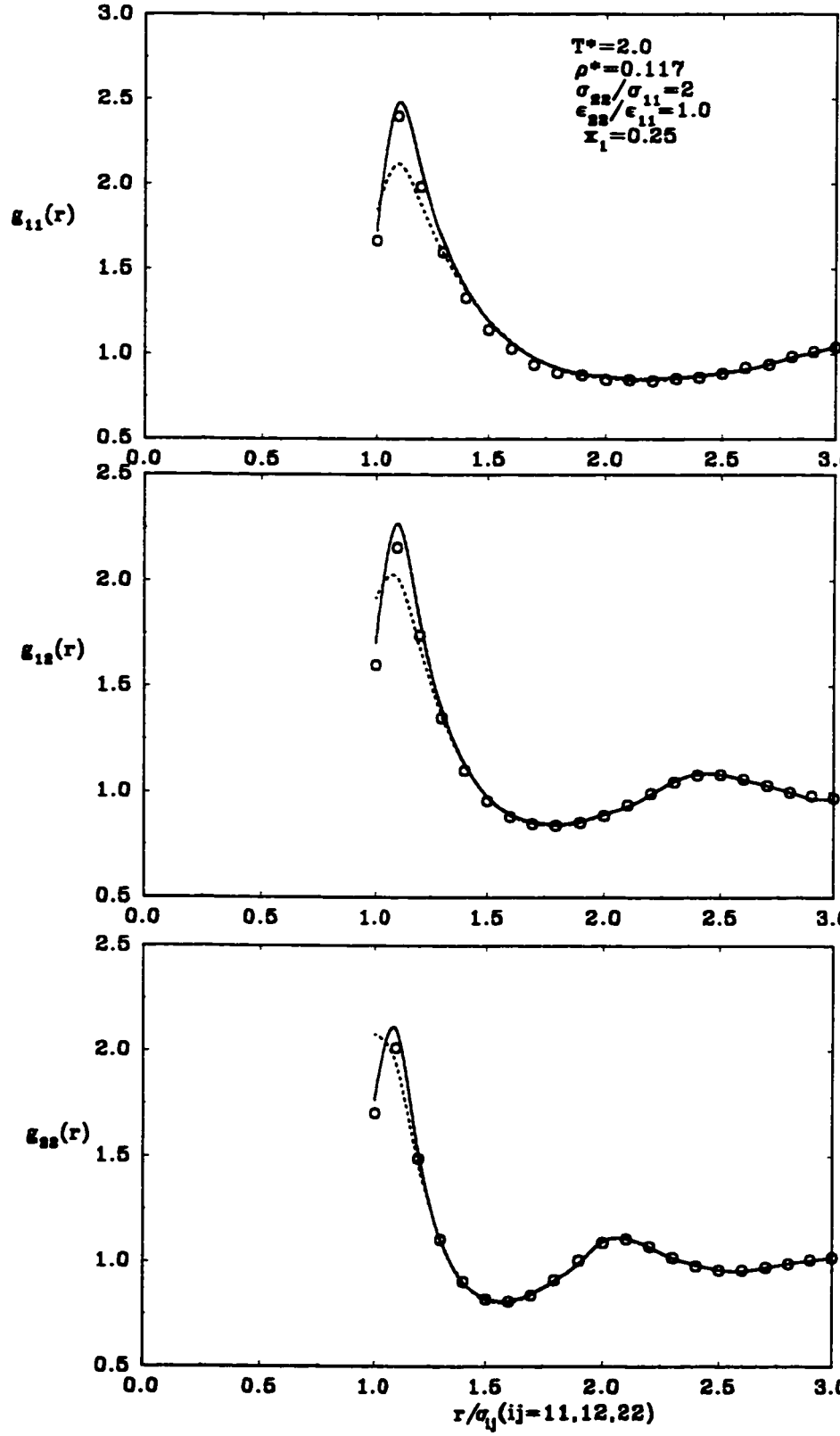

Figure 9. RDF of a LJ mixture. The circles are the MD data (Huber and Ely, 1989). The dashed and solid lines are results from the first-order MSA and SEXP approximation, respectively.

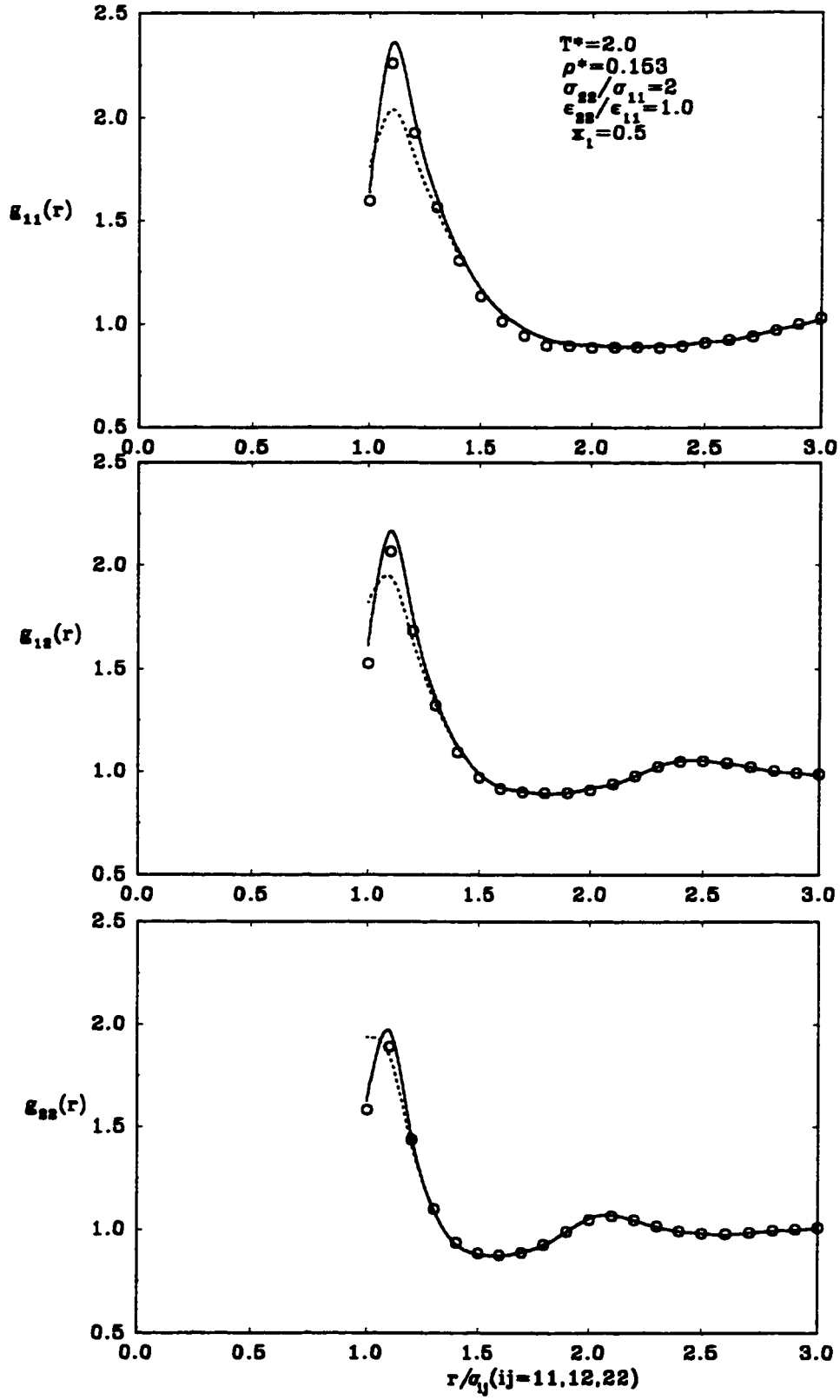

Figure 10. RDF of a LJ mixture. The circles are the MD data (Huber and Ely, 1989). The dashed and solid lines are results from the first-order MSA and SEXP approximation, respectively.

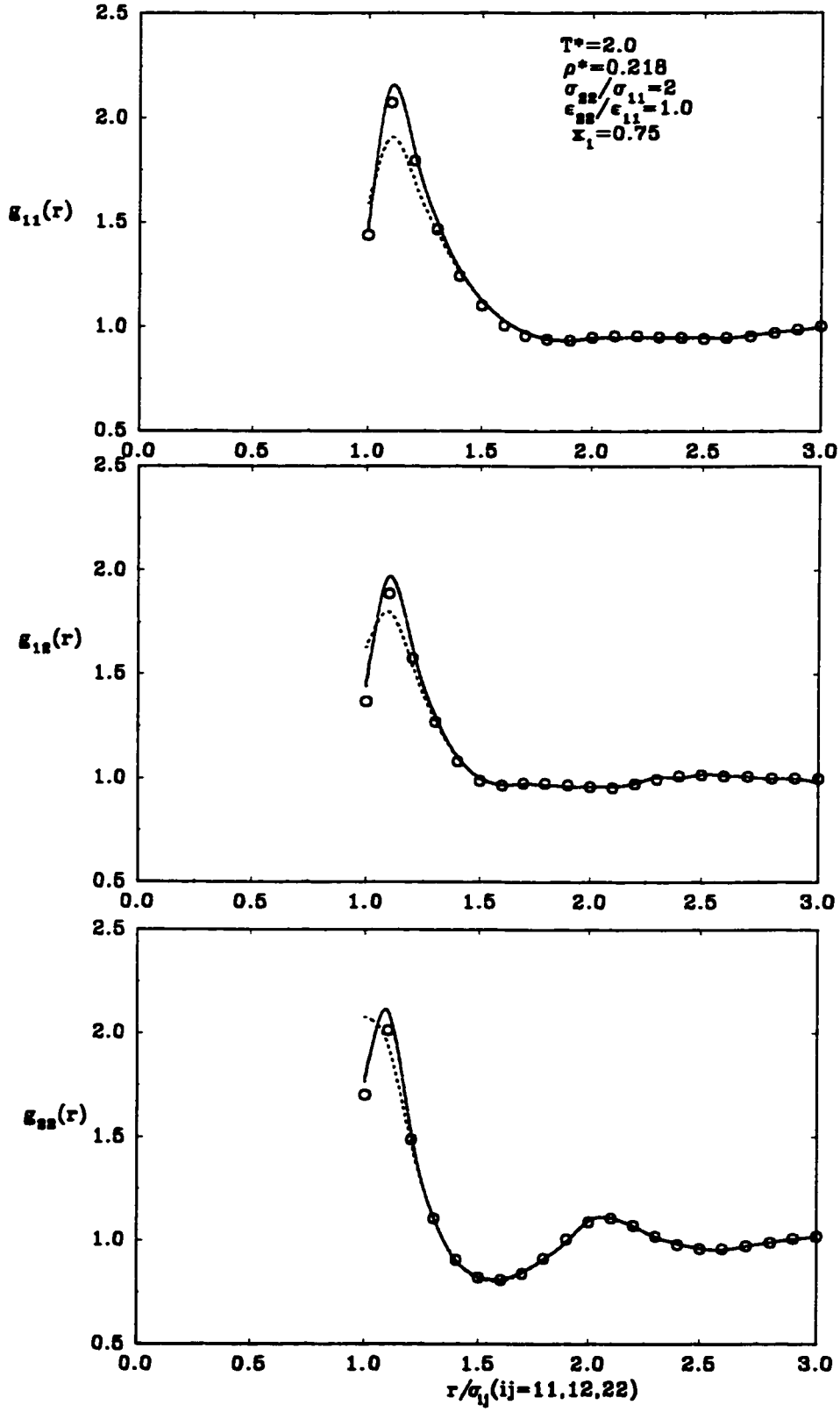

Figure 11. RDF of a LJ mixture. The circles are the MD data (Huber and Ely, 1989). The dashed and solid lines are results from the first-order MSA and SEXP approximation, respectively.

at $r>\sigma_{ij}$ as $c_{ij}(r)=-\beta u_{ij}(r)$, which is the MSA for $R_{ij}<r<\infty$, is valid at $r\to\infty$. It is also evident that the SEXP is a considerable improvement over the MSA at $r\sim\sigma_{ij}$. At large r values, the two approximations are almost indistinguishable. The justification of the SEXP is given in the next section. For both the MSA and the SEXP approximation, RDF is predicted better at higher temperatures than at lower temperatures as found for pure fluids. It appears that $g_{11}(r)$ around $r=2.0$ is slightly underestimated at $T^*=1.0$, but $g_{12}(r)$ and $g_{22}(r)$ are predicted remarkably well. It is notable here that the behavior of $g_{12}(r)$ and $g_{22}(r)$ are a little complicated and different from a standard oscillating and damping function which is utilized to describe the RDF of pure fluids. The remarkable difference suggests that some empirical methods (e. g. Li et al., 1990; Matteoli and Mansoori, 1995; Banaszak et al., 1995) to express the RDF of LJ mixtures by a simple empirical function may be no longer valid even with more fitted parameters. Only a theoretically-based method can yield these RDFs correctly. From comparisons in Figures 6-11, we can conclude that the MSA and the SEXP approximation can provide a reliable RDF for LJ mixtures, although the approximate RDF is not excellent everywhere. The MSA RDF in (156) will serve the development of thermodynamics in later sections for reason of its simplicity. The SEXP approximation, although more accurate than the MSA, is practically difficult to implement due to intensive integration work. It will be shown in later thermodynamic calculations that thermodynamic properties developed by (156) are very satisfactory and its performance is better than other available liquid theories.

3.8. Simplified exponential approximation

The original EXP approximation was proposed some years ago by Andersen et al. (1976) and independently by Stell (1976). By the cluster expansion of the attractive force around the repulsive one, Andersen concluded that the following EXP approximation for the LJ RDF g(r)

$$g(r)=g_0(r)\,e^{g^{MSA}(r)-g_0(r)} \qquad (166)$$

is inherently more accurate than the MSA result $g(r)=g^{MSA}(r)$, although in the EXP approximation a certain number of terms in the cluster expansion of g(r) are neglected.

The subscript 0 in (166) stands for the hard-sphere reference. In the past, the superiority of the EXP approximation has been found for the LJ fluid (Andersen et al., 1976; Stell and Weis, 1980) and the Yukawa fluid(Henderson et al., 1978; Konior and Jedrzejek, 1985). Hφye and Stell (1977) concluded that the EXP approximation can enhance the thermodynamic consistency between two routines: the internal energy and the virial pressure. Here we supply more arguments to justify the EXP approximation. It is known that the exact relation between the indirect correlation function c(r) and the direct correlation function h(r) is

$$c(r) = -\beta u(r) + h(r) - \ln g(r) + B(r) \tag{167}$$

where B(r) is the bridge function. Similarly, for the reference system of hard spheres,

$$c_0(r) = h_0(r) - \ln g_0(r) + B_0(r), \quad r > R \tag{168}$$

Subtracting (168) from (167) yields

$$g(r) = g_0(r)\, e^{\Delta g(r) - \Delta c(r) - \beta u(r) + \Delta B(r)}, \quad r > R \tag{169}$$

where the symbol Δ represents the difference of a quantity from its reference one. The bridge function has been found to be of a certain universality (Rosenfeld and Ashcroft, 1979). Therefore, we may assume $\Delta B(r) = 0$ and (169) can be reduced to

$$g(r) = g_0(r)\, e^{\Delta g(r) - \Delta c(r) - \beta u(r)}, \quad r > R \tag{170}$$

which, when supplemented by the OZ equation,

$$h(r) = c(r) + \rho \int h(r')\, c(\mathbf{r} - \mathbf{r}')\, d\mathbf{r}' \tag{171}$$

can determine in principle an approximate RDF. In order to obtain the RDF, we may design the following iteration procedure to solve Equations (170) and (171). Initially, it is assumed that $g(r) = g_0(r)$ or $\Delta g^{(0)}(r) = 0$. Applying the relation (170) yields

$$\Delta c(r) = -\beta u(r), \quad r > R \tag{172}$$

which is essentially equivalent to the MSA relation

$$c(r) = -\beta u(r), \quad r > R \tag{173}$$

since $c_0(r)$ vanishes rapidly outside of hard core. The solution of (173) and the OZ Equation (171) yields a new relation, $\Delta g^{(1)}(r) = g^{MSA}(r) - g_0(r)$. Substituting $\Delta g^{(1)}(r)$ into (170) gives

$$g(r) = g_0(r)\, e^{g^{MSA}(r) - g_0(r)} \tag{174}$$

which is precisely the EXP approximation. Thus, the EXP approximation is an intermediate result in an iteration solution of (170) and (171). As (170) is generally considered a better approximation, it is conceivable that the EXP approximation is more accurate than the MSA. An algebraic analysis indicates that relation (170) can be equally derived by the HNC approximation (167) after dropping B(r). Since in the HNC approximation, the energy routine gives strictly the same result as that of the virial pressure, it is not surprising to see that the EXP approximation based on (170) yields better thermodynamic consistency. These arguments strongly suggest that the EXP approximation is inherently better than the MSA. A proper utilization of the EXP approximation may overcome some deficiencies of the first-order MSA found above.

In order to incorporate the first-order MSA RDF into the EXP approximation, the following simplified EXP (SEXP) approximation is proposed (Tang and Lu, 1997c)

$$g(r) = g_0(r)\, e^{g_1(r)} \tag{175}$$

In other words, the full MSA RDF is approximately substituted by the sum of the first-order RDF and the reference one. Such a substitution has been proven valid many times in Section 3.4. It should be noted that the RDF of the SEXP approximation is as easily attainable as the first-order MSA RDF. In the EXP approximation, one has to pre-determine the full MSA RDF by a tedious numerical solution. While in the SEXP approximation, g(r) can be obtained in a very straightforward manner by (134).

The superiority of the SEXP approximation is indicated immediately by its limiting value at the zero density. When $\rho = 0$, one can find easily from (171) and (173) that

$$g(r) = 1 - \beta u(r) \tag{176}$$

for the first-order MSA. The SEXP approximation yields

$$g(r) = e^{-\beta u(r)} \tag{177}$$

which is exact at $\rho = 0$, while the first-order MSA result is only a linear approximation of (177). The above observation suggests that the SEXP approximation is more reliable at low densities. The performance of the SEXP approximation at moderate and high densities is demonstrated in Figures 12-14. Figures 12-14 show RDFs predicted by the SEXP approximation as well as by the first-order MSA at the same states as in Figures 4 [the g(r) of the SEXP approximation at $r<R$ in all the figures is extrapolated using values at $r>R$]. These graphical comparisons show that the SEXP approximation is an appreciable improvement over the first-order MSA. The improvement is very pronounced in the vicinity of the first peak of the RDF. Both the peak position and height are correctly shifted by the SEXP approximation. The RDF value at $r \sim \sigma$ is brought down close to MC data. While away from the first peak, the SEXP RDF is practically indistinguishable from the first-order MSA RDF since $g_1(r)$ approaches zero and $g_0(r)$ approaches unity rapidly.

For mixtures, Equation (175) is modified slightly by replacing the reference RDF with that of the mixture and replacing the first-order RDF by $g_{1,ij}(r)$ developed from (156), i. e.

$$g_{ij}(r) = g_{0,ij}(r)\, e^{g_{1,ij}(r)} \tag{178}$$

The good performance of the SEXP approximation for LJ mixtures has been well shown and discussed in the last section in Figures 6-11.

It appears that the performance of the SEXP approximation for the LJ fluid is basically the same as that of the EXP approximation. Stell and Weis (1980) has concluded that overall accuracy of the EXP approximation is excellent even though the excellent results may not be kept at all states. A more subtle inspection shows that the SEXP approximation somewhat overcorrects the first-order MSA at higher

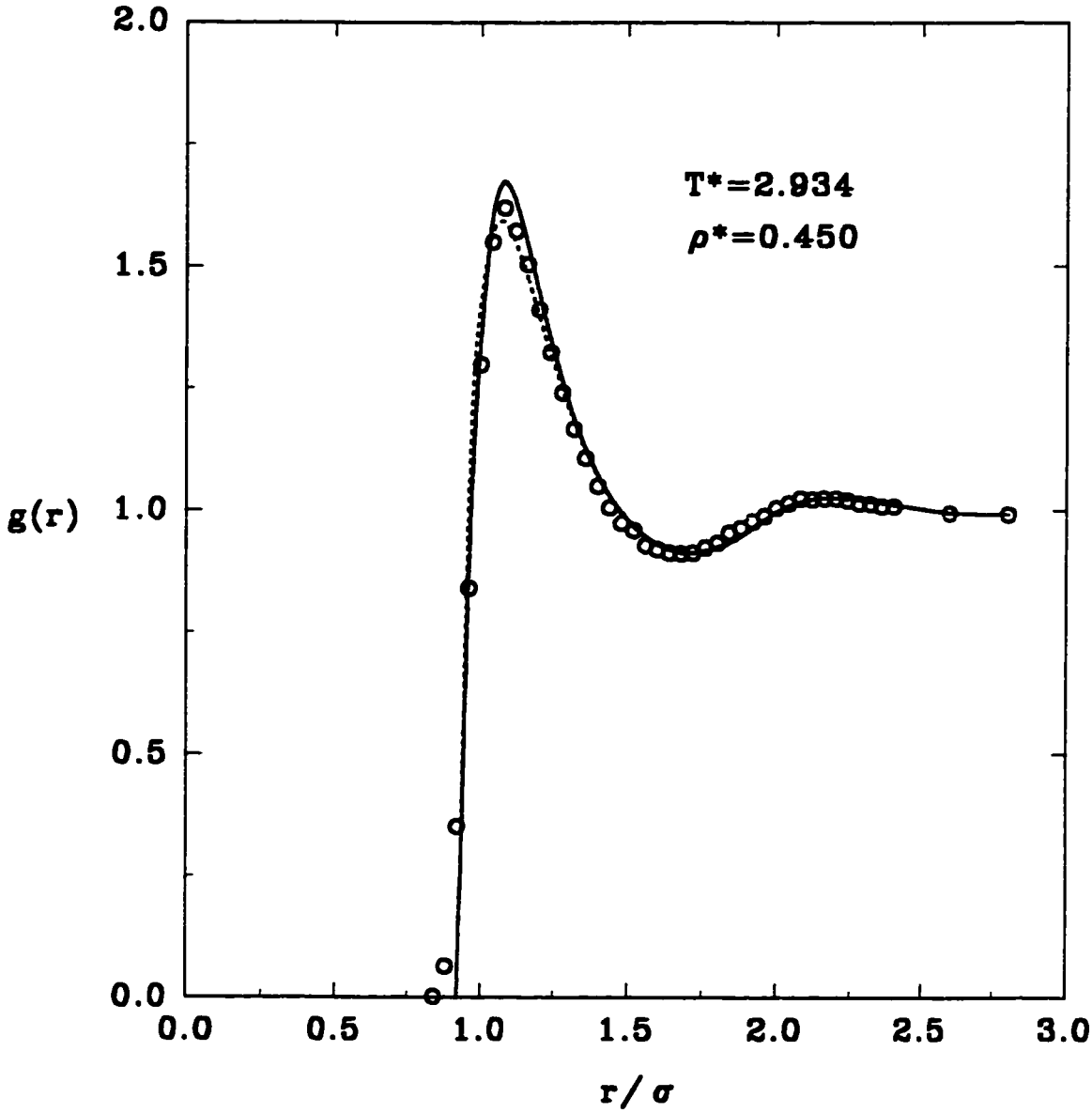

Figure 12. RDF of the LJ fluid. The circles are the MD data (Verlet, 1968). The solid and dashed lines are results from the first-order MSA and SEXP approximations, respectively.

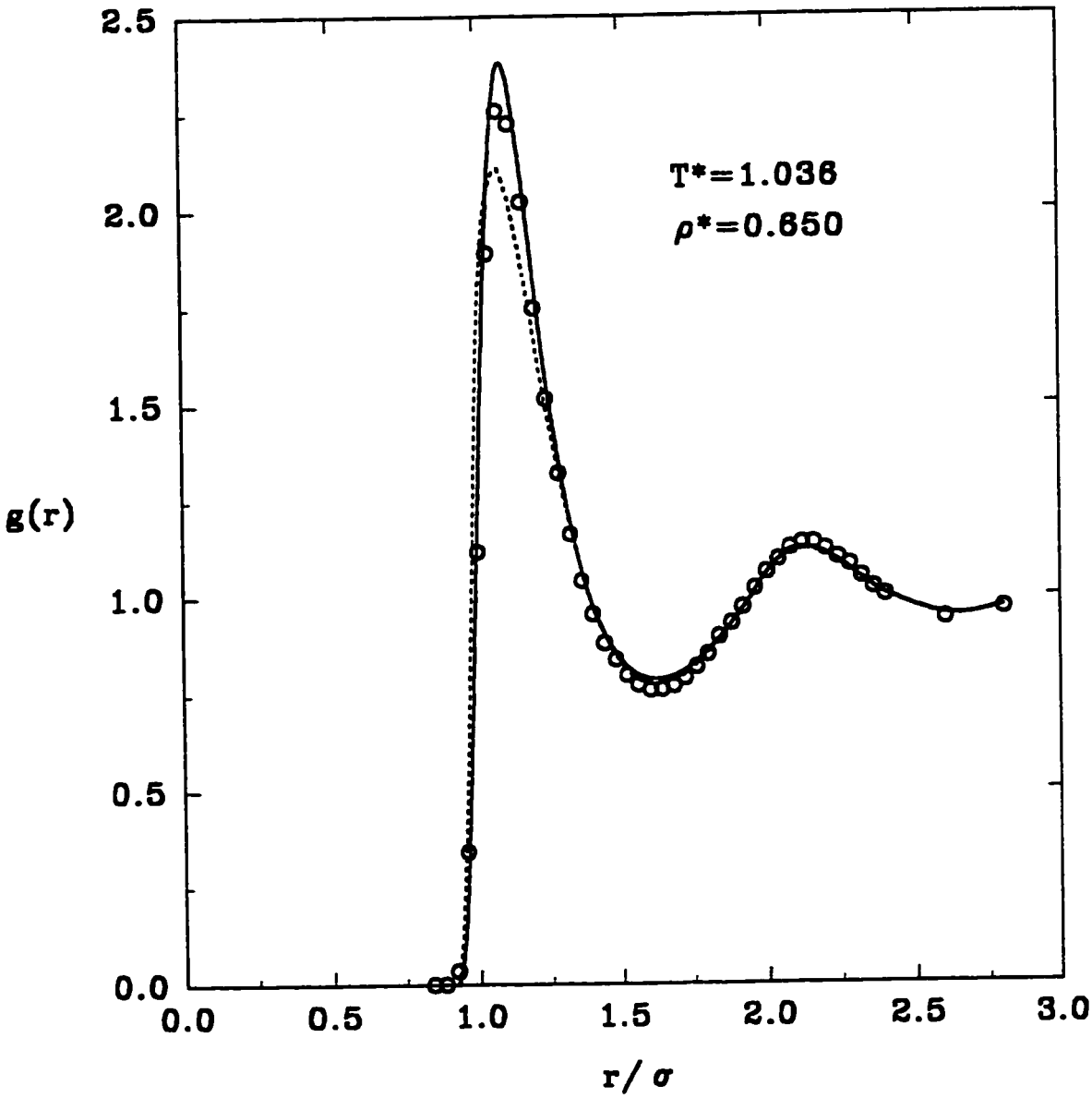

Figure 13. RDF of the LJ fluid. The circles are the MD data (Verlet, 1968). The solid and dashed lines are results from the first-order MSA and SEXP approximations, respectively.

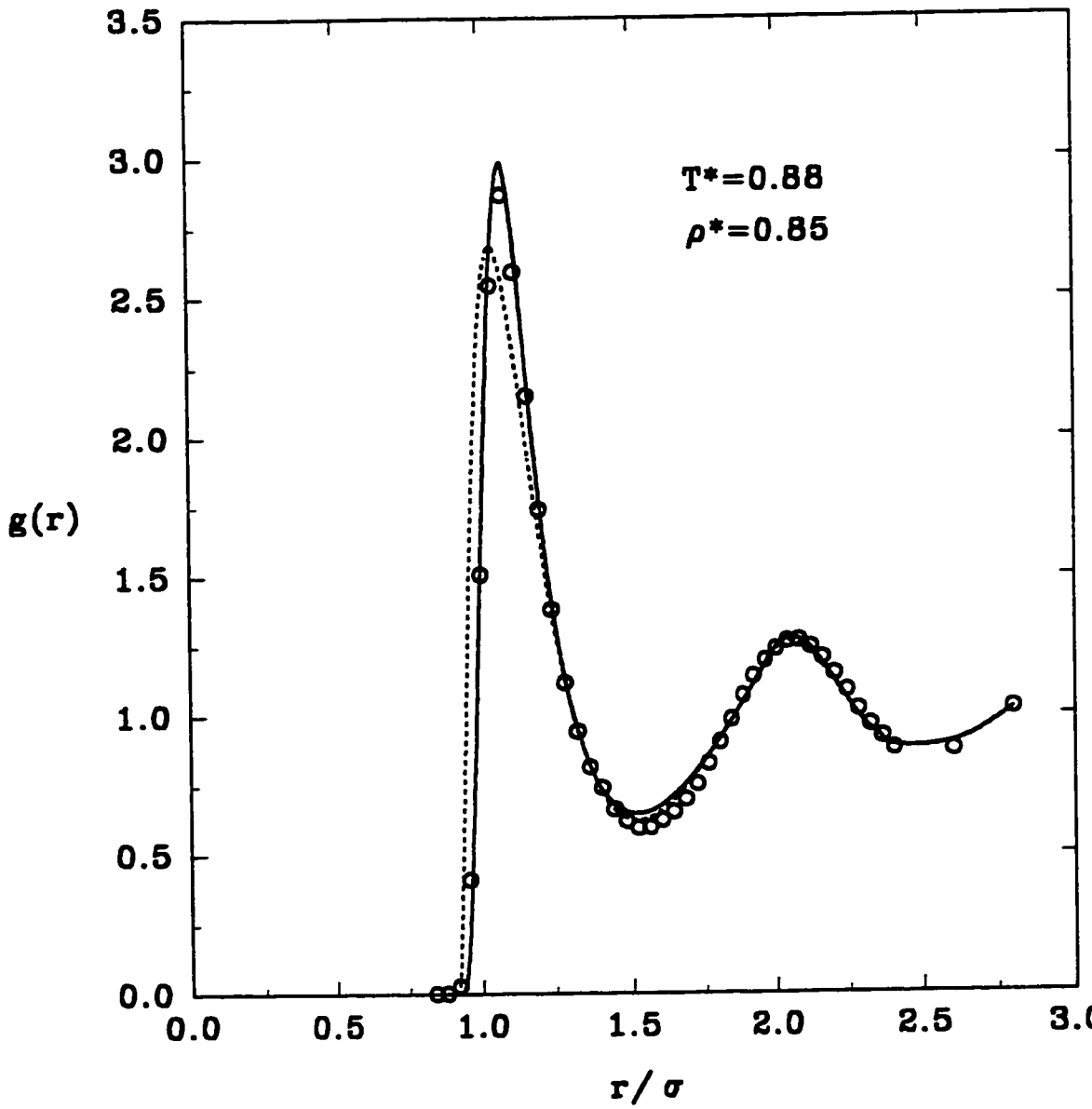

Figure 14. RDF of the LJ fluid. The circles are the MD data (Verlet, 1968). The solid and dashed lines are results from the first-order MSA and SEXP approximations, respectively.

temperatures, which may be inherited from the original EXP approximation. Nevertheless, the EXP approximation, hence possibly the SEXP approximation, remains one of the best liquid theories and any attempts to improve it systematically are extremely difficult (Stell and Weis, 1980).

3.9. RDF for hard-sphere chains

The achievement for spherical molecules demonstrated above provides an efficient way to study nonspherical molecules. Nonspherical molecules cover a much wider range of real fluids than spherical ones. Among the family of nonspherical molecules, the hard-sphere chain fluid is one of the most useful as it represents the skeleton of polymeric molecules. Understanding the fluid will be very helpful to gain knowledge of the properties of polymer solutions. In recent years, hard-sphere chains have been studied extensively by computer simulations (Yethiraj et al., 1990) and integral equation theories such as the polymer-reference interaction site model theory (Chandler and Anderson, 1972; Curro and Schweizer, 1987), Chiew's Percus-Yevick (PY) theory (Chiew, 1990; 1991) and the Chandler-Silbey-Ladanyi equation (Chandler et al., 1982; Lue and Blankschtein, 1995). Considerable progress has been made in exploring the fluid. For example, several equations of state (Chiew, 1990; Lue and Blankschtein, 1995) have been developed analytically from these theories. While compared with the theoretical achievements for spherical fluids, in which we can now obtain (Tang and Lu, 1993) analytically a RDF for an arbitrary potential with a hard core, the work done for hard-sphere chains is less satisfactory. For instance, a simple and relatively reliable RDF expression for the fluid is still absent, and tedious numerical computation has to be made to obtain RDF values. Just like that of hard spheres, the RDF expression of hard-sphere chains is essential to study fluid structure and to explore more complicated chains by perturbation theories.

To develop the RDF expression for hard-sphere chains, the PY integral equation theory implemented by Chiew (1991) is of interest here since it is of higher analytical solvability. In the original work of Chiew (1991), the average RDF g(r) defined as

$$g(r) = \frac{1}{m^2} \sum_{i=1}^{m} \sum_{i=1}^{m} g_{ij}(r) \tag{179}$$

at contact has been analytically obtained. In (179), $g_{ij}(r)$ is the site-site RDF between two chains with a length m. The RDF at an arbitrary value of r has to be calculated by solving numerically an integral equation after imposing the so-called PY2 approximation (Chiew, 1991). Chiew has found that the approximation reproduces excellently the full solution in the PY integral equation theory, where much computation is needed to solve a set of integral equations. Throughout this paper, the PY2 integral equation is adopted to pursue an analytical g(r) expression.

In Chiew's work (1991), the PY2 approximation has ultimately yielded

$$\begin{aligned} rh(r) = -q(r) + 12\eta \int_0^1 dt q(t)\,(r-t)\,h(r-t) + \frac{m-1}{m} q(r-1) \\ + \frac{m-1}{m} \int_0^1 dt (r-t)\,h(r-t), \qquad r>0 \end{aligned} \tag{180}$$

with

$$\begin{aligned} q(r) &= \frac{a}{2}(r^2-1) + b(r-1), \qquad r<1 \\ a &= \frac{1-\eta+3\eta m}{(1-\eta)^2 m}, \quad b = \frac{\eta-1+m(1-4\eta)}{2m(1-\eta)^2} \end{aligned} \tag{181}$$

where $h(r) = g(r)-1$, η is the packing factor of sphere sites. Rewriting Equation (180) for $r>1$ and noting that q(r) is a function valued in [0,1], we have

$$\begin{aligned} rg(r) - r = 12\eta \int_0^1 dt q(t)\,(r-t)\,g(r-t) - 12\eta \int_0^1 dt q(t)\,(r-t) \\ + \frac{m-1}{m} q(r-1) + \frac{m-1}{m} \int_0^1 dt (r-t)\,g(r-t) - \frac{m-1}{m} \int_0^1 dt (r-t), \qquad r>1 \end{aligned} \tag{182}$$

Applying the Laplace transform to both sides of (182) gives

$$\left(1-12\eta Q(s)-\frac{m-1}{m}\frac{1-e^{-s}}{s}\right)G(s)=\frac{1+s}{s}e^{-s}-12\eta\frac{(1+s)e^{-s}}{s^2}\int_0^1 dtq(t)$$
$$+12\eta\frac{e^{-s}}{s}\int_0^1 dttq(t)+\frac{m-1}{m}e^{-s}Q(s)-\frac{m-1}{m}\frac{(1+s)e^{-s}}{s^2}+\frac{m-1}{m}\frac{e^{-s}}{2s} \qquad (183)$$
$$=\frac{e^{-s}}{s^2}(1+4\eta a+6\eta b)+\frac{e^{-s}}{s}\left(1+\frac{5}{2}\eta a+4\eta b\right)+\frac{m-1}{m}e^{-s}\left(Q(s)-\frac{1+s/2}{s^2}\right)$$

where

$$Q(s)=\int_0^\infty q(t)\,e^{-st}=$$
$$-\frac{(1-\eta)/2s^2+3/2\eta^2 s-(1+2\eta)+[(1+\eta/2)s+1+2\eta)e^{-s}}{(1-\eta)^2 s^3}+\frac{m-1}{m}\frac{(s+2)e^{-s}+s-2}{2(1-\eta)s^3} \qquad (184)$$

Further algebraic work shows that

$$1+4\eta a+6\eta b=\frac{(1+\eta+\eta^2)m+\eta(1-\eta)}{(1-\eta)^2 m}$$
$$1+\frac{5}{2}\eta a+4\eta b=\frac{\frac{\eta}{2}(1-\eta)+(1+\eta^2/2)m}{(1-\eta)^2 m} \qquad (185)$$

Consequently, the Laplace transform of rg(r) is obtained

$$G(s)=\frac{\frac{1+2\eta}{(1-\eta)^2}\frac{1}{s^2}+\frac{1+\eta/2}{(1-\eta)^2 s}+\left(Q(s)-\frac{1}{1-\eta}\left(\frac{1}{s^2}+\frac{1}{2s}\right)\right)\omega}{Q_0(s)+\left(\frac{e^{-s}-1}{s}-\frac{6\eta}{1-\eta}\frac{(s+2)e^{-s}+s-2}{s^3}\right)\omega}e^{-s} \qquad (186)$$

where $\omega=(m-1)/m$ and

$$Q_0(s)=\frac{S_0(s)+12\eta L_0(s)e^{-s}}{(1-\eta)^2 t^3},\qquad L_0(s)=(1+\eta/2)s+1+2\eta \qquad (187)$$

$$S_0(s)=(1-\eta)^2 s^3+6\eta(1-\eta)s^2+18\eta^2 s-12\eta(1+2\eta) \qquad (188)$$

Equation (186) immediately suggests that g(r) at contact is

$$g(1)=\frac{1+\eta/2}{(1-\eta)^2}-\frac{1}{1-\eta}\omega \tag{189}$$

which recovers the value of Chiew (1991). If m=1, G(s) in (186) reduces to the PY RDF (87) of hard spheres developed earlier. We have presented a new RDF expression (88) of hard spheres with better performance. The new RDF may provide the possibility to improve (186) by replacing the part of hard spheres with the new one. However, it turns out that the performance of (186) is highly subjected to the chain length m and therefore the resulting improvement may not be substantial.

To serve practical purposes, further mathematic work on the Laplace inverse transform of (186) is needed to obtain g(r). Such an expression can be technically performed by a scheme suggested in Section 3.3, giving

$$\begin{aligned} rg(r)=\sum_{n=0}^{\infty}(-12\eta)^n\Big\{&\Big[1+\frac{\eta}{2}-\omega(1-\eta)\Big]C(2,n,n+1,r-n-1)\\ &+\Big[1+2\eta-\Big(1+\frac{\eta}{2}\Big)\omega+\frac{(1-\eta)}{2}\omega^2\Big]C(1,n,n+1,r-n-1)\\ &+[(1+2\eta)\omega-(1-\eta)\omega^2]C(0,n,n+1,r-n-1)\\ &-\Big[\Big(1+\frac{\eta}{2}\Big)\omega-\frac{(1-\eta)}{2}\omega^2\Big]C(1,n,n+1,r-n-2)\\ &-[(1+2\eta)\omega-(1-\eta)\omega^2]C(0,n,n+1,r-n-2)\Big\} \end{aligned} \tag{190}$$

where

$$C(n_1,n_2,n_3,r)= \tag{191}$$

$$\begin{cases} \displaystyle\sum_{\alpha=0}^{2}\sum_{i=1}^{n_3}\frac{B(n_1,n_2,n_3,i,\alpha)}{(i-1)!}r^{i-1}e^{t_\alpha r}H(r), & n_1+n_2<3n_3 \\ \displaystyle\frac{(1+\eta/2)^{n_2}}{(1-\eta)^{2n_3}}\delta(r)+\sum_{\alpha=0}^{2}\sum_{i=1}^{n_3}\frac{B(n_1,n_2,n_3,i,\alpha)}{(i-1)!}r^{i-1}e^{t_\alpha r}H(r), & n_1+n_2=3n_3 \end{cases}$$

$$B(n_1,n_2,n_3,i,\alpha)=$$

$$\frac{1}{(1-\eta)^{2n_3}}\sum_{k_1=0}^{n_3-i}\sum_{k_2=0}^{n_3-i-k_1}\frac{(-1)^{n_3-i-k_1}(n_3-1+k_2)!\,(2n_3-1-i-k_1-k_2)!}{k_1!\,k_2!\,(n_3-1-k_1-k_2)!\,((n_3-1)!)^2}\qquad(192)$$

$$\frac{A(n_1,n_2,k_1,t_\alpha)}{(t_\alpha-t_\beta)^{n_3+k_2}(t_\alpha-t_\gamma)^{2n_3-i-k_1-k_2}}$$

$$A(n_1,n_2,k_1,\alpha)=$$

$$\sum_{\substack{i,j=0\\ i+j\le n_2\\ i+2j\ge k-n_1}}^{n_2}\frac{n_2!\,(i+n_1+2j)!}{i!\,j!\,(n_2-i-j)!\,(i+2j+n_1-k)!}\left(1+\frac{\eta}{2}-\frac{(1-\eta)}{2}\omega\right)^i\times\qquad(193)$$

$$[1+2\eta-(1-\eta)\,\omega]^{n_2-i-j}\left(\frac{(1-\eta)^2\omega}{12\eta}\right)^j t_\alpha^{n_1+i+2j-k_1}$$

In (191)-(193), $t_\alpha(\alpha=0,1,2)$ are the zeros of S(t):

$$S(t)=(1-\eta)^2t^3+(6\eta(1-\eta)-(1-\eta)^2\omega)\,t^2+(18\eta^2-6\eta(1-\eta)\,\omega)\,t\qquad(194)$$
$$-12\eta(1+2\eta)+12\eta(1-\eta)\,\omega$$

The features of Equation (190) are worthy of note. It is suitable for obtaining g(r) for any value of r and the computation time is conceivably less than the numerical solution of (180) and that of the Laplace inverse transform of (186). As well, Equation (190) is presented in a consistent manner with those RDFs for spherical fluids, and programming (190) is rather simple despite its complicated appearance.

The performance of (190) is virtually the same as Chiew's numerical solution of (180). Namely, it is excellent for short chains but gets worse with increasing chain length m, which seems to be a common defect of theories available today.

Chiew has found that the equation of state of hard-sphere chains is a simple analytical function. In this work, it is shown that the average RDF for the fluid bears an analogously simple form. Since hard-sphere chains are the prototype of chain molecules, these analytical results hopefully will facilitate further theoretical studies of chain fluids. It should be pointed here that a study of chain molecules is much more complex than for spherical ones. The OZ equation for this fluid involves both

intramolecular distribution function and intermolecular RDF as defined in (179). The two quantities are inherently convoluted. This convolution presents a challenging difficulty for studying chain molecules in a traditional manner. For instance, the commonly utilized virial Equation (3) for spherical molecules is apparently no longer valid for a chain fluid. A more disappointing thing is that such a fatal invalidation has not been clarified theoretically. Undoubtedly, these fundamental problems have to be resolved in the future for exploring chain molecules.

4. Equations of State

The success of RDF predictions in previous sections provides the confidence in further developing fluid properties. Subsequent studies are devoted to the SW and LJ fluids. Both SW and LJ potentials have important applications in treating real fluids. For example, the LJ potential can well represent the molecular interactions of simple fluids such as Neon, Argon, Krypton, Xenon (Narten et al., 1974) and CH_4, N_2 (De Souza and Ben-Amotz, 1993). The SW potential is frequently utilized to compute the viscosity and thermal conductivity of real systems (Collings and Mclaughlin, 1980; Dymond, 1987). These practical backgrounds pose the requirement of understanding the SW and LJ fluids more precisely. Although analytical RDFs for the SW and LJ fluids have never been given before, their properties have been studied extensively in past decades. For instance, the Helmholtz free energy for these fluids have been investigated in depth by two well-known perturbation theories proposed respectively by Barker and Henderson (BH) (1967a, 1967b), and by Weeks, Chandler and Anderson (WCA) (1971). As well, the superposition approximation was carried out to treat these fluids (Smith et al., 1971a; 1971b). Recently, Del Rio et al. (1987a; 1987b; Benavides and Del Rio, 1989) made a short range expansion of the Helmholtz free energy in term of λ-1 and a long range expansion in terms of λ to study the SW fluid. In addition, numerous empirical and semiempirical EOS, even containing up to 33 parameters(Nicolas et al., 1979; Johnson et al., 1993), to correlate the MC data have been proposed in the literature. Listing these equations would not serve any practical purposes. These theoretical and empirical treatments are subject considerably to the conditions imposed in their development. At present, developing a suitable equation of state (EOS) which could cover wide ranges of temperature and densities remains a challenging problem in liquid theory. The RDFs in (95) and (132) provide an alternative way to study EOS. Rooted from fluid structure, the resulting EOS is theoretically more rigorous and capable of representing thermodynamic properties in a more systematic manner. We can expect that the EOS developed through RDF will yield better or more reasonable results than other theories.

4.1 EOS and its performance for the SW fluid

Thermodynamic properties can be developed from the energy Equation (2). Once the internal energy of the SW fluid is known, other properties can be derived by using inherent relations between these quantities. Typically

$$\frac{A-A_0}{NkT}=\int_0^{\beta}\frac{U}{N}d\beta \tag{195}$$

$$\frac{P-P_0}{NkT}=\rho\frac{\partial\left(\frac{A-A_0}{NkT}\right)}{\partial\rho} \tag{196}$$

For brevity, we define symbols a, a_0, u, u_0, Z, Z_0 as following:

$$\begin{aligned} a&=\frac{A-A^{id}}{NkT},\quad u=\frac{U-U^{id}}{NkT},\quad Z=\frac{PV}{NkT}\\ a_0&=\frac{A_0-A^{id}}{NkT},\quad u_0=\frac{U_0-U^{id}}{NkT},\quad Z_0=\frac{P_0V}{NkT}\end{aligned} \tag{197}$$

where 0, as mentioned before, stands for the hard-sphere reference and superscript id represents the ideal gas. If the CS equation is used for hard spheres, one has immediately that

$$a_0=\frac{4\eta-3\eta^2}{(1-\eta)^2},\quad u_0=0,\quad Z_0=\frac{1+\eta+\eta^2-\eta^3}{(1-\eta)^3} \tag{198}$$

a). Internal energy

A combination of Equations (2) and (94) yields

$$u=2\pi\rho\beta\int_0^{\infty}g(r)\,u(r)\,r^2dr=u_1+u_2 \tag{199}$$

where

$$u_1=-12\eta\beta\epsilon\int_1^{\lambda}g_0(r)\,r^2dr,\quad u_2=-12\eta\,(\beta\epsilon)^2\int_1^{\lambda}g_1(r)\,r^2dr \tag{200}$$

Although u_1 and u_2 can be obtained by inserting the explicit RDF expressions (119)

and (123) into Equation (200), the final results will become extremely tedious and make any subsequent development difficult. The Hilbert transform suggested earlier is adopted again to calculate the integral in Equation (200). After a careful algebraic analysis (Tang and Lu, 1994b), the following results for the internal energy are obtained

$$u_1=-\left[1+12\eta\sum_{i=0}^{2}\frac{L(t_i)\,(\lambda t_i-1)\,e^{(\lambda-1)t_i}}{t_i S_1(t_i)}\right]\beta\epsilon \tag{201}$$

$$u_2=-12\eta(1-\eta)^8\left\{\sum_i\left(\frac{M(-t_i)F_1(t_i)}{S^2(-t_i)}-\frac{M_1(-t_i)S(-t_i)-2M(-t_i)S_1(-t_i)}{S^3(-t_i)}F(t_i)\right)\right.$$
$$+\sum_i\sum_j\left(F_1(t_i)F_1(t_j)-\frac{F(t_i)F_1(t_j)+F_1(t_i)F(t_j)}{t_i+t_j}+2\frac{F(t_i)F(t_j)}{(t_i+t_j)^2}\right) \tag{202}$$
$$\left.\frac{e^{(t_i+t_j)(\lambda-1)}}{t_i+t_j}\right\}(\beta\epsilon)^2$$

With

$$M=C,\quad M_1=C_1+(\lambda-1)C,\quad C_1=C'(t),\quad C(t)=\lambda t^5-t^4$$
$$F=\frac{M}{S_1^2},\quad F_1=\frac{M_1}{S_1^2}-\frac{MS_2}{S_1^3} \tag{203}$$

b). Helmholtz free energy

Applying Equation (195), the Helmholtz free energy is given by

$$a=a_0+a_1+a_2 \tag{204}$$

with

$$a_1=u_1,\quad a_2=\frac{u_2}{2} \tag{205}$$

c). Compressibility factor

After some straightforward but tedious algebraic work with Equation (196), the following expression of pressure is obtained

$$Z=Z_0+\eta\frac{\partial(a-a_0)}{\partial\eta}=Z_0+Z_1+Z_2 \tag{206}$$

with

$$Z_1=-12\eta\beta\epsilon\sum_i\left[\frac{A_1+(\lambda-1)A}{S_1^2}-\frac{S_2A}{S_1^3}\right]e^{t_i(\lambda-1)} \tag{207}$$

$$\begin{aligned}Z_2=&-6\eta(1-\eta)^7(\beta\epsilon)^2\times\\&\left\{\sum_i\left[\frac{N(-t_i)F_i(t_i)}{S^3(-t_i)}-\frac{N_1(-t_i)S(-t_i)-3N(-t_i)S_1(-t_i)}{S^4(-t_i)}F(t_i)\right]+\right.\\&+\sum_{i,j}\left[\frac{F_1(t_i)E_2(t_j)}{2}-\frac{F(t_i)E_2(t_j)+2F_1(t_i)E_1(t_j)}{2(t_i+t_j)}+\right.\\&\left.\left.\frac{2F(t_i)E_1(t_j)+F_1(t_i)E(t_j)}{(t_i+t_j)^2}-\frac{3F(t_i)E(t_j)}{(t_i+t_j)^3}\right]\frac{e^{(t_i+t_j)(\lambda-1)}}{t_i+t_j}\right\}\end{aligned} \tag{208}$$

Where

$$\begin{gathered}A=\lambda(1-\eta)(1+2\eta)t^4+[\lambda(1+2\eta)^2-(1-\eta)(1+2\eta)]t^3-(1+2\eta)^2t^2\\A_1=A'(t)\end{gathered} \tag{209}$$

$$\begin{gathered}D=(1-\eta)^3t^3-6\eta(1-\eta)(3+\eta)t^2-18\eta^2(7+\eta)t+12\eta(3+19\eta+2\eta^2)\\D_1=D',\quad D_2=D'',\quad C_2=C''\end{gathered} \tag{210}$$

$$\begin{gathered}N=CD,\quad N_1=C_1D+CD_1+(\lambda-1)CD\\N_2=C_2D+CD_2+(\lambda-1)^2CD+2C_1D_1+2(\lambda-1)C_1D+2(\lambda-1)CD_1\end{gathered} \tag{211}$$

$$E=\frac{N}{S_1^3},\quad E_1=\frac{N_1}{S_1^3}-\frac{3NS_2}{2S_1^4},\quad E_2=\frac{N_2}{S_1^3}-\frac{3N_1S_2}{S_1^4}+N\frac{3S_2^2-S_1S_3}{S_1^5} \tag{212}$$

Equations (199), (204) and (206) represent a number of important properties of the SW fluid. It is of interest to compare these properties with those reported in the literature. In Figure 15, the values of the Helmholtz free energy obtained in this work

are compared with those of the long-range expansion (Benavides and Del Rio, 1989), the superposition (Smith et al., 1971) and the local compressibility approximations (Barker and Henderson, 1967). Tables 3 and 4 give comparisons between Equation (206) and the EOS proposed by Lee and Chao (LC) (1987), Lee and Sandler (LS) (1987), Guo et al. (GWL) (1990) and Shen and Lu (SL) (1993). Table 5 gives a comparison among the MC data, Equation (199) and the results from the full MSA solution (Smith et al., 1977). The following conclusions can be drawn from these comparisons:

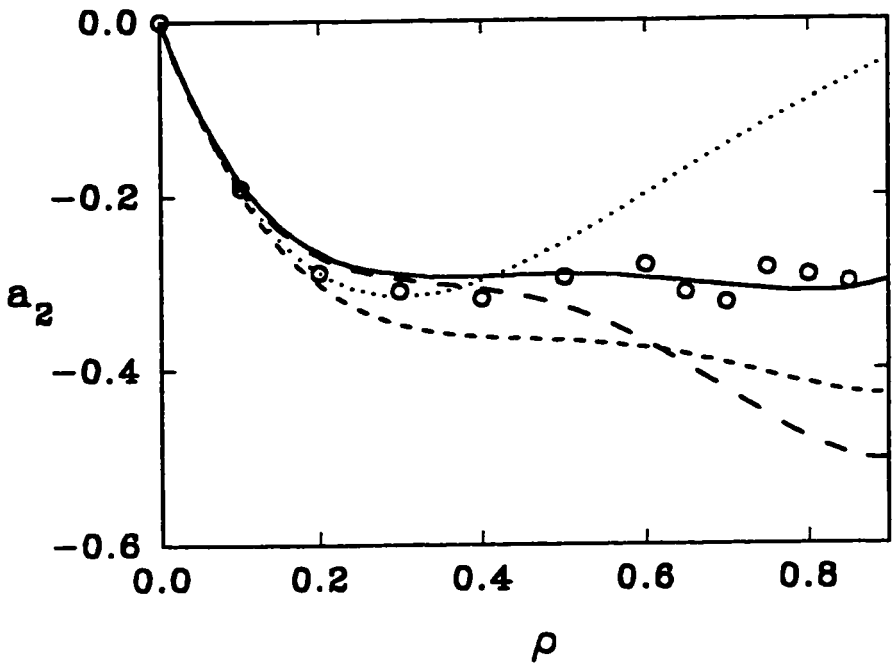

Figure 15. The second term in the free energy expansion of the SW fluid. The circles represent MC results. The solid line is that of this work. The long dashed, the medium dashed and dotted lines are the results of the long-range, the superposition, and the BH approximations, respectively.

Table 3. A comparison of the calculated results for the compressibility factor with Monte Carlo simulation data at λ=1.5

T^*	ρ^*	MC	LC	LS	GWL	SL	this work
1.75	0.05	0.916[a]	0.926	0.878	0.920	0.958	0.930
1.75	0.10	0.853[a]	0.875	0.792	0.855	0.913	0.873
1.75	0.30	0.736[a]	0.880	0.798	0.760	0.856	0.746
1.75	0.50	1.052[a]	1.088	1.489	1.091	1.320	0.999
1.75	0.65	2.073[a]	1.690	2.730	1.898	2.366	2.041
1.75	0.80	4.616[a]	3.935	5.100	3.683	4.556	4.811
2.50	0.05	0.959[a]	0.991	0.960	0.987	1.004	0.991
2.50	0.10	1.081[a]	0.999	0.945	0.985	1.011	0.991
2.50	0.30	1.097[a]	1.211	1.163	1.132	1.189	1.114
2.50	0.50	1.691[a]	1.716	2.008	1.724	1.902	1.678
2.50	0.65	2.909[a]	2.623	3.355	2.766	3.137	2.914
2.50	0.80	5.529[a]	5.041	5.839	4.838	5.514	5.693
3.00	0.05	1.013[a]	1.014	0.989	1.011	1.022	1.013
3.00	0.10	1.035[a]	1.044	1.000	1.032	1.049	1.036
3.00	0.30	1.265[a]	1.339	1.302	1.275	1.319	1.257
3.00	0.50	1.930[a]	1.966	2.213	1.975	2.129	1.942
3.00	0.65	3.168[a]	2.996	3.608	3.114	3.436	3.252
3.00	0.80	5.956[a]	5.480	6.140	5.302	5.887	6.036
4.00	0.50	2.310[b]	2.283	2.473	2.292	2.412	2.273
4.00	0.60	3.130[b]	2.967	3.349	3.047	3.250	3.095
4.00	0.70	4.490[b]	4.132	4.632	4.180	4.495	4.404
4.00	0.80	6.470[b]	6.036	6.526	5.894	6.353	6.464
AAD			0.184	0.209	0.180	0.112	0.045

[a] Guo et al. (1990) [b] Henderson et al. (1976a)

1) Based on the MC results reported in the literature, the Helmholtz free energy obtained in this work is the best. Here, we provide the comparison only for a_2 since a_1 is the same for all theories. Figure 15 indicates that only a_2 of this work gives the right tendency while all other theories give either too high or too low values at high densities.

2) The internal energy for the SW fluid is very accurately given by the analytical expression (199). The accuracy is almost the same as that of the full MSA solution. Although no results from other theories are presented here, it is unlikely for them to compete with Equation (199) since (199) is rigorously developed from the SW RDF.

3) To calculate the compressibility factor, Equation (206) is superior to all other EOS reported in the literature. It is noticeable that Equation (206) is completely predictive whereas other EOS listed in Tables 3 and 4 have one or more parameters to be fitted. As well, Equation (206) is applicable not only to $\lambda = 1.5$ but also to other

λ values. All other equations mentioned above fail obviously in this aspect.

Table 4. A comparison of the calculated compressibility factor with Monte Carlo simulation data at various λ values

λ	T^*	ρ^*	MC[a]	LC	LS	GWL	SL	this work
1.125	1.00	0.40	1.390	2.049	-0.052	2.005	1.484	1.583
1.125	1.00	0.60	2.230	3.416	0.877	3.470	2.604	2.226
1.125	1.00	0.80	3.530	6.601	3.463	6.549	5.430	3.540
1.375	1.50	0.40	0.970	1.306	0.792	1.212	1.172	0.930
1.375	1.50	0.60	1.680	2.018	1.906	2.159	2.178	1.458
1.375	1.50	0.80	4.000	4.777	4.710	4.594	4.890	3.941
1.625	2.00	0.40	0.720	0.629	1.224	0.495	0.800	0.678
1.625	2.00	0.60	1.660	0.726	2.464	0.945	1.642	1.673
1.625	2.00	0.80	5.380	3.097	5.402	2.773	4.188	5.181
1.750	1.43	0.40	-0.220	-0.940	0.708	-1.213	-0.511	-0.543
1.750	1.43	0.60	0.160	-2.169	1.800	-1.769	-0.350	0.148
1.750	1.43	0.80	3.030	-0.726	4.580	-1.233	1.517	3.293
2.000	6.00	0.40	1.480	1.160	2.090	1.083	1.427	1.472
2.000	6.00	0.60	2.820	1.676	3.656	1.835	2.626	2.762
2.000	6.00	0.80	5.500	4.359	6.923	4.063	5.527	5.498
AAD				1.272	0.82	1.316	0.522	0.097

[a] Henderson et al. (1980)

Table 5. A comparison of the calculated internal energy with the Monte Carlo simulation data and the full MSA values

λ	T^*	ρ^*	MC[a]	this work	full MSA[b]
1.500	1.00	0.5	-4.069	-3.910	-3.930
		0.6	-4.774	-4.714	-4.741
		0.7	-5.487	-5.504	-5.499
		0.8	-6.188	-6.213	-6.199
1.250	1.25	0.4	-1.343	-1.199	
		0.6	-2.139	-1.980	
		0.8	-3.081	-3.000	
1.375	1.50	0.4	-1.544	-1.448	
		0.6	-2.353	-2.315	
		0.8	-3.293	-3.286	
1.625	2.00	0.4	-1.866	-1.831	
		0.6	-2.732	-2.744	
		0.8	-3.505	-3.514	
1.750	1.43	0.4	-3.443	-3.312	
		0.6	-4.768	-4.792	
		0.8	-6.034	-6.035	
2.000	3.00	0.4	-2.217	-2.205	
		0.6	-3.246	-3.235	
		0.8	-4.321	-4.294	
AAD				0.023	

[a] Henderson et al., (1980) [b] Smith et al., (1974)

4) Overall, the EOS developed in this work is most accurate to describe the behavior of the SW fluid. The improvement for the Helmholtz free energy, internal energy and compressibility factor is overwhelming and extensive. Additionally, these thermodynamic properties are developed in a consistent and analytical manner. No other theories have ever achieved any of these aspects.

4.2 EOS and its performance for the LJ fluid

With the LJ RDF (156) in hand, one can now proceed to the evaluation of the thermodynamic properties of the LJ fluid. The development of thermodynamics of the LJ fluid is a little different from that of the SW fluid. In the foregoing section for the SW fluid, the internal energy is evaluated first and then for other thermodynamics. In fact, the sequence of calculations for this fluid is optional because its diameter is fixed. However, for the LJ fluid, the Helmholtz free energy must be concerned first for reason of the relevance of its diameter to temperature as shown in (102). In studying the LJ fluid, some extra work is made for the second virial coefficient and the phase diagram because of their usefulness for real fluid calculations.

a). Helmholtz free energy

By utilizing the functional derivative with respect to a potential function, the perturbation theory to second order gives

$$a=a_0+\int\left(\frac{\partial a}{\partial u(r)}\right)_0\delta u(r)\,d\mathbf{r}+\frac{1}{2}\int\int\left(\frac{\partial^2 a}{\partial u(r)\partial u(r_1)}\right)_0\delta u(r)\,\delta u(r_1)\,d\mathbf{r}\,d\mathbf{r}_1 \qquad (213)$$

where 0 represents the reference system or hard spheres in this work. Strictly speaking, the reference system of (213) should be the pseudo fluid interacting through the repulsive part of the LJ force

$$u_{rep}(r)=\begin{cases}u^{LJ}(r), & r<\sigma\\ 0, & r>\sigma\end{cases} \qquad (214)$$

In the BH theory, such a pseudo fluid is made equivalent to a hard-sphere fluid with the diameter selected by (102). The equivalence is utilized here for the calculations of thermodynamics as well as RDF in Section 3.1. $\delta u(r)$ in (213) is a potential

functional variation, or simply the attraction part of the LJ potential:

$$\delta u(r)=\begin{cases} 0, & r<\sigma \\ -k\epsilon\dfrac{e^{-z_1(r-\sigma)}}{r}+k\epsilon\dfrac{e^{-z_2(r-\sigma)}}{r}, & r>\sigma \end{cases} \tag{215}$$

It is already known (Hansen and McDonald, 1986) that

$$\frac{\partial a}{\partial u(r)}=\frac{1}{2}\rho\beta g(r), \quad \int\left(\frac{\partial^2 a}{\partial u(r)\partial u(r_1)}\right)_0\delta u(r_1)\,dr_1=\frac{1}{2}\rho\beta g_1(r) \tag{216}$$

Therefore (213) reduces to

$$a=a_0+a_1+a_2 \tag{217}$$

with

$$a_1=2\pi\rho\beta\int_\sigma^\infty g_0(r)\,u(r)\,r^2dr, \quad a_2=\pi\rho\beta\int_\sigma^\infty g_1(r)\,u(r)\,r^2dr \tag{218}$$

The mathematical work for a_1 and a_2 needs to be further elaborated here:

$$\begin{aligned} a_1&=2\pi\rho\beta\int_R^\infty(g_0(r)-1)\,u(r)\,r^2dr+2\pi\rho\beta\int_R^\infty u^{LJ}(r)\,r^2dr-2\pi\rho\beta\int_R^\sigma g_0(r)\,u(r)\,r^2dr \\ &=-\frac{12\eta\beta\epsilon}{R^3}\left[k_1\left(\frac{L(z_1R)}{z_1^2(1-\eta)^2Q_0(z_1R)}-\frac{1+z_1R}{z_1^2}\right)-k_2\left(\frac{L(z_2R)}{z_2^2(1-\eta)^2Q_0(z_2R)}-\frac{1+z_2R}{z_2^2}\right)\right] \\ &\quad+48\eta\beta\epsilon\left[\frac{1}{9}\left(\frac{\sigma}{R}\right)^6-\frac{1}{3}\left(\frac{\sigma}{R}\right)^6\right]-48\eta\beta\epsilon g_0(R)\left[\frac{1}{9}\left(\frac{\sigma}{R}\right)^{12}-\frac{1}{3}\left(\frac{\sigma}{R}\right)^6+\frac{2}{9}\left(\frac{\sigma}{R}\right)^3\right] \end{aligned} \tag{219}$$

with

$$g_0(R)=\frac{1+\eta/2}{(1-\eta)^2} \tag{220}$$

$$a_2=\pi\rho\beta\int_R^{\infty}g_1(r)\,u(r)\,r^2dr-\pi\rho\beta\int_R^{\sigma}g_1(r)\,u(r)\,r^2dr$$

$$=-\frac{6\eta\beta^2\epsilon^2}{R^3}\left[\frac{k_1^2}{2z_1Q_0^4(z_1R)}+\frac{k_2^2}{2z_2Q_0^4(z_2R)}-\frac{2k_1k_2}{(z_1+z_2)\,Q_0^2(z_1R)\,Q_0^2(z_2R)}\right] \quad (221)$$

$$-24\eta\beta^2\epsilon^2\left[\frac{k_1/R}{Q_0^2(z_1R)}-\frac{k_2/R}{Q_0^2(z_2R)}\right]\left[\frac{1}{9}\left(\frac{\sigma}{R}\right)^{12}-\frac{1}{3}\left(\frac{\sigma}{R}\right)^{6}+\frac{2}{9}\left(\frac{\sigma}{R}\right)^{3}\right]$$

The PY RDF for hard spheres has been utilized in (219) and g(r) over the interval [R,σ] is approximated by its contact value. In order to prevent long-range accumulated errors introduced by the TY function, the LJ potential, $u^{LJ}(r)$, is reused for large values of r. With (219) and (221), the following properties are obtained:

b). Compressibility factor

$$Z=Z_0+Z_1+Z_2 \quad (222)$$

$$Z_1=a_1-\frac{12\eta^2\beta\epsilon}{R^3}\left[k_1\left(\frac{(5/2+\eta/2)\,z_1R+4+2\eta}{z_1^2(1-\eta)^3Q_0(z_1R)}-\frac{L(z_1R)\,Q_{0,\eta}'(z_1R)}{z_1^2(1-\eta)^2Q_0^2(z_1R)}\right)\right.$$

$$\left.-k_2\left(\frac{(5/2+\eta/2)\,z_2R+4+2\eta}{z_2^2(1-\eta)^3Q_0(z_2R)}-\frac{L(z_2R)\,Q_{0,\eta}'(z_2R)}{z_2^2(1-\eta)^2Q_0^2(z_2R)}\right)\right] \quad (223)$$

$$-16\eta\beta\epsilon R\frac{\partial g_0(R)}{\partial R}\left[\frac{1}{9}\left(\frac{\sigma}{R}\right)^{12}-\frac{1}{3}\left(\frac{\sigma}{R}\right)^{6}+\frac{2}{9}\left(\frac{\sigma}{R}\right)^{3}\right]$$

with

$$R\frac{\partial g_0(R)}{\partial R}=\frac{3\eta(5+\eta)}{2(1-\eta)^3} \quad (224)$$

$$Z_2 = a_2 + \frac{12\eta^2\beta^2\epsilon^2}{R^3} \times$$

$$\left[\frac{k_1^2 Q'_{0,\eta}(z_1 R)}{z_1 Q_0^5(z_1 R)} + \frac{k_2^2 Q'_{0,\eta}(z_2 R)}{z_2 Q_0^5(z_2 R)} - \frac{2k_1 k_2 [Q'_{0,\eta}(z_1 R) Q_0(z_2 R) + Q_0(z_1 R) Q'_{0,\eta}(z_2 R)]}{(z_1 + z_2) Q_0^3(z_1 R) Q_0^3(z_2 R)} \right] \quad (225)$$

$$+48\eta^2\beta^2\epsilon^2 \left[\frac{k_1/R}{Q_0^3(z_1 R)} Q'_{0,\eta}(z_1 R) - \frac{k_2/R}{Q_0^3(z_2 R)} Q'_{0,\eta}(z_2 R) \right] \left[\frac{1}{9}\left(\frac{\sigma}{R}\right)^{12} - \frac{1}{3}\left(\frac{\sigma}{R}\right)^6 + \frac{2}{9}\left(\frac{\sigma}{R}\right)^3 \right]$$

where

$$Q'_\eta(t) = \frac{6(1-\eta)t^2 + 36\eta t - 12(1+5\eta) + 12[(1+2\eta)t + 1 + 5\eta]e^{-t}}{(1-\eta)^3 t^3} \quad (226)$$

c). Internal energy

$$u = u_0 + u_1 + u_2 \quad (227)$$

with

$$u_0 = 12\eta \frac{1-\eta/2}{(1-\eta)^3} \frac{d\ln R}{d\ln\beta}, \quad u_1 = a_1 + R\frac{\partial a_1}{\partial R}\frac{d\ln R}{d\ln\beta}, \quad u_2 = 2a_2 + R\frac{\partial a_2}{\partial R}\frac{d\ln R}{d\ln\beta} \quad (228)$$

$$\frac{d\ln R}{d\ln\beta} = \frac{T^* + 2c_2 T^{*2} + 4c_3 T^{*4}}{12c_1\left(1 + \frac{T^* + c_2 T^{*2} + c_3 T^{*4}}{c_1} + \left(1 + \frac{T^* + c_2 T^{*2} + c_3 T^{*4}}{c_1}\right)^{1/2}\right)} \quad (229)$$

$$R\frac{\partial a_1}{\partial R} = \frac{12\eta\beta\epsilon}{R^3}\left[k_1\left(\frac{g_0(R)}{Q_0^2(z_1 R)} - 1\right) - k_2\left(\frac{g_0(R)}{Q_0^2(z_2 R)} - 1\right)\right] \quad (230)$$

$$+48\eta\beta\epsilon(g_0(R) - 1)\left[\left(\frac{\sigma}{R}\right)^{12} - \left(\frac{\sigma}{R}\right)^6\right] - 48\eta\beta\epsilon\, R\frac{\partial g_0(R)}{\partial R}\left[\frac{1}{9}\left(\frac{\sigma}{R}\right)^{12} - \frac{1}{3}\left(\frac{\sigma}{R}\right)^6 + \frac{2}{9}\left(\frac{\sigma}{R}\right)^3\right]$$

$$R\frac{\partial a_2}{\partial R}=\frac{6\eta\beta^2\epsilon^2}{R^2}\times$$

$$\left[\frac{f(z_1R)\,k_1^2}{Q_0^2(z_1R)}+\frac{f(z_2R)\,k_2^2}{Q_0^2(z_2R)}-\frac{2k_1k_2\,[z_1f(z_1R)\,Q_0^2(z_1R)+z_2f(Z_2R)\,Q_0^2(z_1R)\,]}{(z_1+z_2)\,Q_0^2(z_1R)\,Q_0^2(z_2R)}\right] \qquad (231)$$

$$-24\eta\beta^2\epsilon^2\left[\frac{k_1/R}{Q_0^2(z_1R)}-\frac{k_2/R}{Q_0^2(z_2R)}\right]\left[-\frac{10}{9}\left(\frac{\sigma}{R}\right)^{12}+\frac{4}{3}\left(\frac{\sigma}{R}\right)^{6}-\frac{2}{9}\left(\frac{\sigma}{R}\right)^{3}\right]$$

$$+24\eta\beta^2\epsilon^2[k_1z_1f(z_1R)-k_2z_2f(z_2R)]\left[\frac{1}{9}\left(\frac{\sigma}{R}\right)^{12}-\frac{1}{3}\left(\frac{\sigma}{R}\right)^{6}+\frac{2}{9}\left(\frac{\sigma}{R}\right)^{3}\right]$$

where

$$f(t)=\frac{1}{Q^2(t)}+24g_0(R)\,\frac{Q(t)-Q(-t)\,e^{-t}}{t^2Q^3(t)} \qquad (232)$$

d). Second virial coefficient B_2

$$B_2=\frac{\pi R^3}{6}\left[4.0-\frac{32\beta\epsilon}{3}\left(\frac{\sigma}{R}\right)^3-\frac{6\beta^2\epsilon^2}{R^3}\left(\frac{k_1^2}{2z_1}+\frac{k_2^2}{2z_2}-\frac{2k_1k_2}{z_1+z_2}\right)\right. \qquad (233)$$

$$\left.-\frac{24\,(k_1-k_2)\,\beta^2\epsilon^2}{R}\left(\frac{1}{9}\left(\frac{\sigma}{R}\right)^{12}-\frac{1}{3}\left(\frac{\sigma}{R}\right)^{6}+\frac{2}{9}\left(\frac{\sigma}{R}\right)^{3}\right)\right]$$

Development of (223),(225) and (233) is very straightforward, whereas attention is required in the development of Equations (230) and (231). Direct differentiation of (230) and (231) with respect to β will lead to tedious and messy expressions. Instead, the following relation in the development has been utilized:

$$R\frac{\partial(A/NkT)}{\partial R}=\int\frac{\partial(A/Nkt)}{\partial u(r)}\,\frac{\partial u(r)}{\partial R}\,dr=12\eta g(R) \qquad (234)$$

where g(R) is the RDF at contact from the energy routine of the OZ solution and is well discussed by Hφye and Stell (1977).

The achieved expressions (217)-(233) for the LJ fluid are of rather simple analytical forms and are free from tedious numerical integration and differentiation. It is of interest to note that the factorization function Q(t) plays a major role in the derivation

and its nature tremendously reduces the algebraic work in developing (230) and (231) for internal energy. The achieved simplicity will enhance its usefulness in practical calculations. It is also valuable to mention that the development begins with the RDF (138), a basic information for the LJ fluid. Theoretically, this development is more rigorous than the BH theory, which is based on the macroscopic or microscopic compressibility approximation, and the WCA theory, which is just a first-order theory but with a different split of repulsive and attractive forces. We can expect that the new results in this work are more reliable than previous perturbation theories.

Comparing with computer simulation data is necessary to verify the validity of a theory. A detailed comparison among the MC data (Hansen,1970), results from the Verlet and Weis (VW) (1971) equation which is an improved version of the WCA theory, the latest MBWR EOS (Johnson et al., 1993) and the EOS developed in this work is presented in Table 6. The compared properties are the Helmholtz free energy, compressibility factor and internal energy. Four typical isotherms $T^* = 0.75$, 1.15, 1.35 and 2.74 appeared in the literature are included in the comparison. The average absolute deviations (AAD) shown in the last line of the table clearly indicate that the present second-order theory is an improvement over the WCA theory, whose performance is similar to that of the BH theory. The improvement is more impressive for the Helmholtz free energy and compressibility factor. It is also indicated that the proposed theory performs very well at high temperatures but becomes slightly worse at low ones. That performance is understandable since any perturbation theories based on an inverse temperature expansion are more applicable at high temperatures. Even at low temperatures, the present results are better than the WCA values. It is also noted that, over the range of data tested in this work, the present EOS gives comparable accuracy to the latest 33-parameter EOS (Johnson et al, 1993), which is regressed from the MC data of the LJ fluid.

The LJ liquid-vapor phase diagrams obtained from the MC data (Panagiotopoulos, 1987; Lotif et al., 1992) and the proposed second-order theory are shown in Figure 16. The prediction of the phase diagram is generally regarded as a more strict examination of liquid theories. Again, the proposed EOS yields a very successful

prediction except around the critical point, where any other theories suffer the same failure. It is noted that although the phase diagram given by the present theory is slightly worse than the latest 33-parameter EOS, it is better than the original 33-parameter EOS, the PY theory, the hypernetted chain theory, and the soft sphere MSA, and it has a similar performance to the reference hypernetted chain theory from the literature observations (Kalyuzhnyi and Cummings, 1996; Duh and Haymet, 1995; Ferreira et al., 1994). The success obtained in calculating the phase diagram provides a justification to locate the EOS parameters from the measurable phase coexistence envelope, which is used later on in real fluid calculations.

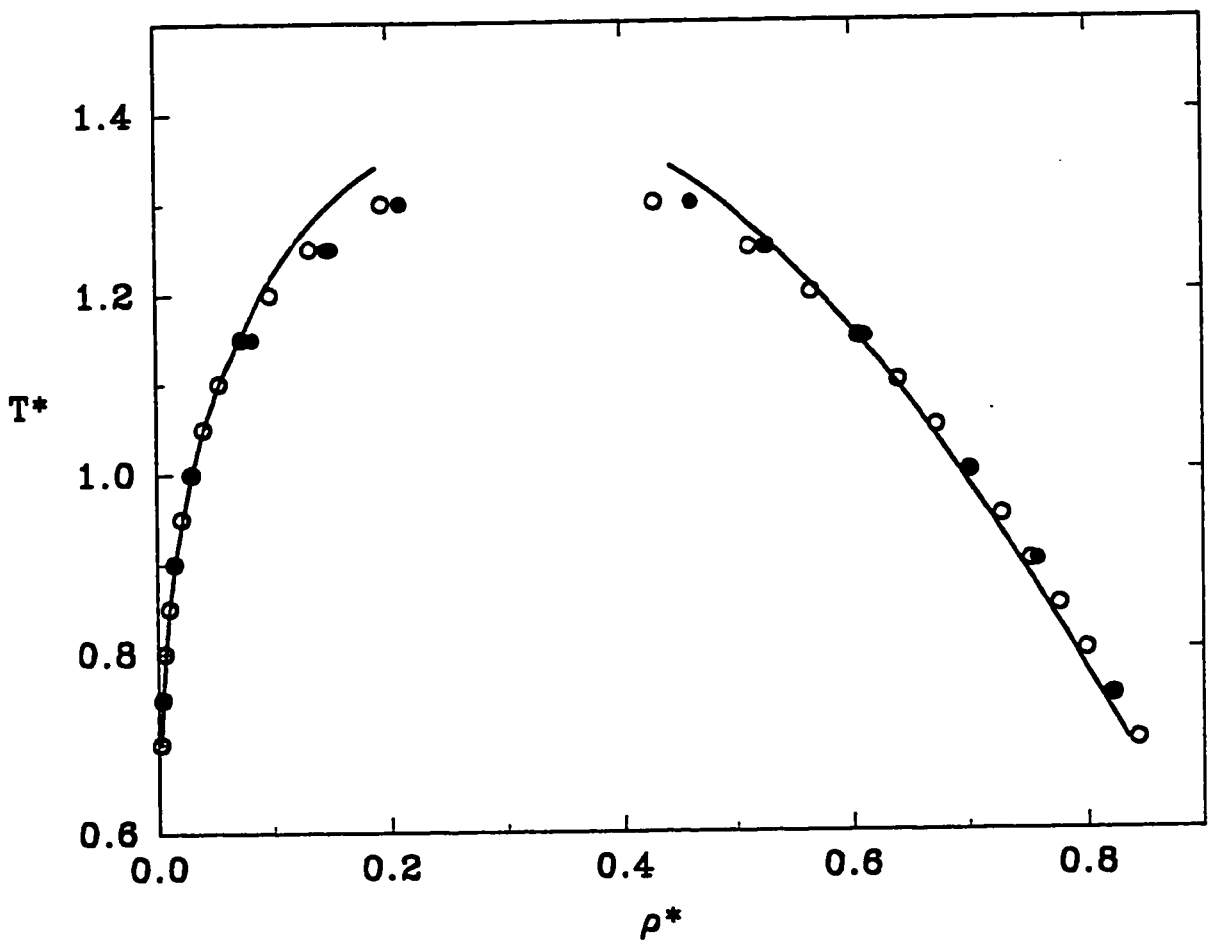

Figure 16. Phase diagram of the LJ fluid. The solid line is results from the present theory. The open and solid circles are the MC data given by Panagiotopoulos (1987) and Lotif (1991), respectively.

Table 6. The LJ properties obtained from various EOS

		a				Z				u			
T^*	ρ^*	MC[1]	VW[2]	MBWR[3]	this	MC	VW	MBWR	this	MC	VW	MBWR	this
0.75	0.10	-0.81	-0.55	-0.87	-0.72	0.23	0.42	0.14	0.33	-1.53	-0.75	-1.62	-1.07
0.75	0.20	-1.48	-1.15	-1.68	-1.37	-0.29	-0.24	-0.50	-0.25	-2.53	-1.59	-3.22	-1.99
0.75	0.30	-2.11	-1.79	-2.35	-1.98	-0.78	-0.93	-0.75	-0.82	-3.44	-2.49	-4.37	-2.87
0.75	0.40	-2.68	-2.43	-2.87	-2.58	-1.20	-1.58	-0.86	-1.35	-4.28	-3.49	-4.98	-3.77
0.75	0.50	-3.23	-3.06	-3.31	-3.15	-1.69	-2.07	-1.19	-1.75	-4.97	-4.53	-5.37	-4.69
0.75	0.60	-3.74	-3.65	-3.75	-3.66	-2.05	-2.24	-1.64	-1.86	-5.81	-5.60	-5.92	-5.64
0.75	0.70	-4.17	-4.12	-4.16	-4.08	-1.71	-1.86	-1.57	-1.45	-6.76	-6.67	-6.75	-6.57
0.75	0.80	-4.47	-4.43	-4.45	-4.34	-0.53	-0.56	-0.42	-0.22	-7.71	-7.67	-7.70	-7.44
0.75	0.84	-4.54	-4.49	-4.50	-4.38	0.37	0.32	0.42	0.60	-8.05	-8.03	-8.05	-7.75
1.15	0.10	-0.39	-0.29	-0.40	-0.37	0.61	0.70	0.62	0.65	-0.75	-0.48	-0.74	-0.62
1.15	0.20	-0.73	-0.61	-0.76	-0.70	0.35	0.37	0.32	0.36	-1.35	-1.02	-1.43	-1.20
1.15	0.30	-1.05	-0.92	-1.07	-1.01	0.12	0.05	0.13	0.10	-1.95	-1.60	-2.03	-1.76
1.15	0.40	-1.33	-1.23	-1.34	-1.30	-0.09	-0.19	0.00	-0.09	-2.48	-2.22	-2.54	-2.34
1.15	0.50	-1.59	-1.51	-1.58	-1.55	-0.13	-0.27	-0.06	-0.14	-3.02	-2.86	-3.04	-2.92
1.15	0.60	-1.79	-1.73	-1.76	-1.74	0.07	-0.08	0.06	0.06	-3.60	-3.50	-3.59	-3.51
1.15	0.65	-1.84	-1.81	-1.83	-1.81	0.31	0.17	0.27	0.31	-3.87	-3.83	-3.88	-3.80
1.15	0.75	-1.88	-1.87	-1.88	-1.85	1.17	1.10	1.16	1.21	-4.46	-4.43	-4.44	-4.34
1.15	0.85	-1.78	-1.76	-1.77	-1.74	2.86	2.83	2.86	2.87	-4.93	-4.94	-4.92	-4.80
1.15	0.92	-1.56	-1.54	-1.55	-1.52	4.72	4.69	4.72	4.68	-5.18	-5.21	-5.16	-5.05
1.35	0.10	-0.30	-0.22	-0.29	-0.28	0.72	0.77	0.72	0.74	-0.58	-0.41	-0.58	-0.51
1.35	0.20	-0.56	-0.46	-0.56	-0.52	0.50	0.53	0.51	0.52	-1.12	-0.86	-1.12	-0.99
1.35	0.30	-0.80	-0.69	-0.78	-0.75	0.35	0.32	0.37	0.35	-1.55	-1.35	-1.61	-1.47
1.35	0.40	-1.00	-0.91	-0.98	-0.95	0.27	0.18	0.30	0.25	-2.04	-1.87	-2.06	-1.95
1.35	0.50	-1.16	-1.09	-1.13	-1.12	0.30	0.20	0.33	0.29	-2.50	-2.40	-2.51	-2.44
1.35	0.55	-1.22	-1.16	-1.19	-1.18	0.41	0.30	0.41	0.39	-2.74	-2.67	-2.74	-2.69
1.35	0.70	-1.29	-1.25	-1.26	-1.25	1.17	1.15	1.20	1.23	-3.47	-3.44	-3.46	-3.39
1.35	0.80	-1.19	-1.15	-1.16	-1.15	2.42	2.42	2.44	2.46	-3.89	-3.88	-3.89	-3.80
1.35	0.90	-0.91	-0.87	-0.88	-0.87	4.58	4.53	4.52	4.52	-4.19	-4.22	-4.20	-4.11
1.35	0.95	-0.67	-0.64	-0.66	-0.64	6.32	5.97	5.98	5.97	-4.23	-4.33	-4.29	-4.21
2.74	0.10	-0.03	-0.02	-0.03	-0.03	0.97	0.98	0.98	0.98	-0.22	-0.22	-0.22	-0.22
2.74	0.20	-0.05	-0.03	-0.05	-0.05	0.99	0.99	0.99	0.99	-0.44	-0.44	-0.44	-0.43
2.74	0.30	-0.05	-0.02	-0.04	-0.04	1.04	1.05	1.06	1.05	-0.65	-0.65	-0.65	-0.64
2.74	0.40	-0.00	0.00	-0.00	-0.00	1.20	1.19	1.20	1.20	-0.86	-0.86	-0.86	-0.86
2.74	0.55	0.06	0.07	0.12	0.11	1.65	1.65	1.66	1.66	-1.17	-1.17	-1.16	-1.16
2.74	0.70	0.37	0.39	0.38	0.37	2.64	2.62	2.62	2.60	-1.42	-1.42	-1.42	-1.43
2.74	0.80	0.65	0.67	0.66	0.65	3.60	3.70	3.67	3.67	-1.56	-1.56	-1.54	-1.55
2.74	0.90	1.04	1.07	1.05	1.05	5.14	5.24	5.17	5.25	-1.62	-1.61	-1.59	-1.61
2.74	1.00	1.58	1.63	1.60	1.61	7.39	7.35	7.29	7.56	-1.53	-1.53	-1.53	-1.58
2.74	1.08	2.16	2.19	2.16	2.21	9.58	9.46	9.52	10.15	-1.39	-1.39	-1.39	-1.44
AAD=			0.16	0.07	0.07		0.23	0.12	0.08		0.09	0.03	0.06

[1] Hansen (1970). [2] Verlet and Weis (1972). [3] Johnson et al. (1993).

4.3. EOS for LJ mixtures

It is known that the LJ potential represents a basic force for real molecules. Consequently, LJ mixtures will represent the prototype of real mixtures, which have tremendous applications in chemical engineering. The behavior of LJ mixtures has produced some very interesting phenomena such as VLE, LLE, aggregation and phase separation, and gas solubility in solvents. Theoretically, the nonideality of LJ mixtures is important for developing more accurate solution models, which may overcome the defects of commonly known models such as the NRTL and UNIFAC models. These practical models have to use two inconsistent sets of parameters for VLE and LLE. Since the LJ molecules studied here are spherical, the nonideality will be attributed only to two LJ parameters, σ_{ij} and ϵ_{ij}. The variation of the two parameters will generate a number of characteristics of nonideal solutions.

At present, there are two types of practical theories to study LJ mixtures. One is the perturbation theory and the other is the conformal solution theory. Lee and Levesque (1973) presented the first reliable perturbation theory for LJ mixtures, which splits the LJ potential into repulsive and attractive parts by the WCA method. This theory is only applicable to slightly nonideal LJ mixtures and was later made sophisticated by a number of authors (Shukla et al., 1986; Bohn et al., 1986; Shukla, 1987; Lotfi and Fisher, 1989; Fotouh and Shukla, 1997). It is valuable to mention that in the theory of Lee and Levesque, the diameters of the hard-sphere reference mixture are independent of composition explicitly, which have brought a number of shortcomings found by later studies (Shukla, 1987; Lotfi and Fisher, 1989). Subsequently, composition-dependent diameters were adopted in these studies by forcing the so-called blip-integrals vanish. The diameter selection presented in Section 3.6 is in a spirit equivalent to those of Shukla (1987) and Lotfi and Fisher (1989), but with less computation. It should be borne in mind that the reference system indicated in (165) is considerably different from all other perturbation theories. The split of the LJ potential in (165) is more similar to that of the BH theory while others are variations of the WCA theory. The WCA-type reference will result in an expensive computational work to obtain hard-sphere diameters due to the number of involved

integrals. In contrast, the diameters used in this work can be easily calculated from an empirical expression (163). It is also noted that all other perturbation theories are first-order type while the present theory is second-order. The accuracy of first-order WCA-type theories is highly subject to the range of densities and is believed to be poor at low densities. Fotouh and Shukla (1997) have utilized recently the random phase approximation to remedy the deficiency but at a cost of extra computation. The present second-order theory developed from the LJ RDF performs equally well from low densities to high densities, based on the observation for the pure LJ fluid. In Section 3.6, it has been seen that the structure of LJ mixtures has been given fairly well by Equation (156). The good performance is expected to be maintained for thermodynamic calculations. As in the pure fluid case, one very powerful advantage of the proposed theory is its analytical simplicity, which is important for practical purposes. At just this point, all other perturbation theories are incompetent because of their tedious numerical integration work.

In addition to perturbation theory, the conformal solution theory is another approach to study LJ mixtures. This theory treats LJ mixtures as a pure LJ fluid with some mixing rules. Obviously, the theory is much less rigorous than perturbation theory and its applicability has to be investigated more carefully. At present, the most successful conformal solution theory is the van der Waals one-fluid (VDW1) theory. The VDW1 theory has been examined over a wide range of conditions (Shukla et al., 1986; Shing et al., 1988; Harismiadis et al., 1991; Fotouh and Shukla, 1997). These studies indicate that the VDW1 theory is unreliable for pressure, thermodynamic excess properties, chemical potential in infinite dilution and liquid density in phase equilibria if parameter ratios (σ_{12}/σ_{11}, $\epsilon_{12}/\epsilon_{11}$) deviate from 1 appreciably, but is good for the calculation of phase equilibria composition of binary mixtures with more relaxed parameter ratios. It is necessary to mention that, as well as the above-mentioned theories, cubic equations of state have been tested (Harismiadis et al., 1994) for LJ mixtures but found unsuccessful even with a number of adjustable parameters. This testing suggests that the application of a simple empirical equation of state for real mixtures is theoretically doubtful.

Computer simulation is another way to study LJ mixtures, and simulation data are indispensable for the development of new liquid theories for LJ mixtures although computational time is very high. Among LJ mixture simulations, Shing and Gubbins (1983) gave data for chemical potential. Shukla et al. (1986) presented the results of a number of thermodynamic excess properties. Lotfi and Fisher (1989) simulated extensively chemical potential at infinite dilution. Phase equilibria has been studied by computer simulation actively in recent years. Harismiadis et al. (1991) gave VLE data over a wide range of conditions by the MC method. Their systems were further investigated by Vrabec et al. (1995) by the MD simulation. Guo at al. (1995) for the first time reported LLE simulation results. These simulation results have greatly prompted the development of theories. In this work, those simulation data will be compared extensively in evaluating the performance of the present EOS of mixtures.

a). Helmholtz free energy

Analogous to pure fluids in Section 4.2, the Helmholtz free energy of a mixture can be expressed by a perturbation expansion in terms of functional derivative to second order:

$$a=a_{rep}+\sum_i\sum_j\int\left(\frac{\partial a}{\partial u_{ij}(r)}\right)_{rep}\delta u_{ij}(r)\,d\mathbf{r}+ \frac{1}{2}\sum_i\sum_j\sum_m\sum_n\iint\left(\frac{\partial^2 a}{\partial u_{ij}(r)\,\partial u_{mn}(r_1)}\right)_{rep}\delta u_{ij}(r)\,\delta u_{mn}(r_1)\,d\mathbf{r}\,d\mathbf{r}_1 \tag{235}$$

where the subscript rep stands for the reference system whose molecules interact through repulsive force alone. This system has to be approximated by a hard sphere mixture for practical calculation. a_{rep} has been developed in Section 3.6, giving

$$a_{rep}=a_0-2\pi\rho\sum_i\sum_j x_i x_j g_{0,ij}(R_{ij})\,R_{ij}^2(R_{ij}-d_{ij}) \tag{236}$$

where R_{ij} is given in (165) and the Helmholtz free energy of hard sphere mixtures is given by (Mansoori et al., 1971)

$$a_0=\frac{1}{\rho}\left[\frac{\left(\frac{\pi}{2}\xi_1\xi_2-\xi_2^3/\xi_3^2\right)}{\Delta}+\frac{\xi_2^3}{\xi_3^2\Delta^2}+\frac{\xi_2^3}{\xi_3^2}\ln\Delta\right]-\ln\Delta \tag{237}$$

The attractive force of the LJ potential, which is the perturbation function in (235), is given by

$$\delta u_{ij}(r)=\begin{cases} 0, & r<\sigma_{ij} \\ -k_{1,ij}\epsilon_{ij}\dfrac{e^{-z_{1,ij}(r-R_{ij})}}{r}+k_{2,ij}\epsilon_{ij}\dfrac{e^{-z_{2,ij}(r-R_{ij})}}{r}, & r>\sigma_{ij} \end{cases} \tag{238}$$

Further assuming that the structure of the reference fluid can be represented by that of the hard sphere mixture, then the subscript rep in the second and third terms of the right-hand side of (235) can be replaced by subscript 0. Utilizing the following relations between RDF and functional derivatives of Helmholtz free energy

$$\begin{gathered}\left(\frac{\partial a}{\partial u_{ij}(r)}\right)_0=\frac{1}{2}\rho\beta x_i x_j g_{0,ij}(r) \\ \sum_m\sum_n\int\left(\frac{\partial^2 a}{\partial u_{ij}(r)\,\partial u_{mn}(r_1)}\right)_0\delta u_{mn}(r_1)\,dr_1=\frac{1}{2}\rho x_i x_j\beta g_{1,ij}(r)\end{gathered} \tag{239}$$

one can obtain

$$a=a_0+a_1+a_2 \tag{240}$$

with

$$\begin{aligned} a_1&=2\pi\rho\beta\sum_i\sum_j\int_{\sigma_{ij}}^{\infty}g_{0,ij}(r)\,u_{ij}(r)\,r^2dr, \\ a_2&=\pi\rho\beta\sum_i\sum_j\int_{\sigma_{ij}}^{\infty}g_{1,ij}(r)\,u_{ij}(r)\,r^2dr \end{aligned} \tag{241}$$

After some algebraic work similar to that in Section 4.2, it is found that

$$a_1=-2\pi\rho\beta\sum_i\sum_j x_i x_j\epsilon_{ij}\left[k_{1,ij}\left(G_{0,ij}(z_{1,ij})\,e^{z_{1,ij}R_{ij}}-\frac{1+z_{1,ij}R_{ij}}{z_{1,ij}^2}\right)-k_{2,ij}\times\right.$$

$$\left.\left(G_{0,ij}(z_{2,ij})\,e^{z_{1,ij}R_{ij}}-\frac{1+z_{2,ij}R_{ij}}{z_{2,ij}^2}\right)\right]+8\pi\rho\beta\sum_i\sum_j x_i x_j\epsilon_{ij}\left[\frac{1}{9}\left(\frac{\sigma_{ij}}{R_{ij}}\right)^6-\frac{1}{3}\left(\frac{\sigma_{ij}}{R_{ij}}\right)^6\right] \quad (242)$$

$$-8\pi\rho\beta\sum_i\sum_j x_i x_j\epsilon_{ij}g_{0,ij}(R_{ij})\left[\frac{1}{9}\left(\frac{\sigma_{ij}}{R_{ij}}\right)^{12}-\frac{1}{3}\left(\frac{\sigma_{ij}}{R_{ij}}\right)^6+\frac{2}{9}\left(\frac{\sigma_{ij}}{R_{ij}}\right)^3\right]$$

$$a_2=-\pi\rho\beta\sum_i\sum_j\epsilon_{ij}\left[k_{1,ij}G_{1,ij}(z_{1,ij})\,e^{z_{1,ij}R_{ij}}-k_{2,ij}G_{1,ij}(z_{2,ij})\,e^{z_{2,ij}R_{ij}}\right] \quad (243)$$

$$-4\pi\rho\beta\sum_i\sum_j x_i x_j\epsilon_{ij}g_{1,ij}(R_{ij})\left[\frac{1}{9}\frac{\sigma_{ij}^{12}}{R_{ij}^9}-\frac{1}{3}\frac{\sigma_{ij}^6}{R_{ij}^3}+\frac{2}{9}\sigma_{ij}^3\right]$$

where

$$g_{0,ij}(R_{ij})=\frac{1}{R_{ij}\Delta}\left(R_{ij}+\frac{\pi R_i R_j\xi_2}{4\Delta}\right) \quad (244)$$

$$g_{1,ij}(R_{ij})=\frac{1}{2\pi\sqrt{\rho_i\rho_j}R_{ij}}\times$$

$$\left[K_{1,ij}+\sum_n K_{1,in}A_{jn}(z_{1,in})+\sum_m K_{1,mj}A_{im}(z_{1,mj})+\sum_m\sum_n K_{1,mn}A_{im}(z_{1,mn})A_{jn}(z_{1,mn})\right. \quad (245)$$

$$\left.-K_{2,ij}-\sum_n K_{2,in}A_{jn}(z_{2,in})-\sum_m K_{2,mj}A_{im}(z_{2,mj})-\sum_m\sum_n K_{2,mn}A_{im}(z_{2,mn})A_{jn}(z_{2,mn})\right]$$

With the Helmholtz free energy (240) in hand, one can easily obtain other thermodynamics of LJ mixtures. Some typical properties are listed as follows:

b). Compressibility factor

$$Z=1+\rho\frac{\partial a}{\partial\rho} \quad (246)$$

c). Internal energy

$$u=-T\frac{\partial a}{\partial T} \tag{247}$$

d). Chemical potential

$$\frac{\mu_i-\mu_i^{id}}{kT}=a+\rho\frac{\partial a}{\partial \rho_i} \tag{248}$$

e). Excess Helmholtz free energy

$$a^{ex}=a-\sum_i x_i a_i \tag{249}$$

with

$$a_i=a(T,\rho_1,\ldots,\rho_N)\,|_{\rho_i=\rho,\,\rho_{j\neq i}=0} \tag{250}$$

It should be borne in mind that

$$a(T,\rho_1,\ldots,\rho_N)=a(T,\rho,x_1,\ldots,x_N) \tag{251}$$

in algebraic work of (246)-(249). More explicit expressions for (246)-(249) may be obtained by using an analogous scheme in Section 4.2 for the pure LJ fluid, but the results will be very tedious and will not benefit the computation more than utilizing a numerical method for partial differentiation. In this work, the numerical differentiation is practically implemented by

$$y\frac{\partial f(y)}{\partial y}=\frac{f(y(1+t))-f(y(1-t))}{2t} \tag{252}$$

where the adjustable parameter t is generally taken as 0.01.

4.4. Comparisons with computer simulation data of LJ mixtures

The following typical properties widely utilized as a criterion for the success of a theory are demonstrated here: pressure, excess Helmholtz free energy, chemical potential, VLE and LLE. The performance of the present theory will be discussed sequentially below. First, a comparison of pressure given by MC simulation, the VDW1 theory, the perturbation theory of Fotouh and Shukla (1997) and Equation (246) is shown in Table 7. The parameter ratios are $\epsilon_{22}/\epsilon_{11}=1.0\sim4.5$, $\sigma_{22}/\sigma_{11}=1.0\sim2.0$, covering a wide range of states. The AAD of the three theories are 8.8, 2.3 and 1.9, respectively and the maximum deviations of these theories are 29, 8 and 6, respectively. Obviously, the VDW1 theory is not reliable for the pressure calculation. It should be mentioned here that the VDW1 results of Fotouh and Shukla (1997) were obtained by a very accurate EOS of the pure LJ fluid. There is almost no more room for improving the pressure prediction of the VDW1 theory for mixtures by adopting a more accurate EOS of the pure LJ fluid. Compared with the perturbation theory of Fotouh and Shukla, the present theory is clearly an improvement. The improvement is further evident in Tables 8 and 9 for excess free energy calculations. The calculations includes two temperatures T = 120 K and T = 300 K and parameter ratios $\epsilon_{22}/\epsilon_{11}=2\sim4$, $\gamma_{12}=0.7071\sim1.4142$, $\sigma_{22}/\sigma_{11}=1$, $l_{12}=1.0$. The proposed theory performs better at higher temperatures than lower ones, which is a nature of perturbation theories. Again, the errors of the VDW1 theory, ranging from 50% to 100%, are intolerable for this excess property. Based on the above results and further comparisons given by Fotouh and Shukla (1997), it is virtually conclusive that the VDW1 theory is inappropriate for the calculations of pressure and thermodynamic excess properties.

Chemical potential is a very important property in describing mixture behavior. Chemical potential at infinite dilution ($x_1\to0$) is of special interest for chemical engineers for reason of its association with Henry's constant H_{12} by

$$H_{12}=\rho_2 RTe^{\frac{\mu_1^{\infty}-\mu_1^{id}}{kT}} \tag{253}$$

where 1 and 2 stands for gas and solvent, respectively. Henry's constant is often utilized to predict the solubility of gases in solvents, especially in supercritical extraction (Boublik, 1997). Table 10 shows that the present theory predicts excellently the chemical potential at infinite dilution, for parameter ratios $\epsilon_{12}/\epsilon_{22}$ = 0.25 ~ 2.0, σ_{12}/σ_{22} = 0.79 ~ 1.26. The prediction is a considerable improvement over the perturbation theory (PT) of Lotif and Fisher (1989). The improvement is more conspicuous at higher σ_{12}/σ_{11} ratios. The performance of the proposed theory for chemical potential at finite concentrations looks less satisfactory in Table 11. However, a more subtle analysis of the MC data and MD data in the table indicates that there may exist a systematic error for the MC data published many years ago (Shing and Gubbins; 1983). Since the MC data at the two terminal points deviate from the MD values severely, there is a reason to doubt the accuracy of the MC data at finite concentrations. The present results are believed more reasonable than either the MC data or the PT results. At this point, it appears desirable to carry out a third computer simulation to verify this speculation.

Phase equilibria including VLE and LLE are always immediately concerned by practical engineers for their industrial applications. In chemical engineering, there are a number of models for calculating phase equilibria, such as NRTL, UNIQAC and UNIFAC models. These models are found successful for different types of mixtures. However, there is a very serious problem unresolved for all these models, i. g., inconsistent sets of parameters are used for the VLE and LLE of the same system. The disturbing inconsistency is believed to come from the empirical nature of these models, resulting in their failure to describe mixture behavior at high densities and low densities simultaneously. Only a model with a rigorous theoretical background is likely to resolve the inconsistency. The present perturbation theory will serve as a preliminary answer to the standing issue of representation of VLE and LLE simultaneously. In phase equilibria calculations, the following equilibrium conditions

$$P^V=P^L,\ \mu_1^V=\mu_1^L,\ \ldots,\ \mu_N^V=\mu_N^L \tag{254}$$

for VLE and

$$P^{L_1}=P^{L_2},\ \mu_1^{L_1}=\mu_1^{L_2},\ \ldots,\ \mu_N^{L_1}=\mu_N^{L_2} \tag{255}$$

for LLE are used to determine the relation between pressure, temperature, concentration and density. In the calculation, the Newton method is utilized to solve a set of Equations (254) or (255) for unknowns. Figures 17 to 36 depict the VLE predictions by means of Equation (254) and the latest MD simulation (Vrabec et al., 1995). Figures 37 to 41 give comparisons between our prediction and the MC simulation (Guo et al., 1995) for LLE.

It is evident that the present theory gives a very good prediction of VLE for LJ mixtures with $\sigma_{22}/\sigma_{11}=1$ and $\epsilon_{22}/\epsilon_{11}=0.5\sim0.75$. Both pressure-composition and pressure-density at two temperatures are obtained equally well. In contrast, a WCA-type perturbation theory demonstrated by Vrabec et al.(1995) is only applicable to the lower temperature $T^*=0.75$ because of its restriction to high densities. The application of the present theory for parameter ratios $\sigma_{22}/\sigma_{11}=1.5$ and $\epsilon_{22}/\epsilon_{11}=0.66\sim1.5$ in Figures 22 to 27 looks less satisfactory. However, when one compares the MD data with the MC data reported earlier (Harismiadis et al., 1991) at these parameter ratios, it is found that there are substantial disagreements between them. Significant uncertainties in both of these two simulations have been claimed in their original papers. Therefore, a more stable computer simulation is needed for examining the applicability of a theory at these parameter ratios. For $\sigma_{22}/\sigma_{11}=0.5$ and $\epsilon_{22}/\epsilon_{11}=0.5\sim1.0$ in Figures 28 to 36, the present theory yields again a rather good description of both pressure-composition and pressure-density relations. It is proper to mention here that the VDW1 theory, although very poor for the pressure and excess property calculations as mentioned above, gives surprisingly a rather good prediction of the pressure-composition relation according to the conclusion of Harismiadis et al. (1991). From the observation in Figures 17 to 36, the prediction is inferior to or at most similar to the present theory for pressure-composition. As

far as pressure-composition is concerned, the VDW1 theory is found disappointing, especially at $\sigma_{22}/\sigma_{11}=0.5$ where liquid densities are systematically overestimated. Therefore, it is proven again that only those robust theories can yield confidently a wide range of thermodynamic properties.

The LLE prediction by the present theory is demonstrated in Figures 37 to 41. Unlike VLE where LJ mixtures may obey the LB combining rule, the interacting parameters of LJ mixtures must deviate from the rule to ensure the occurrence of LLE. In other words, $\gamma_{12}=1$ and $l_{12}=1$ can not exist simultaneously. Figures 37 and 38 indicate that the present theory gives a rather good LLE prediction for two LJ mixtures as long as the temperature is away from the upper critical solution temperature (UCST). As anticipated, the nonclassic behavior of LLE around the UCST is indescribable by a classic theory like the proposed one. The same arguments may be utilized to interpret the relatively less satisfactory prediction in Figure 39 where the MC data are very close to the UCST. Nevertheless, in that figure, the present prediction is still much better that of the VDW1 theory. The LLE prediction for the other two mixtures in Figures 40 and 41 is acceptable in view of the fact that the MC data are not stable and smooth. Unexpectedly in these two figures, the VDW1 theory performs slightly better. Overall, the present theory gives a comparable performance to the VDW1 theory for five LJ mixtures considered here. It should be pointed out that computer simulation data for LLE is very scarce in the literature and we need more simulation data to draw conclusions about the applicability of the present theory for LLE. As well, it would be of value to see other theories to be utilized for the LLE prediction and to see if such a prediction is more sensitive to the accuracy of theories. Only after comparisons with more accurate simulation results and other theories, one can fully answer if the parameter inconsistency of NRTL, UNIQAC and UNIFAC models between VLE and LLE comes from the empirical nature of these models.

Finally, based on the above comparisons, the following conclusions about the performance of the proposed perturbation theory can be drawn:

a) The present theory is the only perturbation theory available today to be implemented in a straightforward and analytical manner. Equation (240) is nearly as

simple as other empirical EOS for mixtures. All other perturbation theories including those of Fotouh and Shukla (1997)and Lotif and Fisher (1989) need extensive integration and their computation is much more time-consuming than the present one.

b) The present perturbation theory is developed from the first-order solution of the OZ equation or the RDF of LJ mixtures. The structure picture is clear in this theory and this distinct feature cannot be expected by any other known perturbation theories. The present theory is applicable at low densities and high densities while a WCA-type theory is only valid for high densities.

c) Extensive comparisons with computer simulation data show that the proposed theory is a considerable improvement over those of Fotouh and Shukla (1997) and Lotif and Fischer (1989). The improvement, covering the calculations of pressure, excess Helmholtz free energy, chemical potential at infinite dilution and phase equilibria, is almost overwhelming.

d) For VLE, to our knowledge, this theory is the only one capable of reproducing simulation results for pressure-concentration and pressure-density simultaneously at low and high temperatures . The perturbation theory of Lotif and Fischer (1989) and the VDW1 theory suffer different failures at this perspective. The performance of the theory of Fotouh and Shukla (1997) for VLE has not yet been reported but is unlikely to surpass the present one, based on the observation of its performance on the calculation of thermodynamic properties.

e) For LLE, this theory has shown promise in predicting the important phase behavior. Further investigation of the theory for LLE needs more computer simulation results.

f) In addition to LLE data, it is desirable to have more computer simulation results for chemical potential and VLE for a comprehensive evaluation of the present theory.

g) There is one straightforward way to make the proposed theory more sophisticated by incorporating the SEXP approximation in Section 3.8. It is conceivable that the SEXP approximation will make the prediction more accurate if the involved extra integration is not a heavy burden.

Table 7. pressure (bar) of LJ mixtures at T=200 K, ϵ_{11}/k=34 K, σ_{11}=2.85Å and $x_1=x_2=0.5$

$\rho\sigma_x^3$	$\epsilon_{22}/\epsilon_{11}$	σ_{22}/σ_{11}	MC[a]	δP% VDW1[b]	δP% PTH[c]	δP% this work
0.90	1.00	1.30	3445	-4	0	0.2
0.90	1.00	2.00	1549	-15	1	1.7
0.90	1.50	1.00	5307	1	1	2.1
0.90	1.50	1.30	3563	-4	1	1.9
0.90	1.50	2.00	1629	-16	5	6.1
0.90	2.50	1.00	5271	4	1	3.6
0.90	2.50	1.30	3691	-4	1	0.8
0.90	2.50	2.00	1778	-21	6	5.0
0.90	3.50	1.30	3680	-3	1	0.1
0.90	3.50	2.00	1851	-24	7	4.2
0.90	4.50	1.00	5159	7	1	0.6
0.90	4.50	1.30	3551	-1	-1	1.0
0.90	4.50	2.00	1905	-29	7	2.4
0.80	1.50	1.05	3323	1	1	1.8
0.80	1.50	1.30	2347	-1	2	2.6
0.80	1.50	1.55	1765	-7	0	0.5
0.80	1.50	2.00	1078	-14	1	1.8
0.80	2.50	1.05	3323	0	0	-0.8
0.80	2.50	1.30	2323	-1	2	1.6
0.80	2.50	1.55	1690	-5	4	4.0
0.80	2.50	2.00	1081	-17	4	3.2
0.80	3.50	1.05	3162	2	0	-1.0
0.80	3.50	1.30	2213	-1	2	1.3
0.80	3.50	1.55	1716	-11	0	-2.0
0.80	3.50	2.00	1097	-23	2	-0.6
0.80	4.50	1.05	2935	6	0	-0.1
0.80	4.50	1.30	2092	-1	1	0.0
0.80	4.50	1.55	1568	-10	2	0.6
0.80	4.50	2.00	1076	-29	0	-3.1
0.69	1.50	1.30	1531	-2	-1	-0.5
0.71	1.50	2.00	711	-10	2	2.2
0.43	4.50	2.00	109	-9	-8	-4.2
AAD %				8.8	2.3	1.9

$\rho\sigma_x^3=\rho(x_1\sigma_{11}^3+x_2\sigma_{22}^3)$, [a] Hoheisel et al. (1983) [b,c] Fotouh and Shukla (1997)

Table 8. Excess free energy (J/mol) of LJ mixtures at T=120 K, $\sigma_{11}=\sigma_{22}=3.405$Å and $\rho\sigma_{11}^3=0.75$

			$x_1=0.25$				$x_1=0.5$				$x_2=0.75$			
ϵ_{11}/k	ϵ_{22}/k	ϵ_{12}/k	MC[a]	VDW1[b]	PTH[c]	this	MC	VDW1	PTH	this	MC	VDW1	PTH	this
84.71	169.42	119.80	134	153	142	126	180	204	188	169	140	153	139	127
69.17	207.50	119.80	335	397	360	319	444	525	476	428	348	394	355	323
59.90	239.60	119.80	546	655	582	513	724	860	771	686	552	642	574	521
84.71	169.42	84.71	670	736	717	655	904	960	954	872	676	704	708	660
84.71	169.42	169.42	-733	-682	-682	-688	-955	-890	-899	-926	-726	-646	-674	-695
79.87	159.73	119.80	15	31	19	12	20	44	27	15	17	37	20	12
59.90	179.70	119.80	37	72	46	28	48	107	64	38	37	94	48	28
47.92	191.68	119.80	51	107	71	44	65	164	96	58	44	149	73	42
AAD=				0.48	0.16	0.11		0.57	0.18	0.10		0.71	0.16	0.11

[a] Shukla et al. (1986) [b,c] Fotouh and Shukla (1997)

Table 9. Excess free energy (J/mol) of LJ mixtures at T=300 K, $\sigma_{11}=\sigma_{22}=3.405$Å and $\rho\sigma_{11}^3=0.75$

			$x_1=0.25$				$x_1=0.5$				$x_2=0.75$			
ϵ_{11}/k	ϵ_{22}/k	ϵ_{12}/k	MC[a]	VDW1[b]	PTH[c]	this	MC	VDW1	PTH	this	MC	VDW1	PTH	this
84.71	169.42	119.80	125	161	132	123	166	216	174	164	125	163	130	123
69.17	207.50	119.80	325	409	337	313	442	549	447	418	315	415	333	314
59.90	239.60	119.80	513	670	546	507	690	884	723	676	520	670	539	508
84.71	169.42	84.71	572	647	581	554	758	824	774	742	571	589	577	559
84.71	169.42	169.42	-576	-547	-561	-566	-771	-694	-744	-758	-586	-478	-560	-571
79.87	159.73	119.80	27	58	32	26	36	84	42	35	27	70	31	26
59.90	179.70	119.80	63	132	76	66	88	202	100	87	56	178	74	63
47.92	191.68	119.80	82	196	117	109	122	307	151	141	72	283	112	102
AAD=				0.58	0.13	0.07		0.64	0.09	0.04		0.98	0.15	0.09

[a] Shukla et al. (1986) [b,c] Fotouh and Shukla (1997)

Table 10. Chemical potential $(\mu_1-\mu_1^{id})/kT$ of LJ mixtures at infinite dilution, $kT/\epsilon_{22}=1.2$ and $\rho\sigma_{22}^3=0.7$

$(\sigma_{12}/\sigma_{22})^3$	$\epsilon_{12}/\epsilon_{22}$	MD[a]	PT[b]	this
0.5	0.250	1.223	1.222	1.204
	0.500	0.408	0.399	0.391
	0.750	-0.559	-0.554	-0.561
	1.000	-1.603	-1.557	-1.575
	1.250	-2.701	-2.587	-2.636
	1.500	-3.840	-3.632	-3.724
	2.000	-6.224	-5.749	-5.993
0.75	0.250	2.245	2.267	2.221
	0.500	1.102	1.080	1.074
	0.750	-0.273	-0.314	-0.289
	1.000	-1.761	-1.788	-1.752
	1.250	-3.324	-3.304	-3.280
	1.500	-4.947	-4.845	-4.849
	2.000	-8.336	-7.968	-8.112
1.00	0.250	3.302	3.365	3.293
	0.375	2.631	2.651	2.613
	0.500	1.842	1.821	1.814
	0.625	0.983	0.928	0.952
	0.750	0.077	-0.004	0.043
	0.875	-0.865	-0.962	-0.887
	1.000	-1.834	-1.938	-1.846
	1.125	-2.826	-2.928	-2.823
	1.500	-5.917	-5.951	-5.860
	2.000	-10.243	-10.050	-10.081
	4.000	-29.084	-26.740	-28.480
1.25	0.250	4.343	4.478	4.333
	0.500	2.555	2.579	2.541
	0.750	0.388	0.329	0.384
	1.000	-1.959	-2.057	-1.921
	1.250	-4.427		-4.338
	1.500	-6.988	-7.011	-6.826
	2.000	-12.340	-12.080	-11.985
1.50	0.250	5.390	5.588	5.383
	0.500	3.300	3.336	3.274
	0.750	0.767	0.666	0.737
	1.000	-1.979	-2.165	-1.993
	1.250	-4.869		-4.839
	1.500	-7.873	-8.044	-7.775
	2.000	-14.170	-14.060	-13.859
2.00	0.250	7.415	7.790	7.438
	0.500	4.709	4.839	4.703
	0.750	1.437	1.339	1.403
	1.000	-2.100	-2.387	-2.138
	1.250	-5.804	-6.155	-5.841
	1.500	-9.629	-10.070	-9.654
	2.000	-17.530	-17.950	-17.560
AAD=			0.06	0.02

[a,b] Lotif and Fischer (1989)

Table 11. Chemical potential $(\mu_1-\mu_1^{id})/kT$ of LJ mixtures at finite concentrations, $kT/\epsilon_{22}=1.2$, $\rho\sigma_x^3=0.7$, $(\sigma_{12}/\sigma_{22})^3=1.5$ and $\epsilon_{11}/\epsilon_{22}=1$

x_1	MC[a]	MD[b]	PT[c]	this
0.0000	-1.870	-1.979	-2.165	-1.990
0.0185	-1.970		-2.176	-2.000
0.0741	-2.060		-2.197	-2.030
0.1481	-2.170		-2.205	-2.040
0.3333	-2.230		-2.172	-2.030
0.5000	-2.160		-2.117	-1.992
0.6667	-2.090		-2.055	-1.942
0.8519	-2.020		-1.988	-1.883
0.9259	-2.000		-1.963	-1.858
1.0000	-1.930	-1.848	-1.938	-1.843

$\rho\sigma_x^3=\rho(x_1\sigma_{11}^3+x_2\sigma_{22}^3)$, [a] Shing and Gubbins (1983) [b,c] Lotif and Fischer(1989)

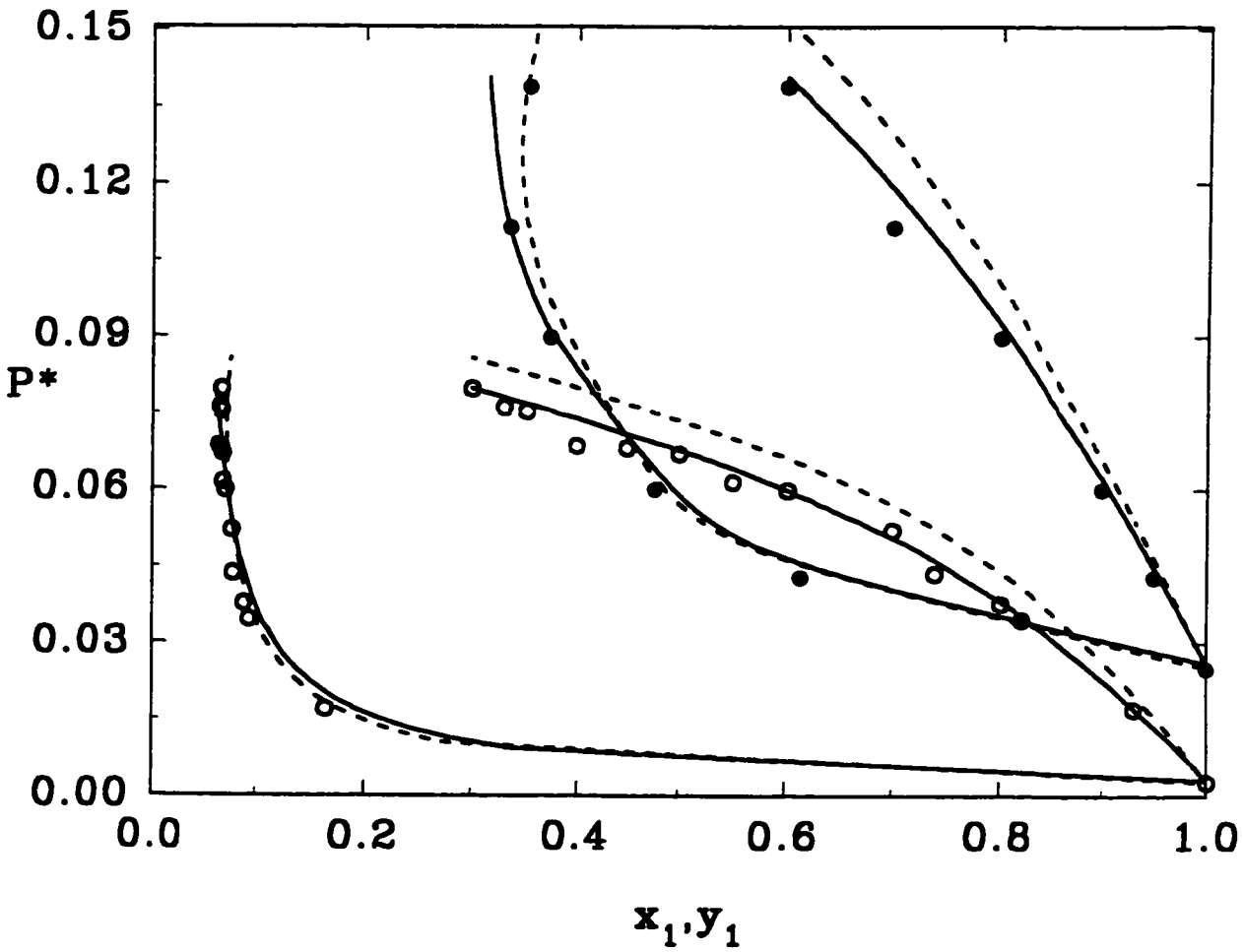

Figure 17. VLE of a LJ mixture with σ_{22}/σ_{11}=1, $\epsilon_{22}/\epsilon_{11}$=0.5. The open and filled circles are the MD data (Vrabec et al., 1995) at T*=0.75 and T*=1.00, respectively. The solid and dashed lines are results from the present and VDW1 theory, respectively.

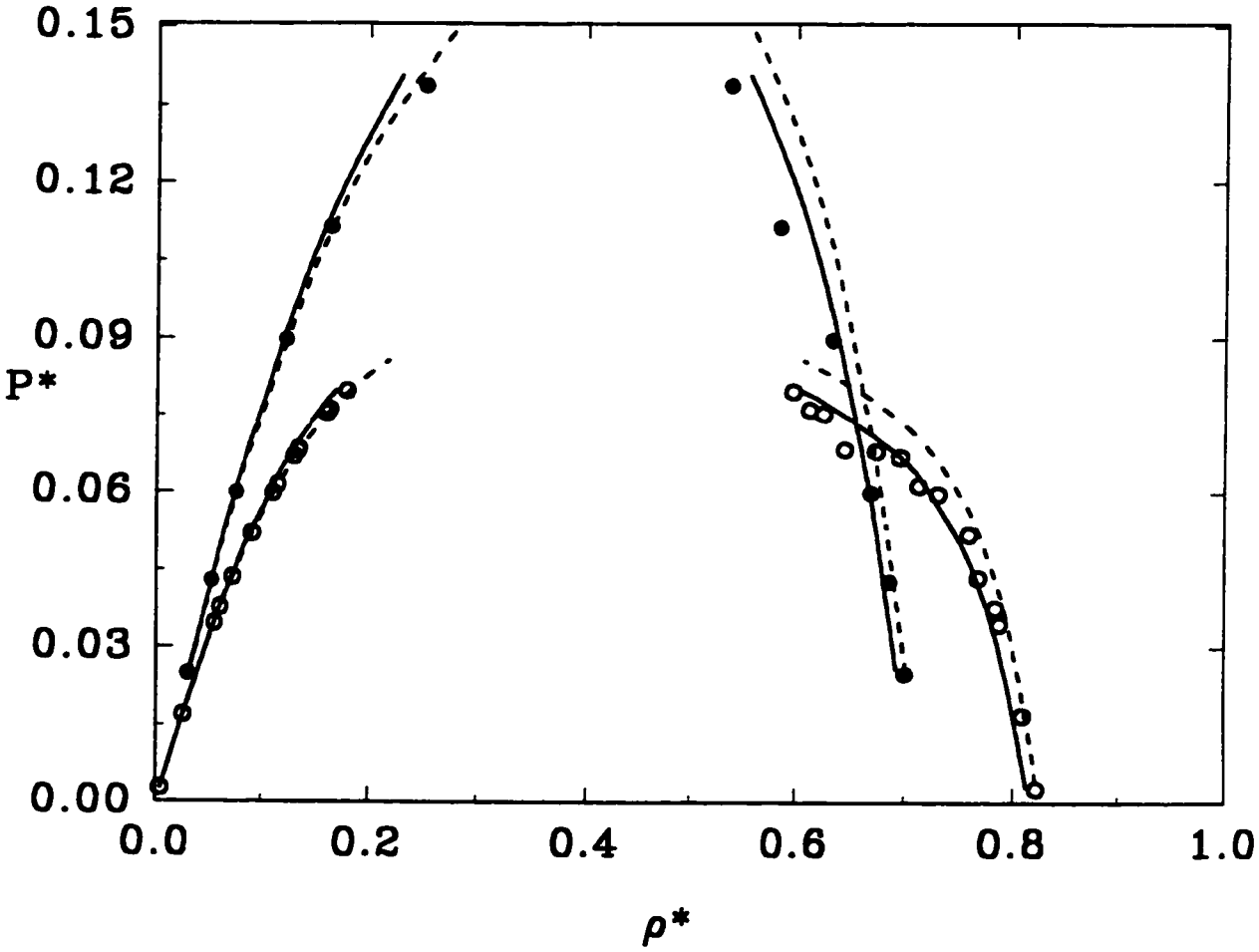

Figure 18. VLE of a LJ mixture with $\sigma_{22}/\sigma_{11}=1$, $\epsilon_{22}/\epsilon_{11}=0.5$. The open and filled circles are the MD data (Vrabec et al., 1995) at $T^*=0.75$ and $T^*=1.00$, respectively. The solid and dashed lines are results from the present and VDW1 theory, respectively.

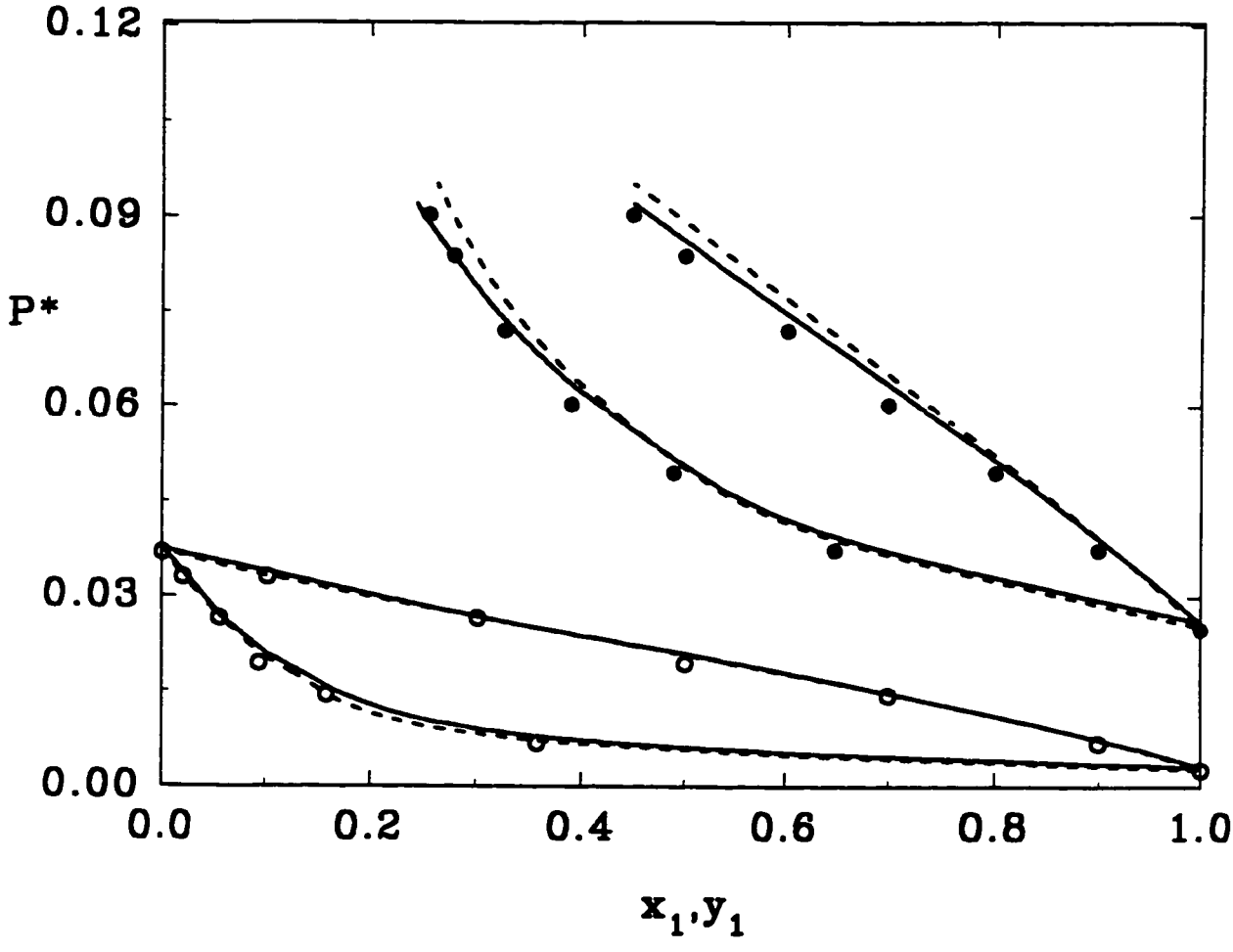

Figure 19. VLE of a LJ mixture with σ_{22}/σ_{11}=1, $\epsilon_{22}/\epsilon_{11}$=0.66. The open and filled circles are the MD data (Vrabec et al., 1995) at T*=0.75 and T*=1.00, respectively. The solid and dashed lines are results from the present and VDW1 theory, respectively.

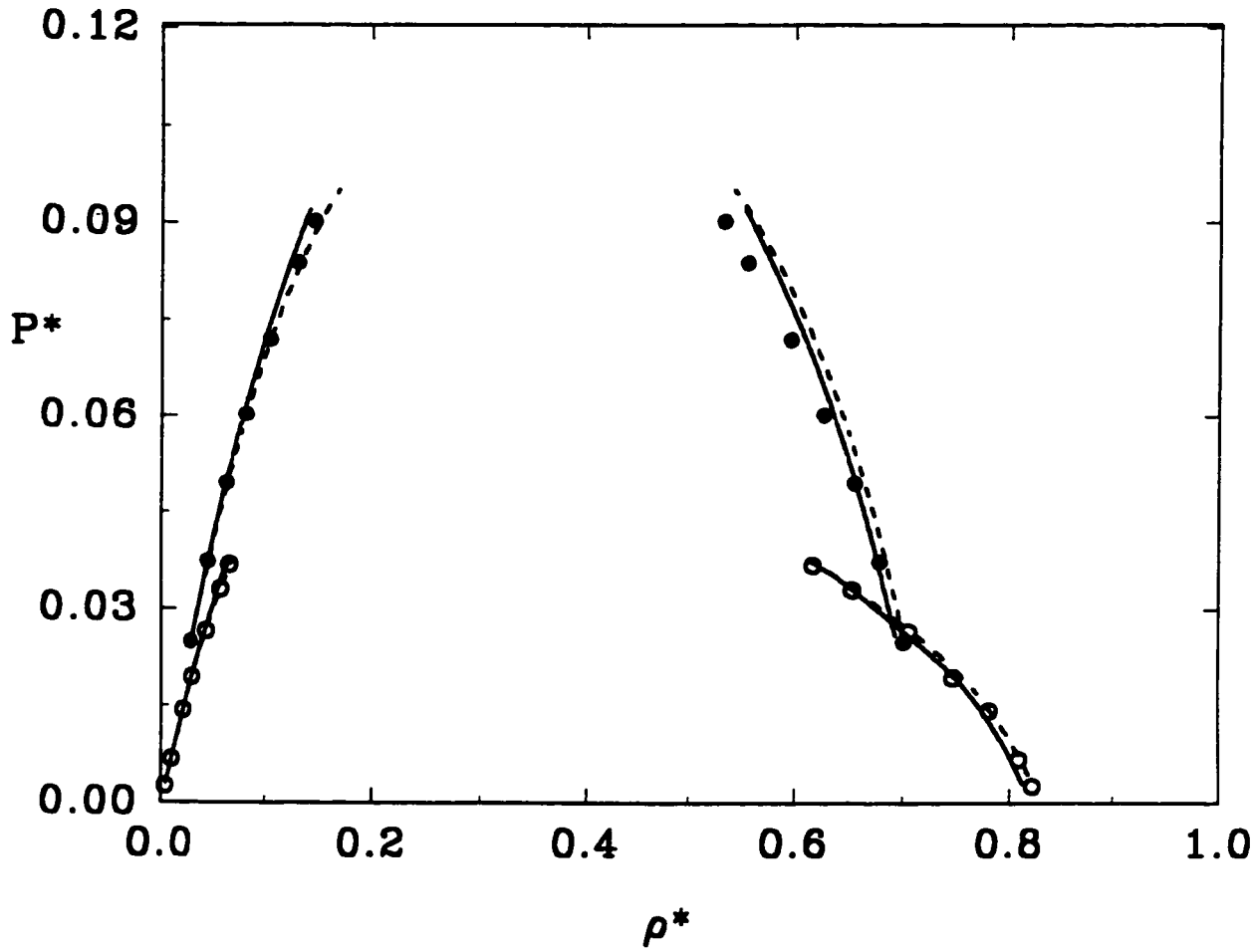

Figure 20. VLE of a LJ mixture with $\sigma_{22}/\sigma_{11}=1$, $\epsilon_{22}/\epsilon_{11}=0.66$. The open and filled circles are the MD data (Vrabec et al., 1995) at T*=0.75 and T*=1.00, respectively. The solid and dashed lines are results from the present and VDW1 theory, respectively.

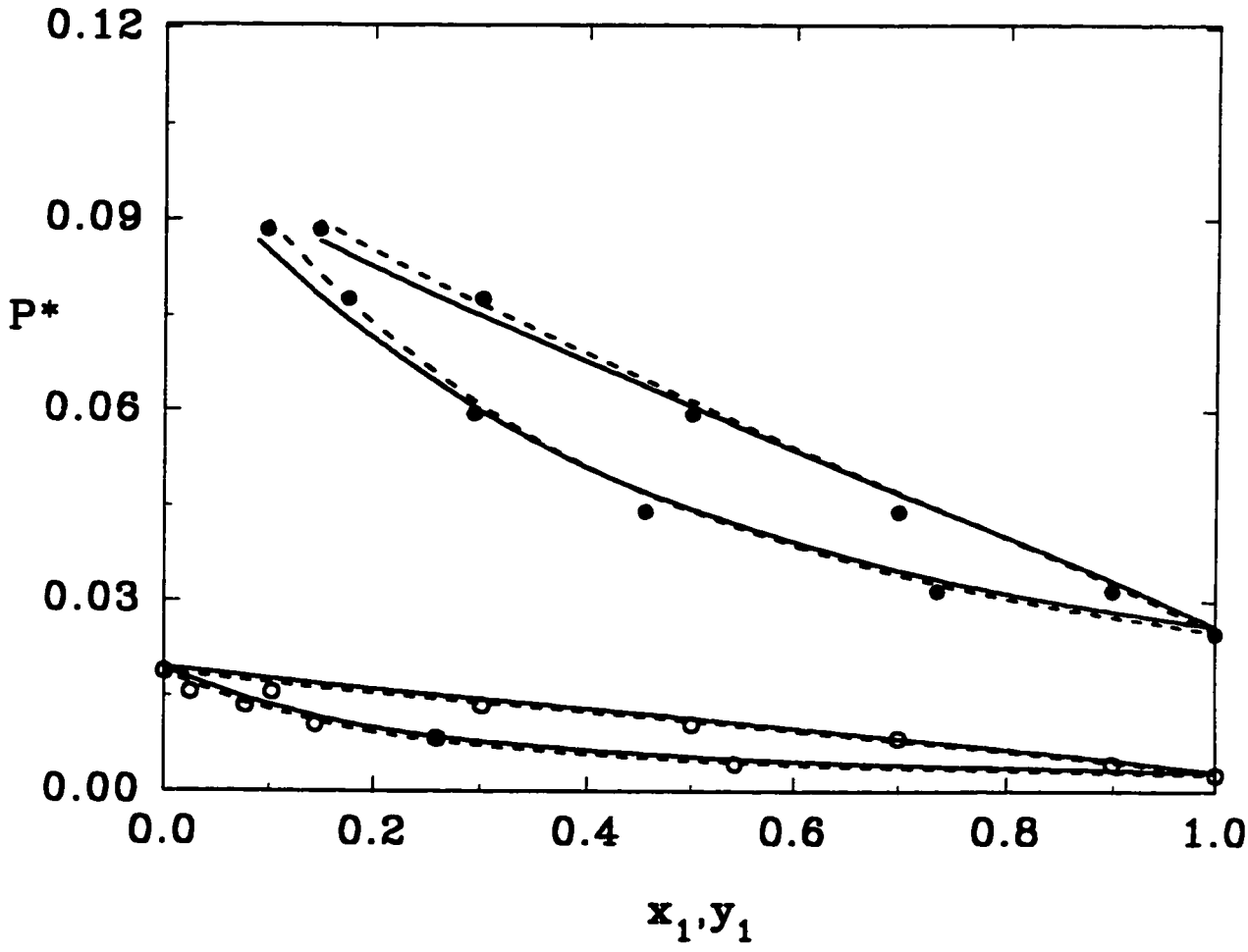

Figure 21. VLE of a LJ mixture with $\sigma_{22}/\sigma_{11}=1$, $\epsilon_{22}/\epsilon_{11}=0.75$. The open and filled circles are the MD data (Vrabec et al., 1995) at T*=0.75 and T*=1.00, respectively. The solid and dashed lines are results from the present and VDW1 theory, respectively.

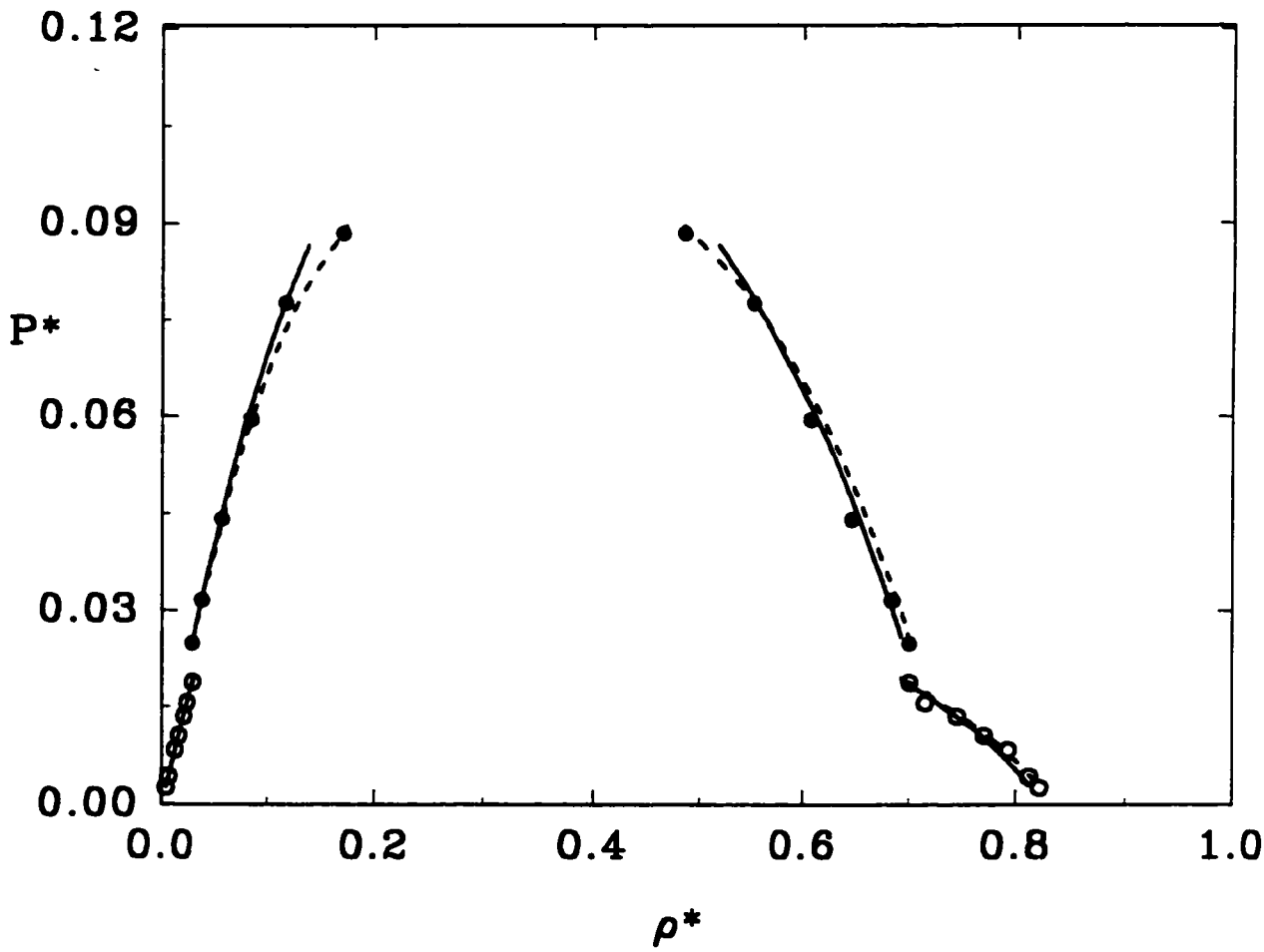

Figure 22. VLE of a LJ mixture with σ_{22}/σ_{11}=1, $\epsilon_{22}/\epsilon_{11}$=0.75. The open and filled circles are the MD data (Vrabec et al., 1995) at T*=0.75 and T*=1.00, respectively. The solid and dashed lines are results from the present and VDW1 theory, respectively.

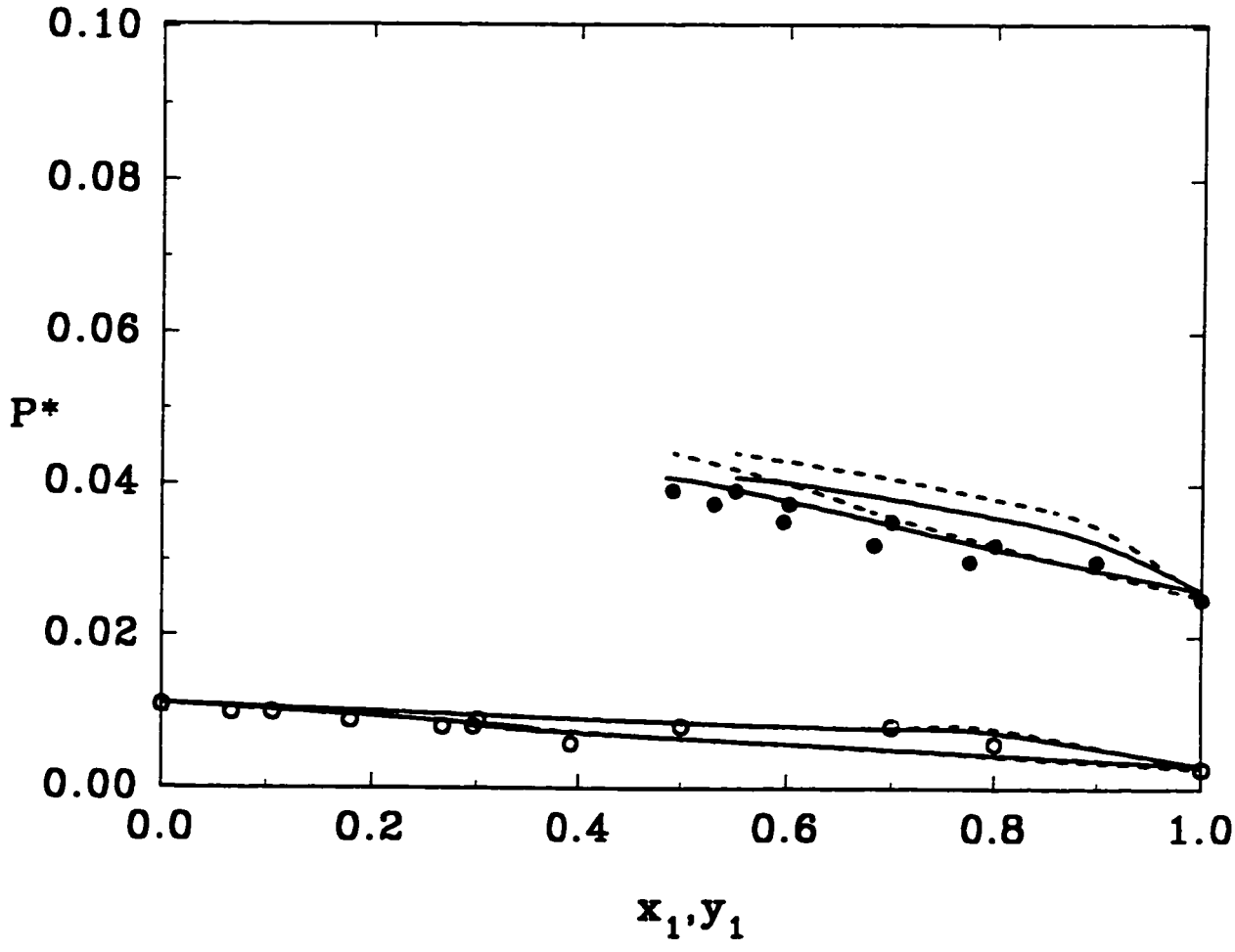

Figure 23. VLE of a LJ mixture with σ_{22}/σ_{11}=1.5, $\epsilon_{22}/\epsilon_{11}$=0.66. The open and filled circles are the MD data (Vrabec et al., 1995) at T*=0.75 and T*=1.00, respectively. The solid and dashed lines are results from the present and VDW1 theory, respectively.

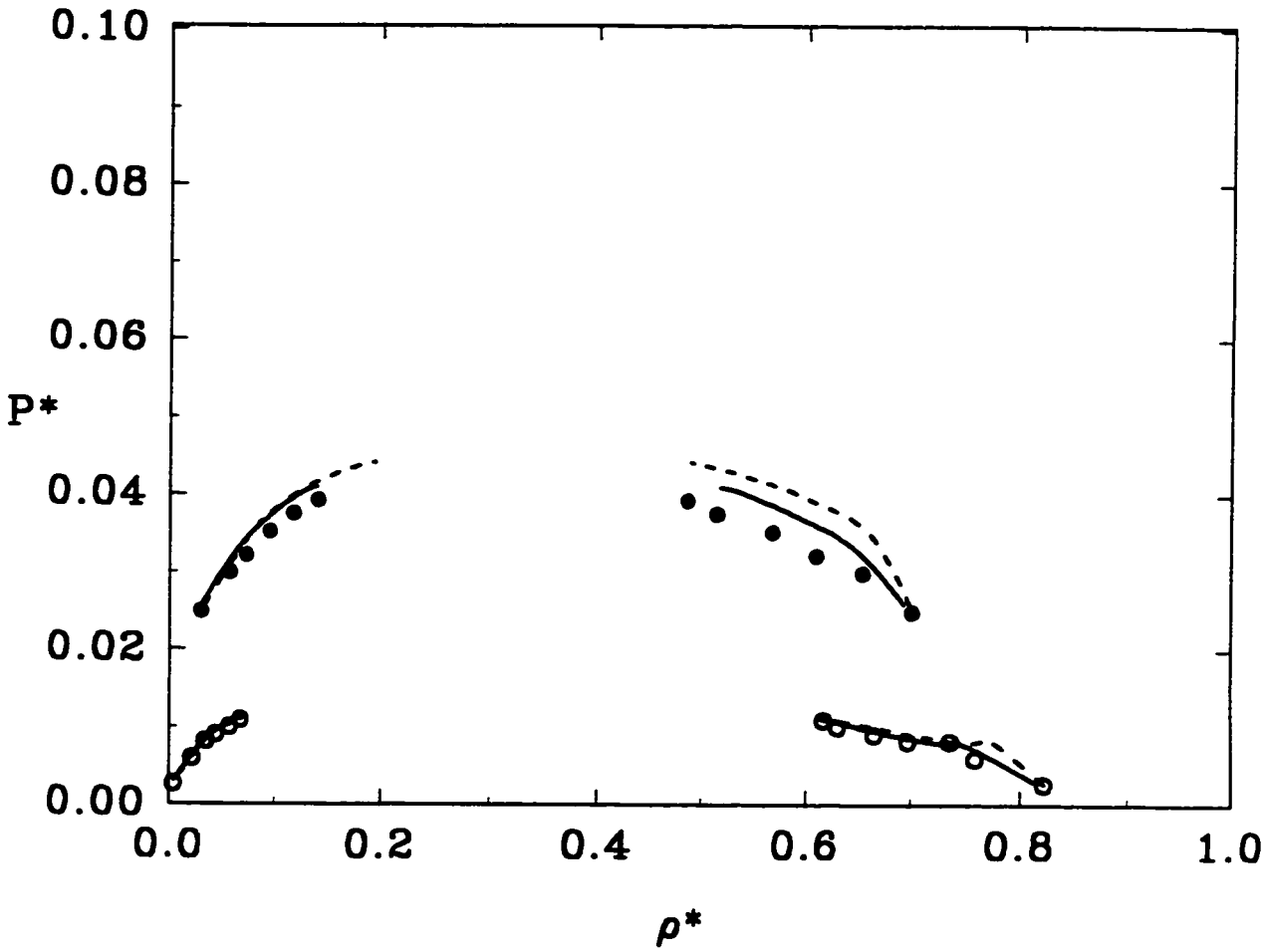

Figure 24. VLE of a LJ mixture with σ_{22}/σ_{11}=1.5, $\epsilon_{22}/\epsilon_{11}$=0.66. The open and filled circles are the MD data (Vrabec et al., 1995) at T*=0.75 and T*=1.00, respectively. The solid and dashed lines are results from the present and VDW1 theory, respectively.

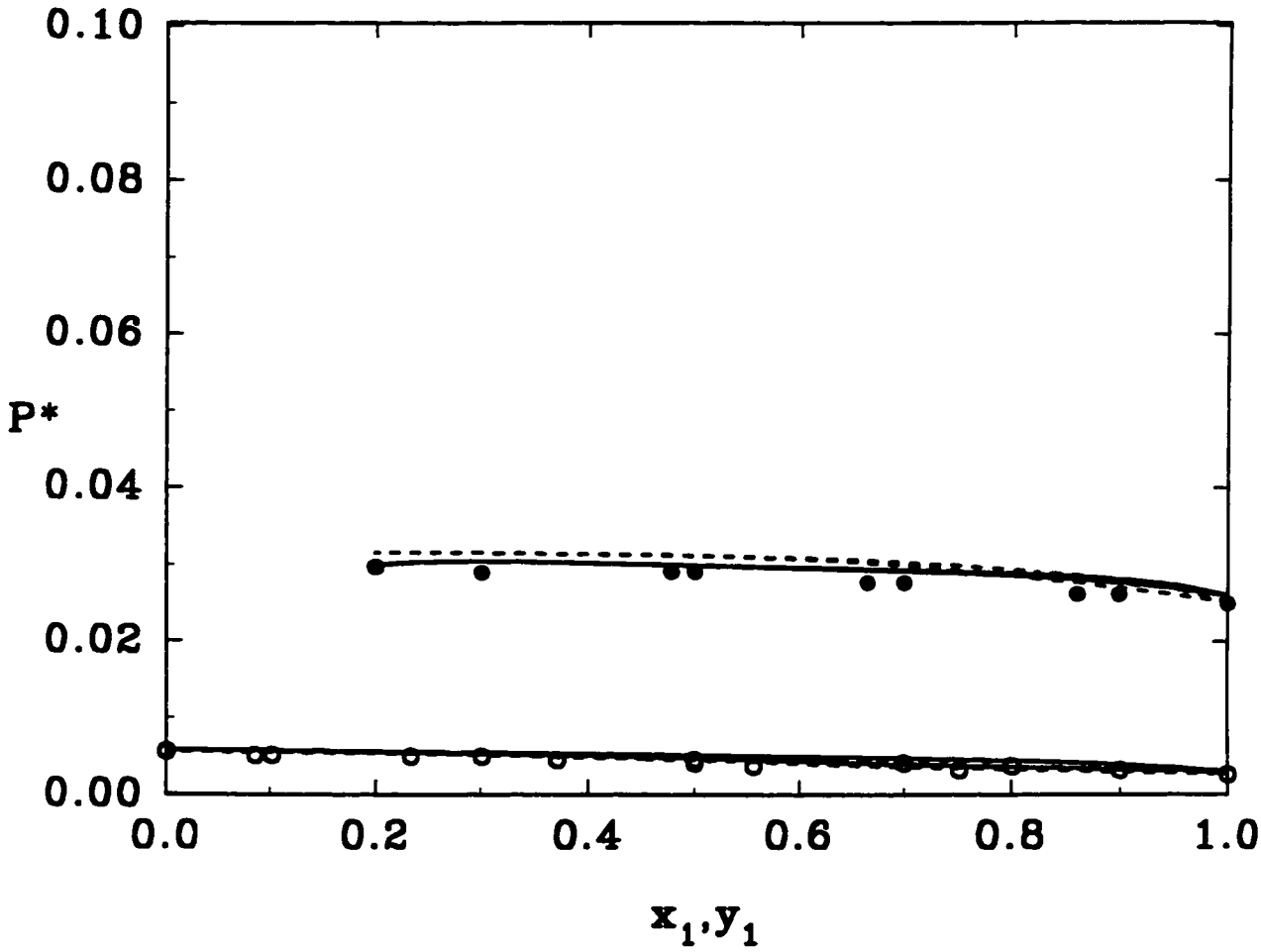

Figure 25. VLE of a LJ mixture with σ_{22}/σ_{11}=1.5, $\epsilon_{22}/\epsilon_{11}$=0.75. The open and filled circles are the MD data (Vrabec et al., 1995) at T*=0.75 and T*=1.00, respectively. The solid and dashed lines are results from the present and VDW1 theory, respectively. The vapor phase is difficult to distinguish from the liquid phase in this case.

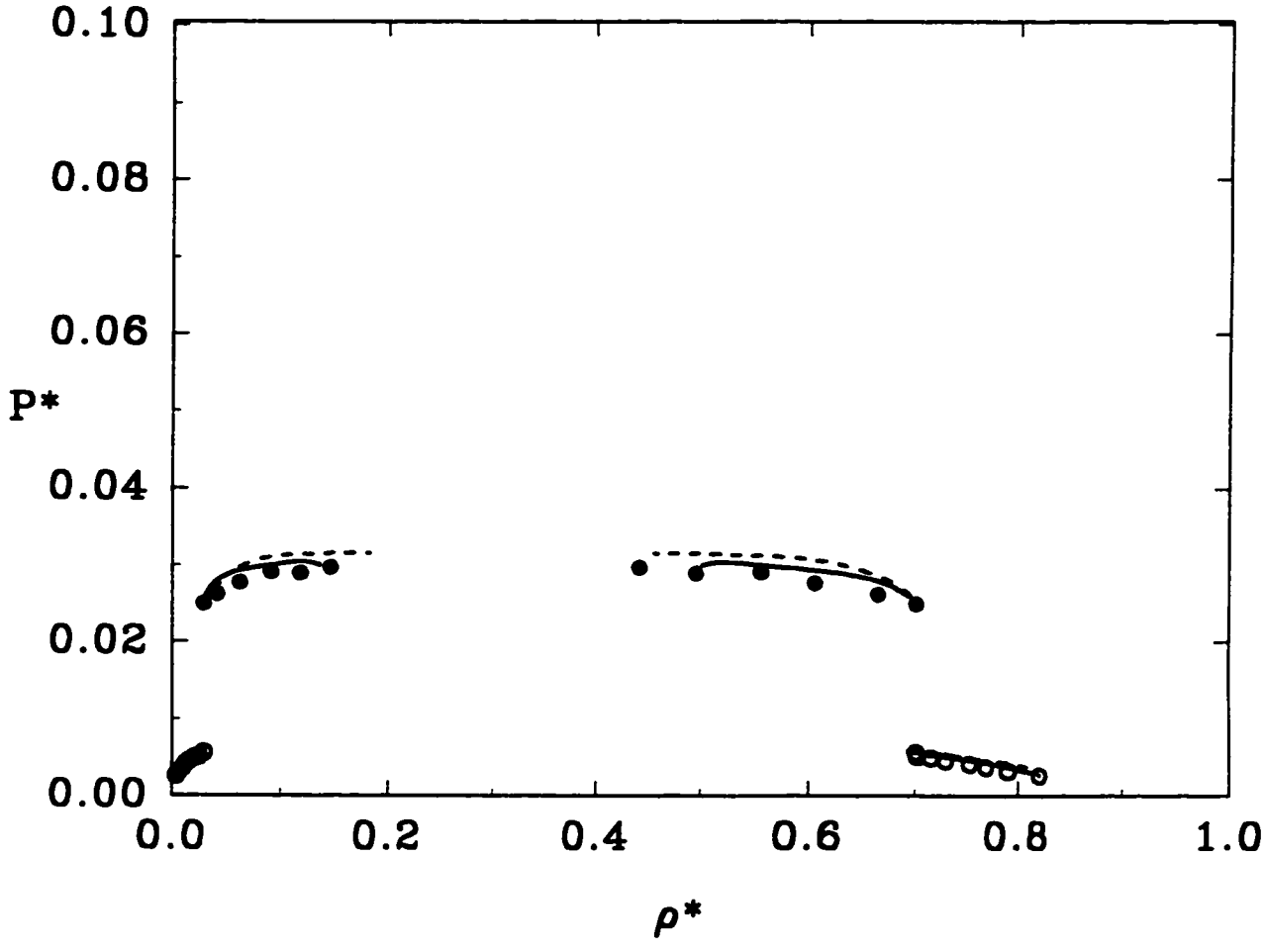

Figure 26. VLE of a LJ mixture with σ_{22}/σ_{11}=1.5, $\epsilon_{22}/\epsilon_{11}$=0.75. The open and filled circles are the MD data (Vrabec et al., 1995) at T*=0.75 and T*=1.00, respectively. The solid and dashed lines are results from the present and VDW1 theory, respectively.

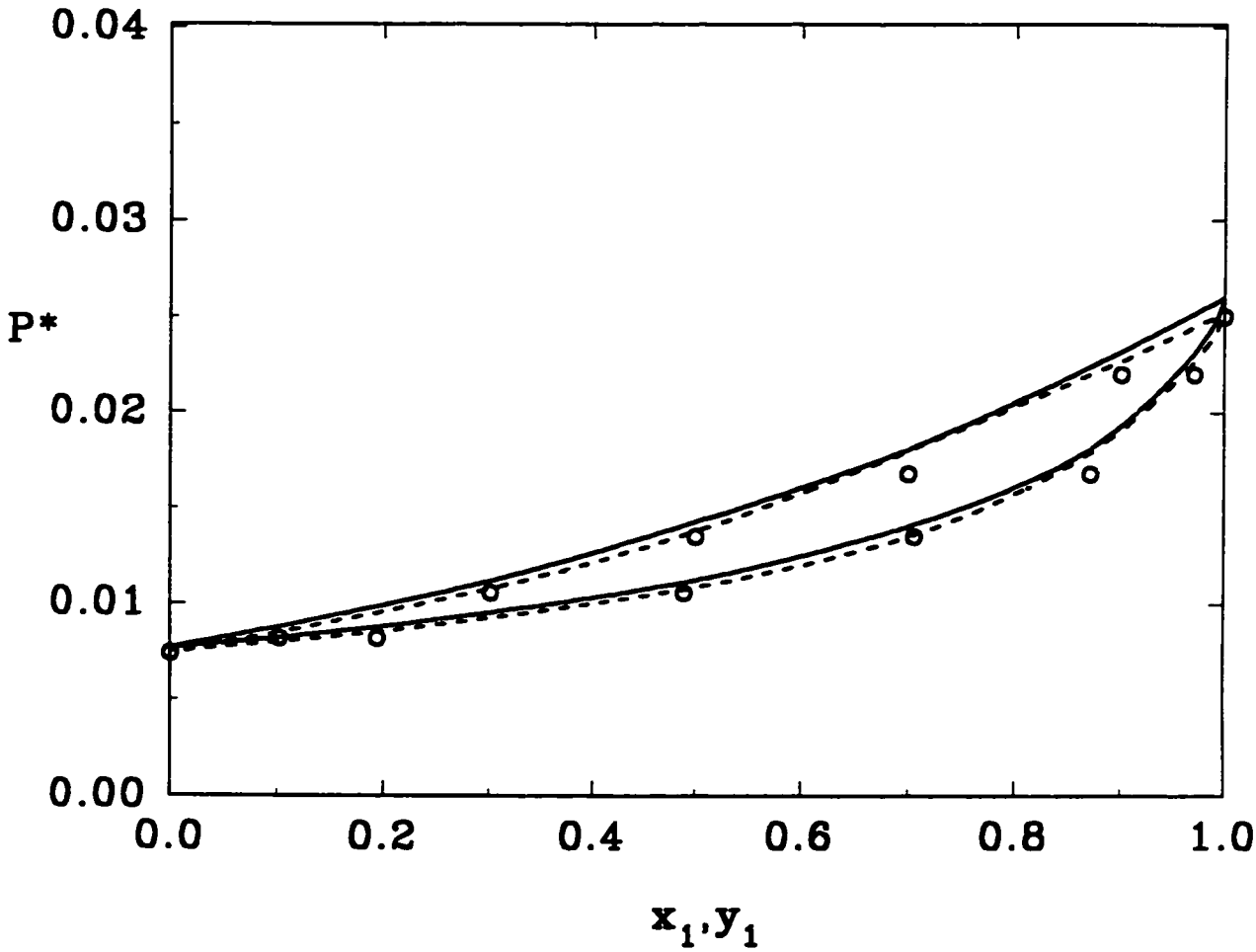

Figure 27. VLE of a LJ mixture with σ_{22}/σ_{11}=1.5, $\epsilon_{22}/\epsilon_{11}$=1.0. The open and filled circles are the MD data (Vrabec et al., 1995) at T*=0.75 and T*=1.00, respectively. The solid and dashed lines are results from the present and VDW1 theory, respectively.

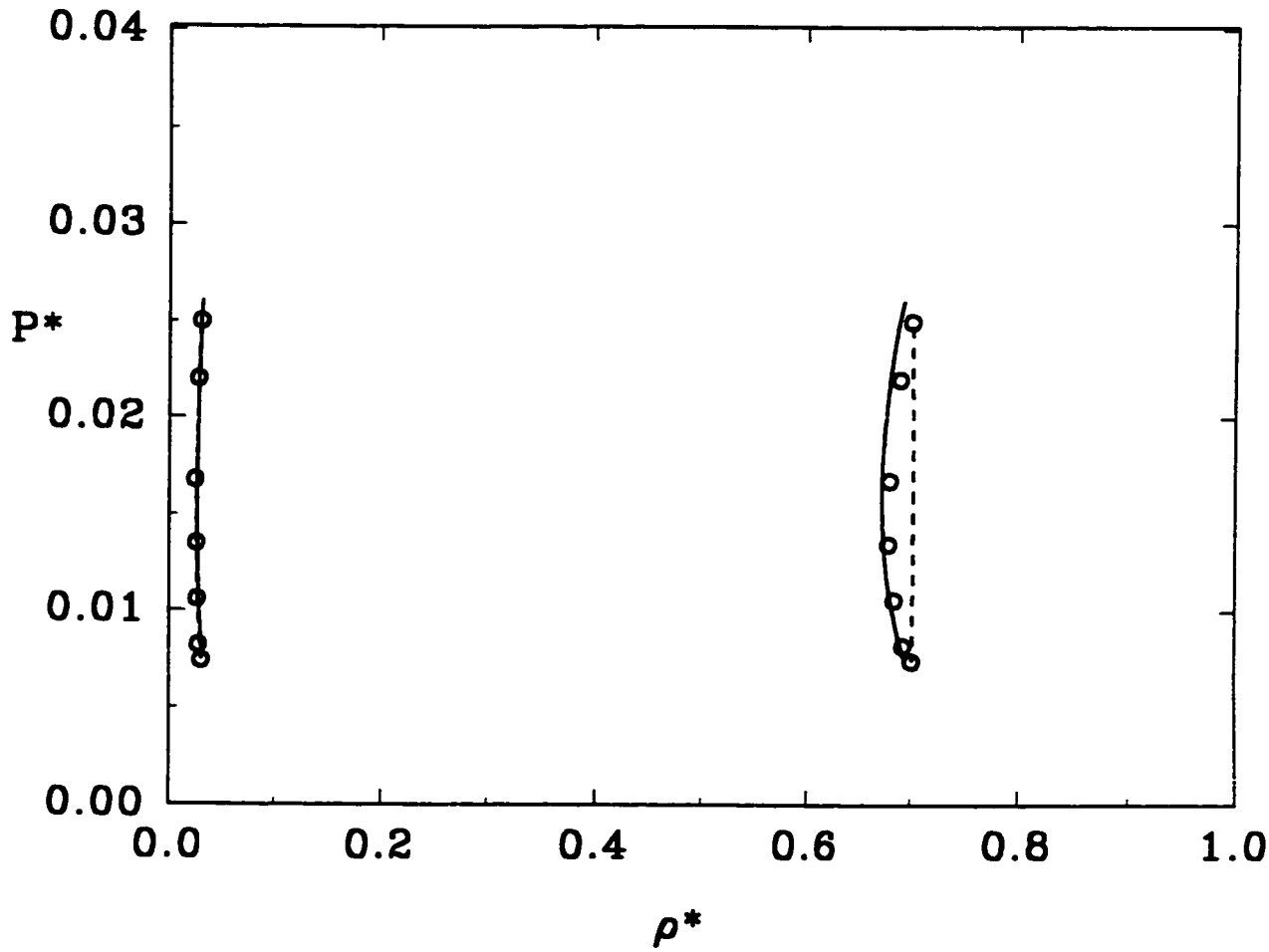

Figure 28. VLE of a LJ mixture with σ_{22}/σ_{11}=1.5, $\epsilon_{22}/\epsilon_{11}$=1.00. The open and filled circles are the MD data (Vrabec et al., 1995) at T*=0.75 and T*=1.00, respectively. The solid and dashed lines are results from the present and VDW1 theory, respectively.

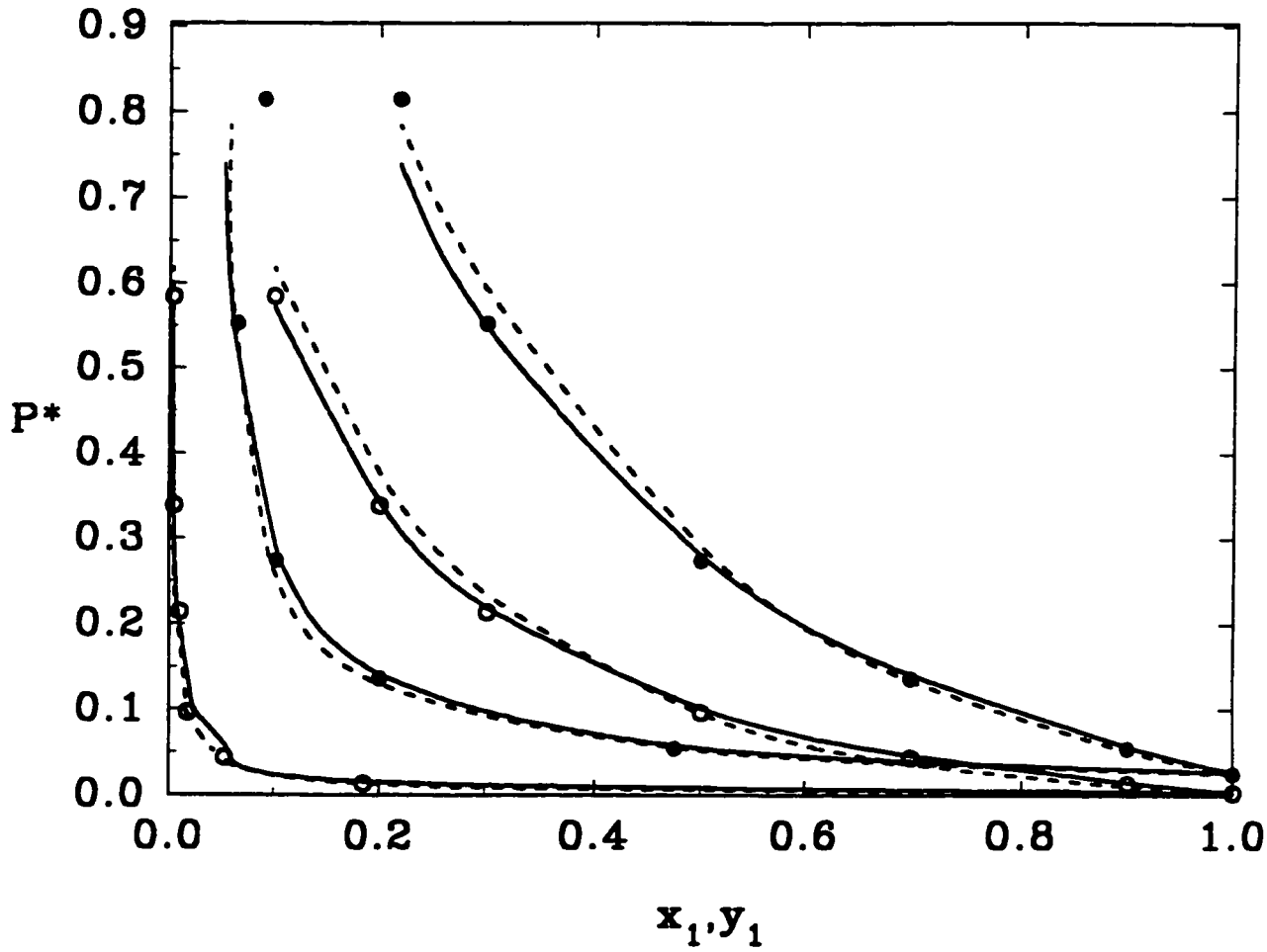

Figure 29. VLE of a LJ mixture with σ_{22}/σ_{11}=0.5, $\epsilon_{22}/\epsilon_{11}$=0.5. The open and filled circles are the MD data (Vrabec et al., 1995) at T*=0.75 and T*=1.00, respectively. The solid and dashed lines are results from the present and VDW1 theory, respectively.

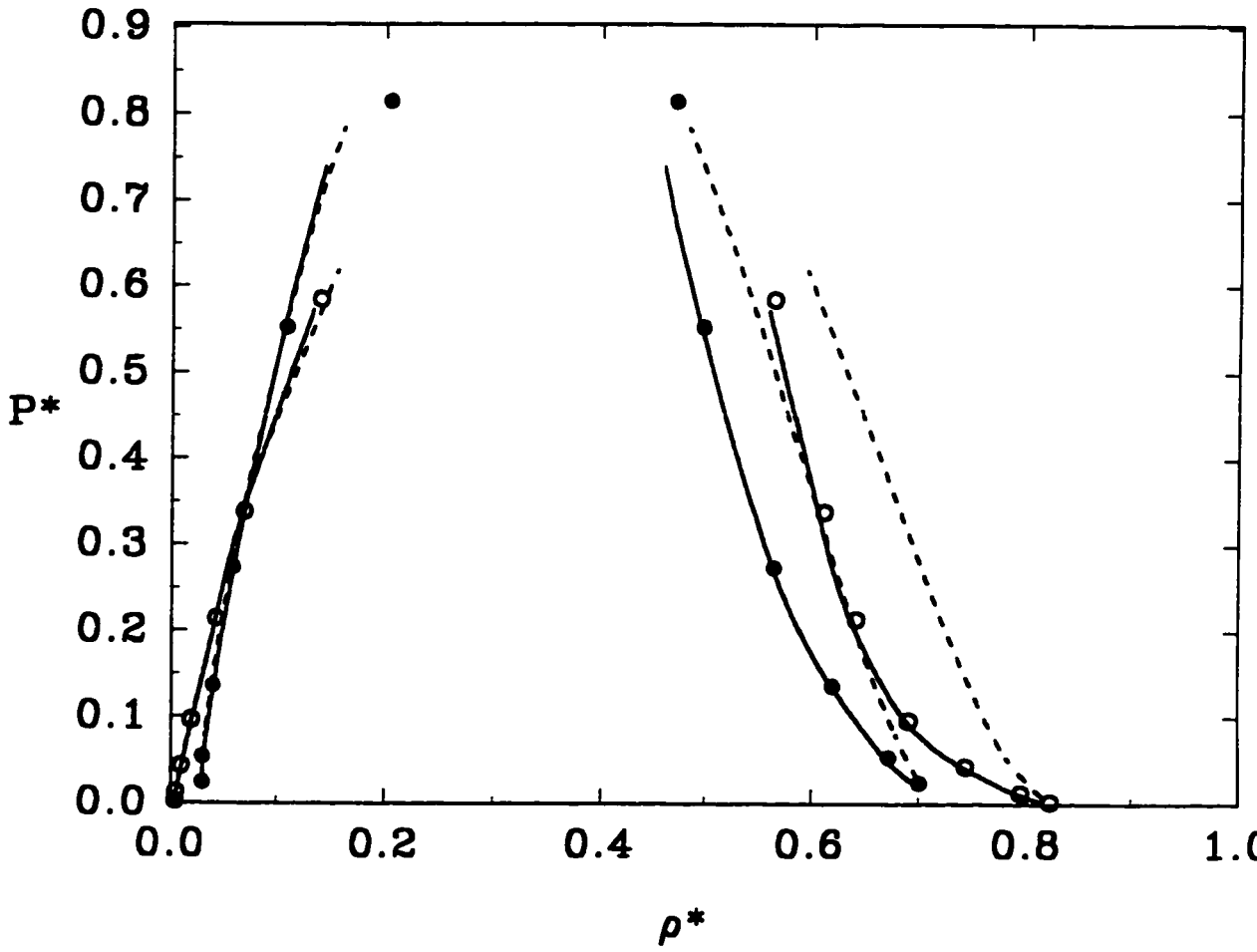

Figure 30. VLE of a LJ mixture with σ_{22}/σ_{11}=0.5, $\epsilon_{22}/\epsilon_{11}$=0.5. The open and filled circles are the MD data (Vrabec et al., 1995) at T*=0.75 and T*=1.00, respectively. The solid and dashed lines are results from the present and VDW1 theory, respectively.

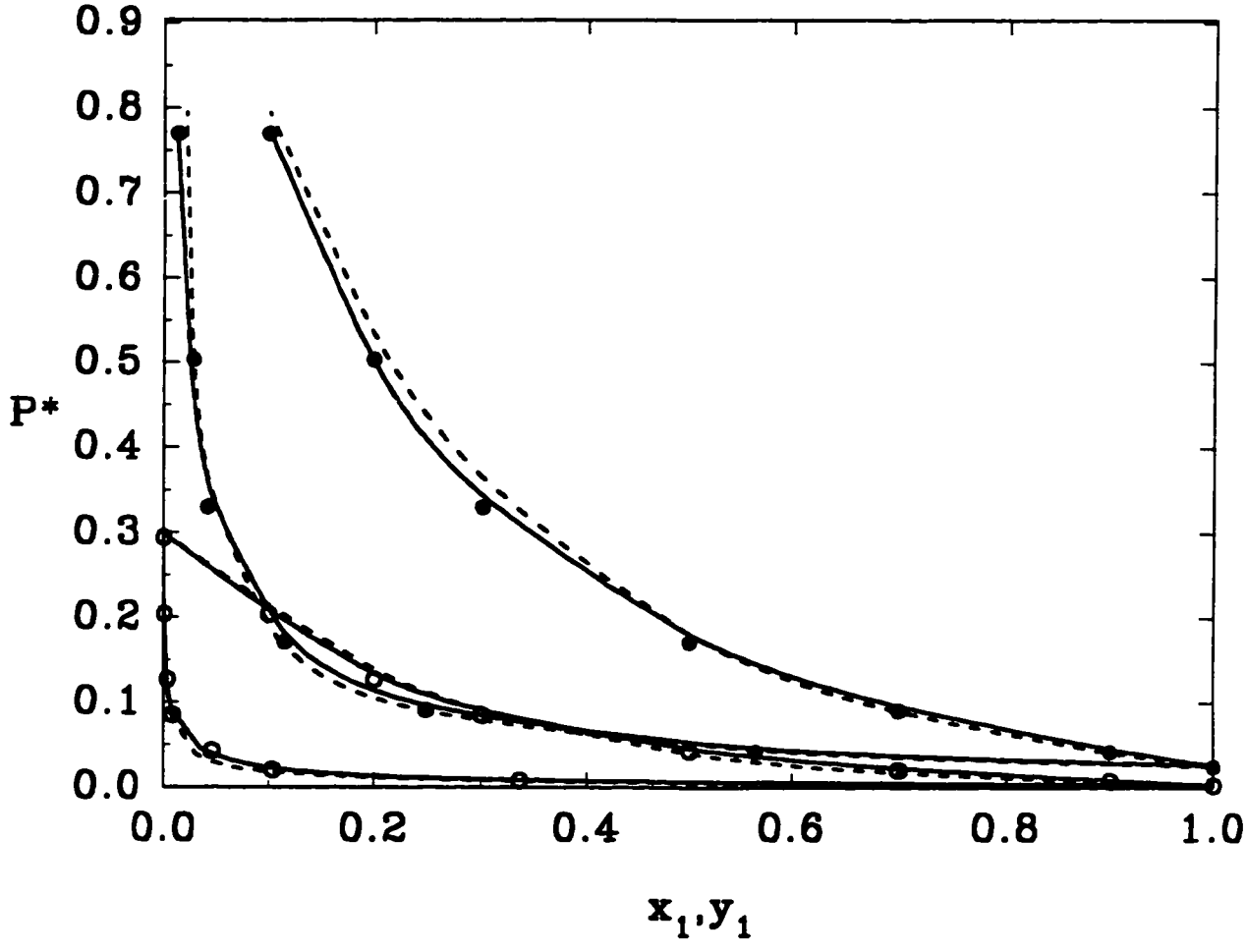

Figure 31. VLE of a LJ mixture with σ_{22}/σ_{11}=0.5, $\epsilon_{22}/\epsilon_{11}$=0.66. The open and filled circles are the MD data (Vrabec et al., 1995) at T*=0.75 and T*=1.00, respectively. The solid and dashed lines are results from the present and VDW1 theory, respectively.

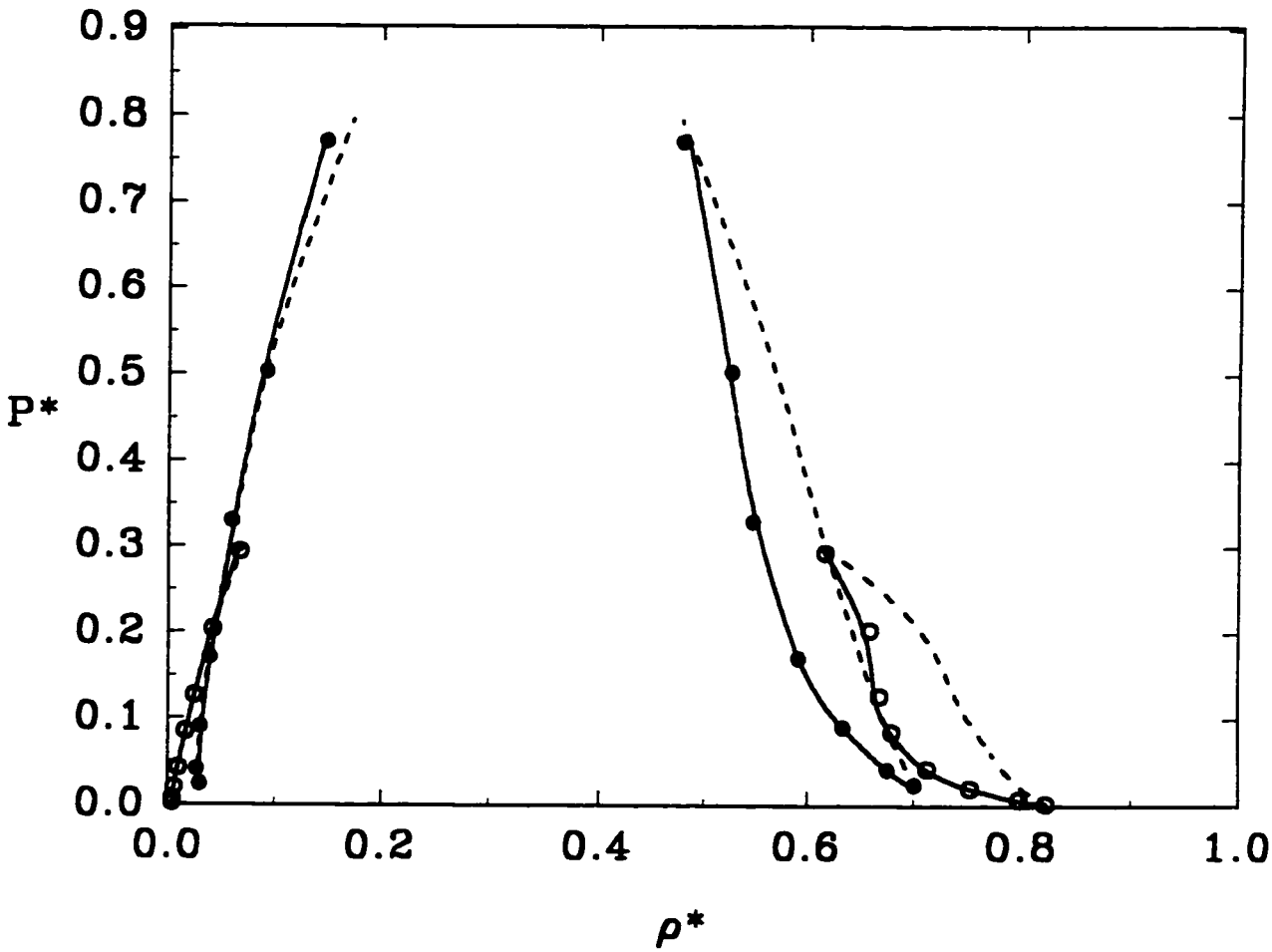

Figure 32. VLE of a LJ mixture with σ_{22}/σ_{11}=0.5, $\epsilon_{22}/\epsilon_{11}$=0.66. The open and filled circles are the MD data (Vrabec et al., 1995) at T*=0.75 and T*=1.00, respectively. The solid and dashed lines are results from the present and VDW1 theory, respectively.

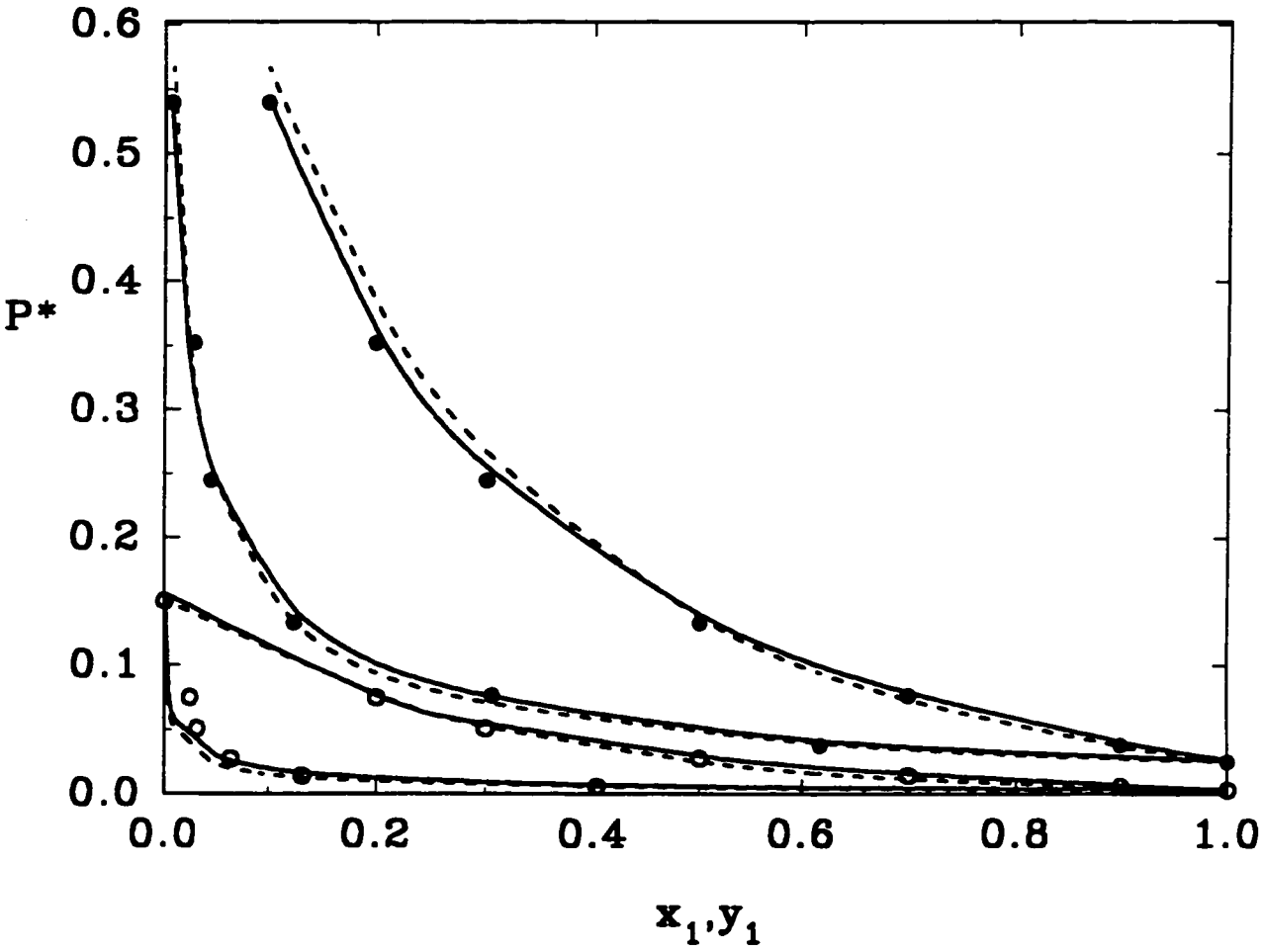

Figure 33. VLE of a LJ mixture with σ_{22}/σ_{11}=0.5, $\epsilon_{22}/\epsilon_{11}$=0.75. The open and filled circles are the MD data (Vrabec et al., 1995) at T*=0.75 and T*=1.00, respectively. The solid and dashed lines are results from the present and VDW1 theory, respectively.

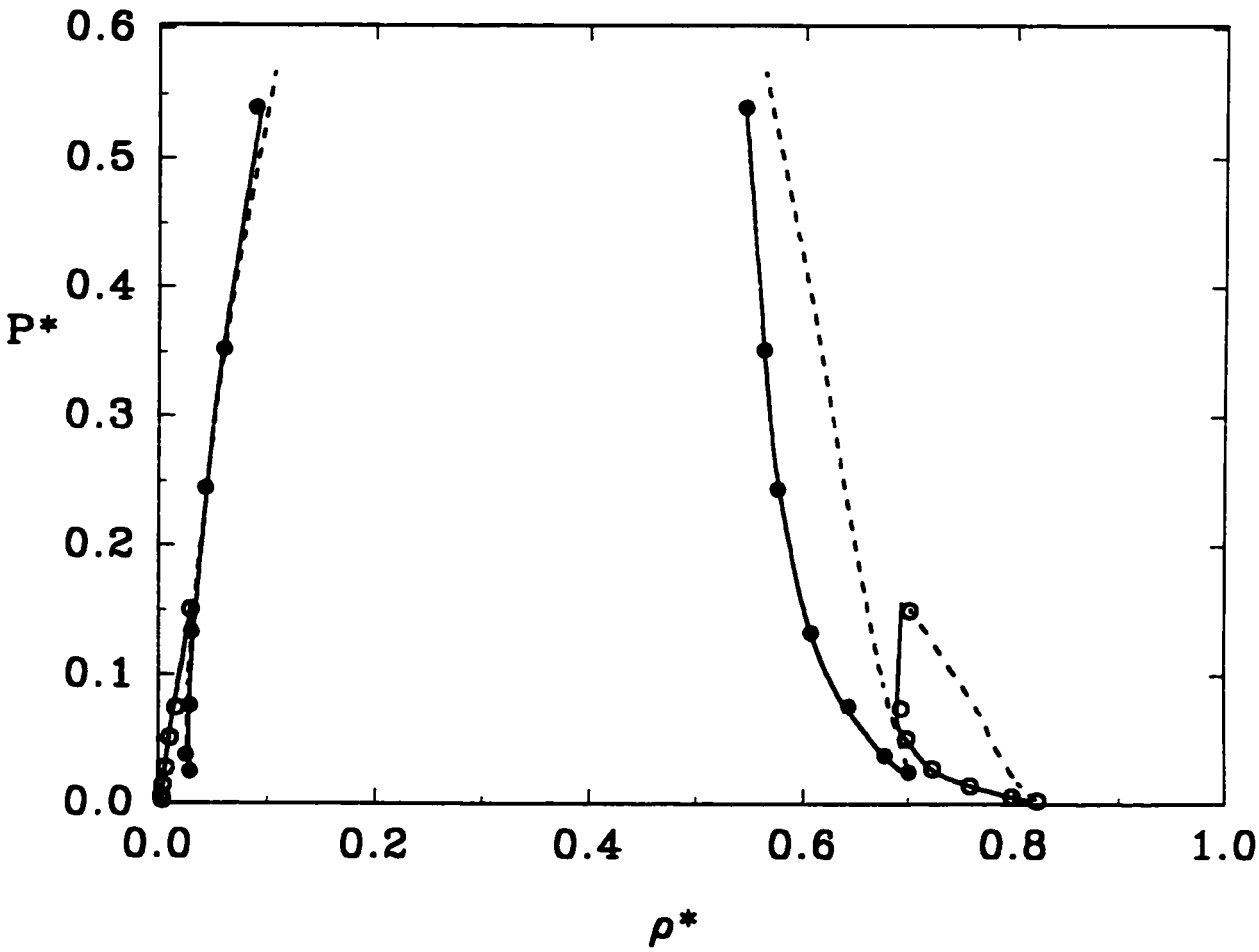

Figure 34. VLE of a LJ mixture with σ_{22}/σ_{11}=0.5, $\epsilon_{22}/\epsilon_{11}$=0.75. The open and filled circles are the MD data (Vrabec et al., 1995) at T*=0.75 and T*=1.00, respectively. The solid and dashed lines are results from the present and VDW1 theory, respectively.

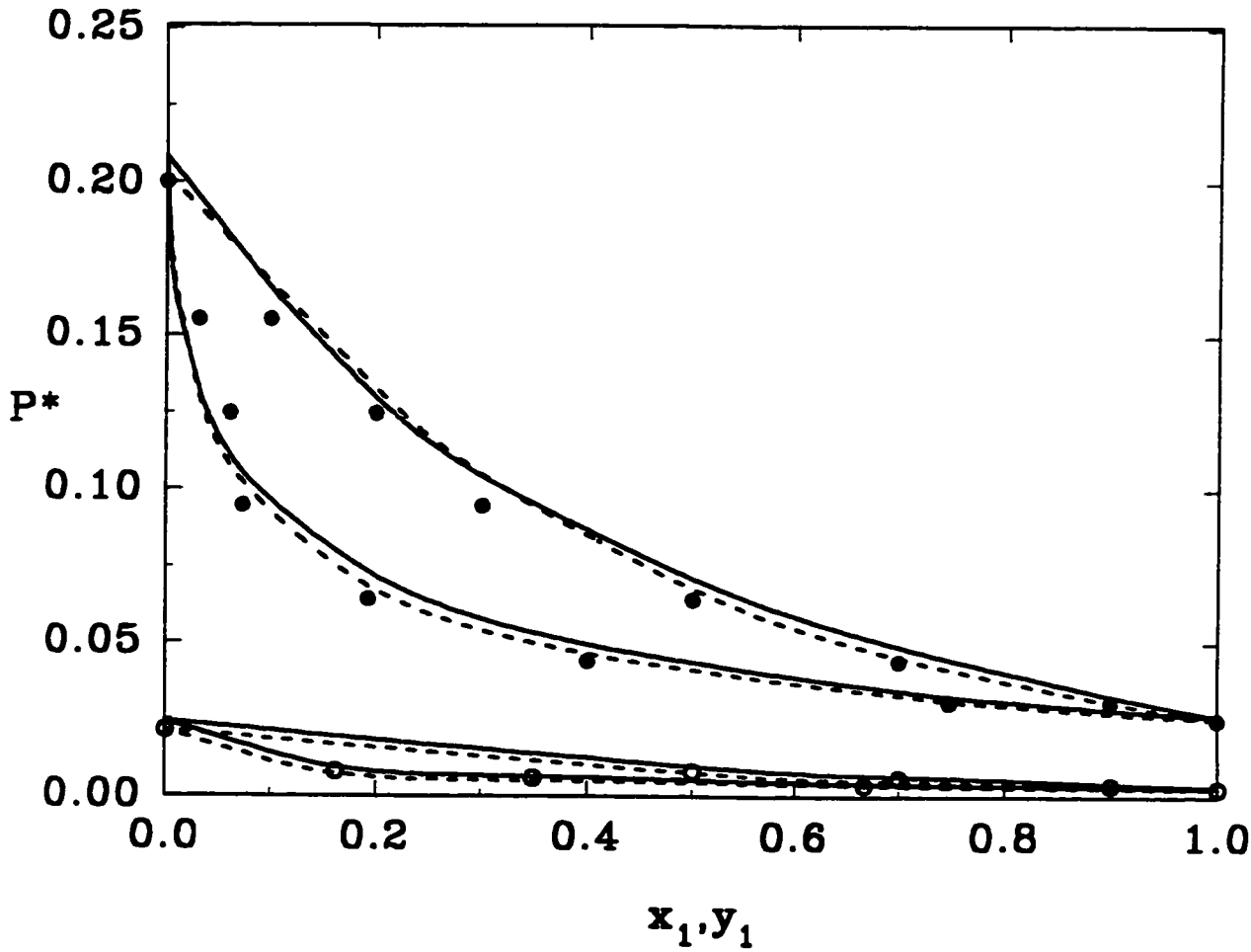

Figure 35. VLE of a LJ mixture with σ_{22}/σ_{11}=0.5, $\epsilon_{22}/\epsilon_{11}$=1.0. The open and filled circles are the MD data (Vrabec et al., 1995) at T*=0.75 and T*=1.00, respectively. The solid and dashed lines are results from the present and VDW1 theory, respectively.

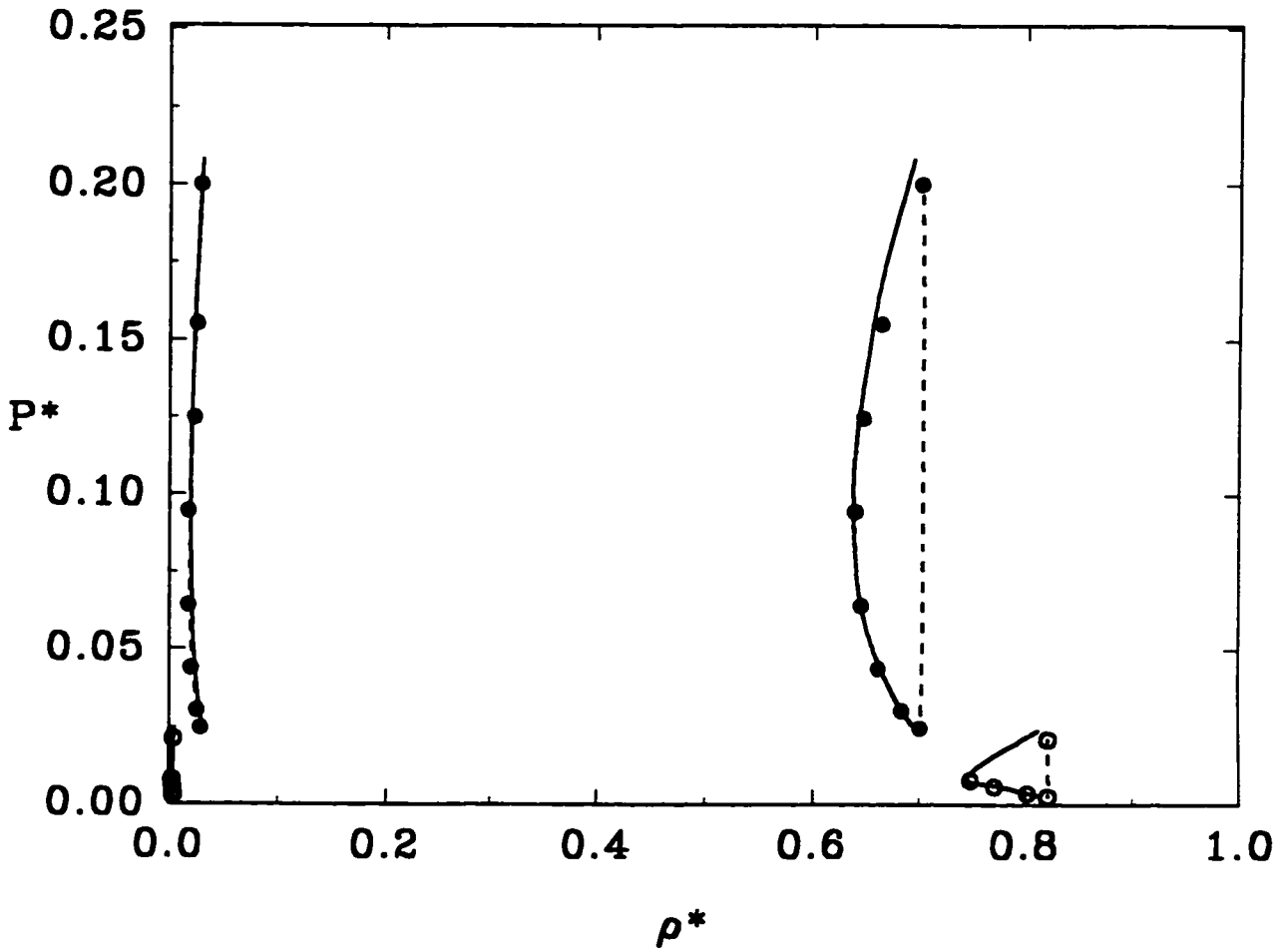

Figure 36. VLE of a LJ mixture with σ_{22}/σ_{11}=0.5, $\epsilon_{22}/\epsilon_{11}$=1.0. The open and filled circles are the MD data (Vrabec et al., 1995) at T*=0.75 and T*=1.00, respectively. The solid and dashed lines are results from the present and VDW1 theory, respectively.

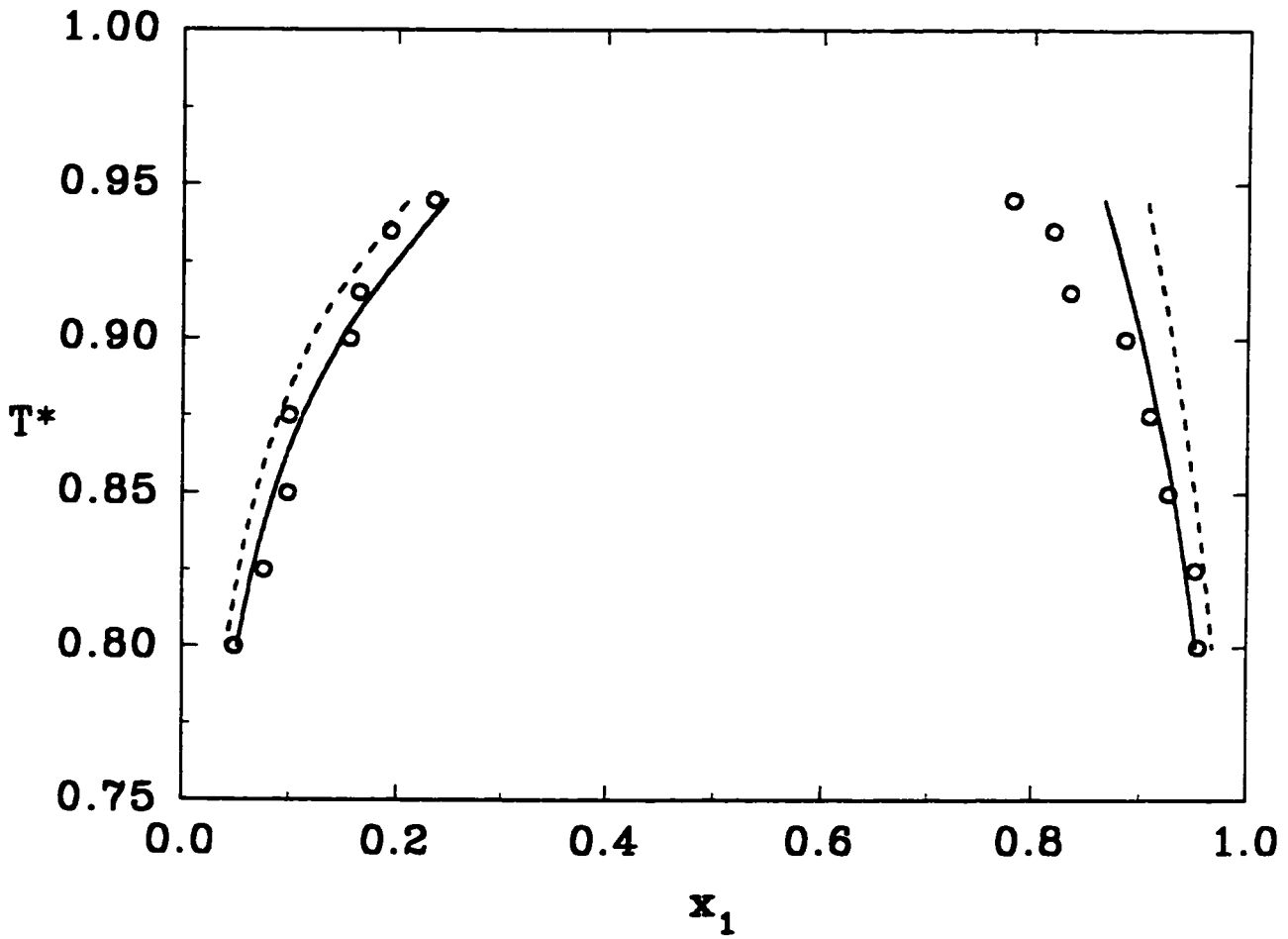

Figure 37. LLE of a LJ mixture with σ_{22}/σ_{11}=0.95, $\epsilon_{22}/\epsilon_{11}$=0.75, γ_{12}=0.70 and l_{12}=1.0 at P*=0.125. The circles are the MC data (Guo et al., 1994).The solid and dashed lines are results from the present and VDW1 theory, respectively.

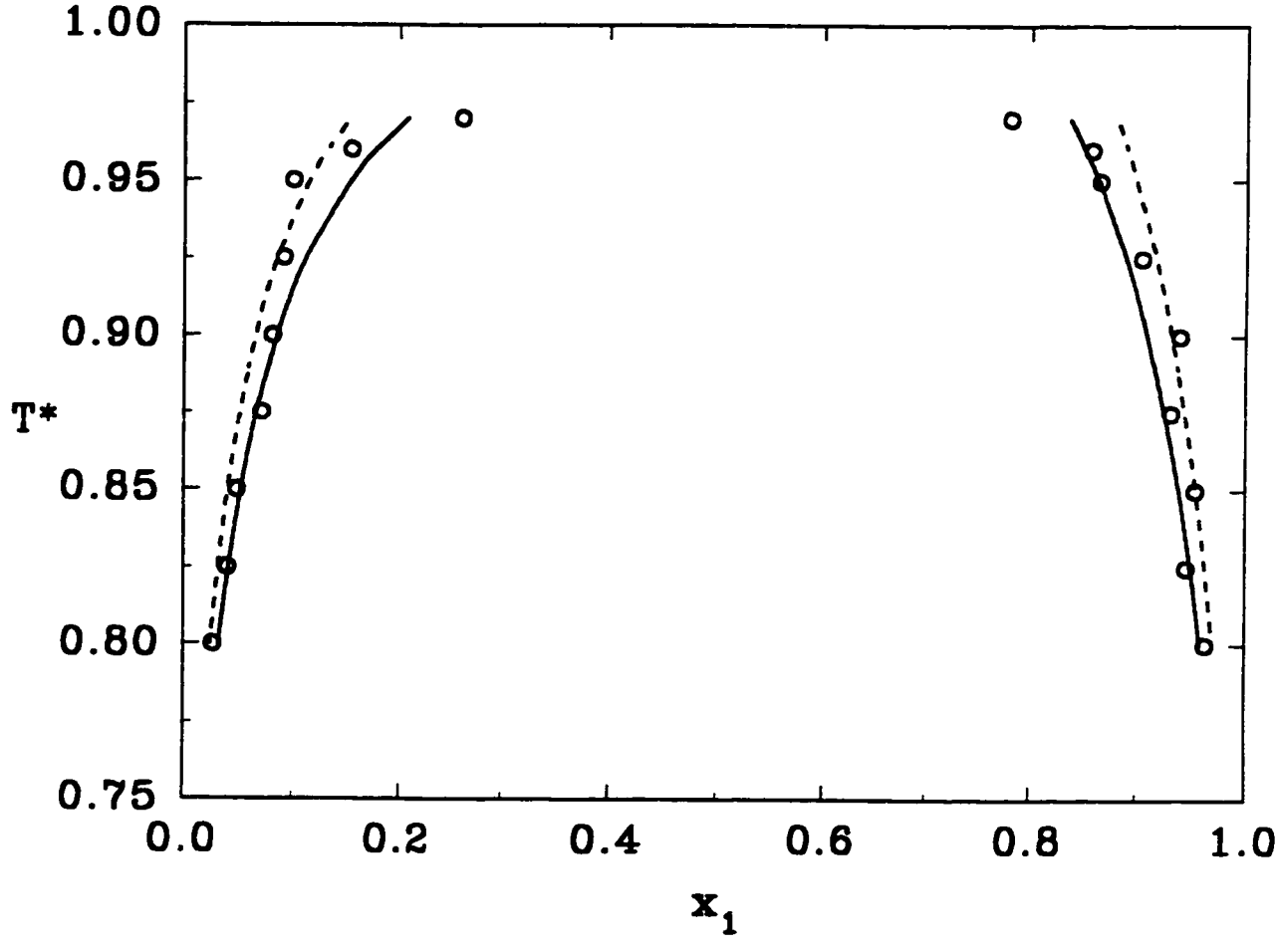

Figure 38. LLE of a LJ mixture with σ_{22}/σ_{11}=0.95, $\epsilon_{22}/\epsilon_{11}$=0.85, γ_{12}=0.70 and l_{12}=1.0 at P*=0.125. The circles are the MC data (Guo et al., 1994).The solid and dashed lines are results from the present and VDW1 theory, respectively.

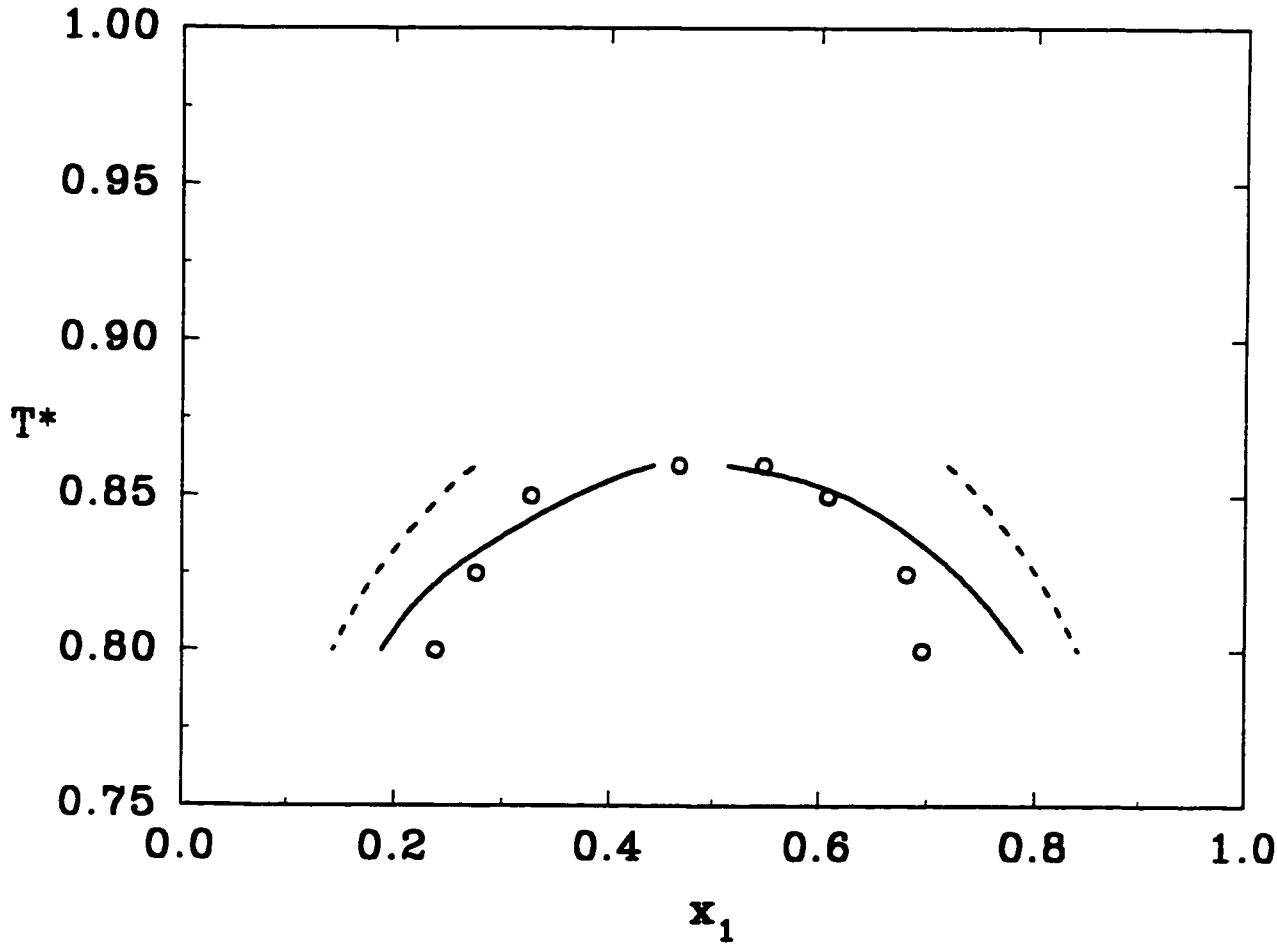

Figure 39. LLE of a LJ mixture with σ_{22}/σ_{11}=0.95, $\epsilon_{22}/\epsilon_{11}$=0.85, γ_{12}=0.80 and l_{12}=1.0 at P*=0.125. The circles are the MC data (Guo et al., 1994).The solid and dashed lines are results from the present and VDW1 theory, respectively.

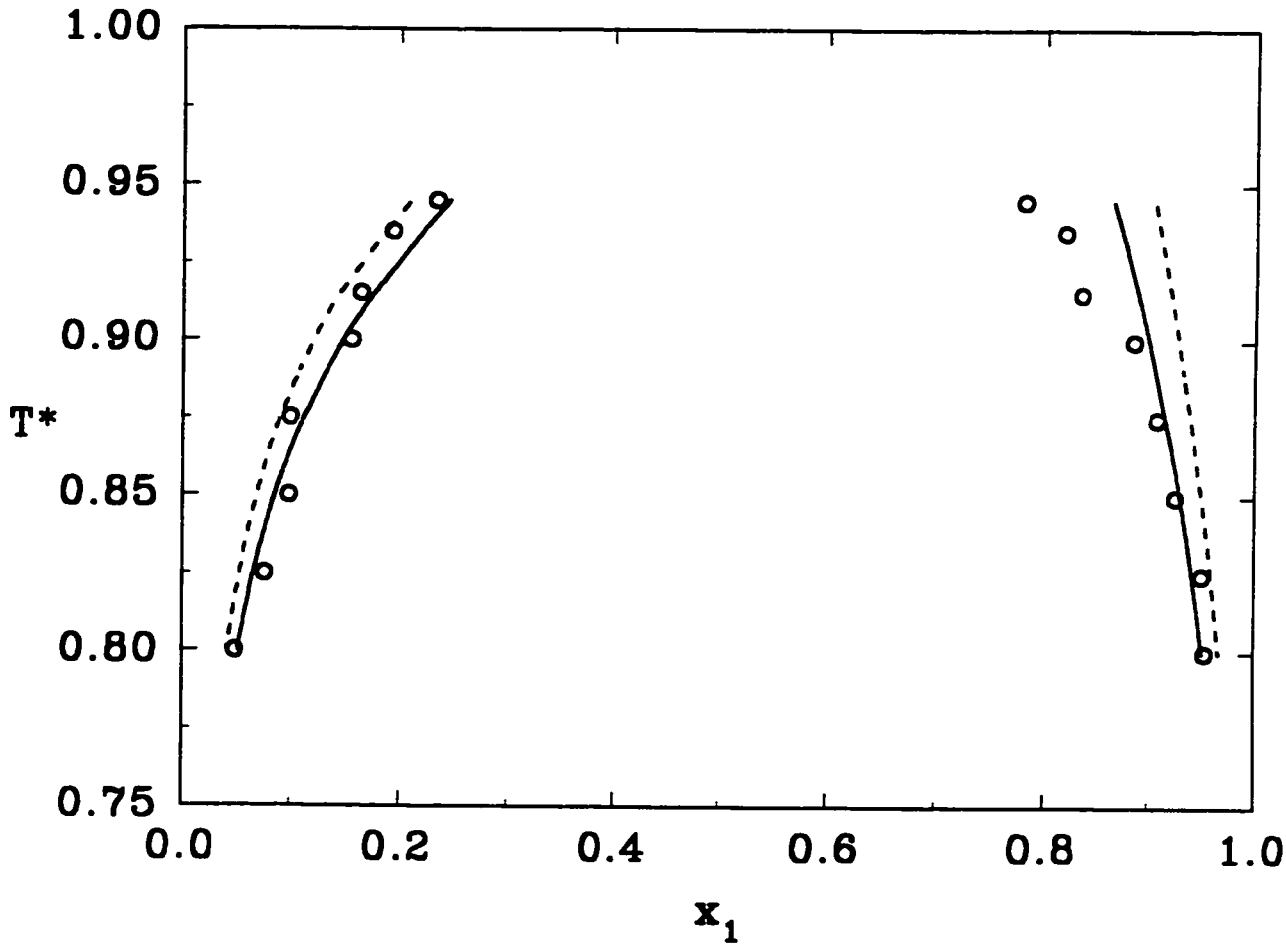

Figure 40. LLE of a LJ mixture with σ_{22}/σ_{11}=0.80, $\epsilon_{22}/\epsilon_{11}$=0.85, γ_{12}=0.70 and l_{12}=1.0 at P*=0.125. The circles are the MC data (Guo et al., 1994).The solid and dashed lines are results from the present and VDW1 theory, respectively.

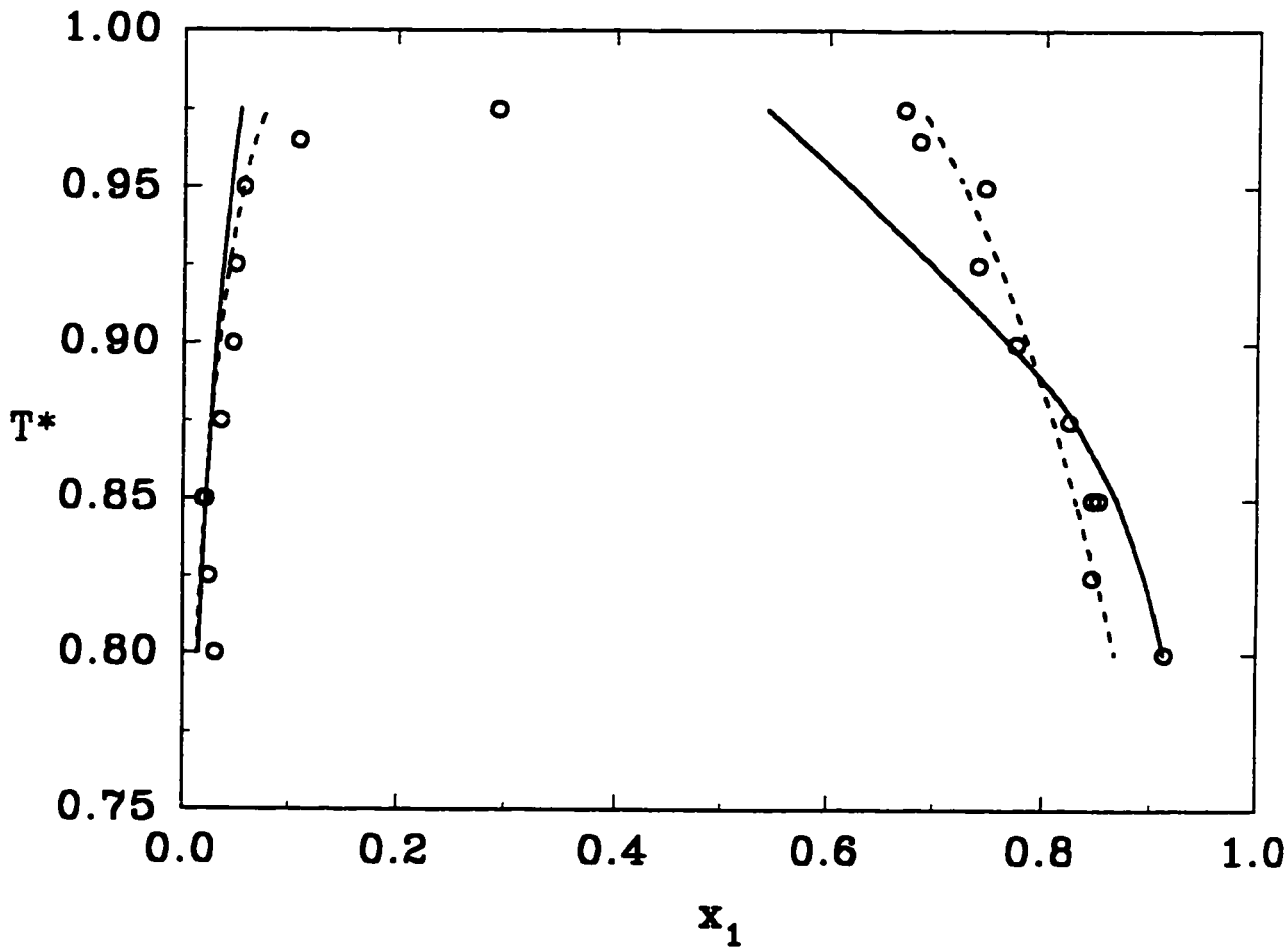

Figure 41. LLE of a LJ mixture with σ_{22}/σ_{11}=0.80, $\epsilon_{22}/\epsilon_{11}$=0.85, γ_{12}=0.70 and l_{12}=0.95 at P*=0.125. The circles are the MC data (Guo et al., 1994).The solid and dashed lines are results from the present and VDW1 theory, respectively.

5. Preliminary Calculations for Real Fluids

The success of Equation (217) provides confidence to apply it in practical calculations. In these preliminary calculations (Tang et al., 1997b), only pure fluids were studied for extracting information about the applicability of a theoretical EOS for real fluids. The information will be very suggestive to apply the theoretical EOS (240) for real mixtures in the future. Four simple fluids, Ar, CH_4, O_2 and N_2 are utilized to test the proposed EOS (217)-(233) for real fluids. Microscopically, all these fluids are very weakly anisotropic. The repulsive force of argon and methane is well known to be spherical. The molecules of oxygen and nitrogen are usually spherically approximated in spite of some orientational dependence. The term $1/r^6$ of the LJ potential is rational to describe the attractive interaction since the dispersion force dominates the attraction.

To determine the parameters ϵ and σ, the data of vapor-liquid phase diagram (Canjar and Manning, 1967) are utilized. Specifically, the equilibrium vapor and liquid densities are utilized to locate ϵ and σ. Their values for the four fluids are listed in Table 12. Unlike the semiempirical EOS which utilize the critical values of real fluids to evaluate their EOS parameters, this fitting takes the data 95% below the critical temperature. The procedure is physically more reasonable because all current theories including the VDW-type EOS are known to be inappropriate to account for the critical and near critical behavior of real fluids, and the information around the critical point is unlikely to yield correct parameters for these EOS. While in the region 95 % below the critical temperature, the proposed EOS has been shown to describe very well the vapor-liquid coexistence curve of the LJ fluid in Figure 16. In Figures 42-45, the phase diagrams calculated by the proposed EOS for the four fluids are shown. The predicted P-T profiles are also supplemented. It is evident that the present EOS represents well the experimental data, except in the region close to the critical point as anticipated. These phase diagrams quite resemble Figure 16 where the saturated T-ρ curve from the proposed EOS is plotted against MC data. The resemblance indicates the rationality of the regressed parameters in the proposed EOS, provided that the LJ

potential represents the interaction of these fluids. To serve as an example, the saturated T-ρ curves are calculated from the PR equation and depicted in Figures 42-45 for comparison. These figures show that the theoretical EOS developed in this work is much better than the PR EOS to calculate saturated liquid densities. The improvement is appreciable for all the four fluids. As far as saturated vapor density and pressure are concerned, the proposed EOS is satisfactory but inferior to the PR EOS because of failure in the critical region. However, one should be aware that the near critical behavior calculated by an empirical EOS is theoretically doubtful even it gives a good description. Overall, the proposed EOS gives a more reliable phase diagram than the empirical one.

The performance of the proposed EOS can be further illustrated by predicting the second virial coefficient B_2. The PR EOS is known to fail in this aspect as depicted in Figures 46-49. Other semiempirical EOS are expected to behave similarly. It is seen that the proposed EOS improves considerably the B_2 calculation for all four fluids. At medium and high temperatures, the proposed EOS gives excellent results, whereas at low temperatures, the results become less satisfactory because the perturbation theory itself becomes less accurate. Equation (233) is only an inverse temperature expansion to second order of the following exact equation:

$$B_2=2\pi\int_0^\infty (1-e^{-\beta u(r)})\, r^2 dr \qquad (256)$$

Furthermore, it is known that the LJ potential is a simple model for real molecules. It is not exact even for argon (Lee, 1988). The inaccuracy of representation may become more pronounced at low than at high temperatures, which is another possible reason to explain the low temperature deterioration.

In summary, the developed two-parameter EOS is found applicable for simple real fluids. The validity is supported by two facts: (1) giving a better phase diagram except around the critical point; and (2) yielding better B_2 values. The theoretical EOS overcomes some shortcomings of semiempirical EOS. These achievements are very encouraging for the future calculation of simple mixtures. We can expect that

Equation (240) will give more consistent results for various thermodynamic properties of these mixtures than other empirical and semiempirical EOS. Equation (240) may need only one set of parameters for both VLE and LLE for simple mixtures, which can not be expected by an empirical model. The investigation of these applications will be carried out in our future studies. Although the proposed EOS is not yet directly applicable for polar fluids with additional intermolecular forces, it provides a foundation to explore these fluids. Developing an EOS for these complex fluids can be facilitated by taking the LJ fluid as the reference system of a perturbation theory and using the developed RDF (134) and property expressions (217)-(233). Of course, such a development will need additional efforts on manipulating perturbation theory and probably more algebraic work on the solution of the OZ equation.

Table 12. The LJ parameters for Ar, CH_4, O_2, N_2

	σ(Å)	ϵ/k(K)
Ar	3.4009	117.18
CH_4	3.7108	149.52
O_2	3.3754	121.72
N_2	3.6060	99.65

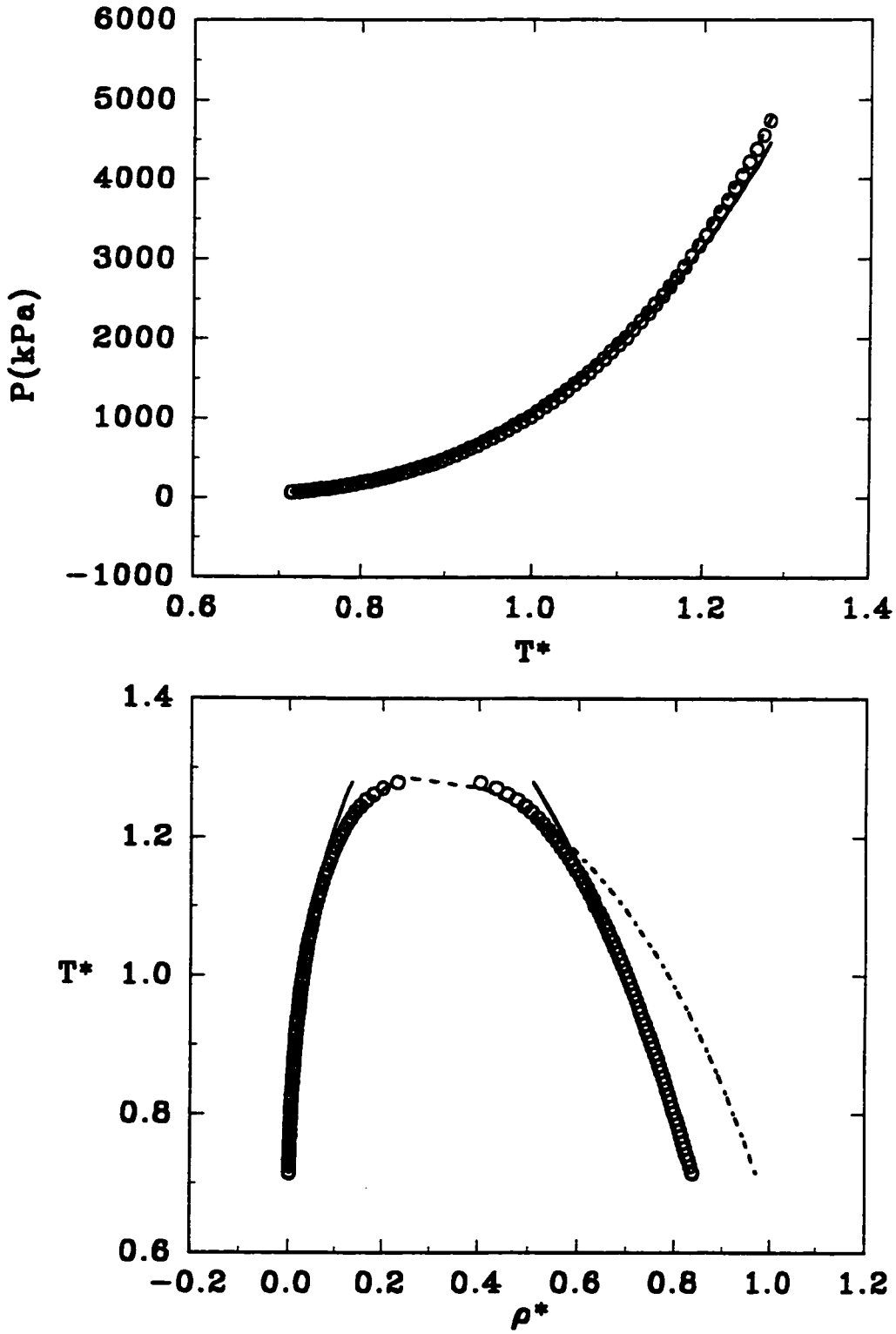

Figure 42. Phase diagram for argon. The solid and dashed lines are given by the present EOS and PR EOS, respectively. The circles are the literature data (Canjar and Manning, 1967).

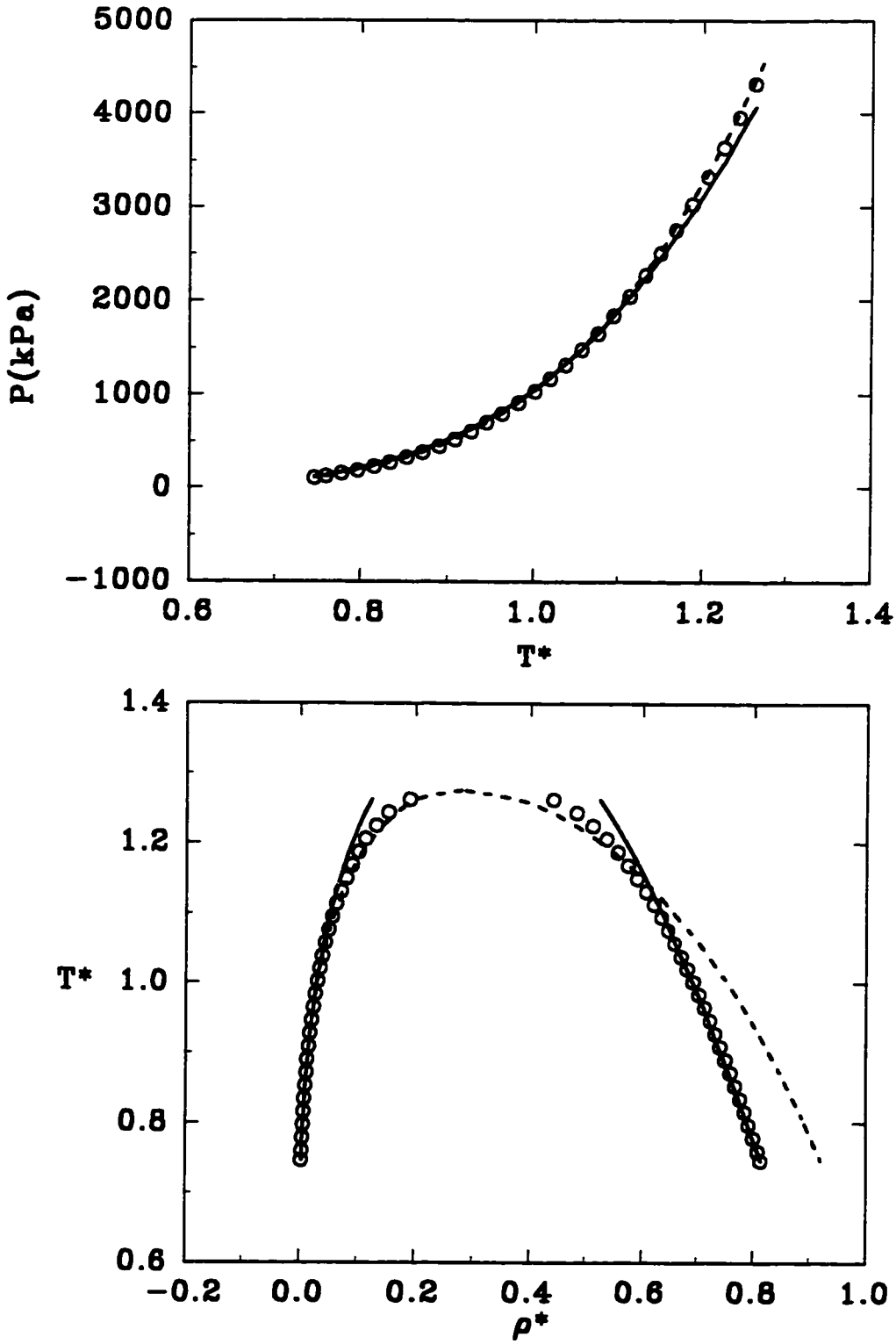

Figure 43. Phase diagram for methane. The solid and dashed lines are given by the present EOS and PR EOS, respectively. The circles are the literature data (Canjar and Manning, 1967).

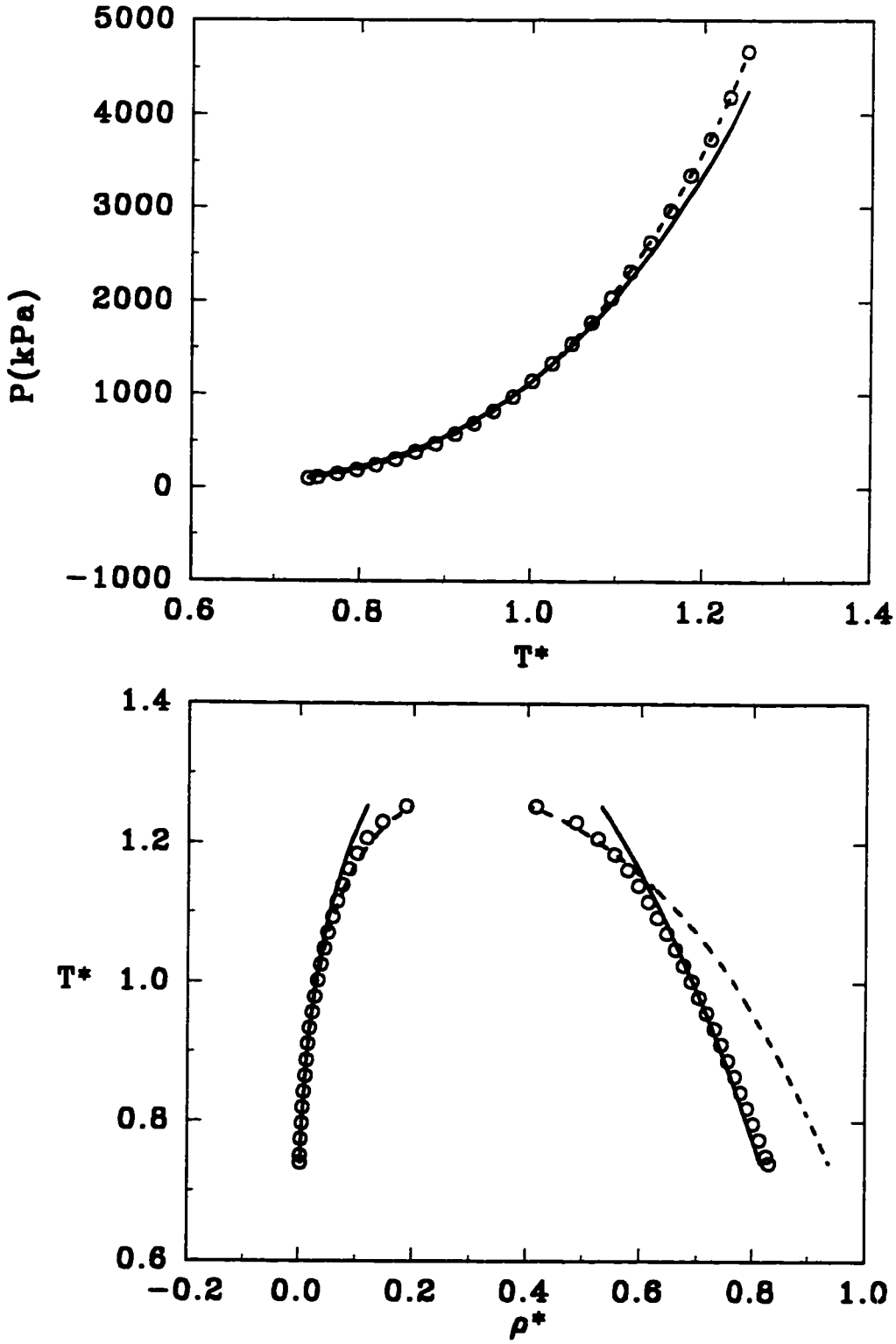

Figure 44. Phase diagram for oxygen. The solid and dashed lines are given by the present EOS and PR EOS, respectively. The circles are the literature data (Canjar and Manning, 1967).

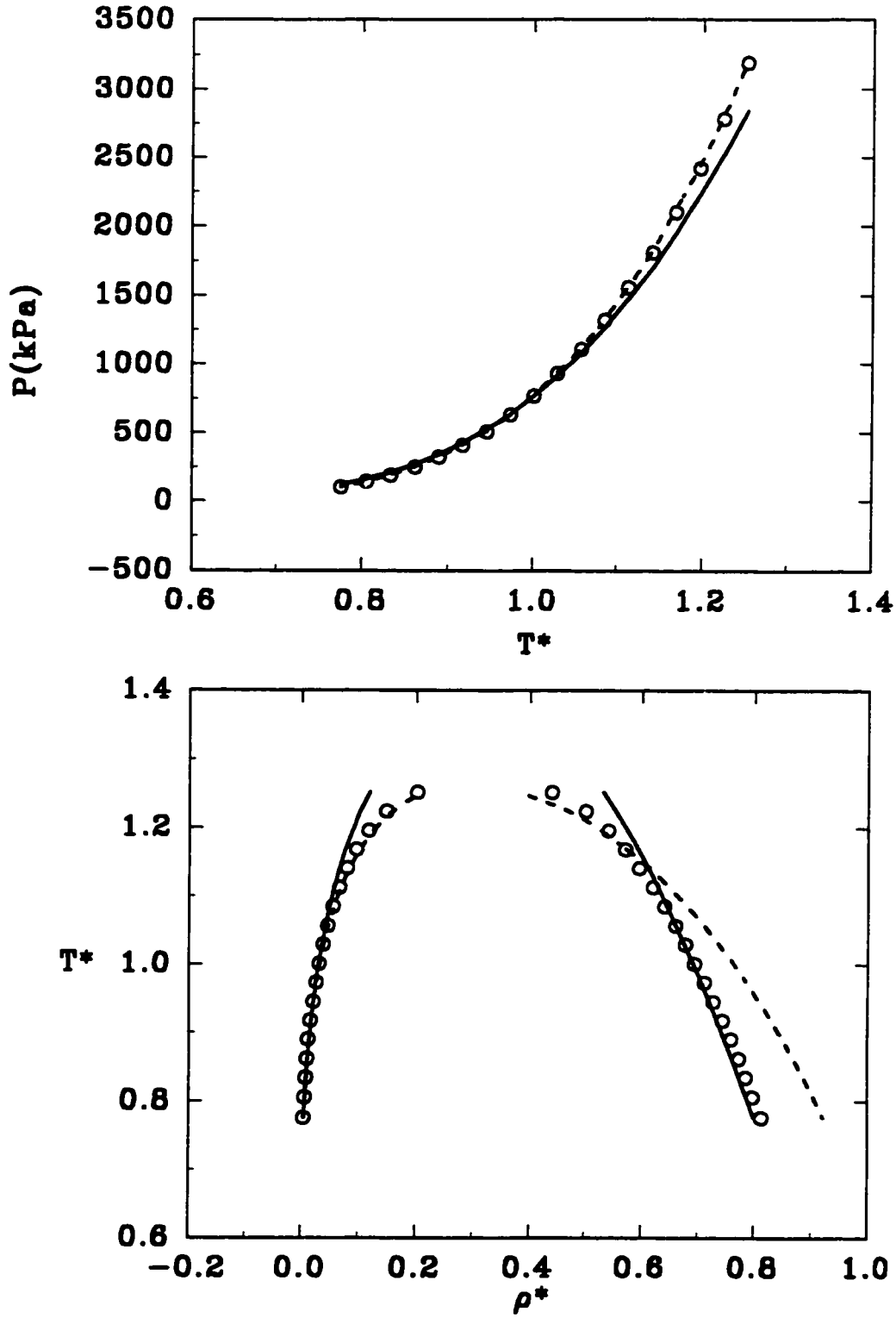

Figure 45. Phase diagram for nitrogen. The solid and dashed lines are given by the present EOS and PR EOS, respectively. The circles are the literature data (Canjar and Manning, 1967).

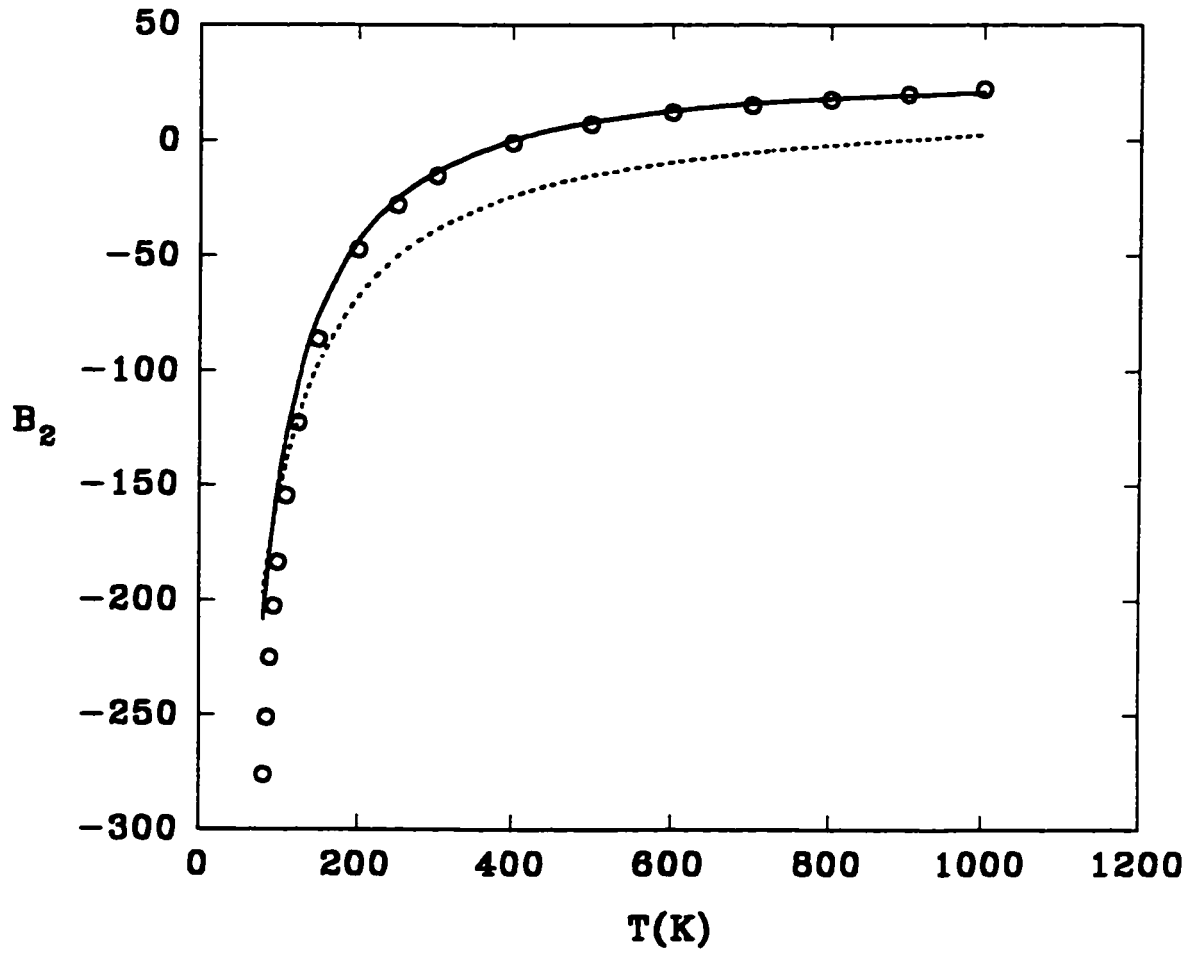

Figure 46. Second virial coefficient for argon. The solid and dashed lines are given by the present EOS and PR EOS, respectively. The circles are the literature data (Dymond and Smith, 1980).

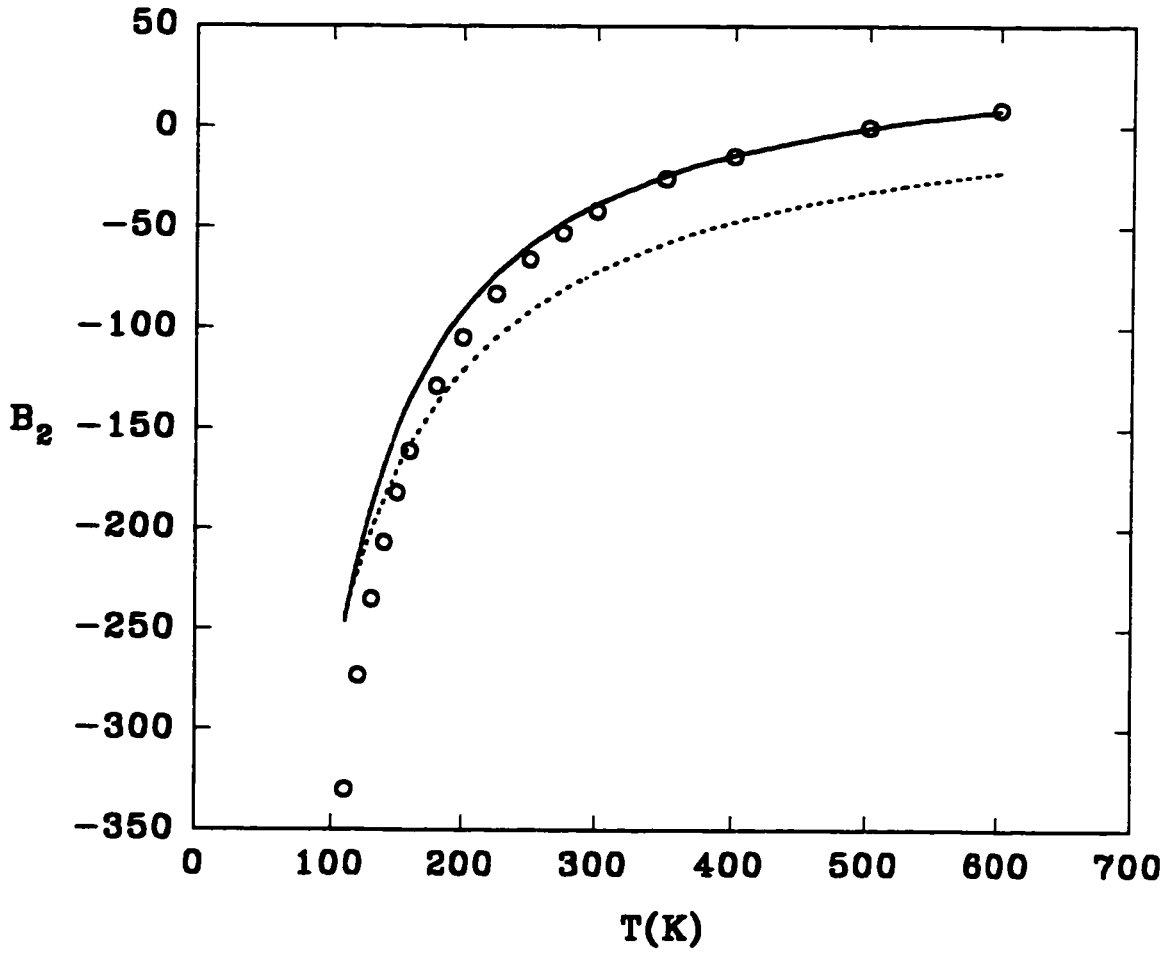

Figure 47. Second virial coefficient for methane. The solid and dashed lines are given by the present EOS and PR EOS, respectively. The circles are the literature data (Dymond and Smith, 1980).

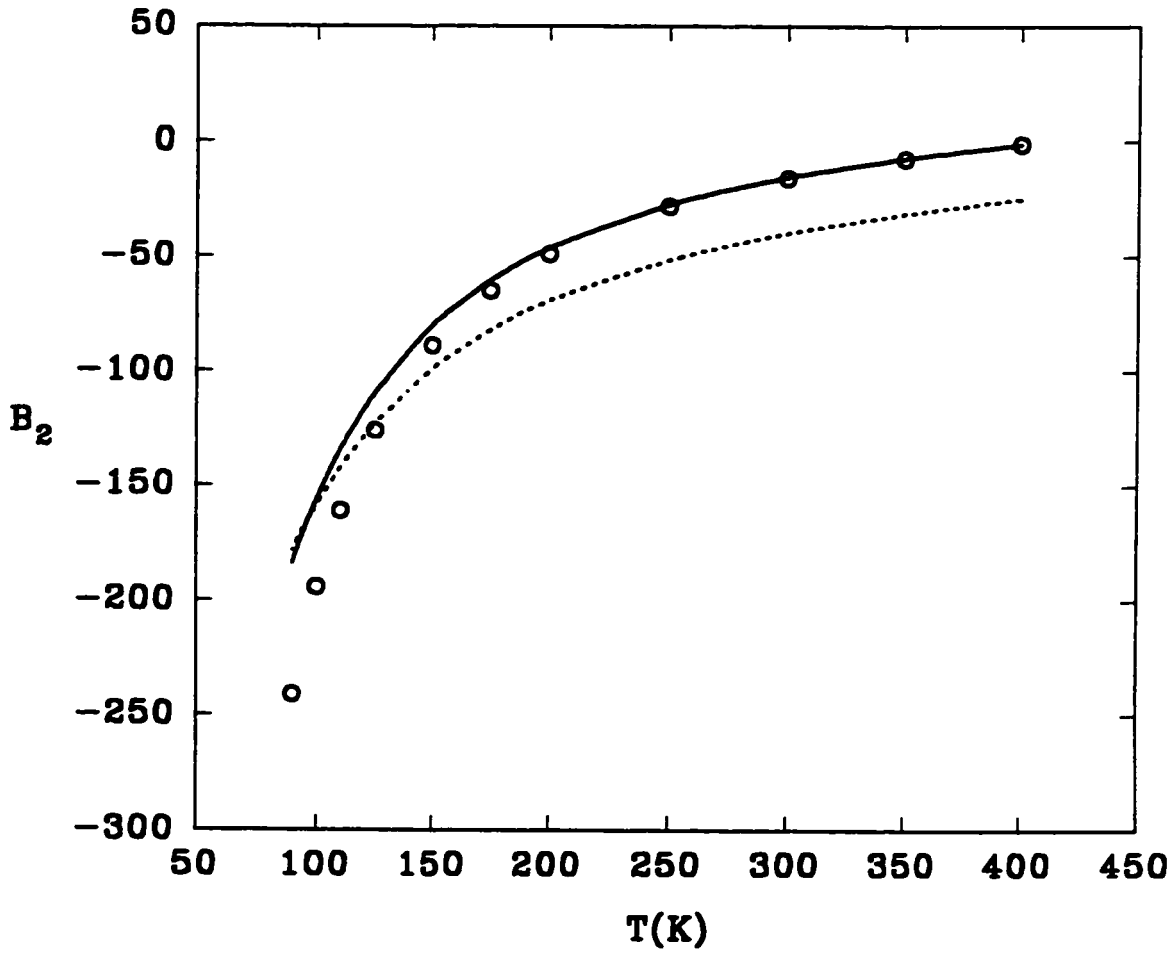

Figure 48. Second virial coefficient for oxygen. The solid and dashed lines are given by the present EOS and PR EOS, respectively. The circles are the literature data (Dymond and Smith, 1980).

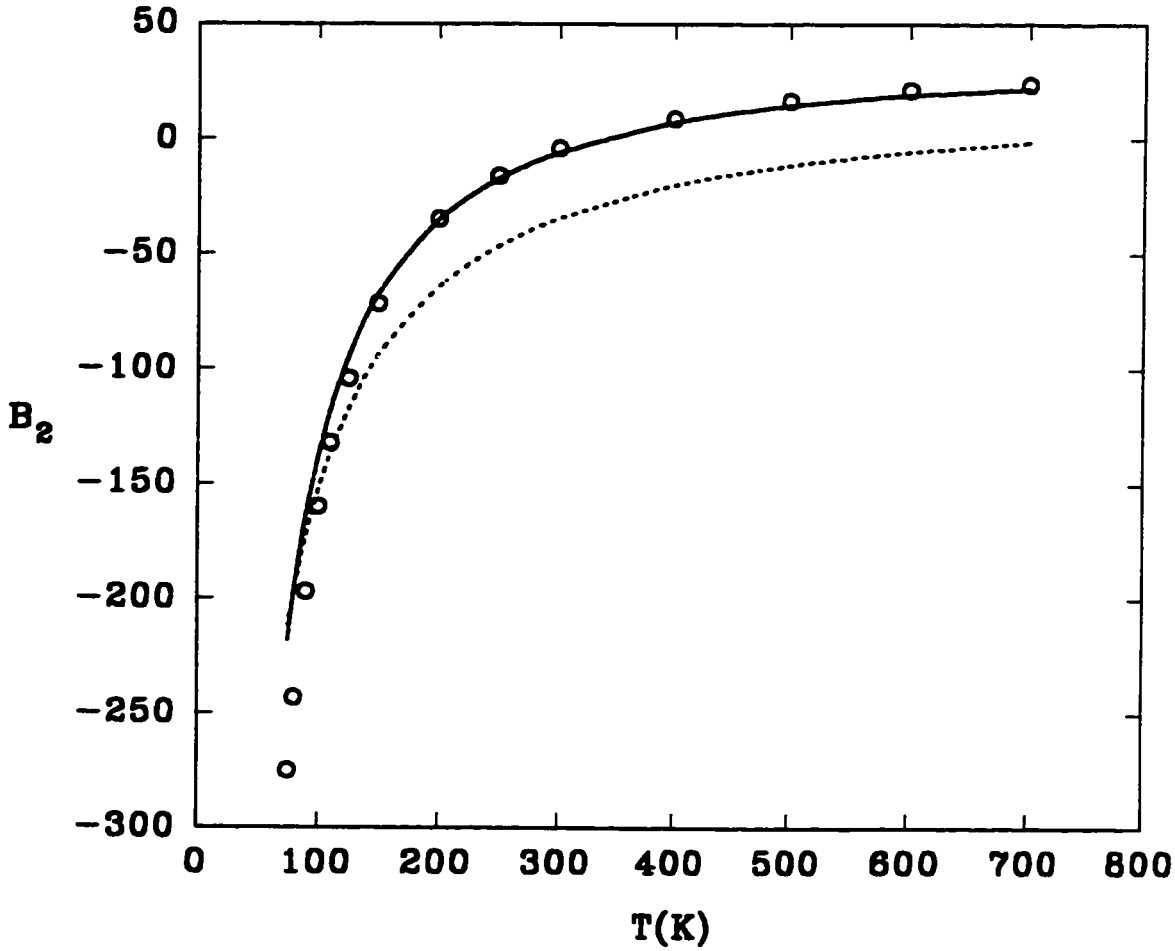

Figure 49. Second virial coefficient for nitrogen. The solid and dashed lines are given by the present EOS and PR EOS, respectively. The circles are the literature data (Dymond and Smith, 1980).

6. Object-oriented Programming with C++ in Studying Fluids

A good liquid theory is important for thermodynamic studies. Equally important is how to implement the liquid theory in practice. The implementation often determines the efficiency of delivering the theory and the progress of developing more sophisticated theories. The accomplishment made in this work is indivisible with the utilization of advanced computer technology. All the calculations mentioned above for classic fluids are programmed by C++. The elegant features of C++, especially Object-oriented Programming (OOP), make the programming for these behaviorly-different but internally-associated fluids like a simple work for a family. The development of the OOP is very similar to the history of OOP itself in computer languages. Originally, C code was written for some of these fluids. C language has provided great convenience in code-writing than other languages, e. g., Fortran. For instance, the treatment of the complex data in Sections 3.1 and 3.3 can be as simple as any real data. The function pointer in C enables one to handle the integrand in an integration as a variable, just like a data variable. Those special features of C have greatly facilitated the program writing. However, as time goes on and more fluids are encountered, these codes for individual fluids become more difficult to manage and wasteful in their reutilization. For instance, one has to copy three sets of code of hard spheres in the programs for SW, Yukawa, LJ fluids individually with only slight modifications. When the TY function and the SEXP approximation are used in the calculations, the code rewriting becomes more irritating and apparently meaningless. At this stage, it comes to the point to re-organize the programs by OOP, the major feature of C++. OOP is a completely new programming design and has considerable differences from the traditional procedure-oriented programming of C and Fortran. Therefore, the transition takes some time and new efforts. But it is proven worthwhile and fruitful. In fact, OOP ideas fit hand in glove in treating the fluids discussed here. Straightforwardly speaking, each fluid in this work is abstracted as a class in OOP. Once temperature, density and potential parameters are given, a concrete object, which is a "real" fluid for calculations, can be created. There are

three major properties to characterize an OOP language: encapsulation, inheritance and polymorphism. These features have made the code more structured, extensible and maintainable. Finally, the whole fluids in this work are manipulated like members of a family. The family tree or the hierarchy of classes is illustrated in Figure 50. The constructors, data and functions of each class are left in Appendix C. Three major features of OOP implemented in this work are explained in detail as follows:

(a) Encapsulation. Encapsulation is used to screen off the members (variables or functions) in a class accessed unnecessarily by other classes or the main function. Encapsulation is implemented by three access controls: private, protected and public, defining if the members of a class are visible from inside, descendants and outside, respectively. Any members of a class must be tagged by one of the above access controls. In the programming of this work, the major quantities concerned are RDF, thermodynamic properties including the Helmholtz free energy, internal energy and compressibility factor. The functions for calculating these quantities may be called from the main program which is outside of the class. Therefore, these functions are treated as public members. Temperature and density are utilized throughout the hierarchy of fluids to describe the state of a fluid. They are designed as protected members since one rarely needs to get them from outside. The universal functions in this work like the factor correlation function $Q_0(s)$ and $A(n_1, n_2, k_1, \alpha)$-$D(n_1,n_2,n_3,z,r)$ in Section 3.3 are protectedly encapsulated. Those functions play only supporting roles for the RDF calculation and are never called in the main program. For the same reasons, $G_i(s)(i=0,1)$ in Section 3.1 and 3.6 is also treated as protected. Private members in programming, for example in the SW class, include all the intermediate functions for calculating the thermodynamic properties of the SW fluid in Section 4.1. These functions are never concerned by us and neither by subclasses. Obviously, encapsulation makes the code very readable and maintainable. In a procedure-oriented programming, all the functions and data mentioned above are open to outside. When the code gets huge, the openness ends up with chaos and difficulty to detect program bugs.

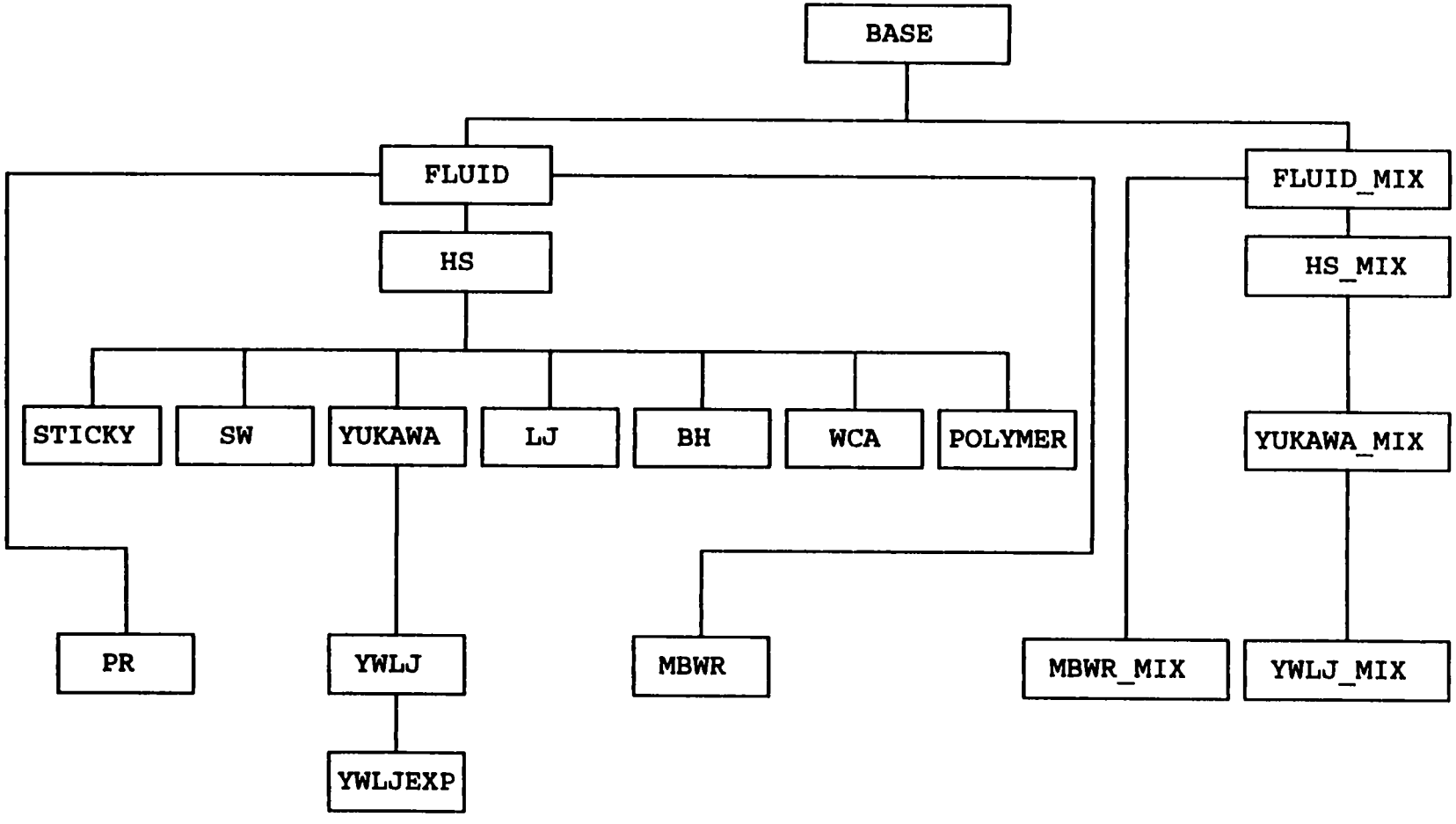

Figure 50. The hierarchy of classes in the OOP design of this work.

(b) Inheritance. Inheritance is an efficient method to make a connection among different classes. Only by inheritance, those classes with similar behavior are organized as a family and unity to the outside. Generally, in a class hierarchy, the toppest class gives the most general behavior of its child classes. A child class automatically inherits all members of its parent class open to it and incorporates some new behavior. Therefore, a parent class is more abstract and a child class is more concrete. This can be perfectly illustrated by the class tree shown in Figure 50. At the top of the tree is class BASE, which provides all the methods necessary in later thermodynamic calculations. These methods include the Simpson method for integration, the Gauss solution method for linear equations, the Newton solution method for nonlinear equations, and numerical Laplace and Fourier transforms. It is notable that these methods are applicable not only for studying fluids but also for any other purposes. In other words, these methods are very general and their container BASE should be defined most abstractly. At the next level, the class hierarchy evolves into two separate subtrees, one for pure fluids and the other for mixtures. The two subtrees behave very similarly and that of pure fluids is further illustrated below. The first class in the subtree, FLUID, is a very abstract class for fluids. It contains the most general characteristics of a fluid, i. e., temperature, density, the Helmholtz free energy, internal energy, compressibility factor and chemical potential. These universal properties are only conceptually created and have to be instantiated in later child classes. It is the conceptual design that makes the function *phase_equilibria* in FLUID applicable for the calculation of phase equilibria of any fluids. The next inheritance is HS, standing for hard spheres. The class is more realistic than the abstract class FLUID. In HS, the RDF and thermodynamic properties are concretely presented. These important quantities are utilized in calculations of perturbation theories for more complex fluids. Therefore, HS is treated as the parent for eight more realistic fluid classes, from STICKY, YUKAWA to POLYMER. The class YWLJ uses the two-Yukawa (TY) function to study the LJ fluid and is naturally designed as the descendant of YUKAWA. The SEXP approximation mentioned in Section 3.8 is encapsulated in YWLJEXP, which is a modification and child of YWLJ.

It should be mentioned here that the MBWR equation is a totally empirical equation for the LJ fluid and is independent of any thermodynamic properties mentioned in this work. Therefore, the class MBWR is created directly as one child of FLUID. The classes in the other subtree for mixtures are developed in a very similar manner.

(c) Polymorphism. This feature is accomplished by virtual functions in C++. A virtual function is a temporary function associated with its class and may be functionally altered in later subclasses while its signature remains the same. Virtual functions greatly enhance the capability of descendants in exhibiting their own characteristics without spending extra code. Virtual functions are utilized extensively in this programming. All the thermodynamic properties are set virtually in FLUID. This setting makes the function *phase_equilibria* to calculate phase equilibria of a fluid using the pressure and chemical potential of that fluid automatically. The virtual function $G_i(s)(i=0,1)$ enables the inverse Fourier transform FFT in BASE to call the proper $G_i(s)$ for the concerned fluid. The Simpson integration, and Newton equation-solving methods also make use of virtual functions to realize their universality. Programming by virtual functions, or the virtual design, is a very important concept in OOP. More virtual functions in programming will make the program more general and more succinct.

Finally, it is pointed that the three features of OOP are inherently connected and have to be considered comprehensively. Without encapsulation, inheritance will not make sense. The design of an inheritance relies on the design of virtual functions. Good virtual functions make a class tree more natural and more flexible for creating new subclasses.

7. Conclusions and Remarks

In this work, the OZ equation is decomposed into a set of new integral equations. The utilization of the Hilbert transform is proposed for the first time to solve analytically these equations under the PY approximation and MSA. Both pure fluids and mixtures are included in the new solution. One extraordinary feature of the solution is that it is applicable to any intermolecular potential. It is found that the first-order solution is of a simple analytical form and sufficient to determine fluid structure and thermodynamics. Subsequently, for the first time, an analytical RDF in terms of the Laplace transform is reported here for the SW and LJ fluids as well as for other fluids in the literature. The reliability of the developed RDF is tested successfully against computer simulation data. Based on the first-order RDF, thermodynamic properties are analytically developed for the SW, LJ fluid and LJ mixtures. Extensive comparisons with computer simulation data show that for the SW fluid the present theory gives best results for various well-width values. For the LJ fluid, the performance of the present theory is superior to the two well-known BH and WCA theories and has a comparable performance to the latest 33-parameter MBWR equation. A number of typical properties of LJ mixtures, including excess free energy, chemical potential at infinite dilution, VLE and LLE, are predicted by the present theory. The predictions are found to be better than those of two WCA-type perturbation theories and the VDW1 theory available in the literature for studying LJ mixtures. One remarkable feature of the proposed theory is its stable performance for various thermodynamic properties while all other theories and empirical EOS mentioned in this work apparently fail in this aspect. Four simple real fluids are calculated by the new EOS in this work. The calculation indicates that the present EOS is an appealing improvement over the empirical PR EOS due to its consistent performance for several typical properties.

As well as theoretical rigorousness and prediction accuracy, the mathematical simplicity achieved by the present theory is very desirable and can not be expected by any other liquid theories based on molecular interactions. By implementing a new

mathematical algorithm for the inverse Laplace transform, RDFs for all mentioned fluids are finally presented in a completely analytical and explicit manner. A new TY function is proposed in this work to map accurately the LJ potential. The mapping successfully gets rid of the integrations intricating the studies of the LJ fluid and mixtures and makes the present theory as easily attainable as other empirical EOS. The accomplishment provides a promising way to develop a new solution model to study real mixtures as well as pure fluids. The theoretically-based model will serve engineering purposes and hopefully eliminate, at least partially, the thermodynamic inconsistencies found in previous empirical models.

In addition to the new OZ solution, this work has incorporated some progress in liquid theory to make the present EOS more sophisticated. By combining the first-order RDF of the Yukawa fluid with the GMSA, a simple and more accurate RDF for both pure hard spheres and mixtures are developed. With importing the EXP approximation, a new approximation, the SEXP approximation, is proposed to eliminate the defects of the MSA for the LJ fluid and mixtures. The PY2 approximation of Chiew for hard sphere chains is for the first time analytically solved in this work. The solution provides a basis to explore nonspherical molecules.

The achievement in this work provides broad prospects for studying more complex molecules and more complex behavior of fluids. One possible application of the mathematical strategy proposed in this work is to nonspherical molecules. The thermodynamic behavior of these fluids is of wider industrial value and is more difficult to describe by an empirical equation. The extensions of the OZ equation for these fluids have been made but fully analytical solutions are very scarce even for simple hard-sphere chains. Since there are many similarities between the extended OZ equation and the original OZ equation, it is feasible to solve analytically the integral equation with the further utilization of the Hilbert transform. The application of the Hilbert transform for the OZ equation of electrolyte solutions is also possible. Electrolyte solutions are an important type of fluids in thermodynamics and their property calculation is always an interesting topic. Although the OZ solutions for these fluids have been reported in the literature, only the basic Coulomb force between

ions is considered in these studied. The Hilbert transform provides the possibility to obtain a solution for more complex interactions between ions, e. g. the Coulomb force plus the LJ potential. In addition to homogeneous fluids, the application of the OZ solutions for non-uniform fluids is of great interest. The analytical, not numerical, structure expressions, for a homogeneous fluid are important input functions to study the corresponding inhomogeneous fluid in the density functional theory. This work has provided a number of more sophisticated RDF expressions than previous ones used in the non-uniform fluid theory. It will be of interest to see in the future whether the new expressions improve the performance of the density functional theory.

Finally, it is valuable to mention here that all the calculations made in this work are programmed by C++ and OOP. The three major features of OOP are used extensively in the work. These features make all the mentioned fluids organized like a family in the programming. The resulting code is concise, easily maintainable and thus greatly facilitates the computational work.

References

Abramo, M. C., C. Caccamo and G. Giunta, " Phase Stability of Fluid Hard-Sphere Mixtures Interacting through an Attractive Tail", Phys. Rev. A. 34, 3279-3287(1986).

Andersen, H. C., D. Chandler and J. D. Weeks, " Roles of Repulsive and Attractive Forces in Liquids: the Equilibrium Theory of Classical Fluids," Adv. Chem. Phys., 34, 105-156 (1976).

Arich B.-N., "Statistical Thermodynamics for Chemists and Biochemists", Plenum Publishing Corporation, New York, Chapter 8 (1992).

Arrieta, E., C. Jedrzejek and K. N. Marsh, "Mean Spherical Approximation Algorithm for Multicomponent Multi-Yukawa Fluid Mixtures: Study of Vapor-Liquid, Liquid-Liquid and Fluid-Glass Transitions", J. Chem. Phys. 95, 6806-6837 (1991).

Attard, P., " Molecular Fluids: Site-site Analysis and Hypernetted Chain Results with Bridge Functions for Lennard-Jones Dimers", Mol. Phys. 83, 273-291 (1994).

Banaszak, M., Y. C. Chiew and M. Radosz, "Mixing Rules for Binary Lennard-Jones Fluid Structures", Fluid Phase Equilibria 111, 161-174 (1995).

Barboy, B., "Solution of the Compressibility Equation of the Adhesive Hard-Sphere Model for Mixtures", Chem. Phys. 11, 357-371 (1975).

Barker, J. A. and D. Henderson, "Perturbation Theory and Equation of State for Fluids: The Square-Well Potential", J. Chem. Phys. 47, 2856-2861 (1967a).

Barker, J. A. and D. Henderson, "Perturbation Theory and Equation of State for Fluids. II. A Successful Theory of Liquid", J. Chem. Phys. 47, 4714-4721 (1967b).

Baxter, R. J. "Percus-Yevick Equation of Hard Spheres with Surface Adhesion", J. Chem. Phys. 49, 2270-2275 (1968a).

Baxter, R. J. "Ornstein-Zernike Relation for a Disordered Fluid", Aust. J. Phys. 21, 563-569 (1968b).

Baxter, R. J. "Ornstein-Zernike Relation and Percus-Yevick Approximation for Fluid Mixtures", J. Chem. Phys. 52, 4559-4562 (1970).

Benavides, A. L. and F. Del Rio, "Properties of the Square-Well Fluid of Variable Width. III, Long-Rang Expansion", Mol. Phys. 68, 983-1000 (1989).

Blum, L., " Mean Spherical Model for Asymmetric Electrolytes, I. Method of Solution", Mol. Phys. 30, 1529-1535, (1975).

Blum, L. and J. S. Hφye, " Mean Spherical Model for Asymmetric Electrolytes, 2. Thermodynamic Properties and the Pair Correlation Function", J. Phys. Chem. 81, 1311-1316, (1977).

Blum, L. and J. S. Hφye, "Solution of the Ornstein-Zernike Equation with Yukawa Closure for a Mixture", J. Stat. Phys. 19, 317-324 (1978).

Blum, L., "Solution of the Mean Spherical Approximation for Hard Ions and Dipoles of Arbitrary Size", J. Stat. Phys. 18, 451-474 (1978).

Blum, L. and D. Wei, " Analytical Solution of the Mean Spherical Approximation for an Arbitrary Mixture of Ions in a Dipolar Solvent", J. Chem. Phys. 87, 555-567 (1987).

Bohn, M., J. Fischer and F. Kohler, "Prediction of Excess Properties for Liquid Mixtures: Results from Perturbation Theory for Mixtures with Linear Molecules", Fluid Phase Equilibria 31, 233-252(1986).

Boublik, T., "Phase Equilibria of Systems Considered in Supercritical Fluid Extraction Determined from Perturbation Theory", Mol. Phys. 90, 585-591 (1997).

Caccamo, C. and G. Giunta, "Liquid-Liquid and Liquid-Vapor Separation in Hard Sphere Yukawa Mixtures", Phys. Lett. A 158, 325-330 (1991).

Caccamo, C. and G. Giunta, "Microscopic Theoretical Description of Phase Stability in Hard Sphere Yukawa Mixtures", Mol. Phys. 78, 83-93 (1993).

Canjar, L. N. and F. S. Manning, "Thermodynamic Properties and Reduced Correlations for Gases", Gulf Publishing Company, Houston, Texas (1967).

Carnahan, N. F. and K. E. Starling, "Intermolecular Repulsions and the Equation of State for Fluids", AIChE J. 18, 1184-1189 (1972).

Castano, F., J. J. Brey and A. Santos, "Nonclassical Critical Exponents in the Mean Spherical Approximation", Mol. Phys. 66, 695-700 (1989).

Chandler, D. and H. C. Andersen, "Optimized Cluster Expansion for Classical Fluids. II. Theory of Molecular Liquids", J. Chem. Phys. 57, 1930-1937 (1972).

Chandler, D., R. Silbey and B. M. Ladanyi, "New and Proper Integral Equations for Site-Site Equilibrium Correlations in Molecular Fluids", Mol. Phys. 46, 1335-1345 (1982).

Chang, J. and S. I. Sandler, "A Real Function Representation for the Structure of the Hard-Sphere Fluid", Mol. Phys. 81, 735-744 (1994).

Chialvo, A. A. and P. T. Cummings, " Solute-Induced Effects on the Structure and Thermodynamics of Infinitely Dilute Mixtures", AIChE J. 40, 1558-1573 (1994).

Chiew, Y. C., "Percus-Yevick Integral-Equation Theory for Athermal Hard-Sphere Chains", Mol. Phys. 70, 129-143 (1990).

Chiew, Y. C., "Intermolecular Site-Site Correlation Functions of Athermal Hard-Sphere Chains: Analytic Integral Equation Theory", J. Chem. Phys. 93, 5067-5074 (1990).

Chiew, Y. C., "Percus-Yevick Integral-Equation Theory for Athermal Hard-Sphere Chains. II. Average Intermolecular Correlation Functions", Mol. Phys. 73, 359-373 (1991).

Chiew, Y. C., D. Kuehner, H. W. Blanch and J. M. Prausnitz, "Molecular Thermodynamics for Salt-Induced Protein Precipitation", AIChE J. 41, 2150-2159 (1995).

Collings, A. F. and I. L. Mclaughlin, " The Transport Coefficients for Polyatomic Liquids", J. Chem. Phys. 73, 3390-3395 (1980).

Curro, J. G. and K. S. Schweizer, "Equilibrium Theory of Polymer Liquids: Linear

Chains", J. Chem. Phys. 87, 1842-1846 (1987).
Davies, B. and B. Martin, "Numerical Inversion of the Laplace Transform: a Survey and Comparison of Methods", J. Comput. Phys. 33, 1-32 (1979).
Del Rio, F. and L. Lira, "Properties of the Square-Well Fluid at Variable Width. I. Short-Range Expansion", Mol. Phys. 61, 275-297 (1987a).
Del Rio, F. and L. Lira, "Properties of the Square-Well Fluid at Variable Width. II. the Mean Field Term.", J. Chem. Phys. 87, 7179-7184 (1987b).
De Souza, L. E. S. and D. Ben-Amotz, "Optimized Perturbed Hard Sphere Expressions for the Structure and Thermodynamics of Lennard-Jones Fluids", Mol. Phys. 78, 137-149 (1993).
Duh Der-Ming, and A. D. J. Haymet, "Integral Equation Theory for Uncharged Liquids: the Lennard-Jones Fluid and the Bridge Function", J. Chem. Phys. 103, 2625-2633 (1995).
Dymond, J. H. and E. B. Smith, "The Virial Coefficients of Pure Gases and Mixtures", Clarendon Press, Oxford(1980).
Dymond, J. H., "Corrections to the Enskog Theory for Viscosity and Thermal Conductivity", Physica 144B, 267-276 (1987).
Ferreira P. G., R. L. Carvalho and M. M. Telo da Gama,"Singularities in the Consistent Hypernetted Approximation". J. Chem. Phys. 101, 594-602 (1994).
Foiles, S. M. and N. W. Aschcroft, "Variational Theory of Phase Separation in Binary Liquid Mixtures", J. Chem. Phys., 75, 3594-3598 (1981).
Fotouh, K. and K. Shukla, "An Improved Perturbation Theory and van der Waals One-Fluid Theory of Binary Fluid Mixtures: Part 1. Total and Excess Thermodynamic Properties", Fluid Phase Equilibria 127, 45-70 (1997).
Gubbins, K. E., W. R. Smith, M. K. Tham and E. W. Tiepel, "Perturbation Theory for the Radial Distribution Function", Mol. Phys. 22, 1089-1105 (1971).
Guo, M., W. Wang and H. Lu, "Equations of State for Pure and Mixture of Square-Well Fluids, II. Equation of State", Fluid Phase Equilibria 60, 221-237 (1990).
Guo, M., Y. Li, Z. Li and J. Lu, "Molecular Simulation of Liquid-liquid Equilibria for Lennard-Jones Fluids", Fluid Phase Equilibria 98, 129-139 (1994).
Hansen, J. P. and I. R. McDonald, "Theory of Simple Liquids", 2nd. Ed. Academic Press, London (1986).
Hansen, J. P., "Phase Transition of the Lennard-Jones System. II. High-Temperature Limits", Phys. Rev. A 2, 221-230(1970).
Harismiadis, V. I., A. Z. Panagiotopoulos, and D. P. Tassios, "Phase Equilibria of Binary Lennard-Jones Mixtures with Cubic Equations of State", Fluid Phase Equilibria 94, 1-18 (1994).
Harismiadis, V. I., N. K. Koutras, D. P. Tassios and A. Z. Panagiotopoulos, "How Good is Conformal Solution Theory for Phase Equilibrium Prediction?", Fluid Phase Equilibria 65, 1-18 (1991).

Henderson, D., W. G. Madden and D. D. Fitts, " Monte Carlo and Hypernetted Chain Equation of State for the Square-Well Fluid", J. Chem. Phys. 64, 5026-5034 (1976a).

Henderson, D., F. F. Abraham and J. A. Barker, " The Ornstein-Zernike Equation for a Fluid in Contact with a Surface", Mol. Phys. 31, 1291-1295 (1976b).

Henderson, D., E. Waisman, J. L. Lebowitz and L. Blum, "Equation of State of a Hard-Core Fluid with a Yukawa Tail", Mol. Phys. 35, 241-255 (1978).

Henderson, D., O. H. Scalise and W. R. Smith, "Monte Carlo Calculation of the Equation of State of the Square-Well Fluid as a Function of Well Width", J. Chem. Phys. 72, 2431-2438 (1980).

Hochstadt, H., "Integral Equations", Wiley, New York, Chapter 5 (1973).

Hoheisel, C., U. Deiters and K. Lucas, "The Extension of Pure Fluid thermodynamic Properties to Supercritical Mixtures. A Comparison of Current Theories with Computer Data over a Large Region of State", Mol. Phys. 49, 159-170 (1983).

Hoheisel, C. and R. Zhang, "Structure and Phase Separation Behavior of Yukawa Mixtures Studied by the Mean Spherical Approximation and Computer Calculations", Phys. Rev. A 43, 5332-5336 (1991).

Huber, M. L. and J. F. Ely, "Properties of Lennard-Jones at Various Temperatures and Energy Ratios with a Size Ratio of Two", NIST Technical Note #1331 (1989).

Hφye, J. S. and L. Blum, "Solution of the Yukawa Closure of the Ornstein-Zernike Equation", J. stat. Phys. 16, 399-413 (1977).

Hφye, J. S. and G. Stell,"Thermodynamics of the MSA for Simple Fluids," J. Chem. Phys., 67, 439-445 (1977).

Jedrzejek, C. and G. A. Mansoori, "Equation of State of a Hard Core Fluid with a Two-Yukawa Tail: Toward a Simple Analytic Theory", Acta Phys. Pol. 57, 107-118 (1980).

Johnson, J. K., J. A. Zollweg and K. E. Gubbins, "The Lennard-Jones Equation of State Revisited", Mol. Phys. 78, 591-618 (1993).

Kalyuzhnyi Yu. V., and P. T. Cummings, "Phase Diagram for the Lennard-Jones Fluid Modelled by the Hard-Core Yukawa Fluid", Mol. Phys. 87, 1459-1462(1996).

Kenkare, P. U. and C. K., Hall, "Modelling of Phase Separation in PEG-Salt Aqueous Two-Phase Systems", AIChE J. 42, 3508-3522 (1996).

Konitor, J. and C. Jedrzejek, "Analytic Formulation of the WCA Type Perturbation Theory for a Hard-Core with One-Yukawa Tail Fluid", Mol. Phys., 55, 187-198 (1985).

Lebowitz, J. L., "Exact Solution of Generalized Percus-Yevick Equation for a Mixture of Hard Spheres", Phys. Rev. 133, A895-A899 (1964).

Lebowitz, J. L. and J. K. Percus, " Mean Spherical Model for Lattice Gases with Extended Hard Cores and Continuum Fluids", Phys. Rev. 144, 251-258 (1966).

Lee, K. H. and S. T. Sandler, "The Generalized Van Der Waals Partition: IV. Local

Composition Models for Mixtures of Unequal-Size Molecules", Fluid Phase Equilibria 50, 53-77 (1987).
Lee, L. L., "Molecular Thermodynamics of Nonideal Fluids", Butterworths Series in Chemical Engineering, Chapter II (1988).
Lee, L. L. and D. Levesque, "Perturbation Theory for Mixtures of Simple Liquids", Mol. Phys. 26, 1351-1370 (1973).
Lee,R. J. and K. C. Chao, "Coordination Number and Thermodynamics of Square-Well Fluid Mixtures", Mol. Phys. 61, 1431-1442 (1987).
Lee, R. J. and K. C. Chao, "Equation of State for Square-Well Fluids", Mol. Phys. 65, 1253-1256 (1988).
Levesque, D. and L. Verlet, "Perturbation Theory and Equation of State for Fluids", Phys. Rev. 182, 307-316 (1969).
Li, J., Y. Li, J. Lu and T. Teng, "A New Analytic Formula for Molecular Radial Distribution Function in Fluid and Fluid Mixtures. Fluid Phase Equilibria 55, 75-85 (1990).
Lotif, A. and J. Fisher, "Chemical Potential of Model and Real Dense Fluid Mixtures from Perturbation Theory and Simulations", Mol. Phys. 66, 199-219 (1989).
Lotif, A., J. Vrabec and J. Fisher, "Vapour-Liquid Equilibria of the Lennard-Jones Fluid from the NPT plus Test Particle Method", Mol. Phys. 76, 1319-1460 (1992).
Lue, L. and D. Blankschtein, "Analytical Solutions of the Proper Integral Equations for Interactions Site Fluids: Molecules Composed of Hard-Sphere Interaction Sites", J. Chem. Phys. 103, 7086-7097 (1995).
Madden, W. G. and D. D. Fitts, "A New Perturbation Technique for the Radial Distribution Function of Simple Fluids", Mol. Phys. 28, 1095-1099 (1974).
Mandel, F., R. J. Bearman and M. Y. Bearman, "Numerical Solutions of the Percus-Yevick Equation for the Lennard-Jones (6-12) and Hard-Sphere Potentials", J. Chem. Phys. 52, 3315-3323 (1970).
Mansoori, G. A., N. F. Carnahan, K. E. Starling and T. W. Leland, 1971,"Equilibrium Thermodynamics Properties of the Mixtures of Hard Spheres", J. Chem. Phys., 54, 1523-1525 (1971).
Matteoli, E. and G. A. Mansoori, "A Simple Expression for Radial Distribution Function of Pure Fluids and Mixtures", J. Chem. Phys. 103, 4672-4677(1995).
Munoz, F., T. W. Li and E. H. Chimowitz, "Henry's Law and Synergism in Dilute Near-Critical Solution: Theory and Simulation", AIChE J. 41, 389-401 (1995).
Narten, A. H., L. Blum and R. H. Fowler, "Mean Spherical Model for the Structure of Lennard-Jones Fluids", J. Chem. Phys. 60, 3378-3381 (1974).
Nicolas, J. J., K. E. Gubbins and W. B. Streett, "Equation of State for the Lennard-Jones Fluid", Mol. Phys. 37, 1429-1454 (1979).
Ornstein, L. S. and F. Zernike, "Accidental Deviations of Density and Opalescence at the Critical Point of a Single Substance", Pro. Akad. Sci. 17, 793(1914).

Panagiotopoulos, A. Z., "Direct Determination of Phase Coexistence Properties of Fluids by Monte Carlo Simulation in a New Ensemble", Mol. Phys. 61, 813-826 (1987).
Peng, D.-Y. and D. B. Robinson, "A New Two-Constant Equation of State", Ind. Eng. Chem. Fundam. 15, 59-64 (1976).
Percus, J. K. and G. J. Yevick, "Analysis of Classical Mechanics by Means of Collective Coordinates", Phys. Rev. 110, 1-13 (1958).
Perram, J. W., "Hard Sphere Correlation Functions in the Percus-Yevick Approximation", Mol. Phys. 30, 1505-1509 (1975).
Perram, J. W. "The Analytical Solution of the Percus-Yevick and Mean Spherical Equations for Potentials of Finite Range", Mol. Phys. 49, 461-473 (1983).
Redlich, O. and J. N. S. Kwong, "On the Thermodynamics of Solutions V", Chem. Rev. 44, 233(1949).
Reed, J. M. and K. E. Gubbins, "Applied Statistical Mechanics", Mcbraw-Hill, Inc, Chapter 13, (1973).
Rosenfeld, Y. and N. W. Ashcroft, "Theory of Simple Classical Fluid: Universality in the Short-Range Structure," Phys. Rew. A, 20, 1208-1235 (1979).
Rudisill E. N. and P. T. Cummings, "Gibbs Ensemble Simulation of Phase Equilibrium in the Hard Core Two-Yukawa Fluid Model for the Lennard-Jones Fluid", Mol. Phy. 68, 629-635 (1989).
Sadus, R. J., " Calculating Critical Transitions of Fluid Mixtures Theory vs. Experiment", AIChE Journal 40, 1376-1403 (1994).
Shen, S. and B. C.-Y. Lu, "A Simple Perturbed Equation of State from a Pseudopotential Function", Fluid Phase Equilibria 84, 9-22 (1993).
Shing, K. S. and K. E. Gubbins, "The Chemical Potential in Non-Ideal Liquid Mixtures. Computer Simulation and Theory", Mol. Phys. 49, 1121-1138 (1983).
Shing, K. S., K. E. Gubbins and K. Lucas, "Henry Constants in Non-Ideal Fluid Mixtures. Computer Simulation and Theory", Mol. Phys. 65, 1235-1252 (1988).
Shukla, K. P., M. Luckas, H. Marquardt and K. Lucas, "Conformal Solutions: Which Model for Which Application?", Fluid Phase Equilibria 26, 129-147 (1986).
Shukla, K. P.,"Thermodynamic Properties of Simple Fluid Mixtures from Perturbation Theory", Mol. Phys. 62, 1143-1163 (1987).
Smith, E. R., "Mean Spherical Approximation for Simple Hard Sphere Fluids I. Methods of Solution", Mol. Phys. 38, 823-841 (1979).
Smith, W. R. and D. Henderson,"Analytical Representation of the Percus-Yevick Hard-Sphere Radial Distribution Function", Mol. Phys. 19, 411-415 (1970).
Smith, W. R., D. Henderson and J. A. Barker, "Approximate Evaluation of the Second-Order Term in the Perturbation Theory of Fluids", J. Chem. Phys. 53, 508-515 (1971).
Smith, W. R., D. Henderson and J. A. Barker, "Perturbation Theory and the Radial

Distribution Function of the Square-Well Fluid", J. Chem. Phys. 55, 4027-4033 (1971).
Smith, W. R., "Mean Spherical Approximation and Optimized Cluster Theory for the Square-Well fluid", J. Chem. Phys. 67, 5308-5316 (1977).
Stell, G., " Fluids with Long-Range Forces: Toward a Simple Analytic Theory," Phase Transition and Critical Phenomena, Vol. 5, 47-84 (1976).
Stell, G. and J. J. Weis,"Structure and Thermodynamics of a Simple Fluid," Phys. Rev. A., 21, 645-657 (1980).
Tang, Y. and B. C.-Y. Lu, "A New Solution of the Ornstein-Zernike Equation from the Perturbation Theory", J. Chem. Phys. 99, 9828-9835 (1993).
Tang, Y. and B. C.-Y. Lu, "First-Order Radial Distribution Functions Based on the Mean Spherical Approximation for Square-Well, Lennard-Jones, and Kihara Fluids", J. Chem. Phys. 100, 3079-3084 (1994a).
Tang, Y. and B. C.-Y. Lu, "An Analytical Analysis of the Square-Well Fluid Behaviors", J. Chem. Phys. 100, 6665-6671 (1994b).
Tang, Y. and B. C.-Y. Lu, "Equation of State Based on the Mean Spherical Approximation", Proceedings of Second Beijing International Symposium on Thermodynamics in Chemical Engineering and Industry, Vol 1, 75-82 (1994c).
Tang, Y. and B. C.-Y. Lu, "Analytical Solution of the Ornstein-Zernike Equation for Mixtures", Mol. Phys. 84, 89-103 (1995).
Tang, Y. and B. C.-Y. Lu, "Improved Expressions for the Radial Distribution Function of Hard Spheres", J. Chem. Phys. 103, 7463-7470 (1995).
Tang, Y. and B. C.-Y. Lu, "Direct Calculation of Radial Distribution Function for Hard-Sphere Chains", J. Chem. Phys. 105, 8262-8265 (1996).
Tang, Y. and B. C.-Y. Lu, "Analytical Representation of Radial Distribution Function for Classical Fluids", Mol. Phys. 90, 215-224 (1997).
Tang, Y., Z. Tong and B. C.-Y. Lu, "An Analytical Equation of State Based on the Ornstein-Zernike Equation", Fluid Phase Equilibria 134, 21-42(1997).
Tang, Y. and B. C.-Y. Lu, "Analytical Prediction of Structure and Properties of the Lennard-Jones Fluid", AIChE J. (in press).
Thiele, E., "Equation of State for Hard Spheres", J. Chem. Phys. 39, 474-479 (1963).
Troop, G. J. and R. J. Bearman, "Numerical Solution of the Percus-Yevick Equation for the Hard-Sphere Potential", J. Chem. Phys. 42, 2408-2411 (1965).
Toda, M., R. Kubo, N. Saito,"Statistical Physics I", Springer-Verlag, 101-102 (1992).
Verlet, L., "Computer "Experiments" on Classical Fluids II. Equilibrium Correlation Functions", Phys. Rev. 165, 201-214 (1968).
Verlet, L., and J. Weis, "Equilibrium Theory of Simple Liquids", Phys. Rev A. 5, 939-952 (1972).
Vrabec, J., A. Lotif and J. Fisher, "Vapor Liquid Equilibria of Lennard-Jones Model Mixtures from the NPT plus Test Particle Method", Fluid Phase Equilibria 112, 173-197 (1995).
Waisman, E. and J. L. Lebowitz, "Exact Solution of an Integral Equation for the

Structure of A Primitive Model of Electrolytes", J. Chem. Phys. 52, 4301-4307 (1970).
Waisman, E., " The Radial Distribution Function for a Fluid of Hard Spheres at High Densities: Mean Spherical Integral Equation Approach", Mol. Phys. 25, 45-48(1973).
Weeks, J. D., D. Chandler and H. C. Anderson, "Roles of Repulsive Forces in Determining the Equilibrium Structure of Simple Liquids", J. Chem. Phys. 54, 5237-5245 (1971).
Wei, D., and L. Blum, " The Mean Spherical Approximation for an Arbitrary Mixture of Ions in a Dipolar Solvent: Approximate Solution, Pair Correlation Functions and Thermodynamics", J. Chem. Phys. 87, 2999-3007 (1987).
Wei, D., and L. Blum, "Nonprimitive Model of Electrolyte: Analytical Solution of the Mean Spherical Approximation for an Arbitrary Mixture of Sticky Ions and Dipoles", J. Chem. Phys. 88, 1091-1100 (1988).
Wertheim, M. S., "Exact Solution of the Percus-Yevick Integral Equation for Hard Spheres", Phys. Rev. Lett. 10, 321-323 (1963).
Wertheim, M. S., "Exact Solution of the Mean Spherical Model for Fluid of Hard Spheres with Permanent Electric Dipole Moment", J. Chem. Phys. 55, 4291-4298 (1971).
Yethiraj, A. and C. K. Hall, "Site-site Correlations in Short Chain Fluids", J. Chem. Phys. 93, 4453-4461 (1990).

Appendix A: The Hilbert Transform

For any $\phi(x)$, the one-dimensional Fourier transform is defined by

$$\hat{\phi}(k) = \int_{-\infty}^{\infty} \phi(x)\, e^{-ikx} dx \tag{A1}$$

The Hilbert transform denoted by the operator H is defined as

$$H\hat{\phi}(k) = \frac{1}{\pi} \int_{-\infty}^{\infty} \frac{\hat{\phi}(y)}{k-y} dy \tag{A2}$$

If the inverse Fourier transform is symbolled by F^{-1}, the Hilbert transform holds the following main properties.

1)

$$H^2\hat{\phi}(k) = -\hat{\phi}(k) \tag{A3}$$

2)

$$F^{-1}[H\hat{\phi}(k)] = isgn(x)\, F^{-1}[\hat{\phi}(k)] = isgn(x)\,\phi(x) \tag{A4}$$

where

$$sgn(x) = \begin{cases} 1 & x \geq 0 \\ -1 & x < 0 \end{cases}$$

3) Defining two new functions($-\infty < c < \infty$) as follows:

$$\hat{\phi}_{c^+}(k) = \frac{1}{2}\{\hat{\phi}(k) + ie^{-ikc} H[\hat{\phi}(k)\, e^{ikc}]\} \tag{A5}$$

$$\hat{\phi}_{c^-}(k) = \frac{1}{2}\{\hat{\phi}(k) - ie^{-ikc} H[\hat{\phi}(k)\, e^{ikc}]\} \tag{A6}$$

then we will have

i)

$$\hat{\phi}(k) = \hat{\phi}_{c^+}(k) + \hat{\phi}_{c^-}(k)$$

ii)

$$F^{-1}[\hat{\phi}(k)] = F^{-1}[\hat{\phi}_{c^+}(k)] + F^{-1}[\hat{\phi}_{c^-}(k)]$$

iii)

$$F^{-1}[\hat{\phi}_{c^+}(k)] \in [-\infty, c], \quad F^{-1}[\hat{\phi}_{c^-}(k)] \in [c, \infty] \qquad \textbf{(A7)}$$

in other words

$$F^{-1}[\hat{\phi}_{c^+}(k)] = \begin{cases} 0, & x > c \\ \phi(x), & x \le c \end{cases}$$

$$F^{-1}[\hat{\phi}_{c^-}(k)] = \begin{cases} \phi(x), & x \ge c \\ 0, & x < c \end{cases}$$

Definitions (A5) and (A6) which decompose ϕ(k) into two parts have an important application in our OZ equation solution.

Appendix B: Solution of the OZ Equation for Mixtures

The analytical solution of the OZ equation for mixtures can be carried out in a similar manner to that in Section 2.1. The development is made in terms of matrix, which basic properties have been mentioned in the OZ solution of hard-sphere mixtures (Baxter, 1970).

The first-order OZ equation given in Section 2.2 is

$$\tilde{H}_1(k)\,(I-\tilde{C}_0(k)) = (I+\tilde{H}_0(k))\,\tilde{C}_1(k) \tag{B1}$$

The Baxter (1970) factorization gives

$$I-\tilde{C}_0(k) = Q_0(k)\,Q_0^T(-k) \tag{B2}$$

where $Q_0(k)$ is the factor correlation matrix of hard sphere mixtures detailed in Section 2.2 and the superscript T denotes the transpose of matrix. $C_0(k)$ is a symmetric matrix and its component is an even function of k, leading to(Baxter, 1970)

$$Q_0(k)\,Q_0^T(-k) = Q_0(-k)\,Q_0^T(k) \tag{B3}$$

By combining (B2) and (B3), Equation (B1) may be translated into

$$Q_0^T(k)\,\tilde{H}_1(k)\,Q_0(k) = [Q_0(-k)]^{-1}\tilde{C}_1(k)\,[Q_0^T(-k)]^{-1} \tag{B4}$$

If further defining matrices $H_1(k)$ and $C_1(k)$ with their components given by

$$\begin{aligned}\{\hat{H}_1(k)\}_{ij} &= 2\pi\sqrt{\rho_i\rho_j}\int_0^\infty r h_{1,ij}(r)\,e^{-ikr}dr \\ \{\hat{C}_1(k)\}_{ij} &= 2\pi\sqrt{\rho_i\rho_j}\int_0^\infty r c_{1,ij}(r)\,e^{-ikr}dr\end{aligned} \tag{B5}$$

we have

$$\tilde{H}_1(k) = \frac{\hat{H}_1(-k)-\hat{H}_1(k)}{ik}, \quad \tilde{C}_1(k) = \frac{\hat{C}_1(-k)-\hat{C}_1(k)}{ik} \tag{B6}$$

Making a substitution of the above relations into Equation (B4) yields

$$Q_0^T(k)\,\hat{H}_1(k)\,Q_0(k) = Q_0^T(k)\,\hat{H}_1(-k)\,Q_0(k) + [Q_0(-k)]^{-1}\hat{C}_1(k)\,[Q_0^T(-k)]^{-1} - [Q_0(-k)]^{-1}\hat{C}_1(-k)\,[Q_0^T(-k)]^{-1} \quad \text{(B7)}$$

If $C_1(k)$ is further decomposed into two parts

$$\hat{C}_1(k) = U_1(k) + S_1(k) \quad \text{(B8)}$$

with each component of $U_1(k)$ and $S_1(k)$ represented by

$$\{U_1(k)\}_{ij} = 2\pi\sqrt{\rho_i\rho_j}\int_{R_{ij}}^{\infty} rC_{1,ij}(r)\,e^{-ikr}dr$$
$$\{S_1(k)\}_{ij} = 2\pi\sqrt{\rho_i\rho_j}\int_{0}^{R_{ij}} rC_{1,ij}(r)\,e^{-ikr}dr \quad \text{(B9)}$$

Equation (B7) can be written as

$$Q_0^T(k)\,\hat{H}_1(k)\,Q_0(k) = Q_0^T(k)\,\hat{H}_1(-k)\,Q_0(k) + [Q_0(-k)]^{-1}U_1(k)\,[Q_0^T(-k)]^{-1} + [Q_0(-k)]^{-1}S_1(k)\,[Q_0^T(-k)]^{-1} - [Q_0(-k)]^{-1}\hat{C}_1(-k)\,[Q_0^T(-k)]^{-1} \quad \text{(B10)}$$

The first-order OZ equation can now be treated by analyzing each term of (B10) in the n × n dimensional r-space. The component of matrix in the left-hand side, which is a multiplication of three matrices, can be explicitly expressed by

$$\{Q_0^T(k)\,H_1(k)\,\hat{Q}_0(k)\}_{ij} = \sum_m \sum_n \{Q_0(k)\}_{mi}\{\hat{H}_1(k)\}_{mn}\{Q_0(k)\}_{nj} \quad \text{(B11)}$$

An investigation of Equation (B11) shows that the functions $\{Q_0(k)\}_{mi}$, $\{H_1(k)\}_{mn}$ and $\{Q_0(k)\}_{nj}$ are in the r-space $[\lambda_{mi}, R_{mi}]$, $[R_{mn}, \infty]$ and $[\lambda_{nj}, R_{nj}]$, respectively. So their multiplication will lie in the space $[R_{ij}, \infty]$. Therefore, the term on the left-hand side of Equation (B10) will be in the n × n r-space $[R_{11},\infty][R_{12},\infty].....[R_{NN},\infty]$ which is later denoted as $[R,\infty]$. A similar analysis shows that the first, the third, the fourth terms on the right-hand side of Equation (B10) lie either in the space $[-\infty,R]$ or in its subspace. Only the second term which covers the entire Space $[-\infty,\infty]$ $[-\infty,\infty].....[-\infty,\infty]$ makes contribution to our concerned space $[R,\infty]$. That term has to be further split into two spaces $[-\infty, R]$ and $[R, \infty]$ as indicated below:

$$[Q_0(-k)]^{-1}U_1(k)\,[Q_0^T(-k)]^{-1}=\left[[Q_0(-k)]^{-1}U_1(k)\,[Q_0^T(-k)]^{-1}\right]^{[R,\infty]} +\left[[Q_0(-k)]^{-1}U_1(k)\,[Q_0^T(-k)]^{-1}\right]^{[-\infty,R]} \tag{B12}$$

It implies that for each matrix component of Equation (B12),

$$\left\{[Q_0(-k)]^{-1}U_1(k)\,[Q_0^T(-k)]^{-1}\right\}_{ij}=\left\{[Q_0(-k)]^{-1}U_1(k)\,[Q_0^T(-k)]^{-1}\right\}_{ij}^{[R_{ij},\infty]} +\left\{[Q_0(-k)]^{-1}U_1(k)\,[Q_0^T(-k)]^{-1}\right\}_{ij}^{[-\infty,R_{ij}]} \tag{B13}$$

The split in (B12) and (B13) can be technically performed by the Hilbert transform, viz.

$$\left\{[Q_0(-k)]^{-1}U_1(k)\,[Q_0^T(-k)]^{-1}\right\}_{ij}^{[R_{ij},\infty]}=\frac{1}{2}\left\{[Q_0(-k)]^{-1}U_1(k)\,[Q_0^T(-k)]^{-1}\right\}_{ij} - \frac{e^{-ikR_{ij}}}{2\pi i}\int_{-\infty}^{\infty}\frac{dy}{y-k}\left\{[Q_0(-y)]^{-1}U_1(y)\,[Q_0^T(-y)]^{-1}\right\}_{ij}e^{iyR_{ij}} \tag{B14}$$

$$\left\{[Q_0(-k)]^{-1}U_1(k)\,[Q_0^T(-k)]^{-1}\right\}_{ij}^{[-\infty,R_{ij}]}=\frac{1}{2}\left\{[Q_0(-k)]^{-1}U_1(k)\,[Q_0^T(-k)]^{-1}\right\}_{ij} + \frac{e^{-ikR_{ij}}}{2\pi i}\int_{-\infty}^{\infty}\frac{dy}{y-k}\left\{[Q_0(-y)]^{-1}U_1(y)\,[Q_0^T(-y)]^{-1}\right\}_{ij}e^{iyR_{ij}} \tag{B15}$$

which read more conveniently in the following form of matrix

$$\left[[Q_0(-k)]^{-1}U_1(k)\,[Q_0^T(-k)]^{-1}\right]^{[R,\infty]}=\frac{1}{2}[Q_0(-k)]^{-1}U_1(k)\,[Q_0^T(-k)]^{-1} -\frac{E(k)}{2\pi i}\int_{-\infty}^{\infty}\frac{dy}{y-k}\left[E(-y)\,[Q_0(-y)]^{-1}U_1(y)\,[Q_0^T(-y)]^{-1}E(-y)\right]E(k) \tag{B16}$$

$$\left[[Q_0(-k)]^{-1}U_1(k)\,[Q_0^T(-k)]^{-1}\right]^{[-\infty,R]}=\frac{1}{2}[Q_0(-k)]^{-1}U_1(k)\,[Q_0^T(-k)]^{-1} +\frac{E(k)}{2\pi i}\int_{-\infty}^{\infty}\frac{dy}{y-k}\left[E(-y)\,[Q_0(-y)]^{-1}U_1(y)\,[Q_0^T(-y)]^{-1}E(-y)\right]E(k) \tag{B17}$$

In Equations (B16) and (B17), integration is operated with each component of matrix

in the bracket. E(k) is a diagonal matrix defined by

$$E(k) = \begin{bmatrix} e^{\frac{-ikR_1}{2}} & 0 & . & . & . \\ 0 & e^{\frac{-ikR_2}{2}} & 0 & . & . \\ . & . & . & . & . \\ . & . & . & 0 & e^{\frac{-ikR_M}{2}} \end{bmatrix}$$

Substituting Equation (B12) into (B10) and making a slight rearrangement yields

$$\begin{aligned} &Q_0^T(k)\hat{H}_1(k)Q_0(k) - \left[[Q_0(-k)]^{-1}U_1(k)[Q_0^T(-k)]^{-1}\right]^{[R,\infty]} = \\ &\left[[Q_0(-k)]^{-1}U_1(k)[Q_0^T(-k)]^{-1}\right]^{[-\infty,R]} + Q_0^T(k)\hat{H}_1(-k)Q_0(k) + \\ &[Q_0(-k)]^{-1}S_1(-k)[Q_0^T(-k)]^{-1} - [Q_0(-k)]^{-1}\hat{C}_1(-k)[Q_0^T(-k)]^{-1} \end{aligned} \qquad \text{(B18)}$$

The left-hand side of the above equation is in space [R, ∞], while the right-hand side of the above equation belongs to the space [-∞, R]. Both sides should vanish. Hence,

$$Q_0^T(k)\hat{H}_1(k)Q_0(k) = \left[[Q_0(-k)]^{-1}U_1(k)[Q_0^T(-k)]^{-1}\right]^{[R,\infty]} \qquad \text{(B19)}$$

In terms of Equation (B16), one has

$$\begin{aligned} Q_0^T(k)\hat{H}_1(k)Q_0(k) &= \frac{1}{2}[Q_0(-k)]^{-1}U_1(k)[Q_0^T(-k)]^{-1} \\ -\frac{E(k)}{2\pi i}\int_{-\infty}^{\infty}\frac{dy}{y-k}&\left[E(-y)[Q_0(-y)]^{-1}U_1(y)[Q_0^T(-y)]^{-1}E(-y)\right]E(k) \end{aligned} \qquad \text{(B20)}$$

which is the first-order OZ solution for mixtures presented in Section 2.2. A very similar analysis can yield the following ith-order OZ solution:

$$
\begin{aligned}
Q_0^T(k)\,\hat{H}_\gamma(k)\,Q_0(k) = &\frac{1}{2}\,[Q_0(-k)]^{-1}U_\gamma(k)\,[Q_0^T(-k)]^{-1} - \\
&\frac{ik}{4\pi}\sum_{m=1}^{\gamma-1} Q_0^T(k)\,\tilde{H}_m(y)\,\tilde{C}_{\gamma-m}(y)\,[Q_0^T(-k)]^{-1} - \\
&\frac{E(k)}{2\pi i}\int_{-\infty}^{\infty}\frac{dy}{y-k}\Bigg\{E(-y)\Bigg[[Q_0(-y)]^{-1}U_\gamma(y)\,[Q_0^T(-y)]^{-1} - \\
&\frac{iy}{2\pi}\sum_{m=1}^{\gamma-1} Q_0^T(y)\,\tilde{H}_m(y)\,\tilde{C}_{\gamma-m}(y)\,[Q_0^T(-y)]^{-1}\Bigg]E(-y)\Bigg\}E(k)
\end{aligned}
\tag{B21}
$$

Appendix C: Body of Classes in OOP

```
class BASE{
  private:
    void find_ab(void (BASE::*f_set)(float [9], float [9]),
      float x[9], float a[9][9], float b[9], int n);
    void find_ab(float (BASE:: *f[9])(float [9]),
      float x[9], float a[9][9], float b[9], int n);
    complex (BASE::*FFTDF)(complex);
    float FFTr,FFTc,FFTF(float k);
    float FFTint(float (BASE::*fun)(float),float a, float b, float err);
  protected:
    float factorial(int);
    int max(int, int);
    void sloeq3(float,float,float,float, complex r[3]);
    void Gauss(float a[9][9], float b[9], int n);
    void Newton (void (BASE::*f_set)(float [9], float [9]),
      float x[9], int n, float err);
    virtual void f_set(float [9], float [9]){}
    void Newton (float (BASE::*f[9])(float [9]),
      float x[9], int n, float err);
    float integral(float (BASE::*fun)(float),
      float a, float b, float err,int flag);
    virtual float integrand_1(float){return 0;}
    virtual float integrand_2(float){return 0;}
    virtual float integrand_3(float){return 0;}
    virtual float integrand_4(float){return 0;}
    virtual float integrand_5(float){return 0;}
    float FFT(complex (BASE::*fun)(complex),float r);
    virtual complex G(complex){return 0;}
    virtual complex G0(complex){return 0;}
    virtual complex G1(complex){return 0;}
  public:
      BASE(){
      }
      virtual ~BASE(){
      }
};

class FLUID: virtual public BASE{
  private:
```

```
    virtual void P_mu_equal(float x[9],float f[9]);
  protected:
    float tstar,rho;
    void f_set(float x[9],float f[9]);
  public:
    FLUID(){}
    ~FLUID(){}
    virtual void initial(void){}
    virtual float a(void){return 0;}
    virtual float a(float rho){
      FLUID::rho=rho;
      return a();
      }
    virtual float Z(void);
    virtual float Z(float rho){
      FLUID::rho=rho;
      return Z();
      }
    virtual float u(void);
    virtual float u(float rho){
      FLUID::rho=rho;
      return u();
      }
    float mu(void){return a()+Z();}
    float mu(float rho){return a(rho)+Z(rho);}
    void phase_equilibria(float &Rho_l,float &Rho_v, float &Pstar);
};

class HS: public FLUID{
  protected:
    float eta;
    void roots(void);
    complex t[3];
    complex S(complex),S1(complex),S2(complex),L(complex);
    float S(float),L(float);
    float Q_0(float),Q1eta(float),Q1s(float);
    float IQ2(float),Q2(float);
    virtual complex A(int,int,int,int);
    float CC(int,int,int,float);
    complex B(int,int,int,int,int),EE(int,int,int,complex,float),
```

```
    DD(int,int,int,complex,float);
   complex G(complex);
 public:
   HS(float pack){
     eta=Pi*pack/6;
     roots();
     }
   HS(float tstar,float pack){
     HS::tstar=tstar;
     eta=Pi*pack/6;
     roots();
     }
   HS(){
     }
   ~HS(){
     }
   virtual  float g0(float);
   virtual  float g(float r){return g0(r);}
   float g0msa(float);
   float c0(float, char*);
   virtual float a(void){return a0();}
   virtual float a(float pack){
     eta=Pi/6*pack;
     return a();
     }
   virtual float Z(void){return Z0();}
   virtual float Z(float pack){
     eta=Pi/6*pack;
     return Z();
     }
   virtual float u(void){return 0;}
   virtual float u(float pack){
     eta=Pi/6*pack;
     return u();
     }
   float a0(void);
   float Z0(void);
};

class SW: public HS{
```

```
  private:
    complex D(complex),D1(complex),D2(complex);
    complex E(complex),E1(complex),E2(complex);
    complex F(complex),F1(complex);
    complex M(complex),M1(complex),M2(complex);
    complex N(complex),N1(complex),N2(complex);
    complex Z(complex),Z1(complex),Z2(complex);
  protected:
    float lm;
  public:
    SW(float tstar,float pack,float lm):HS(tstar,pack){
      SW::lm=lm;
      }
    SW(){}
    ~SW(){}
    float g1(float);
      float g(float r){
        return g0(r)+g1(r);
        }
    float a(void){return a0()+a1()+a2();}
    float a(float pack){
      eta=pack*Pi/6;
      return a0()+a1()+a2();
      }
    float a1(void);
    float a2(void);
    float Z(void){return Z0()+Z1()+Z2();}
    float Z(float pack){
      eta=pack*Pi/6;
      return Z0()+Z1()+Z2();
      }
    float Z1(void);
    float Z2(void);
    float u(void){
      return a1()+2*a2();
      }
};

class YUKAWA: public HS{
  protected:
```

```
    float z;
  public:
    YUKAWA(float tstar, float pack, float z):HS(tstar,pack){
    YUKAWA::z=z;
    }
    YUKAWA(){}
    ~YUKAWA(){}
    float g1(float);
    float g(float r){
      return g0(r)+g1(r);
      }
    float a(void){
      return a0()+a1()+a2();
      }
    float a(float pack){
      eta=Pi/6*pack;
      return a0()+a1()+a2();
      }
    float a1(void);
    float a2(void);
    float Z(void){
      return Z0()+Z1()+Z2();
      }
    float Z(float pack){
      eta=Pi/6*pack;
      return Z0()+Z1()+Z2();
      }
    float Z1(void);
    float Z2(void);
    float u(void){
      return a1()+2*a2();
      }
};

class YWLJ: public YUKAWA{
  private:
    float z1,z2,k,k1,k2;
    float F(float);
  protected:
    float R;
```

```
    float gext(float);
    void initial(void);
  public:
    YWLJ(float tstar,float rho){
      YWLJ::tstar=tstar;
      YWLJ::rho=rho;
      initial();
      }
    YWLJ(){}
    ~YWLJ(){}
    float g1(float);
    float g(float r){
      if(r>=R)return g0(r/R)+g1(r);
      else return gext(r);
      }
    float a1(void);
    float a2(void);
    float a(void){
      return a0()+a1()+a2();
      }
    float a(float pack){
      eta=pack*Pi/6*pow(R,3);
      return a0()+a1()+a2();
      }
    float Z1(void);
    float Z2(void);
    float Z(void){
      return Z0()+Z1()+Z2();
      }
    float Z(float pack){
      eta=pack*Pi/6*pow(R,3);
      return Z0()+Z1()+Z2();
      }
    float u(void);
    float B2(float,float);
};

class YWLJEXP: public YWLJ{
  private:
    float integrand_1(float r), integrand_2(float r);
```

```
protected:
public:
  YWLJEXP(float tstar,float pack):YWLJ(tstar,pack){}
  YWLJEXP(){}
  ~YWLJEXP(){}
  float g(float r){
    if(r>=R)return g0(r/R)*exp(g1(r));
    else return gext(r);
    }
  float ar(void){
    return integral(&BASE::integrand_1,1.0,1.5,0.001,0);
    }
  float a(void){
    return a0()+a1()+a2()+ar();
    }
  float a(float pack){
    eta=pack*Pi/6*pow(R,3);
    return a0()+a1()+a2()+ar();
    }
  float Zr(void){
    float eta0,temp1,temp2,temp;
    float h=0.005;
    eta0=eta;
    eta=eta0*(1-h);temp1=ar();
    eta=eta0*(1+h);temp2=ar();
    temp=(temp2-temp1)/2/h;
    eta=eta0;
    return temp;
    }
  float Z(void){
    return Z0()+Z1()+Z2()+Zr();
    }
  float Z(float pack){
    eta=pack*Pi/6*pow(R,3);
    return Z0()+Z1()+Z2()+Zr();
    }
  float ur(void){
    float tstar0,eta0,R0,temp1,temp2,temp;
    float h=0.005;
    tstar0=tstar; R0=R; eta0=eta;
```

```
      tstar=tstar0*(1-h);eta=eta0;initial();temp1=ar();
      tstar=tstar0*(1+h);eta=eta0;initial();temp2=ar();
      temp=-(temp2-temp1)/2/h;
      tstar=tstar0; R=R0; eta=eta0;
      return temp;
      }
    float u(void){
      return YWLJ::u()+ur();
      }
    float B2(float tstar,float sigma);
};

class BH: public HS{
  private:
    float pack,R;
    void initial(void);
    float integrand_1(float r);
  protected:
  public:
    BH(float tstar,float pack):HS(tstar,pack){
      BH::pack=pack;
      }
    BH(){}
    ~BH(){}
    float g(float);
    float a(void);
    float a(float pack){
      BH::pack=pack; initial();
      return a();
      }
    float Z(void);
    float Z(float pack){
      BH::pack=pack; initial();
      return Z();
      }
    float u(void);
};

class WCA: public HS{
  private:
```

```
    float pack,R;
    void initial(void);
    float y0(float);
    float integrand_1(float r);
  protected:
  public:
    WCA(float tstar,float pack):HS(tstar,pack){
      WCA::pack=pack;
      }
    WCA(){}
    ~WCA(){}
    float g(float);
    float a(void);
    float a(float pack){
      WCA::pack=pack; initial();
      return a();
      }
    float Z(void);
    float Z(float pack){
      WCA::pack=pack; initial();
      return Z();
      }
    float u(void);
};

class POLYMER: public HS{
  protected:
    int m;
    float ratio;
  public:
    POLYMER(float pack, int m0):HS(pack){
      m=m0;
      ratio=1.-1/float(m);
      }
    POLYMER(){}
    ~POLYMER(){}
    float g0(float);
    complex A(int,int,int,int);
};
```

```
class STICKY: public HS{
  protected:
  public:
    STICKY(float tstar, float pack):HS(tstar,pack){}
    STICKY(){}
    ~STICKY(){}
    float g1(float);
    float g(float r){
      return g0(r)+g1(r)/tstar;
      }
};

class LJ: public HS{
  private:
    float x;
    float integrand_1(float);
    float integrand_2(float);
    float integrand_3(float);
    float integrand_4(float);
    float integrand_5(float);
    float gext(float);
    float fexp(float);
  protected:
    float R;
    void initial(void);
  public:
    LJ(float tstar,float rho){
      LJ::tstar=tstar;
      LJ::rho=rho;
      initial();
      }
    LJ(){}
    ~LJ(){}
    float g1(float);
    float g(float r){
      if(r>=R)return g0(r/R)+g1(r);
      else return gext(r);
      }
    float a1(void);
    float a2(void);
```

```
    float a(void){
      return a0()+a1()+a2();
      }
    float a(float rho){
      eta=rho*Pi/6*pow(R,3);
      return a();
      }
    float Z(void);
    float Z(float rho){
      LJ::rho=rho;
      return Z();
      }
    float u(void);
};

class MBWR: public FLUID{
  private:
    float aa,ZZ,uu;
    void calculation(void);
  protected:
  public:
    MBWR(float tstar,float pack);
    MBWR(){}
    ~MBWR(){}
    float a(void){ return aa;}
    float a(float pack){rho=pack;calculation();return aa;}
    float Z(void){ return ZZ;}
    float Z(float pack){rho=pack;calculation();return ZZ;}
    float u(void){ return uu;}
};

class PR: public FLUID{
  private:
    float Tc,Pc,omega;
    float R,uu,ww;
    float aa,bb;
  protected:
    void initial(void);
  public:
    PR(float T,float v,float Tc, float Pc, float omega);
```

```
    PR(){}
    ~PR(){}
    float a(void);
    float Z(void);
};

class FLUID_MIX: virtual public BASE{
  private:
    float Rho_l, Rho_v, x_l[9], x_v[9], P_constant;
    char *phase_flag;
    void P_mu_equal(float x[9], float f[9]);
  protected:
    int N,I,J;
    float tstar,Rho,rho[9],x[9];
    virtual void initial(float, float [9], float){}
    virtual void initial(float [9], float){}
    void f_set(float x[9], float f[9]);
  public:
    FLUID_MIX(){
      }
    ~FLUID_MIX(){
      }
    virtual float a(void){return 0;}
    float a_ex(void);
    float Z(void);
    float u(void);
    float mu(int);
    void phase_equilibria(float &Rho_l,float &Rho_v,
         float &Pstar, float x[9],float y[9], char *flag);
};

class HS_MIX: public FLUID_MIX{
  private:
    float JJ[9][9],z;
    void initial(int N,float rho[9],float R[9]);
    void initial(int N,float rho[9],float R[9], float tstar);
  protected:
    float R[9];
    float xi0,xi1,xi2,xi3,xi4,delta;
    complex q1(complex,float),q2(complex,float);
```

```
    float q1(float,float),q2(float,float);
    complex det(complex),W(complex, int, int);
    float det(float),W(float, int, int);
    complex A(complex,int,int);
    float A(float,int,int);
    complex G0(complex);
    float G0(float);
    complex G1(complex);
    float G1(float);
    void initial(float Rho, float x[9], float tstar);
    void initial(float rho[9], float tstar);
  public:
    HS_MIX(int N,float rho[9],float R[9])
      {initial(N,rho,R);}
    HS_MIX(int N,float rho[9],float R[9],float tstar)
      {initial(N,rho,R,tstar);}
    HS_MIX(){
      }
    ~HS_MIX(){
      }
    float g0_PY(float,int,int);
    float g0_GMSA(float,int,int);
    float g0_VW(float,int,int);
    float g0_contact_PY(int,int);
    float a0_MCSL(void);
    float a(void){return a0_MCSL();}
};

class YUKAWA_MIX: public HS_MIX{
  private:
    complex b(complex s, int i, int j);
    float b(float s, int i, int j);
  protected:
    float z[9][9];
    float K[9][9];
  public:
    YUKAWA_MIX(int N,float rho[9],float R[9],
      float tstar,float k[9][9],float z[9][9]);
    YUKAWA_MIX(){
      }
```

```
    ~YUKAWA_MIX(){
     }
    float g(float,int,int);
    float g1(float,int,int);
    float g1_contact(int,int);
    complex G1(complex s);
    float G1(float s);
};


class YWLJ_MIX: public YUKAWA_MIX{
  private:
    float z1[9][9],z2[9][9];
    float d[9][9];
    float K1[9][9],K2[9][9];
    float F(float);
  protected:
    float sigma[9][9],epsilon[9][9];
    virtual void initial(int N,float rho[9],float sigma[9][9],float tstar,
      float epsilon[9][9]);
    void initial(float Rho,float x[9],float tstar);
    void initial(float rho[9],float tstar);
    complex G1(complex s);
    float G1(float s);
  public:
    YWLJ_MIX(int N,float rho[9],float sigma[9][9],float tstar,
      float epsilon[9][9]);
    YWLJ_MIX(){
     }
    ~YWLJ_MIX(){
     }
    float g(float,int,int);
    float g1(float,int,int);
    float g1_contact(int,int);
    float a(void);
    float a0(void),a1(void),a2(void);
};

class MBWR_MIX: public FLUID_MIX{
  private:
```

```
    void initial(int N,float rho[9],float sigma[9][9],float tstar,
      float epsilon[9][9]);
  protected:
    float sigma[9][9],epsilon[9][9];
    void initial(float Rho, float x[9], float tstar);
    void initial(float rho[9], float tstar);
  public:
    MBWR_MIX(int N,float rho[9],float sigma[9][9],float tstar,
      float epsilon[9][9]);
    MBWR_MIX(){
      }
    ~MBWR_MIX(){
      }
    float a(void);
};
```

IMAGE EVALUATION
TEST TARGET (QA-3)

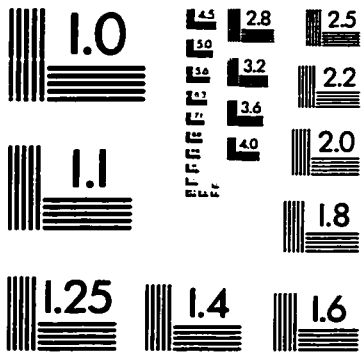

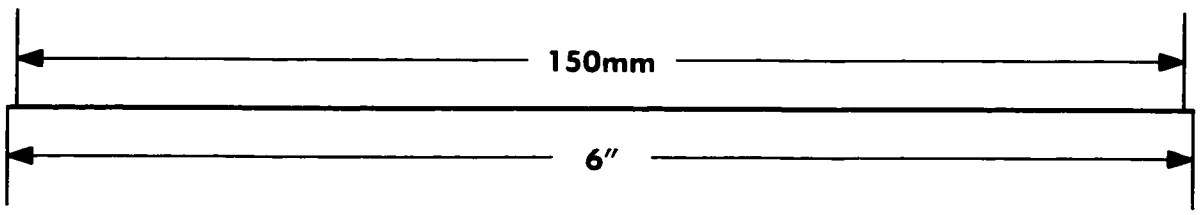

APPLIED IMAGE, Inc
1653 East Main Street
Rochester, NY 14609 USA
Phone: 716/482-0300
Fax: 716/288-5989